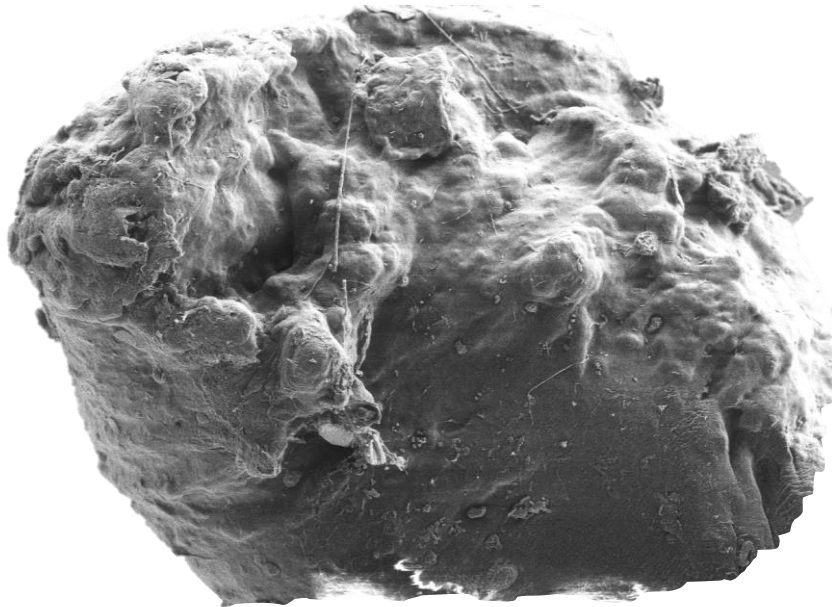


Diversity and specificity of microplastic-associated bacterial communities: evidences from a marine coral microcosm system




Dissertation zur Erlangung des akademischen Grades
Doktor der Naturwissenschaft
- Dr. rer. nat. -

vorgelegt von

M. Sc. Ángel Germán Franco Franco

Gießen, April 2020

JUSTUS-LIEBIG-
 UNIVERSITÄT
GIESSEN

Die vorgelegte Arbeit wurde am Institut für Angewandte Mikrobiologie, Fachbereich 09 (Agrarwissenschaften, Ökotoxikologie und Umweltmanagement) der Justus-Liebig-Universität Gießen, in der Zeit von Oktober 2015 bis Mai 2019 unter der Leitung Prof. Dr. Dr.-Ing. Kämpfer und der Betreuung von Dr. Stefanie Glaeser angefertigt.

Dekan

Prof. Dr. Jürgen Janek

Physikalisch-Chemisches Institut
FB08 der Justus-Liebig-Universität Gießen
Heinrich-Buff-Ring 17, 35392 Gießen

Gutachter

1. Prof. Dr. Peter Kämpfer

Institut für Angewandte Mikrobiologie
FB09 der Justus-Liebig-Universität Gießen
Heinrich-Buff-Ring 26-32, 35392 Gießen, Deutschland

2. Prof. Dr. Thomas Wilke

Institut für Tierökologie und Spezielle Zoologie
FB08 der Justus-Liebig-Universität Gießen
Heinrich-Buff-Ring 26-32, 35392 Gießen, Deutschland

3. Prof. Dr. Catalina Arévalo-Ferro

Department of Biology
Faculty of Sciences, National University of Colombia
Av. Carrera 30 # 45-03, Bogotá, Colombia

Ángel Germán Franco Franco (2020). Diversity and specificity of microplastic-associated bacterial communities: evidences from a marine coral microcosm system. Dissertation zur Erlangung des Doktorgrades der Naturwissenschaftlichen Fachbereiche der Justus-Liebig-Universität Gießen, Deutschland.

Cover: Scanning electron microscope micrograph of a microplastic particle incubated in the CEMarin aquarium system.

“Excellence is never an accident. It is always the result of high intention, sincere effort, and intelligent execution; it represents the wise choice of many alternatives – choice, not chance, and determines your destiny”

Aristotle

Table of contents

Summary.....	1
Zusammenfassung.....	2
Abbreviations.....	4
1. Introduction.....	6
1.1 State of the art.....	6
1.1.1 The ocean and its coral reefs: threatened ecosystems	6
1.1.2 Global stressors that affect the health of coral reefs	7
1.1.3 Plastic pollution and effects of MP on coral health	8
1.1.4 Influence of global stressors on coral diseases induced by bacteria	10
1.1.5 The importance of bacteria-coral interactions	12
1.2 Knowledge gaps and objectives.....	14
1.3 Hypothesis	16
2. Background.....	18
2.1 The prokaryotic life on microplastics in marine environments	18
2.1.1 Bacterial colonisation of surfaces and biofilm formation	18
2.1.2 Bacterial communities on MP surfaces	19
2.2 The genus <i>Vibrio</i> is a common member of marine environments	21
2.2.1 The genus <i>Vibrio</i> , a ubiquitous and pathogenic genus in the ocean	21
2.2.2 The importance of cultivation-based studies and the taxonomy of <i>Vibrio</i>	23
2.3 Marine habitats as hotspot of new bacterial species	24
2.3.1 Bacteria from the marine <i>Roseobacter</i> clade are primary colonisers.....	25
2.3.2 <i>Winogradskyella</i> sp. is a common genus from marine environments.....	27
3. Materials and methods.....	29
3.1 Revealing the bacterial assemblages developed in the marine system	29
3.1.1 Setup of the CEMarin aquatic system and experiment	29
3.1.2 Collection of MP, sandy sediments, detritus, and water samples	30
3.1.3 DAPI staining of MP and colonisation experiment	31
3.1.4 Scanning electron microscopy (SEM) of the particles	31
3.1.5 DNA extraction from particles and water samples	32
3.1.6 Microbial community fingerprinting using PCR-DGGE	32
3.1.7 16S rRNA gene amplicon Illumina MiSeq sequencing	33

3.1.8	<i>Vibrio</i> -specific primer design	34
3.1.9	Quantification of <i>Vibrio</i> spp. 16S rRNA gene targets by qPCR.....	34
3.1.10	Clone library construction and screening.....	36
3.1.11	Cultivation, isolation, and maintenance of bacteria.....	36
3.1.12	Genotypic differentiation of isolates.....	37
3.1.13	Phylogenetic identification and phylotyping of isolates	37
3.1.14	Statistical Analyses	38
3.2	Genome sequencing and genome-based analyses	38
3.2.1	Genome sequencing of selected strains	38
3.2.2	Analyses of genome sequences	39
3.3	Diversity of <i>Vibrio</i> spp. cultivated from the marine aquarium system.....	40
3.3.1	Amplification of housekeeping genes and genotyping of bacterial isolates....	40
3.3.2	Phylogenetic analysis based on MLSA	40
3.4	Polyphasic characterization of new bacterial species	41
3.4.1	Isolation of the strains	41
3.4.2	Phylogenetic analyses and G+C content calculation.....	41
3.4.3	Morphological characterization and growth and degradation tests.....	41
3.4.4	Enzyme activity tests.....	43
3.4.5	Pigment extraction and analysis.....	43
3.4.6	Chemotaxonomy	43
4.	Results	45
4.1	The prokaryotic life on MP, natural particles, and water fractions in a marine system containing small-polyp stony corals	45
4.1.1	Bacterial colonisation of MP occurs within 24 hours	45
4.1.2	SEM visualization indicated a specific colonisation of MP	45
4.1.3	Bacterial community fingerprinting confirmed intra- and inter-tank stability of samples	47
4.1.4	Specificity of bacterial assemblages of MP	48
4.1.5	Alpha diversity reveals similarities between particle-bacterial assemblages ..	49
4.1.6	Specific families dominated the bacterial assemblages on MP	50
4.1.7	Bacterial assemblages of MP contain exclusive phylogenetic groups	52
4.1.8	Quantification of <i>Vibrio</i> spp. based on qPCR.....	55
4.1.9	Cloning and specificity of the <i>Vibrio</i> spp. primer sets	57
4.1.10	Cultivation-dependent characterization of MP-specific bacteria	59

4.2	Revealing the information contained in the genomes	66
4.2.1	Genome structure and the genetic potential of MP-colonizing bacteria	66
4.2.2	Putative virulence-associated genes in <i>Vibrio</i> spp. genomes	74
4.3	The genus <i>Vibrio</i> as a key member of the marine system.....	76
4.3.1	High diversity of <i>Vibrio</i> spp. phylotypes detected in the marine system.....	76
4.3.2	MLSA-based phylogeny of <i>Vibrio</i> spp. isolates	79
4.3.3	Different distribution of <i>Vibrio</i> spp. phylotypes in the marine system.....	88
4.3.4	Genotypic differentiation and specific occurrence of <i>Vibrio</i> spp. genotypes..	88
4.3.5	Analysis of the genome of the strain THAF100	90
4.3.6	Presence of putative pathogenicity-related genes in <i>Vibrio</i> sp. THAF100	92
4.4	The CEMarin microcosm system harbours new bacterial species	95
4.4.1	<i>Winogradskyella pocilloporae</i> sp. nov. isolated from healthy tissues of the coral <i>Pocillopora damicornis</i>	96
4.4.2	<i>Pseudomaribius plastisphaeris</i> sp. nov. a new moderately halophilic species isolated from the surface of a polyethylene microplastic particle incubated in a marine aquarium system.....	103
4.4.3	<i>Ruegeria sedimentorum</i> sp. nov., a moderately halophilic bacterium isolated from the surface of a sandy sediment	109
4.4.4	<i>Vibrio aquimaris</i> sp. nov. a novel member of <i>Vibrionaceae</i> with putative pathogenicity-related genes, isolated from the water of a marine aquarium system	115
5.	Discussion.....	123
5.1	Bacterial assemblages developed on MP differed from those on natural particles	123
5.2	Potential bacterial degradation of PE-MP	125
5.3	MP as a refuge of potential pathogens for the marine biota.....	127
5.4	The genus <i>Vibrio</i> is an important member of the bacterial community of the marine system	128
5.5	MP carried <i>Vibrio</i> spp. with putative pathogenic genes	129
5.6	<i>Vibrio aquimaris</i> THAF100 also contain putative pathogenic genes.....	131
5.7	Conclusions and perspectives	133
	References	135
	Appendix	153
	Acknowledgements	156
	Curriculum Vitae	157
	Declaration.....	160

List of figures

1	Main stressors and their effects on marine environments and coral reefs.....	11
2	Graphical hypothesis of MP as vectors involved in coral health impairment.....	16
3	Stages of biofilm formation.....	19
4	Cell counts per mL of water for each tank of the marine system.....	30
5	Graphic description of the experimental tanks.....	30
6	Comparison of the binding regions of the primer sets used in this study.....	35
7	Bacterial colonisation of MP in the system and under optimal conditions.....	45
8	Scanning electron micrographs of the particles.....	46
9	Bacterial community fingerprinting analyses.....	47
10	Fractions of sequences per sample.....	48
11	NMDS of the composition of bacterial assemblages analysed by samples.....	49
12	Alpha diversity of bacterial assemblages.....	50
13	Relative abundances of the dominant phyla associated to the samples.....	51
14	Relative abundances of selected phyla and families in the samples.....	52
15	Relative abundances of phylogenetic groups in the different samples and their classification at higher taxonomic levels.....	54
16	Occurrence of the most abundant taxa in the different sample types.....	56
17	Total abundance of <i>Vibrio</i> spp. calculated by qPCR	57
18	Phylogenetic affiliation of cloned 16S rRNA gene sequences.....	59
19	Diversity of cultured bacteria per sample based on the phylotyping.....	63
20	Phylogenetic placement of bacterial isolates from the system.....	64
21	Circular visualization of genomes of <i>Roseivivax</i> strains.....	70
22	Circular visualization of genomes of <i>Marinobacter</i> strains.....	71
23	Circular visualization of genomes of <i>Erythrobacter</i> strains.....	72
24	Circular visualization of genomes of <i>Vibrio</i> strains.....	73
25	Presence and absence of putative virulence-associated genes in <i>Vibrio</i> strains.....	74
26	Phylogenetic placement of <i>Vibrio</i> spp. based on 16S rRNA gene sequences.....	78
27	Phylogenetic placement of <i>Vibrio</i> spp. based on MLSA with five 5 genes.....	80
28	Phylogenetic placement of <i>Vibrio</i> spp. based on partial sequences of <i>recA</i>	82
29	Phylogenetic placement of <i>Vibrio</i> spp. based on partial sequences of <i>pyrH</i>	83
30	Phylogenetic placement of <i>Vibrio</i> spp. based on partial sequences of <i>rpoD</i>	84
31	Phylogenetic placement of <i>Vibrio</i> spp. based on partial sequences of <i>gyrB</i>	85
32	Phylogenetic placement of <i>Vibrio</i> spp. based on partial sequences of <i>rctB</i>	86
33	Seriation analysis of phylotypes based on an absence-presence (0/1) matrix.....	88
34	Genotyping of <i>Vibrio</i> spp. isolates based on their genomic fingerprint patterns.....	89
35	Seriation analysis of genotypes based on an absence-presence (0/1) matrix.....	90
36	Distribution of genes in the genome of strain the THAF100.....	91
37	Core genome phylogenetic tree based on nucleotide sequences.....	93
38	Core genome phylogenetic tree based on amino acid sequences.....	94
39	Gene products associated to pathogenicity detected in the strain THAF100.....	95

40	Phylogenetic placement of strain AFPH31 ^T within the genus <i>Winogradskyella</i>	97
41	Absorption spectra of cellular pigments of <i>Winogradskyella</i> strains.....	98
42	Polar lipid profile of the strain AFPH31 ^T	100
43	Phylogenetic placement of strain THAF1 with members of the <i>Roseobacter</i> clade..	104
44	Thin-layer chromatography of the polar lipid profile of the strain THAF1.....	108
45	Phylogenetic placement of strain THAF57 with members of <i>Rhodobacteraceae</i>	110
46	Polar lipid profile of the strain THAF57.....	114

List of tables

1	Pairwise comparison using PERMANOVA based on Monte Carlo permutations.....	49
2	Relative abundances calculated for the most abundant phyla for each sample.....	51
3	Significance values for pairwise comparisons between the samples.....	53
4	Absolute quantification of <i>Vibrio</i> spp. and <i>Bacteria</i> 16S rRNA gene targets.....	57
5	Taxonomic assignment of the clones.....	58
6	Phylotype assignments of the isolated bacteria from the marine system.....	60
7	Main characteristics of complete genomes of MP-colonizers.....	66
8	Gene products potentially involved in polymer degradation and virulence.....	69
9	Overview of <i>Vibrio</i> spp. phlotypes and number of isolates per sample.....	77
10	Accession numbers of the gene sequences employed in the MLSA.....	87
11	Phenotypic characteristics that differentiate the strain AFPH31 ^T	99
12	Physiological characterisation of the strain AFPH31 ^T obtained with the test panel...	100
13	Fatty acid composition of strain AFPH31 ^T and its closest related type strains.....	101
14	Phenotypic characteristics that distinguish the strain THAF1.....	105
15	Physiological characterisation of the strain THAF1 obtained with the test panel....	106
16	Cellular fatty acid composition of strain THAF1 and its closest related type strains.	107
17	Differential characteristics of the strain THAF57 and its related species.....	111
18	Physiological characterisation of the strain THAF57 obtained with the test panel...	112
19	Cellular fatty acids profile of the strain THAF57 and its related species.....	113
20	Phenotypic characteristics differentiating the strain THAF100.....	117
21	Physiological characterisation of the strain THAF100 obtained with the test panel..	118
22	Cellular fatty acids composition of strain THAF100 and its related type strains.....	119

Summary

Corals are complex organisms in a delicate balance with symbiotic algae, fungi, bacteria, archaea, and viruses, which constitute the coral holobiont. Coverage and survival of coral reefs decrease rapidly due to changes in environmental conditions induced by human activities including, among others, the plastic pollution. Few studies have focused on the effects of plastic pollution on coral health, even though the research on microplastics (MP) in the ocean is imperative since MP are ubiquitous in aquatic systems, subjected to bacterial colonisation, dispersion among ecosystems, and ingestion by animals being transferred within the food web.

The hypothesis on which the study is based suggests that MP harbour specific bacterial assemblages that differ from those on other particles and that MP act as vectors of non-native and potential pathogenic bacteria that may be involved in the health impairment of corals, which was observed in corals exposed to MP in the CEMarin aquatic system. Bacterial assemblages associated with different habitats within the system: MP, sandy sediments, detritus, and present in the $> 5\mu\text{m}$, the $0.22\text{-}5\mu\text{m}$, and the total water fractions, were investigated by cultivation-dependent and independent approaches. A closer examination of isolates of genera *Roseivivax*, *Marinobacter*, *Roseivivax*, and especially *Vibrio* was performed due to their relevance as potential coral pathogens.

Differences in structure and composition of the bacterial assemblages associated with the particles and water fractions were observed, as well as MP-specific bacterial assemblages with high abundances of *Jejudonia*, *Roseivivax*, *Marinobacter*, and *Erythrobacter*, not present in any other sample. Quantitative PCR revealed a higher abundance of *Vibrio* spp. 16S rRNA gene copies per ng total DNA from MP compared to sandy sediments. The most abundant genera identified in the 16S rRNA gene amplicon sequencing were also isolated from the different samples. This approach indicated that *Vibrio* was the most abundant genus of the cultured community, and through a deep analysis based on 16S rRNA gene phylotyping, multilocus sequence analysis (MLSA), and genotyping, a higher genetic diversity of *Vibrio* spp. was observed. The strains were more closely related to *Vibrio alginolyticus*, *Vibrio fortis*, *Vibrio coralliilyticus*, *Vibrio mediterranei*, and *Vibrio owensii*, most of them coral pathogens. The genome of selected MP-associated bacteria was sequenced and by using comparative genomics, genes involved in the degradation of complex polymers, as well as genes associated to pathogenicity were detected, which may be related to coral diseases and the health impairment observed in corals incubated in the CEMarin aquarium system. In addition, four isolates from the strain collection represented new species, described as *Winogradskyella pocilloporae*, *Pseudomaribius plastisphaeri*, *Ruegeria sedimentorum*, and *Vibrio aquimaris*.

These findings validate the proposed hypothesis and represent a starting point to unravel the potential effects of MP-associated bacterial communities on coral's health. The strain collection may serve as base for future studies aimed to strengthen the knowledge of plastic biodegradation and bacterial pathogenicity on corals to identify the causes, mitigate their effects, and contribute to the conservation of these ecosystems.

Zusammenfassung

Korallen sind komplexe Organismen, die in einem empfindlichen Gleichgewicht mit symbiotischen Algen, Pilzen, Bakterien, Archaeen und Viren den Korallen-Holobionten bilden. Die Ausbreitung und das Überleben der Korallenriffe nehmen aufgrund der durch den Menschen verursachten Veränderungen der Umwelt, u.a. durch die Verschmutzung durch Plastikreste, rapide ab. Bisher haben sich nur wenige Studien auf die Auswirkungen dieser Verschmutzung auf die Gesundheit der Korallen konzentriert. Dabei ist die Erforschung von Mikroplastik im Ozean unerlässlich, da diese Partikel in aquatischen Systemen allgegenwärtig sind, einer bakteriellen Besiedlung ausgesetzt sind und von Tieren aufgenommen und im Nahrungsnetz übertragen werden könnten.

Die Hypothese, auf die sich die Studie stützt, legt nahe, dass MP spezifische Bakterielle Gemeinschaften aufweisen, die sich von denen auf anderen Partikeln unterscheiden, und dass MP als Vektoren nicht einheimischer und potenziell pathogener Bakterien fungieren. Diese Bakterien könnten die Gesundheitsschädigung von Korallen induzieren, welche bei Korallen beobachtet wurde, die MP im aquatischen System von CEMarin ausgesetzt waren. Aus diesem System wurden bakterielle Gemeinschaften durch kultivierungs-abhängige und -unabhängige Ansätze untersucht, die mit verschiedenen Lebensräume assoziiert sind (Mikroplastik-Partikel, sandige Sedimente, Detritus, > 5µm Wasserfraktionen, 0,22-5µm Wasserfraktionen und den Gesamtwasserfraktionen). Eine genauere Untersuchung von Isolaten der Gattungen *Roseivivax*, *Marinobacter*, *Erythrobacter*, und insbesondere *Vibrio* wurde aufgrund ihrer Relevanz als potentielle Korallenpathogene durchgeführt.

Es wurden Unterschiede in Struktur und Zusammensetzung der mit den Partikeln und Wasserfraktionen assoziierten bakteriellen Gemeinschaften sowie Mikroplastik-spezifische bakterielle Gemeinschaften beobachtet. Die Mikroplastik-assozierte Gemeinschaft wies hohe Abundanzen von *Jejundonia*, *Roseivivax*, *Marinobacter* und *Erythrobacter* auf, die in keiner anderen Probe vorhanden waren. Die Quantitative PCR zeigte eine höhere Häufigkeit von *Vibrio* spp. 16S rRNA Genkopien pro ng Gesamt-DNA aus Mikroplastik-Fractionen im Vergleich zu den 16S rRNA Genkopien pro ng Gesamt-DNA aus sandigen Sedimenten. Die häufigsten Gattungen, die in der 16S rRNA-Gen-Amplicon-Sequenzierung identifiziert wurden, wurden ebenfalls aus den verschiedenen Proben isoliert. *Vibrio* war die am häufigsten vorkommende Gattung der bakteriellen Gemeinschaft. Eine Tiefenanalyse auf der Grundlage der 16S rRNA-Genphylogenisierung, die Multilocus-Sequenzanalyse (MLSA) und die Genotypisierung, konnte zeigen, dass eine hohe genetische Diversität vorliegt. Die Stämme waren eng verwandt mit *Vibrio alginolyticus*, *Vibrio fortis*, *Vibrio coralliilyticus*, *Vibrio mediterranei* und *Vibrio owensii*, wovon die meisten Korallenpathogene sind. Mit Hilfe der vergleichenden Genomik wurden Gene entdeckt, die am Abbau komplexer Polymere beteiligt sind und die mit Virulenzfaktoren und Pathogenität assoziiert sind, die mit der gesundheitlichen Beeinträchtigung der Korallen im System zusammenhängen können. Aus dieser Gruppe wurden zusätzlich vier Stämme isoliert, die neue Arten darstellen: *Winogradskyella pocilloporae*, *Paramaribius plastisphaeri*, *Ruegeria sedimentorum* und *Vibrio aquimaris*.

Diese Ergebnisse validieren die vorgeschlagene Hypothese und stellen einen Ausgangspunkt dar, um die möglichen Auswirkungen von Mikroplastik-assoziierten Bakteriengemeinschaften auf die Gesundheit der Korallen zu entschlüsseln. Die angelegte Stammsammlung kann als Grundlage für zukünftige Studien dienen, die das Wissen über die bakterielle Pathogenität von Korallen stärken sollen. Diese Erkenntnisse können genutzt werden, um die Ursachen der Schädigung der Gesundheit zu identifizieren, ihre Auswirkungen zu mildern und zur Erhaltung dieser Ökosysteme beizutragen.

Abbreviations

AHL	Acyl homoserine lactone
ASW	Artificial seawater
BBD	Black band disease
BLAST	Basic Local Alignment Search Tool
BMC	Beneficial microorganisms for corals
BSA	Bovine serum albumin
CO ₂	Carbon dioxide
Det	Detritus
DGGE	Denaturing gradient gel electrophoresis
DNA	Deoxyribonucleic acid
dNTP	Dideoxyribonucleoside triphosphate
DOC	Dissolved organic carbon
FL	Free-living
LDPE	Low-density polyethylene
MA	Marin agar
MaPa	Maximum-Parsimony
MB	Marine broth
ML	Maximum-Likelihood
MLSA	Multilocus sequence analysis
MP	Microplastic particles
MRC	Marine <i>Roseobacter</i> clade
MT	Metric tons
NJ	Neighbour-Joining
NMDS	Non-metric multidimensional scaling
OA	Ocean acidification
OTU	Operational taxonomic unit
PA	Particle-associated
PCA	Principal component analysis
PCR	Polymerase chain reaction
PE	Polyethylene
PET	Polyethylene terephthalate
qPCR	Quantitative Polymerase chain
rRNA	Ribosomal ribonucleic acid
Sed	Sandy sediment
SEM	Scanning electron microscopy
SST	Sea surface temperature
UPGMA	Unweighted pair-group method using arithmetic average
WPD	White plague disease

CHAPTER I

1. Introduction

1.1 State of the art

1.1.1 The ocean and its coral reefs: threatened ecosystems

The oceans are the base of the food web and the source and reserve of millions shapes of life that are essential for the biology of the planet and innumerable processes within it, from photosynthesis (absorption of CO₂ and production of O₂) to the regulation of the global temperature (Hoegh-Guldberg and Bruno, 2010). The life that oceans harbour is also tremendously affected by climate change, which has occurred naturally since millions of years. However, since the industrial revolution began, environmental conditions have changed drastically in a short time period to which nature cannot totally adapt, causing reduction of native ecosystems, shifts in the land use, decrease in animal populations, and even total extinction of numerous species (Hoegh-Guldberg *et al.*, 2007). The increasing concentrations of anthropogenic-produced greenhouse gases accumulated since the industrial era have induced global warming, modifying the natural conditions of the ocean, causing an irreversible ecological transformation (Pomeroy, 1974; Hoegh-Guldberg and Bruno, 2010). For instance, the atmospheric CO₂ levels have increased by 40 % over the past 250 years (Doney *et al.*, 2009), and estimations for the next 50 years exceed the conditions under which marine ecosystems thrived for millions of years (Hughes *et al.*, 2003; Hoegh-Guldberg *et al.*, 2007).

Coral reefs are the most complex and taxonomically diverse marine ecosystems, providing habitat to thousands of vertebrates and invertebrates, for this reason they are called the rainforest of the sea (Jackson *et al.*, 2001; Mulhall, 2009). They offer a wide variety of good and services to coastal and inland populations and bear complex ecological relationships within the ocean's biota. Corals are affected by high atmospheric CO₂ concentrations, which modify the chemical conditions of the ocean's water inducing ocean acidification (OA). This threat hard corals since their skeletons tend to be weaker, reduce the coral larval settlement, and the accretion of coral reefs (Pandolfi *et al.*, 2011; Doropoulos *et al.*, 2012).

Another stressor that threat corals and other marine ecosystems is the water pollution due to inappropriate industrial waste disposal and especially solid material as plastic debris. Those are hazardous due to their chemical constituents (including toxic compounds) and pollutants absorbed from the environment, but also due to the physical entanglement or ingestion of macro and microplastic (MP) particles by the wildlife (Engler, 2012; Cole *et al.*, 2013; Setälä *et al.*, 2014; Rochman, 2015). It is also suggested that MP are vectors of non-native and potential pathogenic bacteria that impair the health condition of the wildlife (Zettler *et al.*, 2013; Kirstein *et al.*, 2016; Viršek *et al.*, 2017; Reichert *et al.*, 2018). The water temperature affects the gene expression of coral-associated bacteria, such as coral pathogens of the genus *Vibrio*, which may explain coral mortality events observed during thermal stress (Ben-Haim *et al.*, 2003; Vezzulli *et al.*, 2010; Kimes *et al.*, 2012; Ushijima *et al.*, 2016).

Besides, Galloway *et al.*, in 2017 stated that MP might have potential negative impacts ranging from subcellular modifications to the malfunction of entire ecosystems.

These and other threats have caused a reduction of coral reefs, with about 30 % seriously damaged and predictions indicate that approximately 60 % will be lost by 2030 (Hughes *et al.*, 2003). Studies focused on erosion rates found a loss of carbonate material that represent about 0.5 m of erosion in coral crests by 2100 due to a reduced carbonate production by stressed corals (Harris *et al.*, 2018). The main stress factors will be explained in more detail in the next sections, focusing in the negative effects on coral health.

1.1.2 Global stressors that affect the health of coral reefs

Current global warming induced by the addition of anthropogenic-produced greenhouse gases to the atmosphere impacts both terrestrial and marine ecosystems, reflected in an increment of global average temperatures of ~ 0.2 °C per decade in the last 30 years (Hansen *et al.*, 2006). Global warming leads to high sea surface temperature (SST) that modifies several biological processes from cellular- to ecosystem-scale. For instance, differential gene expression, decreased ocean productivity, altered food web dynamics, reduced abundance of habitat-forming species, changes in species distributions, and incidence of diseases of the marine biota (Hoegh-Guldberg and Bruno, 2010; Vezzulli *et al.*, 2015; Lamb *et al.*, 2018). Corals are particularly sensitive to SST increments because they suffer a disruption of the symbiosis with zooxanthellae (endosymbiotic algae) inducing coral bleaching and affecting the health of the coral due to the absence of these algae that provide nutrients to the host (Pandolfi *et al.*, 2011). Variations in SST also affects the metabolic regulation of microorganisms as bacteria of the genus *Vibrio*, responsible of massive bleaching outbreaks. This involves bacterial penetration and multiplication in the coral epidermal layer and the subsequent production of extracellular peptide toxins that inhibits algal photosynthesis, especially at temperatures above 25 °C (Ben-Haim *et al.*, 2003; Rosenberg *et al.*, 2009; Kimes *et al.*, 2012). As SST increases worldwide, bleaching events are expected to occur not only during summer months, but also more frequent in other seasons and constantly in tropical waters.

A second stressor is the ocean acidification (OA), caused by the increasing atmospheric carbon dioxide (CO₂), whose levels have increased nearly 40 % in the last 250 years (Doney *et al.*, 2009). Current concentration of CO₂ is 384 ppmv (parts per million by volume), while during preindustrial level was of 280 ppmv (Jansen *et al.*, 2007), indicating a substantial increment. The CO₂ reacts with water producing carbonic acid, which dissociates to produce bicarbonate ions and protons. The protons react with carbonate ions producing more bicarbonate ions, reducing the availability of carbonate for biological processes as calcification (Hoegh-Guldberg *et al.*, 2007). This process is performed by several marine animals such as foraminifera, molluscs, crustaceans, echinoderms, corals, etc., to build shells and outer structures. Besides, high CO₂ concentrations reduce seawater pH, increasing dissolved inorganic carbon, also suggested as cause of coral decline (Rosenberg *et al.*, 2007; Doney *et al.*, 2009). OA has a negative effect on coral reefs, decreasing calcification and growth rates

since the production of aragonite (crystalline form of calcium carbonate that corals deposit) is inhibited; therefore, the skeletal density of corals decreases (Cooper *et al.*, 2008). The reduced skeletal density increases erosion rates, making coral reefs more susceptible to storms and favour the action of fish that remove carbonate, both reducing the structural complexity of the ecosystem (Hoegh-Guldberg *et al.*, 2007). Under OA corals might maintain stable growth rates and skeletal density by investing more energy in these processes, but this diminishes for instance, the production of gametes, impairing the sexual reproduction and reducing the larval recruitment and settlement (Szmant and Gassman, 1990; Doropoulos *et al.*, in 2012). However, little is known about responses of organisms, populations, and communities to elevated CO₂, as well as potential adaptations to this condition, which should be a call for research.

Coastal communities have exploited the goods and services provided by coral reefs, influencing the degradation of the natural conditions of this ecosystem, affecting the ecology of the oceans at higher levels, especially in the last 50 years (Pandolfi *et al.*, 2011). Overfishing to fulfil the demand of the growing human population is an additional stressor that affect coral reefs, as well as habitat destruction causing population declines and loss of biodiversity (Hughes *et al.*, 2003; McDevitt-Irwing *et al.*, 2017; Boström-Einarsson *et al.*, 2018). The main impact of overfishing on coral reefs turns around the reduced grazing pressure due to the diminishing abundance of herbivorous fish that graze on algae, causing an increment in the concentration of macroalgae that compete with corals for space (McDevitt-Irwin *et al.*, 2017). Additional negative effects of algae include shading, abrasion, overgrowth, source of potential pathogens, and allelopathy, harmful effects caused by the release of chemical compounds from one organism to another (Rosenberg *et al.*, 2007). Likewise, some algae release dissolved compounds that are detected by bacteria, enhancing their activity and inducing coral mortality (Smith *et al.*, 2006). The habitat destruction caused by human activities as overfishing, tourism, industrialisation, etc., impacts several ecological levels within coral reefs due to the loss of critical resources as food or shelter for other animals (Boström-Einarsson *et al.*, 2018). The habitat loss decrease coral population sizes and fragment them, affecting their adaptation to warmer and more acidic conditions of the water, reducing their capacity to evolve in response to additional stressors (Pandolfi *et al.*, 2011).

Marine ecosystems are threatened by disturbances triggered by human activities that to date, do not show any improvement. As measurements of SST and CO₂ concentrations are still increasing and laws protecting the oceans by controlling sustainable fishing activities are not completely implemented, negative consequences on the health of marine ecosystems will keep increasing in the next decades if human activities are not regulated to mitigate their impact.

1.1.3 Plastic pollution and effects of MP on coral health

Plastic production has increased exponentially since its commercial development in the 1940s due to low cost production, versatility, and multiple applications (Andrady, 2011). In 2012, the global plastic resin production reached 288 million metric tons (MT), an increment of 620 % since 1975 (Jambeck *et al.*, 2015). The huge demand, the production of single-use plastic, the lack of awareness for the responsible purchase of plastic, and low recycling rates,

produce an accumulation of plastic debris worldwide in terrestrial and aquatic environments. Plastic pollution was first reported in the early 1970s in the North Atlantic Ocean (Carpenter and Smith, 1972; Colton *et al.*, 1974) and calculations indicated that 4.8 to 12.7 million MT of plastic entered into the ocean in 2010 (Jambeck *et al.*, 2015).

Due to their low density, plastic debris mainly float in the water surface, facing weathering conditions as mechanical abrasion, hydrolysis, biological-, thermooxidative-, and UV radiation-degradation, which fragment the plastic debris into smaller pieces (Andrady, 2011; Galloway *et al.*, 2017). In addition, there are also primary MP used in industrial, domestic, and even medical applications, such as abrasive scrubbers in cleaning products for machinery, body, and also in drug delivery systems, which are likely to be transported in the waste water until they enter aquatic habitats (Browne *et al.*, 2007). Nowadays, plastic litter is classified according to the size: macroplastics > 25 mm, mesoplastics between 5 and 25 mm, microplastics (MP) between 20 μm and 5 mm, and nanoplastics < 20 μm (Wagner *et al.*, 2014). Estimations indicate that MP concentrations have reached 100 000 particles m^3 not only in the water column but also present in marine sediments (Wright *et al.*, 2013). Most MP are found in the water column or floating in the water surface and may be dispersed over long distances by oceanographic currents, but MP might also sink to the seabed, accumulating and being in contact with sessile organisms, which threatens the marine ecosystems (Andrady *et al.*, 2011; Carson *et al.*, 2013; Wright *et al.*, 2013). Galloway *et al.*, in 2017, suggested that the presence of MP in the ocean might impact negatively all levels of biological organization, from subcellular changes in gene expression or enzyme activities to malfunctions of entire ecosystems and community shifts within them.

In recent years an increasing number of negative impacts have been proved for the presence of MP in fresh water and marine ecosystems. MP are dangerous particles *per se* since during the plastic production several toxic compounds and monomers are added to their surfaces. Some of the contaminants are antioxidants (nonylphenol), catalysts (organotin), flame retardants (polybrominated diphenyl ethers), bisphenol A (BPA), antimicrobials (triclosan), and phthalate plasticizers. Plastics also act as sinks and vectors of toxic chemicals accumulating intermediate compounds from partial degradation (styrene and aromatic compounds), hydrophobic organic chemical (HOC), persistent organic pollutants (POPs), polychlorinated biphenyls (PCBs), and dioxins, absorbed and concentrated on MP (Mato *et al.*, 2001; Browne *et al.*, 2007; Andrady, 2011; Engler 2012; Rochman, 2015; Koelmans *et al.*, 2016). These toxic compounds are slowly leached from the MP surface to the seawater reaching low concentrations. However, the real ecological risk is that these toxic compounds are several orders of magnitude more concentrated on MP than in the seawater and might enter easily to animals through MP ingestion, bio-accumulated, and transferred in the food web (Browne *et al.*, 2013; Koelmans *et al.*, 2016). In the last years the MP ingestion by marine biota has been widely documented, becoming an important topic in marine ecology since it has been reported in all trophic levels of the food web: zooplankton, molluscs, fish, turtles, birds, and mammals (Cole *et al.*, 2011; Carson, 2013; Cole *et al.*, 2013; Lusher *et al.*, 2013; Wright *et al.*, 2013, Setälä *et al.*, 2014; Gall and Thompson, 2015; Nelms *et al.*, 2018; Duncan *et al.*, 2019).

Scleractinian corals confused MP during prey detection, capturing and ingesting these particles, leading to an accumulation of MP in their internal tissues (Hall *et al.*, 2015). However, corals can also recognize and reject indigestible material after a prior ingestion and retention of the particles as observed in *Montastraea cavernosa*, *Orbicella faveolata*, and other species of reef-building corals (Hankins *et al.*, 2018; Reichert *et al.*, 2018). Additional factors were evaluated to elucidate the driving elements that stimulate MP ingestion. Allen *et al.*, in 2017, suggested that MP consumption may be influenced by phagostimulents present on MP surfaces that could be recognized by chemoreceptors of corals. Recently, additional studies were conducted in order to determine the effect and responses of corals after MP exposure. For instance, Chapron *et al.*, (2018) showed that MP exposure reduced skeletal mineralization and growth rates of the deep water reef-building coral *Lophelia pertusa*. During MP exposure, species-specific responses such as MP retention in the mucus layer, ingestion, egestion, tissue overgrowth, bleaching, or necrosis of tissues were observed in six species of small-polyp stony corals: *Acropora humilis*, *Acropora millepora*, *Pocillopora verrucosa*, *Pocillopora damicornis*, *Porites lutea*, and *Porites cylindrica* (Reichert *et al.*, 2018). These responses were observed in experiments performed in the CEMarin aquarium system, the same where the experiments of the present study were carried out.

The main global stressors that affect marine environments and corals are depicted in the Fig. 1, especially the plastic pollution and the negative effects of MP on coral health. Despite the growing evidence of this phenomenon, the processes and participants (viruses, archaea, bacteria, fungi, algae, and/or protozoans) involved in the coral responses to MP ingestion and exposure are still unknown. However, most of the studies have been focused on the bacterial communities that colonise MP, suggesting that they are key players in the interaction between MP and corals, and the observed responses.

1.1.4 Influence of global stressors on coral diseases induced by bacteria

Global stressors as high SST, OA, overfishing, and water pollution reduce the ability of corals to regulate its own microbiome or exclude invasive bacterial taxa from the surrounding environment, leading to infection and disease events. The bacterial communities of stressed corals show higher richness and diversity for members of potential pathogenic taxa as *Cyanobacteria*, *Flavobacteriales*, *Rhodobacterales*, and *Vibrionales*, which tend to be overrepresented, while symbionts as *Endozoicomonas* tend to be underrepresented (Pantos *et al.*, 2003; Meyer *et al.*, 2015; McDevitt-Irwin *et al.*, 2017). However, exceptions occur depending on the studied coral species, sampling and analysis methods, locations, and environmental conditions. Thurber *et al.*, in 2009 evaluated structural and functional changes of the coral microbiome in presence of four local stressors: increased temperature, elevated nutrients, dissolved organic carbon (DOC) loading, and reduced pH were evaluated. These stressors increased the number of bacterial genes involved in virulence, stress resistance, sulphur and nitrogen metabolism, motility, chemotaxis, etc. Increments in bacterial richness and diversity of certain bacterial groups and the expression of virulence factors, indicates a malfunction of the microbiome's ability to auto-regulate its own composition affecting its metabolic activity and threatening the overall health of the holobiont.

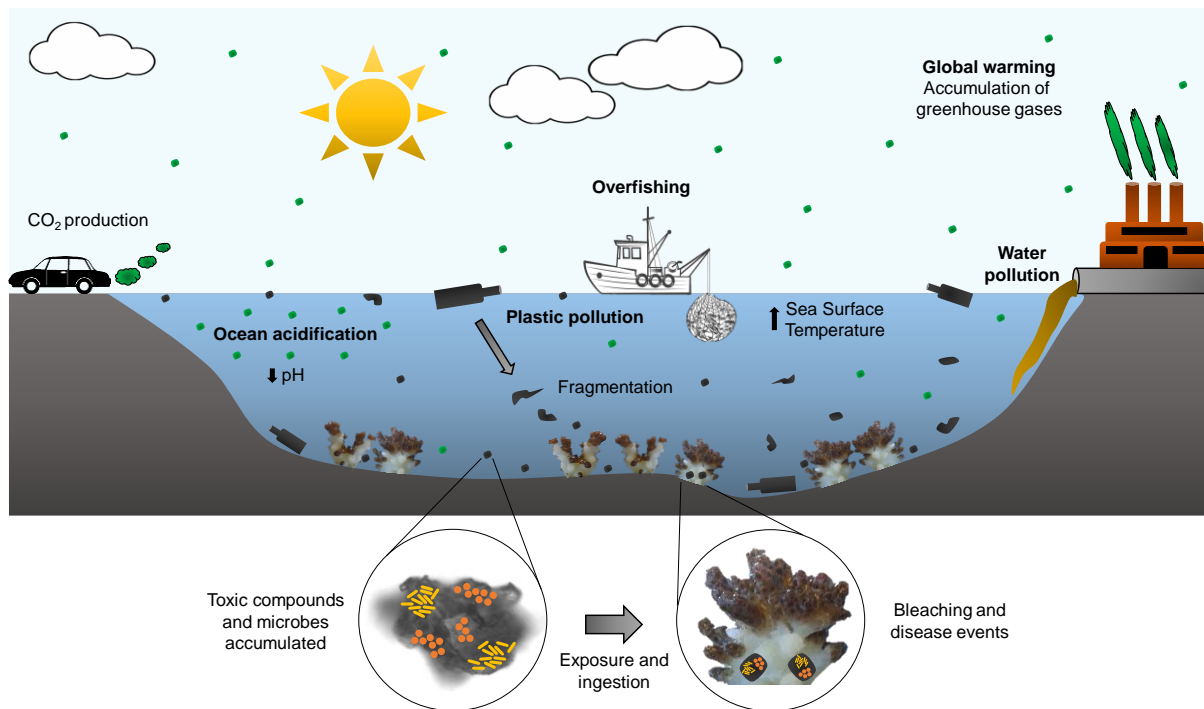


Fig. 1: Main stressors (bold) and their effects on marine environments and coral reefs. Rising concentrations of greenhouse gases increase SST, as well as CO₂ affect the chemical conditions of the seawater inducing OA. Overfishing disturbs fish populations that control the proliferation of algae that compete with corals for space. Water pollution with toxic waste and plastic debris impacts the marine biota. MP, result of the fragmentation of larger particles, accumulate toxic compounds and are colonised by microbes, which might affect coral health after exposure and ingestion of MP.

Vibrio is an important genus in marine ecosystems that includes several potential pathogenic species acting as single etiologic agents or being part of a consortium that triggers the diseases in marine animals (Thompson *et al.*, 2004a, Thompson *et al.*, 2005a; Cervino *et al.*, 2008; Kimes *et al.*, 2012; Ushijima *et al.*, 2014; Wang *et al.*, 2015; Kemp *et al.*, 2018). The infections occur through the expression of certain virulence genes, which are highly regulated by quorum sensing systems, and therefore, by the cell density, but also by environmental conditions as observed in strains of *Vibrio coralliilyticus* (Kimes *et al.*, 2012; Liu *et al.*, 2018). Virulence factors involved in motility, host degradation, antimicrobial resistance, and transcriptional regulation, are upregulated at water temperatures above 27 °C (Kimes *et al.*, 2012).

Besides the genus *Vibrio*, environmental conditions induce changes in the composition of other bacterial groups and disturbances in the coral microbiome, often related to the appearance of diseases as white plague disease (WPD) or black band disease (BBD), caused by polymicrobial consortiums (Cárdenas *et al.*, 2011). WPD-consortiums are generally dominated by members of the *Cytophaga–Flavobacterium–Bacteroides* complex, *Neisseriales*, *Rickettsiales*, *Vibrionales*, and families *Alteromonadaceae* and *Rhodobacteraceae*, while a *Cyanobacteria*-dominated microbial mat with sulphur-cycling

bacteria and MRC members dominate BBD-consortiums (Sekar *et al.*, 2008; Sunagawa *et al.*, 2009; Miller *et al.*, 2011; Garcia *et al.*, 2013; Meyer *et al.*, 2016; Sato *et al.*, 2016).

MRC contains species that play important roles for the global carbon and sulfur cycles, as well as pioneer colonisers of surfaces and potential pathogens (Boettcher *et al.*, 2005; Buchan *et al.*, 2005; Wagner-Döbler and Biebl, 2006). Therefore, the hypothesis of MP as vectors that transport non-native and potential pathogenic bacteria into internal animal tissues starts playing a role. MRC members have been detected in high abundances on MP, also observed for *Alteromonadaceae* or *Vibrionaceae* (Zettler *et al.*, 2013; De Tender *et al.*, 2017b; Frère *et al.*, 2018). Algae are also important members of microbial communities on MP, as observed in scanning electron microscopy (SEM) micrographs (Zettler *et al.*, 2013; De Tender *et al.*, 2017b). Exudates produced by algae are rich in dissolved neutral sugars that stimulate fast-growing bacteria as members of *Pseudoalteromonadaceae*, *Erythrobacteraceae*, *Hyphomonadaceae*, or *Vibrionaceae*, which also carry several virulence factors (Nelson *et al.*, 2003). Other taxa that also contain potential pathogens found on MP are *Aeromonas*, *Arcobacter*, *Campylobacteraceae*, *Leptolyngbya*, *Phormidium*, *Pseudomonas*, *Tenacibaculum*, etc. (McCormick *et al.*, 2014; Oberbeckmann *et al.*, 2016; Dussud *et al.*, 2018b). The cell density of these potential pathogens on MP, likely forming biofilms, are higher than in the water column. This promotes the expression of virulence factors through regulation mechanisms as quorum sensing that might be one of the reasons of the health condition impairment of corals once the MP have reach and colonised internal tissues.

The influence of water temperature in the regulation of virulence genes and the structure of the populations of *Vibrio* and other genera of the coral microbiome, indicates an increasing relevance of global warming-associated stressors on the health of marine ecosystems (Vezzulli *et al.*, 2010; Tout *et al.*, 2015b). As warmer water temperatures are becoming more frequent in all latitudes due to high SST as consequence of the climate change, it is expected that potential pathogens as *Vibrio* spp. infect corals causing multiple diseases. Although these stressors disrupt the coral-bacteria interactions affecting the health of the holobiont, native bacterial communities are essential for the health of the coral. These communities participate in processes that lead to resilience even under adverse environmental conditions, decreasing the negative impacts on the reef ecosystem.

1.1.5 The importance of bacteria-coral interactions

Most bacteria are found mainly in open ocean waters and oceanic surfaces, with 1.2×10^{29} and 3.5×10^{30} cells, respectively (Whitman *et al.*, 1998). McDevitt-Irwin *et al.*, in 2017, provided an overview of the number of bacterial operational taxonomic units (OTUs) found in different organisms that inhabit coral reefs. Bacterial OTUs are groups of organisms clustered according to their DNA sequence similarity, normally 97 % based on the 16S rRNA gene. The number of OTUs ranged from 10^2 to 10^4 in corals and in sediments and tropical reef water column from 10^3 to 10^5 , indicating the ubiquity of bacterial communities in the ocean.

Corals are complex metaorganisms in a close relationship with *Symbiodinium*, a dinoflagellate that secretes photosynthesis products to the coral, producing up to 95 % of the coral's energy requirements, allowing them to thrive in nutrient-poor waters (Muscattine *et al.*, 1981; Burriesci *et al.*, 2012; Krediet *et al.*, 2013). The corals also keep a close symbiosis with its microbiome, which includes viruses, archaea, bacteria, fungi, protists, and other algae, all in a delicate balance that collectively constitute the coral holobiont (Rosenberg *et al.*, 2007; Ainsworth *et al.*, 2009; Blackall *et al.*, 2015). However, questions as when and how the corals get their microbiome, especially the bacterial component, are still matter of research. Blackall *et al.*, suggested in 2015 that bacteria (primarily members of *Alphaproteobacteria*) are inherited mainly horizontally from adult corals to their planula larvae or in postsettlement stages. Vertical heritance has been also observed in less extent, where chemotaxis or quorum sensing favour this transfer of bacteria (Ransome *et al.*, 2014; Tout *et al.*, 2015a).

Corals provide several internal and external habitats for microbe colonisation, scleractinian corals for instance, are compartmentalized in mucus, tissue, and skeleton. It has been proven that bacterial assemblages differ in community composition, richness, and response to host and environmental variables according to the compartment they inhabit (Blackall *et al.*, 2015; Zhang *et al.*, 2015a; Bourne *et al.*, 2016; Pollock *et al.*, 2018). Likewise, corals can harbour particular species-specific bacterial communities that might be disturbed even by small changes in the surrounding environmental conditions (Vega-Thurber *et al.*, 2009; Sunagawa *et al.*, 2010). On the other hand, reports also indicate that even under the adverse conditions propitiated by humans, corals will change rather than disappear, since some species tolerate climate change conditions better than others, likely due to a joint action of the coral and its bacterial communities, leading to a higher ecological success (Hughes *et al.*, 2003).

The physiology of the hosts is also improved by the distribution of functions within the members of the microbiome depending on the specific compartments that bacteria colonise (Ainsworth *et al.*, 2016). It has been proposed that corals have i) a ubiquitous core microbiome with bacteria present in all corals even from separated geographical habitats; ii) a core microbiome with regional-bacterial members, and iii) a highly diverse bacterial community (Ainsworth *et al.*, 2015; Hernandez-Agreda *et al.*, 2016). These bacterial members of the microbiome enhance the health, resilience, and disease resistance of the holobiont and have been named “beneficial microorganisms for corals” (BMC) (Reshef *et al.*, 2006; Rosenberg *et al.*, 2007; Vega-Thurber *et al.*, 2009; Krediet *et al.*, 2013; McDevitt-Irwin *et al.*, 2017; Peixoto *et al.*, 2017). BMC contribute to nutrient acquisition and nitrogen, carbon, sulphur, and phosphorous fixation or cycling for the coral and *Symbiodinium* (Raina *et al.*, 2009; Sellstedt and Richau, 2013; Zhang *et al.*, 2015b; Bourne *et al.*, 2016; Hernandez-Agreda *et al.*, 2016). Members of genera *Halomonas* or *Endozoicomonas*, some of the main symbionts of healthy corals, help to prevent mitochondrial dysfunction, promote gluconeogenesis, transport proteins and carbohydrates to the host, and protect *Symbiodinium* from pathogens as *Vibrio* spp. (Pantos *et al.*, 2015; Ding *et al.*, 2016; Neave *et al.*, 2017; Quintanilla *et al.*, 2018). Health condition is also stimulated by the production of antimicrobial compounds that prevent invasion of potential pathogens, exogenous bacteria, fungi, and algae, as well as the increment of opportunist bacteria (Ritchie, 2006; ElAhwany *et al.*, 2013; Raina *et al.*, 2016). Coral-associated bacteria

are also able to exclude potential pathogenic bacteria from the host surfaces and disrupt quorum sensing by producing inhibitory compounds (Alagely *et al.*, 2011; Krediet *et al.*, 2013).

Corals can adapt quickly to changing environmental conditions as high temperatures or even develop resistance to specific pathogens by altering their own population of symbiotic bacteria within the holobiont (Brown *et al.*, 2000; Reshef *et al.*, 2006). This bacteria-mediated resistance and tolerance led to propose the “coral probiotic hypothesis” where compounds produced by a renovated coral-associated bacterial community lysed the cells of the pathogen *V. shilonii* that had induced bleaching in previous experiments (Reshef *et al.*, 2006). Several studies support this hypothesis by showing experience-mediated tolerance to bleaching, antagonism within members of the microbiome, or coral species no longer susceptible to pathogens previously identified as etiological agents of diseases (Brown *et al.*, 2000; Richardson and Aronson, 2002; Rypien *et al.*, 2010; Ainsworth and Gates, 2016).

Coral-associated bacteria participate in diverse processes that regulate the holobiont’s health during all the stages of development. The bacterial component of coral microbiomes is fundamental for the resilience of single organisms and hence of the whole reef ecosystem, as they can buffer the cumulative environmental impacts and pressures. Disturbances in this interaction affect not only the fitness, stability, and functioning of coral reefs but also their responses to environmental pressures resulting, for example, in coral disease outbreaks.

1.2 Knowledge gaps and objectives

The bacterial component of the coral holobiont have received increasing attention since 2001 when Rohwer *et al.*, used cultivation-dependent and -independent methods to describe bacterial communities associated to *Montastraea franksi*. From then on, hundreds of studies have been performed to characterise bacterial communities of coral holobionts from different geographical locations, as well as disturbances caused by global warming stressors or diseases. In the last decades, the negative impacts of the plastic pollution in marine ecosystems have been evaluated, mainly the threats represented by entanglement of animals with fishing gear and plastic ropes and the ingestion of plastic debris by fish, birds, reptiles and mammals. However, to date, few studies have integrated corals into these analyses, becoming increasingly important since recent reports indicated that corals can ingest MP, entering the food web.

In the last decade, several studies have investigated the composition and diversity of the bacterial assemblages growing on MP and the differences induced by environmental conditions, geographical locations, or plastic material in open waters and artificial marine systems. Likewise, due to the buoyancy characteristics of MP, it has been suggested that this particles transport non-native and potential pathogenic bacteria among ecosystems by the action of sea currents, as well as potential plastic-degrading bacteria.

Even though in the last years numerous studies have deciphered the role of bacteria in certain corals diseases, several phenomena are still unclear. For instance, how corals get the bacterial communities that trigger diseases, the environmental conditions that favour the presence of these bacterial groups, the different stages of the infection process, etc. Most of the studies have used culture-independent techniques to compare the bacterial communities of healthy and diseased corals to identify candidate bacterial groups or etiological agents involved in the diseases' development. However, most of these studies have ignored cultivation-based approaches, which have been scarcely evaluated, even though the study of bacterial isolates can provide the physiological and metabolic characteristics of the isolated bacteria, allowing infection and ecotoxicology assays, the study of the genomes, etc.

Despite the growing evidence regarding the adverse effects of MP ingestion and exposure to coral health and the roles that bacteria play in coral diseases, the question whether the MP *per se* or the MP-associated microbes (viruses, archaea, bacteria, fungi, algae, and/or protozoans) are responsible of the disease outbreaks observed in corals exposed to MP has not been fully addressed. This is the first time that MP-associated bacterial communities are investigated as the factor that link the MP presence in marine systems with the impairment of coral health evidenced by coral bleaching, tissue loss, and development of diseases worldwide.

Under the consideration of these knowledge gaps, this thesis is focused on one main and three specific objectives aimed to provide a better understanding of the bacterial assemblages able to colonise PE-MP present in the CEMarin aquarium system, as well as their potential effects on coral health.

Main objective:

- (1) To investigate by cultivation-dependent and -independent approaches the composition and structure of bacterial assemblages on MP, sandy sediments, detritus, and present in the > 5µm, the 0.22-5µm, and the total water fractions of the marine system and the most relevant genera associated to MP.

Specific objectives:

- (1) To investigate the diversity of the strains belonging to the genus *Vibrio* from the marine system through a deep taxonomic and genotypic analysis and assess its relevance as potential coral pathogens.
- (2) To detect putative genes involved in the biodegradation of complex polymers and pathogenicity in the most abundant strains isolated from MP by total genome sequencing and comparative genomics.
- (3) To obtain a strain collection from the most abundant particle- and water-associated heterotrophic bacteria from the marine system and by means of the polyphasic taxonomy describe new bacterial species.

1.3 Hypothesis

Lamb *et al.*, in 2018 associated the increment of health impairment observed in 159 coral reefs from the Asia-Pacific region to the contact of these corals with plastic waste. These debris are hazardous due to its chemical constituents and compounds accumulated and absorbed from the environment and the non-native microbial communities carried by the debris that can be ingested by corals and other marine animals (Hall *et al.*, 2015; Allen *et al.*, 2017).

Given the mentioned lack of knowledge and the observations from previous studies (Lamb *et al.*, 2018; Reichert *et al.*, 2018), two hypotheses were formulated on which this study is based: (i) the composition of the bacterial assemblages developed on MP differ from the composition of those formed on the natural particles of the same marine system and (ii) the health impairment of corals registered worldwide due to plastic debris exposure is, to a certain extent, influenced by the non-native bacteria present on these particles.

Then, MP might act as vectors that promote the invasion of non-native and potential pathogenic bacteria that require a minimum number of cells to infect internal tissues of the host and express pathogenicity genes (e.g. *Vibrio* spp. and other potential pathogenic species), leading to disturbances of the holobiont's natural microbiome altering its physiology, and/or triggering disease outbreaks (Fig. 2).

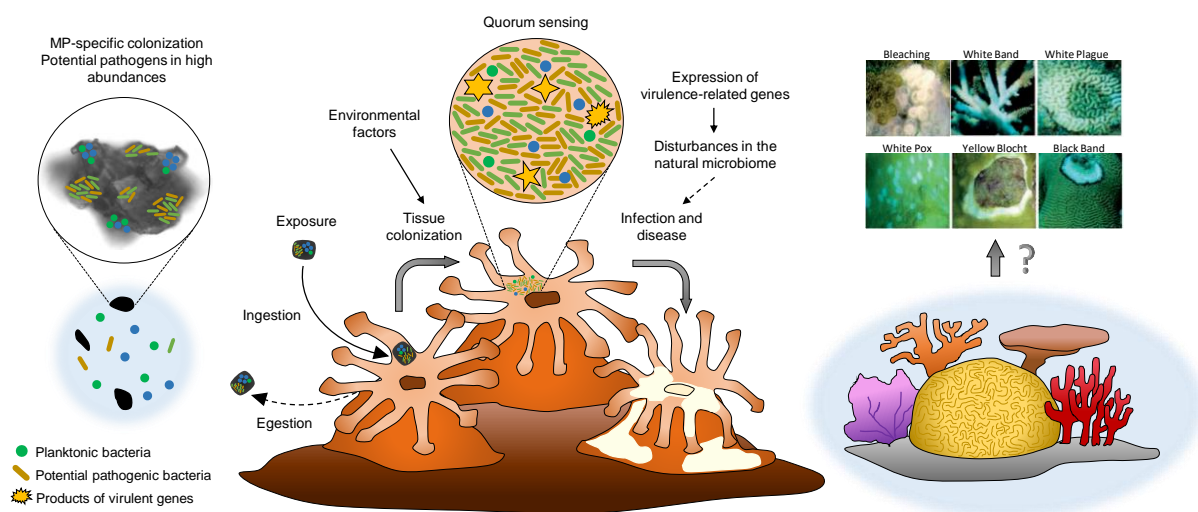


Fig. 2: Graphical hypothesis of MP as vectors involved in the coral health impairment. MP are colonised by specific bacterial assemblages including pathogenic bacteria, whose abundances may be higher compared to those in the water column. Corals exposed to MP might ingest these particles transferring non-native bacteria into internal tissues altering the native microbiome of the holobiont. Once in the tissues, and depending of environmental conditions, bacteria from the non-native communities can reach high densities. At high densities, quorum sensing systems are activated regulating the expression, among others, of pathogenicity genes, whose products (toxins, enzymes, virulence factors, etc.) affect *Symbiodinium* inducing bleaching, as well as other diseases where bacteria as *Vibrio* spp. play pivotal roles. Photographs of diseased corals were taken from Rosenberg *et al.*, 2007.

CHAPTER II

2. Background

2.1 The prokaryotic life on microplastics in marine environments

2.1.1 Bacterial colonisation of surfaces and biofilm formation

Bacteria thrive in both the sunlit surface layer and in the dark waters of the ocean in two different lifestyles, either as planktonic (free-living) or surface-associated (biofilm-forming) cells. In marine waters, innumerable types of biotic and abiotic surfaces exist that are rapidly colonised by bacteria forming biofilms. This colonisation might be influenced by characteristics of the surfaces as pigment content, absorbed chemicals, and pollutants (De Tender *et al.*, 2015). The interaction between bacteria and surfaces also depend in great extent on the physicochemical and biological properties of the substratum, such as hydrophobicity, roughness, microtopography, vulnerability to wear, nutrients availability, accumulation of organic molecules, among others (Palmer *et al.*, 2007). All these surface properties may then explain the differences found in bacterial assemblages associated to plastic debris and natural surfaces (Oberbeckmann *et al.*, 2014; Dussud *et al.*, 2018a; Oberbeckmann *et al.*, 2018).

The first steps of bacterial surface colonisation start with the accumulation and adsorption of diverse organic and inorganic molecules on any submerged surface. These molecules might be sensed by bacteria that eventually attach to those surfaces to initiate the biofilm formation (Dang and Lovell, 2000). Bacteria can also recognize specific conditions of the microenvironment (redox potential, degradable substrates, and electron donors and acceptors) responding and adapting to them through sensing and communication mechanisms. These communication mechanisms include two-component signal transduction systems, chemotaxis, quorum sensing, posttranscriptional regulation by small RNAs, or regulation by second messengers as cyclic di-GMP (c-di-GMP) (Szurmant and Ordal, 2004; Ng and Bassler, 2009; Capra and Laub, 2012; McDougald *et al.*, 2012; Chambers and Sauer, 2013; Römling *et al.*, 2013; Dang and Lovell, 2016; Flemming *et al.*, 2016).

Once bacteria detect appropriate conditions of a surface, the biofilm formation starts (Fig. 3). Pioneer species or primary colonisers sense environmental cues on the surfaces and attach to the surface forming a bacterial monolayer by cell division, modifying the characteristics of the surface by production of biopolymers (exopolysaccharides), shaping the surface suitable (or unsuitable) for subsequent colonisation (O'Toole *et al.*, 2000). Additional cells of pioneer species are recruited to the growing biofilm, as well as secondary colonisers might interact with them, resulting in a primary biofilm community and the development of microcolonies (O'Toole *et al.*, 2000; Dang and Lovell, 2016). Synergic and competitive interactions among the biofilm members and the recruitment of additional bacterial colonisers, as well as the loss of others, are complementary steps involved in the maturation of biofilms (Flemming *et al.*, 2016). Availability of N, P, and Fe, may induce surface-adapted lifestyles or trigger dispersive behaviours of cells from established biofilms towards more favourable

surfaces to colonise (Tang and Grossart, 2007; Kim *et al.*, 2009). The biofilm formation stages are regulated by quorum sensing and other type of cell-cell communication mechanisms, making any surface “hot spots” of microbial activity (O’Toole *et al.*, 2000; Labbate *et al.*, 2004; McDougald *et al.*, 2012). As in biofilms bacterial cells are spatially close to each other, interactions among them favour genetic exchange, metabolic cooperation, and community responses, making biofilms cooperative consortiums formed by one or multiple species (Ng and Bassler, 2009; Burmølle *et al.*, 2014; Claessen *et al.*, 2014; Flemming *et al.*, 2016). Biofilms are survival mechanism that provides advantages such as greater access to nutritional resources, environmental stability, protection against predators, viruses, antibiotics, toxins, UV radiation, and deleterious environmental pressures (McDougald *et al.*, 2012; Salta *et al.*, 2013; Dang and Lovell, 2016).

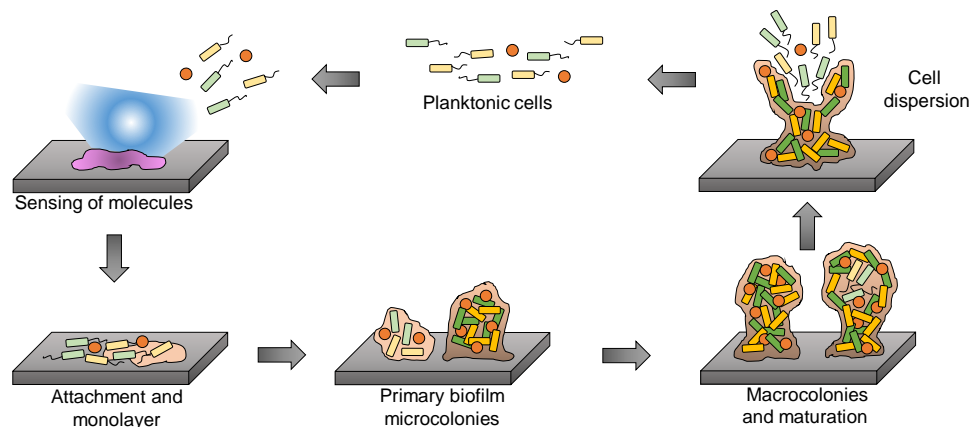


Fig. 3: Stages of biofilm formation. Planktonic cells interact with surfaces after recognizing cues on their surfaces. Following the attachment, cell-to-cell interactions in the monolayer induce the formation of microcolonies, which mature into macrocolonies where cells are differentiated. Environmental conditions trigger the dispersion of cells from the biofilms that return to a planktonic lifestyle.

Polar holdfast structures as stalks or prosthecae are produced by several marine bacteria, such as members of the marine *Roseobacter* clade (MRC), to facilitate colonisation of surfaces (Dang and Lovell, 2016). The expression of these structures is regulated by the contact with a surface or other bacteria, specific environmental conditions, or the internal physiological status (Langille and Weiner, 1998; Heindl *et al.*, 2014). These structures offer competitive advantages over other bacteria, as more efficient surface colonisation during early stages of biofilm formation on biotic and abiotic surfaces. Evidence indicates that these bacterial biofilms that colonise natural and artificial surfaces in the ocean have additional impacts in biological interactions. For instance, these biofilms influence the recruitment, settlement, and/or metamorphosis of corals and other marine invertebrates through the production of chemical cues recognized by their larvae (Chung *et al.*, 2010; Tebben *et al.*, 2012; Sharp *et al.*, 2015; Franco *et al.*, 2019).

2.1.2 Bacterial communities on MP surfaces

In the last years, ecological consequences derived from plastic debris and MP in marine and freshwater environments have been widely documented. For instance, the effects of debris

ingestion by animals (Andrady *et al.*, 2011; Carson, 2013; Cole *et al.*, 2013; Wright *et al.*, 2013; Hall *et al.*, 2015), the occurrence of MP in rivers and lakes (McCormick *et al.*, 2014), or the plastic-associated toxins and their impact on the food web (Mato *et al.*, 2001). Microorganisms play key roles in aquatic environments in nutrient cycling and primary production, being the base of food web and pioneer surface colonisers, which can easily adapt to new emerging habitats as plastics (Dang *et al.*, 2008; Harrison *et al.*, 2014). Law *et al.*, for instance, reported in 2010 a plastic debris concentration up to 5×10^5 pieces/km² in the North Atlantic Subtropical Gyre. Some marine bacteria can produce adhesion structures as pili, fimbriae, flagella, curli, stalks, or prosthecae that facilitate attachment to particles as plastic debris, which represent advantages as increased nutrient uptake, genetic transfer, enzymatic activity, or biofilm formation, over other bacteria (Zettler *et al.*, 2013; Dang and Lovell, 2016; Dussud *et al.*, 2018b; Oberbeckmann *et al.*, 2018).

To characterise this new habitat, Zettler *et al.*, (2013) introduced the term “plastisphere”, which is the habitat where microbial communities formed by heterotrophs, autotrophs, predators, symbionts, and pathogenic organisms coexist. These microbial communities have been studied by 16S rRNA gene-based fingerprinting and other molecular-based methods, reflecting diverse and specific microbial assemblages compared to the surrounding water and other natural particles (Zettler *et al.*, 2013; Oberbeckmann *et al.*, 2016; De Tender *et al.*, 2017a; Oberbeckmann *et al.*, 2018). Microscopy techniques such as scanning electron microscopy (SEM) or catalysed reporter deposition fluorescence in situ hybridization (CARD-FISH), have been also used to characterise bacterial communities on plastic debris (Carson *et al.*, 2013; Harrison *et al.*, 2014; McCormick *et al.*, 2014; Reisser *et al.*, 2014; Wagner *et al.*, 2014; Van Cauwenberghe *et al.*, 2015).

Evidence indicates that the composition of bacterial communities on MP differs according to the plastic material, geographical location, environmental conditions, among others; however, they share, in certain extent, a common core bacteriome. This includes members of *Rhodobacteraceae*, *Alteromonadaceae*, *Pseudoalteromonadaceae*, *Flavobacteriaceae*, *Erythrobacteraceae*, *Saprospiraceae*, *Sphingomonadaceae*, *Hyphomonadaceae*, *Vibrionaceae*, *Verrucomicrobiaceae*, *Flammeovirgaceae*, and the JTB255 marine benthic group (Zettler *et al.*, 2013; Oberbeckmann *et al.*, 2016; De Tender *et al.*, 2017a; De Tender *et al.*, 2017b; Dussud *et al.*, 2018b; Frère *et al.*, 2018; Oberbeckmann *et al.*, 2018; Keszy *et al.*, 2019). Likewise, some studies have stated that MP are a new kind of surface in the aquatic systems that may act as vectors for the dispersal of pollutants (nonylphenol and phenanthrene) and additives (Triclosan), as well as non-native microbes, and potential bacterial pathogens for the marine wildlife and humans as well, such as members of genera *Pseudomonas*, *Staphylococcus*, *Vibrio*, *Tenacibaculum*, *Phormidium*, among others (Browne *et al.*, 2013; Zettler *et al.*, 2013; Oberbeckmann *et al.*, 2014; Wagner *et al.*, 2014; Keswani *et al.*, 2016; Kirstein *et al.*, 2016; Dussud *et al.*, 2018b). However, this is actively discussed, since other studies have shown that the abundance of pathogenic bacteria as *Vibrio* spp. on the surface of MP is not particularly high compared to other samples and there are no clear proofs of diseases caused by MP-transmitted *Vibrio* spp. (Van Cauwenberghe *et al.*, 2015; Oberbeckmann *et al.*, 2016; Dussud *et al.*, 2018b; Jacquin *et al.*, 2019).

Bacteria on MP might be transferred from the surface of the particles into the tissues of eukaryotic organisms after ingestion or during exposure and accumulated in the marine food web starting with the zooplankton (Karjalainen *et al.*, 2005, Setälä *et al.*, 2014). Likewise, bacteria present on MP could lead to disease events through production of toxins and the expression of virulence factors, some of them influenced by environmental conditions as water temperature, as determined for the coral pathogen *Vibrio coralliilyticus* (Kimes *et al.*, 2012; Vezzulli *et al.*, 2015; Ushijima *et al.*, 2016). Then, these genes might be involved in the emergence of disease outbreaks observed worldwide and especially in temperate regions as response of climate change, causing the disruption of the balance and composition of the native bacterial communities associated to corals and other animals (Baker-Austin *et al.*, 2012).

As some bacterial groups are able to degrade plastic polymers and use them as source of energy, studies have also focused on the polymer degradation by bacteria on MP. Evidence indicate that taxa *Actinobacteria*, *Burkholderiales*, *Sphingomonadales*, *Rhodobacteraceae*, *Flavobacteriaceae*, *Cryomorphaceae*, *Hyphomonadaceae*, *Saprospiraceae*, *Alteromonadaceae*, or *Erythrobacteriaceae*, are associated with natural organic polymers and contain hydrocarbonoclastic bacteria (Dang and Lovell, 2016; Oberbeckmann *et al.*, 2016; Dussud *et al.* 2018a; Oberbeckmann *et al.*, 2018; Ogonowski *et al.*, 2018; Curren and Leong, 2019). These bacteria have the metabolic potential to induce chemical changes in the polymer chains by the expression of diverse enzymes as lipases, depolymerases, esterases, proteinases, ureases, dehydratases, or hydrolases, involved in the breakdown of complex polymers (Pathak and Navneet 2017; Morohoshi *et al.*, 2018; Urbanek *et al.*, 2018; Jacquin *et al.*, 2019). Despite this increasing information regarding polymer-degrading bacteria, more studies should be performed in order to use these bacteria in biodegradation and bioremediation approaches oriented to mitigate the plastic pollution.

The effects of MP-associated bacteria on the health of marine ecosystems and their wildlife need to be further investigated. An appropriate target might be the study of infective processes caused by the pathogenic members of the genus *Vibrio*, which are responsible of disease outbreaks observed in coral reefs, mainly at high latitudes in response to ocean warming as seen by Rubio-Portillo *et al.*, in 2018. As response to this need and instead of more descriptive molecular-based studies, the present study also comprises the isolation of MP-associated bacteria in order to unveil their influence on the impairment of coral health. However, detailed ecotoxicology studies with these bacteria, an especially *Vibrio* strains, in regards to their virulence on corals and other animals should be performed.

2.2 The genus *Vibrio* is a common member of marine environments

2.2.1 The genus *Vibrio*, a ubiquitous and pathogenic genus in the ocean

Vibrio is one of the largest bacterial genera cultured from a broad range of aquatic ecosystems worldwide, from brackish to deep-sea water (Colwell, 2006; Thompson *et al.*,

2004a). *Vibrio* spp. are heterotrophic bacteria found as planktonic cells in water columns in concentrations ranging from 10^2 to 10^4 *Vibrio* spp. cells per mL and 10^1 to 10^3 colony forming units (CFU) per mL seawater, as calculated by qPCR and CFU counting on TCBS, respectively (Thompson *et al.*, 2005a; Kemp *et al.*, 2018). The occurrence of members of this genus depends on the temperature, salinity, and nutrient availability of the water, showing a seasonal variability that shape the structure and diversity of the communities. Therefore, the abundance of *Vibrio* spp. is higher in tropical regions and in seasons with warm-waters at high latitudes (Thompson *et al.*, 2004b; Tout *et al.*, 2015b; Rubio-Portillo *et al.*, 2018). The ability to use a wide variety of carbon and nitrogen sources, as well as diverse adaptation strategies depending on their lifestyle explain their success in diverse aquatic niches (Chimetto *et al.*, 2008; Payne *et al.*, 2016). Members of the genus *Vibrio* have been found in high abundances associated to sediments, plankton, algae, seagrass, aquatic animals, and even on artificial surfaces as plastics or glass (Heidelberg *et al.*, 2002; Vandenberghe *et al.*, 2003; Thompson *et al.*, 2004a; Oberbeckmann *et al.*, 2016; Zettler *et al.*, 2013). *Vibrio* spp. are able to form biofilms on submerged surfaces, inducing communal behaviours regulated by specialized cell-to-cell communication systems as quorum sensing, providing several advantages compared to other bacteria inhabiting the same aquatic environments (McDougald *et al.*, 2006; Liu *et al.*, 2018).

One additional key aspect of the genus *Vibrio* is that it harbours several potential pathogenic species, which cause diseases to vertebrate and invertebrate marine animals as corals, bivalves, shellfish, fish, other animals of the aquaculture industry, and mammals including humans (Ben-Haim *et al.*, 2003; Austin and Zhang, 2006; Vezzulli *et al.*, 2010, Roth *et al.*, 2012; Wang *et al.*, 2016). Diseases on marine animals caused by members of the genus are increasing worldwide and are linked to the expression of a broad set of virulence-related pathogenicity genes, which seems to be an ancestral trait within certain *Vibrio* clades and might be exchanged between members of the genus (Bruto *et al.*, 2018).

Tout *et al.*, (2015b) documented an increment in four orders of magnitude of the abundance of *Vibrio* spp. and other potential pathogens over the native coral-associated bacteria, as well as its physiological activity, which was caused by heat stress. In natural conditions the microbiome regulates the populations of these potential pathogens, but at high abundances, bacteria may become causative agents of coral diseases: bleaching, yellow band disease, *Montipora* white syndrome, *Porites* white patch syndrome, etc. (Ben-Haim *et al.*, 2003; Rosenberg *et al.*, 2007; Cervino *et al.*, 2008; Ushijima *et al.*, 2012; Ushijima *et al.*, 2014; Séré *et al.*, 2015; Kemp *et al.*, 2018). Evidence indicates that environmental conditions influence the regulation of the expression of pathogenicity-associated genes in *Vibrio* through quorum sensing systems, which depends on the cell density (Jung *et al.*, 2015; Liu *et al.*, 2018). For instance, at water temperatures above 27 °C, virulence factors involved in host degradation, antimicrobial resistance, and transcriptional regulation, as well as phenotypic changes in motility, antibiotic resistance, haemolysis, cytotoxicity, and bioluminescence are upregulated in *Vibrio* (Rosenberg *et al.*, 2009; Kimes *et al.*, 2012; Vezzulli *et al.*, 2010; Vezzulli *et al.*, 2015). The infection mechanism of *Vibrio* at warm temperatures includes the expression of adhesins to attach to the coral surface, Toxin P to inhibit the photosynthesis of *Symbiodinium*, superoxide dismutase for survival inside the coral, proteinases, etc. (Rosenberg *et al.*, 2007).

Therefore, it is suggested that mass mortality events of benthic invertebrates as corals and diverse vertebrates, as well as their more frequent occurrence, are associated to higher SST as consequence of global warming conditions. The influence of these factors on the regulation of pathogenicity genes in the genus *Vibrio* has been already documented in corals of the Mediterranean Sea (Baker-Austin *et al.*, 2012; Vezzulli *et al.*, 2013; Vezzulli *et al.*, 2015). This, combined with the ability of *Vibrio* spp. to form biofilms on particles present in the ocean, such as MP, represents an increasing problematic in aquatic ecosystems that might affect the wildlife and human health (Zettler *et al.*, 2013; Quilliam *et al.*, 2014; Keswani *et al.*, 2016; Kirstein *et al.*, 2016).

2.2.2 The importance of cultivation-based studies and the taxonomy of *Vibrio*

Vibrio spp. are usually easy to isolate from environmental or clinical samples since they are able to grow well between 15 and 30 °C (and even higher temperatures) and use a wide range of nutrients. However, certain species require supplements added to the media, for instance vitamins or growth factors (Thompson *et al.*, 2004a). The ubiquity and isolation easiness of *Vibrio* spp. have allowed detailed studies in terms of pathogenic, metabolic, and physiologic traits and their importance in nutrient cycling in the marine environments. The isolation of *Vibrio* spp. from habitats as seawater, sediments, or coral reefs from the Mediterranean, Baltic, or North Seas, and the Pacific, Caribbean, or Atlantic Oceans, have highlighted the broad physiological plasticity, biodiversity, and geographical distribution of this group (Chimetto *et al.*, 2008; Kirstein *et al.*, 2016; Kemp *et al.*, 2018; Rubio-Portillo *et al.*, 2018).

On the other hand, due to the upgrade and development of new molecular techniques, cultivation-based studies have been partially relegated. This led to an underestimation of the diversity of the genus *Vibrio* in cultivation-independent studies that are based only on 16S rRNA gene-sequences. Therefore, a combination of culture-dependent and -independent methods are highly recommended to obtain a wider picture of the *Vibrio* spp. communities in a determined ecosystem. For instance, Thompson *et al.*, (2005b) showed that a coastal bacterioplankton population of *Vibrio splendidus* consist of at least a thousand distinct genotypes present in extremely low concentrations in the seawater. Likewise, genomic fingerprinting (genotyping), MALDI-TOF MS, and 16S rRNA gene-based analyses were used by Rubio-Portillo *et al.*, (2018) to evaluate the diversity and genetic relatedness at strain level of *Vibrio* spp. from ecological niches including healthy and diseased coral tissues and seawater from two different locations in the Mediterranean Sea. In that study, numerous genotypes were found in the analysed niches, several were shared among distant sampling locations or present in diseased corals; however, 19 genotypes were found associated only to one of the ten analysed niches, indicating the specificity of those *Vibrio* strains.

The extraordinary expansion in the number of known species from the genus *Vibrio* has brought some difficulties represented by their correct phylogenetic assignment within the genus (Sawabe *et al.*, 2013). The phylogeny of the genus *Vibrio* is problematic and challenging due to the narrow boundaries delimiting species based on the high 16S rRNA gene sequence similarities, often resolved based on phenotypic characteristics, which frequently leads to

species misidentification (Thompson *et al.*, 2004a; Cano-Gomez *et al.*, 2011). Species of certain clades, especially those that include numerous representatives, such as the Harveyi, Splendidus, or Halioticoli clades, cannot always be differentiated based on the 16S rRNA gene sequence phylogeny (Urbanczyk *et al.*, 2013). Therefore, additional methods should be implemented to achieve a higher phylogenetic resolution, which has been obtained through core genome sequence phylogeny and MLSA based on few protein coding housekeeping genes (Thompson *et al.*, 2005a; Thompson *et al.*, 2007; Urbanczyk *et al.*, 2007; Thompson *et al.*, 2009; Lin *et al.*, 2010; Pascual *et al.*, 2010; Cano-Gomez *et al.*, 2011; Sawabe *et al.*, 2013; Urbanczyk *et al.*, 2013). In order to validate the use of MLSA approaches for the resolution of *Vibrio* spp., Pascual *et al.*, (2010) correlated pairwise DNA-DNA hybridisation (DDH) values with nucleotide sequence similarity values obtained by the comparison of concatenated partial nucleotide sequences of the 16S rRNA gene and the three most resolving genes of the MLSA scheme: *rpoD*, *rctB*, and *toxR*. Based on this analysis, a cut-off value for species designation was calculated, sequence similarity values above 90.3% indicate that strains can be considered as members of the same species.

These cultivation-dependent approaches using, besides the 16S rRNA gene sequence-based phylogeny, MLSA with diverse schemes of housekeeping genes and whole genome-based analyses, led to a more reliable classification of *Vibrio* spp., including the creation of new clades, the re-classification of former *Vibrio* species as new genera within *Vibrionaceae*, and the identification and description of numerous new species (Urbanczyk *et al.*, 2007; Cano-Gomez *et al.*, 2011; Hoffmann *et al.*, 2012; Sawabe *et al.*, 2013; Tarazona *et al.*, 2014; Doi *et al.*, 2017).

2.3 Marine habitats as hotspot of new bacterial species

The incubation experiment of the present study was conducted as part of the Ocean 2100 global change simulation project and performed in the CEMarin aquarium system located at the animal facility of the Justus Liebig University. This system contains marine biota and vegetation that emulate a realistic coral reef environment. Coral reefs harbour a huge diversity of wildlife; therefore, they have been called the rainforest of the sea (Mulhall, 2009). Coral reefs are also highly diverse in terms of bacterial diversity, since estimations indicate that 10^3 to 10^5 bacterial OTUs are present in the tropical reef water column and reef sediments, while 10^2 to 10^4 OTUs are associated to corals (McDevitt-Irwin *et al.*, 2017). This bacterial diversity is reflected in the numerous strains isolated from the MP, sediments, detritus, water samples, and coral tissues from the system, some of them representing potential new species based on the 16S rRNA gene similarity values lower than the proposed threshold for differentiating two species ($< 98.65\%$) with respect to the closest related type species (Kim *et al.*, 2014). These potential new species belong to genera of known primary surface colonisers (*Pseudomonas* and *Ruegeria*), common members of bacterial communities associated to marine animals (*Winogradskyella*), and the already mentioned potential coral pathogens (*Vibrio*).

2.3.1 Bacteria from the marine *Roseobacter* clade are primary colonisers

Numerous halophilic or moderately halophilic bacteria have been classified as members of the family *Rhodobacteraceae*, specifically within the MRC, one of the most abundant groups in marine environments that comprises about the 25% of marine microbial communities (Buchan *et al.*, 2005; Wagner-Döbler and Biebl, 2006). The tolerance, as well as the requirement of high salt concentrations explain why these bacteria thrive and are ubiquitous in several hostile environments and why many of them have been isolated from solar salterns, hypersaline soils, mudflats, seawater, marine sediments, coastal biofilms and even from a deep marine canyon and associated to marine animals or algae (Martínez-Checa *et al.*, 2005; Choi *et al.*, 2007; Albuquerque *et al.*, 2015; Kim *et al.*, 2015; Lee *et al.*, 2018; Park *et al.*, 2018). In recent years, members of *Rhodobacteraceae* and especially of the MRC, have gained attention in ecological studies of marine and freshwater ecosystems due their importance as primary surface-colonisers of natural (marine snow, particulate material, wood) and artificial surfaces (glass, steel, plastic) (Dang *et al.*, 2008; Lee *et al.*, 2008; Oberbeckmann *et al.*, 2018). The high number of OTUs in 16S rRNA gene amplicon sequence data assigned to *Rhodobacteraceae* indicated that members of the family were abundant in bacterial communities on polyethylene (PE), polyethylene terephthalate (PET), and polystyrene (PS) particles, sampled across different sites and seasons (De Tender *et al.*, 2017; Oberbeckmann *et al.*, 2018; Ogonowski *et al.*, 2018). Likewise, it was reported that *Roseobacter* sp., together with other members of the MRC clade, were the primary colonisers of diverse plastic materials after 24 hours of exposure, which evidences the key role of this group in the colonisation and establishment of biofilms on submerged surfaces (Dang and Lovell, 2000; Dang *et al.*, 2008; Lee *et al.*, 2008; Debroas *et al.*, 2017; Dussud *et al.*, 2018b).

A strain designated as THAF1 was isolated from a PE-MP, which was incubated in the CEMarin aquarium system. Based on its 16S rRNA gene sequence, the strain THAF1 showed highest sequence similarity to type strains of three different genera from the MRC. The first: *Palleronia* sp., proposed by Martínez-Checa *et al.*, in 2005, which includes three valid species isolated from a hypersaline soil of a saline saltern, the deep Mediterranean Sea, and soil of a tidal land (Martínez-Checa *et al.*, 2005; Choi *et al.*, 2007; Albuquerque *et al.*, 2015; Kim *et al.*, 2015, respectively). The second: *Maribius* sp., proposed by Choi *et al.*, in 2007 including bacteria from the surface water of the Sargasso Sea, a hypersaline water of a solar saltern, and from a tidal mudflat (Choi *et al.*, 2007; Lee *et al.*, 2018). The third: *Pseudomaribius* sp., which includes so far, only one species isolated from a tidal flat sediment (Park *et al.*, 2018).

These three genera are characterised by Gram negative, non-motile, strictly aerobic, heterotrophic, and catalase-positive rod-shaped cells. The predominant isoprenoid quinone is UQ-10. The major fatty acid is C_{18:1} ω7c. The major polar lipids are phosphatidylglycerol, a phosphoglycolipid, and an aminolipid (Martínez-Checa *et al.*, 2005; Choi *et al.*, 2007; Lee *et al.*, 2018; Park *et al.*, 2018).

Another genus from the MRC that was also isolated from MP and sediments incubated in the aquarium system was *Ruegeria* sp. Evidence indicated that *Ruegeria* sp. was an

important member of the community growing on PE fragments incubated at the sea surface and highly present in the coral mucus layer (Rubio-Portillo *et al.*, 2016; Pinto *et al.*, 2019). Similarly, *Ruegeria* sp. was highly abundant, together with other members of the MRC on polyhydroxyalkanoate (PHA) films, which are biodegradable polymers, indicating a potential degradation of plastics by *Ruegeria* sp. (Morohoshi *et al.*, 2018). It is known that during the surface attachment process, motile species of *Ruegeria* sp. might use the flagella, as well as regulatory pathways such as d-ci-GMP or the production of acyl homoserine lactones (AHLs) involved in quorum sensing systems to modulate biofilm formation (Wagner-Döbler and Biebl, 2006; Golberg *et al.*, 2011; Dang and Lovell, 2016).

Members of the genus *Ruegeria* are present in the marine water column, sediments, sand, or associated with animals. The genus was proposed by Uchino *et al.*, in 1998 and it has been emended several times. *Agrobacterium* species included in a subdivision proposed by Rüger and Höfle in 1991, which contained the marine star-shaped aggregate-forming bacteria, were accommodated in new groups. Misclassified species as *Agrobacterium atlanticum*, *Agrobacterium gelatinovorum*, and *Roseobacter algicola* were transferred to the genus *Ruegeria* (Uchino *et al.*, 1998) and classified as *Ruegeria atlantica*, *Ruegeria gelatinovirans* (later reclassified as *Thalassobius gelatinovorus* by Arahal *et al.*, 2005), and *Ruegeria algicola* (later reclassified later as *Marinovum algicola* by Martens *et al.*, 2006). Likewise, *Silicibacter lacuscaerulensis* and *Silicibacter pomeroyi* were reclassified as *Ruegeria lacuscaerulensis* and *Ruegeria pomeroyi* (Yi *et al.*, 2007). In 2018, Wirth and Whitman reassigned several species within the *Roseobacter* clade, *Tropicibacter litoreus* and *Tropicibacter mediterraneus* were integrated to *Ruegeria* as *Ruegeria litorea* and *Ruegeria mediterranea*, and *Ruegeria mobilis* and *Ruegeria scottomollicae* were transferred to the new genus *Epibacterium*.

With these modifications, the genus is currently comprised by 18 valid species including *Ruegeria arenilitoris* (Park and Yoon, 2012), *Ruegeria conchae* (Lee *et al.*, 2012), *Ruegeria denitrificans* (Arahal *et al.*, 2018), *Ruegeria faecimaris* (Oh *et al.*, 2011), *Ruegeria halocynthiae* (Kim *et al.*, 2012), *Ruegeria intermedia* (Kämpfer *et al.*, 2013), *Ruegeria kandeliae* (Zhang *et al.*, 2018), *Ruegeria lutea* (Kim *et al.*, 2019), *Ruegeria marina* (Huo *et al.*, 2011), *Ruegeria marisrubri* and *Ruegeria profundus* (Zhang *et al.*, 2017), *Ruegeria meonggei* (Kim *et al.*, 2014), and *Ruegeria sediminis* (Baek *et al.*, 2020). Most of the species of the genus were isolated from marine environments and associated to marine animals, with the exception of *R. lacuscaerulensis*, obtained from a geothermal lake. Five species have been isolated from marine sediments or sand (Uchino *et al.*, 1998; Park and Yoon, 2012; Oh *et al.*, 2011; Huo *et al.*, 2011; Baek *et al.*, 2020) as the isolate THAF57 obtained from the sandy sediments.

Ruegeria sp. is characterised by ovoid to rod-shaped Gram-negative cells unable to form spores, catalase and oxidase-positive, motile with a polar flagella or non-motile, and required sea salt for growth. Cells are non-phototrophic and most of the species are aerobic but some can grow facultative anaerobically via nitrate reduction. The major respiratory quinone is ubiquinone 10, G+C content is usually high (55-59 mol %), and C_{18:1} ω7c or summed feature 8 (C_{18:1} ω7c/ ω6c) are the dominant fatty acids (Pujalte *et al.*, 2013).

2.3.2 *Winogradskyella* sp. is a common genus from marine environments

Winogradskyella is a monophyletic genus of marine bacteria belonging to the family *Flavobacteriaceae* within the phylum *Bacteroidetes*. Nedashkovskaya *et al.* in 2005 proposed the genus based on phylogenetic, phenotypic, and chemotaxonomic analyses of three species of marine bacteria: *Winogradskyella thalassocola* (type species), *Winogradskyella epiphytica*, and *Winogradskyella eximia*. The genus has been successively emended, and the last emendation occurred in 2013 (Ivanova *et al.*, 2010; Yoon *et al.*, 2011; Nedashkovskaya *et al.*, 2012; Begum *et al.*, 2013). Currently, the genus is comprised by 33 valid species, most of them have been isolated from seawater, marine sediments, green and brown algae, or solar salterns. Likewise, other species have been isolated from diverse marine invertebrates, for instance *Winogradskyella echinorum* from a sea urchin (Nedashkovskaya *et al.* 2009), *Winogradskyella exilis* from a starfish (Ivanova *et al.*, 2010), *Winogradskyella crassostreae* from an oyster (Park *et al.*, 2015), *Winogradskyella poriferorum* and *Winogradskyella haliclonae* from sponges (Lau *et al.*, 2005; Schellenberg *et al.*, 2017), the latter isolated from the CEMarin aquarium system. By last, *Winogradskyella pocilloporae* strain AFPH31^T, was isolated from the tissues of a healthy coral (*Pocillopora damicornis*) incubated in the CEMarin aquarium system as well (Franco *et al.*, 2018).

Similarly, through 16S rRNA gene amplicon sequencing, OTUs assigned to *Winogradskyella* sp. were detected only in the microbiome of the black coral *Antipathes dichotoma*, as a sign of species-specific variation within black corals (Liu *et al.*, 2018). Interestingly, *Winogradskyella* sp. was also found in biofilms developed on the surface of polystyrene particles obtained from the Mediterranean Sea and it is known that members of the genus are able to degrade complex polysaccharides, such as xylan and cellulose (Delacuvellerie *et al.*, 2019).

Within the genus *Winogradskyella*, the morphology of cells vary between rod- or coccoid-shaped, the pigmentation of the colonies could be yellow- or orange-pigmented but flexirubin pigments are not produced. The cells are Gram-stain negative, oxidase-positive or negative, catalase-positive, strictly aerobic or facultative anaerobic, and with a gliding motility in most of the species. The polar lipid profile comprises phosphatidylethanolamine and one or two unknown aminolipids. The major respiratory quinone is the menaquinone MK-6 and the main fatty acids are straight-chain C_{15:0}, branched-chain iso-C_{15:0}, iso-C_{15:1}, anteiso-C_{15:0} and fatty acids with hydroxy groups iso-C_{15:0} 3-OH, iso-C_{16:0} 3-OH and iso-C_{17:0} 3-OH (Franco *et al.*, 2018).

CHAPTER III

3. Materials and methods

3.1 Revealing the bacterial assemblages developed in the marine system

3.1.1 Setup of the CEMarin aquatic system and experiment

The incubation of the particles was performed at the aquaculture facility of the Center of Excellence in Marine Science (CEMarin) at the Justus Liebig University Giessen, Germany. Three independent 80-liter tanks (independent biological replicates) were filled with artificial seawater (ASW) (ATI-Aquaristik, Coral Ocean plus, Premium Quality Reef Salt, Germany) containing in mg L⁻¹, Ca²⁺: 410, Mg²⁺: 1230, PO₄³⁻ <0.03, and a salinity of 3.3%. Alkalinity was maintained at 2.52 mmol L⁻¹ by the addition of NaHCO₃. The aquaria system had a constant water flow and a filtration system that replaced 3.5 L water per hour from one 4000 L tropical seawater system that harbour marine biota, which emulated a realistic marine environment. Water parameters were kept constant during the experiment (12 weeks). The tanks were equipped with horizontal and vertical pumps to generate currents and 300 W heaters that maintained the water temperature at 26 °C using a feedback controlled regulation (Profilux 3, Aquatic Bus, GHL Advanced Technology GmbH & Co. KG, Germany), with a 10:14 light:dark photoperiod using T5 tubes (Aquablue Special, ATI-Aquaristik, Germany). Coral fragments of the species *Acropora millepora*, *Pocillopora damicornis*, and *Porites lutea* were placed randomly in the tanks. The system was acclimatized for two weeks before addition of pristine and surface-sterilised MP and sandy sediments. The setup of the system was led by Dr. Patrick Schubert and Dr. Jessica Reichert from the research group of Prof. Dr. Thomas Wilke.

The MP used in the experiment (low-density polyethylene - LDPE, Novosint) represent a self-adhesive thermoplastic black powder used for indoor and outdoor coatings, as corrosion protection, electrostatic and heavy-duty coatings (Novoplastik, Germany). The size of the MP was between 37 mm to 163 mm with a mean diameter of 112.7 ± 11.1 mm (mean \pm SD) with a density of 0.95 g cm⁻³. Their planar surface area ranged from 819 to 32 487 mm² with a median of 4 477 mm². The irregularly shaped particles exhibit a rough surface structure with a specific surface area of 0.0204 m² g⁻¹, determined in a Mastersizer 2000 (Malvern, Worcestershire, UK) (Reichert *et al.*, 2018).

Before the addition, both particle types were sterilised by incubation in 70% (v/v) ethanol for 24 hours, then the particles were rinsed with filtered (0.22 µm pore-size Sterivex filters) and autoclaved ambient water (collected from the tanks). MP were added to the tanks at a concentration of approximately 200 particles per litre (0.003 g L⁻¹ or 250 mg/aquarium), where approximately 5% floated in the water column, while 90 g of sandy sediments were added. The concentration of MP was controlled weekly by manual counting under a stereo microscope and additional MP was added when the amount was below the initial concentration. Investigation of pooled MP instead of single particles was performed to minimize bias, which may have been caused by the younger biofilm present on the later added particles. The concentration of

bacterial cells in the tank water was monitored by SYBR Green I (SG-I) staining as described previously (Glaeser *et al.*, 2010) using the method of Lunau *et al.*, (2005) with an epifluorescence microscope DM5000B, a DFC 3000G camera system, and the LAS X software (all Leica, Germany) used for cell counting. The concentration of bacterial cells was in the range of 10^5 to 10^6 cells mL⁻¹ tank water. (Fig. 4). A graphic description of the marine system is shown in the Fig. 5.

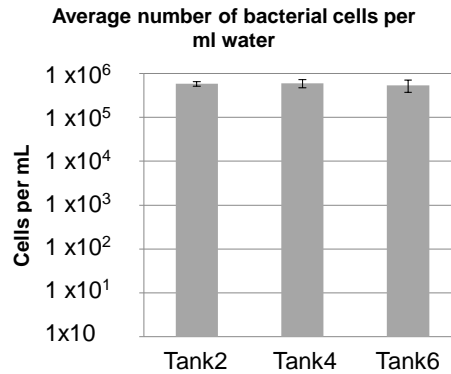


Figure 4: Cell counts per mL of water for each tank of the marine system. Number of cells was calculated according to Lunau *et al.*, (2005) by filtering 6 mL of water from the tanks in black polycarbonate filters (0.2 μ m, 25 mm). Cells were stained with SYBR Green I and counted using the epifluorescent microscope DM5000 B, the DFC 3000 G camera system, and the LAS X software (Leica, Germany). Depicted values represent mean values and standard deviations determined from the three tanks. Mean values were determined based on 10 counted pictures per tank.

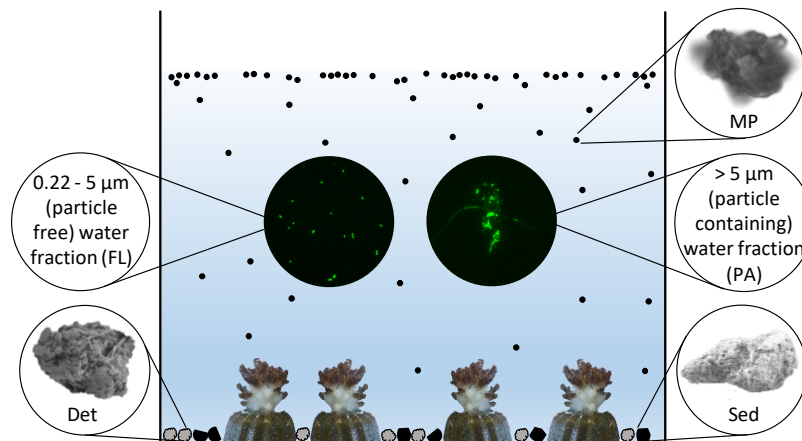


Figure 5: Graphic description of the experimental tanks. Microplastic particles (MP), sandy sediments (Sed), detritus (Det), particle-associated (PA) and free-living (FL) bacterial communities. Water circulation system not shown. PA and FL fractions are indicated by SybrGreen I staining of bacteria from water fractions after collection on membrane filters. 1000-fold magnification.

3.1.2 Collection of MP, sandy sediments, detritus, and water samples

After the incubation, four MP, sediments, and detritus samples (intra-tank replicates) were randomly collected from each of the three independent tanks. MP distributed in the water column and on the water surface were collected with a sterile micropipette and sterile pipette

tips. Sediments and detritus were collected from random areas of the bottom of the tanks with sterile 20 mL glass pipettes. All samples were placed separately in sterile 2 mL tubes containing 1 mL of 0.22 μm -filter sterilised and autoclaved ASW and stored at $-20\text{ }^{\circ}\text{C}$ until DNA extraction. Two litres of water per tank were collected from the water column (20 cm below water surface) using 60 mL syringes and filtered immediately. PA-bacterial communities were collected on sterile 5 μm Minisart syringe filters (Sartorius), and FL-bacterial communities were collected from the flow through on sterile 0.22 μm Sterivex-GP filter units (Millipore, Schwalbach, Germany). Filters were stored immediately at $-20\text{ }^{\circ}\text{C}$ until DNA extraction.

3.1.3 DAPI staining of MP and colonisation experiment

To visualise the MP colonisation, cells were stained with DAPI and observed under the microscope. Surface-sterilised MP added to the marine system were collected immediately and after 24, 48, and 72 hours of incubation. MP were rinsed twice with PBS buffer (pH 7.2) to remove the loosely-attached bacteria, fixed in 1 mL of a 2 % GDA solution and incubated for a minimum of 4 hours at $4\text{ }^{\circ}\text{C}$. Then, MP were placed on gelatine-coated slides and dried at $37\text{ }^{\circ}\text{C}$. Bacterial cells were stained with 15 μL of a $1\text{ }\mu\text{g mL}^{-1}$ DAPI (4',6-diamidino-2-phenylindole) solution (diluted in pure water) and incubated for 8 minutes in dark at RT. MP were carefully rinsed with ice-cold pure water to remove the excess of DAPI and dried in dark at RT. Finally, a drop of Citifluor AF1 (Science Services) was applied on the particles and covered with a cover glass. Microscopy was performed with the DM 5000 B epifluorescence microscope and the images were taken with the camera DFC 3000 G and the Application Suit (LAS X) software (all Leica Microsystems, Germany). In parallel, 50 μL of fresh liquid cultures of pure strains at 0.5 McFarland density were added separately to 3 mL of MB in 24-well plates. Surface-sterilised MP were added to the wells and incubated for 24 to 48 hours at $25\text{ }^{\circ}\text{C}$ and 100 rpm in dark. Fixation, staining, and microscopy were done as described above.

3.1.4 Scanning electron microscopy (SEM) of the particles

The collected MP, sediments, and detritus were washed with 0.2 μm filtered, autoclaved seawater and pre- fixed for 1 hour at $4\text{ }^{\circ}\text{C}$ in a solution of 0.1 M sodium cacodylate buffer (CB, pH 7.4) containing 8% sucrose, 1.5% paraformaldehyde, and 2.5% glutaraldehyde. Samples were rinsed in CB buffer at $4\text{ }^{\circ}\text{C}$, and immersed in the fixative overnight at $4\text{ }^{\circ}\text{C}$. After several washes in buffer, samples were incubated in 2% OsO_4 , washed again in buffer, and subsequently in ddH₂O. Samples were dehydrated in increasing ethanol series [30, 50, 70, 80, 90, 96, 100% (v/v)] (20 minutes each) after osmium fixation, critical point dried, mounted on SEM holders and gold sputtered. Samples were analysed using a Zeiss DSM982 field emission scanning electron microscope (FESEM; Carl Zeiss AG, Germany) at 3–5 kV. Images were taken using a secondary electron (SE)-detector with the voltage of the collector grid biased to + 300 V in order to improve the signal-to-noise ratio and to reveal optimal topographical contrast. For element analysis, energy-dispersive X-ray microanalysis (EDX) was done at 15 kV acceleration voltage using a 10 mm² Si(Li) detector (Oxford instruments plc, UK). The SEM microscopy was performed in cooperation with Dr. Martin Hardt in the Image Unit at the Biomedizinisches Forschungszentrum Seltersberg (BFS) in Giessen, Germany.

3.1.5 DNA extraction from particles and water samples

For the analysis of particle and water associated bacterial assemblages, total community DNA (TC-DNA) was extracted from particles and filters used to collect PA- and FL-bacteria. About 20-30 MP and 10 sediments or detritus were collected and filters were removed from cartridges of the Minisart and Sterivex units after being pre-frozen in liquid nitrogen and broken with a hammer. Filters were cut with a sterile scalpel into three pieces, used as intra-tank replicates. TC-DNA from particles and filters was extracted according to Bižić-Ionescu *et al.*, (2015), with few modifications. Samples were incubated for 30 min at 100 °C in 1 mL of lysis buffer (100 mM Tris-HCl, 50 mM EDTA, 100 mM NaCl and 1% SDS at pH 8.0), followed by a 15 min incubation at 65 °C after addition of phenol:chloroform:isoamyl alcohol 25:24:1 (1 mL). For the filter pieces, prior the first incubation, a mixture of 0.1 and 0.5 mm zirconia/silica beads (0.3 g each, Roth) was added to the lysis buffer and filters were bead beaten twice for 1 minute in 30 seconds interval. Samples were centrifuged for 15 min at 4 °C and aqueous phases were transferred into new tubes. An identical volume of chloroform:isoamyl alcohol 24:1 was added, samples were mixed and centrifuged again for 15 minutes at 4 °C; aqueous phases were transferred into new tubes. DNA was precipitated by incubation for 3 hours at RT after addition of ¼ volume 7.5 M filter sterilised ammonium acetate and 1 volume of 99 % isopropanol and centrifugation at 17,000 g at 4 °C for 40 min. DNA pellets were washed twice in ice-cold 70% (v/v) ethanol (10 min centrifugation), the tubes were drained upside down, and dried in a Speed Vac at RT for 5 minutes. DNA pellets were dissolved in 100 µL molecular grade water (Roth). To ensure the complete dissolution of the DNA, samples were incubated at 37 °C for 10 minutes. Due to the presence of inhibitory compounds, undiluted, 1:10, 1:20, 1:50, and 1:100 diluted DNA extracts were tested as PCR templates and 1:10 dilutions were selected for further analyses. DNA was stored at -20 °C.

3.1.6 Microbial community fingerprinting using PCR-DGGE

Bacterial 16S rRNA gene fragments (568 bp length) were PCR-amplified using bacterial 16S rRNA gene targeting universal primers 339F (5'-CTC CTA CGG GAG GCA GCA G-3') and 907R (5'-CCG TCA ATT CMT TTG AGT TT-3') (Muyzer *et al.*, 1993). A 40 bp GC clamp (5'-CGC CCG CCG CGC CCC GCG CCC GGC CCG CCG CCC CCG CCC C-3') was added at the 5'-end of primer 339F to stabilize the migration of DNA fragments in the DGGE gels. PCR reactions were performed in a total volume of 50 µL containing 5 µL of 1:10 diluted DNA extracts, 1x Dream Taq buffer, 0.4 µM of each primer, 0.1 µM of each dNTPs, 0.4 mg mL⁻¹ BSA, and 0.02 U µL⁻¹ Dream Taq DNA polymerase (all chemicals except primers from Thermo Scientific). PCR was done as follows: initial denaturing at 95 °C for 3 min followed by 34 cycles of 95 °C for 30 sec, 55 °C for 30 sec, and 72 °C for 40 sec, and a final extension step at 72°C for 30 min to prevent the formation of double bands during DGGE. PCR products were checked by 1.4 % (w/v) agarose gel electrophoresis. Equal amounts of the PCR products were loaded on DGGE gels containing 7 % (v/v) polyacrylamide and a 40–70 % linear denaturing gradient. Denaturing agents of 100 % were thereby defined as 7 M urea and 40 % (v/v) formamide (Brinkhoff and Muyzer, 1997). Electrophoresis was carried out at 60 °C and 100 V for 24 h in a INGENY Phor U System (Ingeny International BV, GP Goes,

Netherlands) in 1X TAE buffer (pH 7.4, adjusted with acetic acid). DNA bands were stained with ethidium bromide and documented in a Quatum ST5 system (Vilber Lourmat). Cluster analysis of DGGE patterns was performed in GelCompar II version 4.5 (Applied Maths, Sint-Martens-Latem, Belgium) with unweighted pair-group method using arithmetic average (UPGMA) clustering based on a dissimilarity matrix generated by the Pearson correlation, considering the presence, absence, and intensity of DGGE bands. Band matching was used to determine the relative abundance of individual DNA bands in the DGGE patterns. Non-metric Multidimensional Scaling (NMDS) and ranked distance analyses were performed in PAST3 and based on a similarity matrix generated with the Bray-Curtis similarity index.

3.1.7 16S rRNA gene amplicon Illumina MiSeq sequencing

Amplicon sequencing was performed with the universal *Bacteria* 16S rRNA gene targeting primer system 341F (5'-CCT ACG GGN GGC WGC AG-3') and 785R (5'-GAC TAC HVG GGT ATC TAA KCC-3') (Klindworth *et al.*, 2013). PCRs, product quantification and purification, and Illumina 300 bp paired-end read sequencing using an Illumina MiSeq V3 system was performed by LGC Genomics (Berlin, Germany). Sequence libraries were demultiplexed with the Illumina bcl2fastq 1.8.4 software, reads were sorted by amplicon inline barcodes allowing one barcode mismatch. Reads with missing barcodes, one-sided barcodes, or conflicting barcode pairs were discarded. Sequence adaptors were clipped in the following step and all reads with a length <100 bp were discarded (adaptor clipping). Subsequently, primers (3 mismatches allowed) were detected and used for sequence orientation and clipped. Forward and reverse reads were combined using BBMerge 34.48 (<http://bbmap.sourceforge.net/>). The combined read pair data set was used for further analysis. FASTQC files were converted to fasta files using Galaxy (<https://usegalaxy.org/>) and fasta files were submitted to the NGS analysis pipeline of the SILVA rRNA gene database project (SILVAngs 1.3; Quast *et al.*, 2013). All combined reads were aligned by the SILVA Incremental Aligner (SINA version 1.2.10 for ARB SVN, revision 21008) (Pruesse *et al.*, 2012) against the SILVA SSU rRNA SEED database, and quality controlled (Quast *et al.*, 2013). Reads < 50 aligned nucleotides and with more than 2% ambiguities or 2% homopolymers were excluded from further processing. Reads with a low alignment quality (50 alignment identity, 40 alignment score reported by SINA) were seen as putative contaminations and artefacts, and excluded from downstream analysis. After these initial quality control steps, identical reads were identified (dereplication), the unique reads were clustered on a per-sample basis, and clusters were defined as OTUs. A reference read per OTU was classified. Dereplication and clustering was done using cd-hit-est (version 3.1.2; <http://www.bioinformatics.org/cd-hit>; Li and Godzik, 2006) using accurate mode, ignoring overhangs, and applying identity criteria of 1.00 and 0.98, respectively. The classification was performed by local nucleotide BLAST search against the non-redundant version of the SILVA SSU Ref dataset (release 123; <http://www.arb-silva.de>) using blastn (version 2.2.30+; <http://blast.ncbi.nlm.nih.gov/Blast.cgi>) with standard settings (Camacho *et al.*, 2009). The classification of each OTU reference read was mapped onto all reads that were assigned to the respective OTU. This yields quantitative information (number of individual reads per taxonomic path), within the limitations of PCR and sequencing technique biases, as well as

multiple rRNA operons. Reads without any BLAST hit or reads with weak BLAST hits, where the function “(% sequence identity + % alignment coverage)/2” did not exceed the value of 93, remain unclassified. These reads were assigned to the group of “No Relative” in the SILVAngs fingerprint and Krona charts (Ondov *et al.*, 2011). Archaeal, chloroplast, mitochondria, and “No Relative” reads were excluded from the analysis. Only reads assigned to the bacterial phyla were used for further analysis. The sequence analysis was done by Dr. Stefanie Glaeser. Amplicon sequence data were deposited in the sequence read archive (SRA) of NCBI as SRA project with accession number SRP194562 (experiments SRX5781870 to SRX5781884) assigned to the BioProject PRJNA540740 and BioSample SAMN11554495, respectively.

3.1.8 *Vibrio*-specific primer design

Absolute abundance of *Vibrio* spp. 16S rRNA gene fragments in DNA samples of MP, sediments, detritus, and water fractions was quantified by qPCR by using two *Vibrio*-specific primer sets. The binding specificity of the *Vibrio* primer system 567F (5'-GGC GTA AAG CGC ATG CAG GT-3') and 680R (5'-GAA ATT CTA CCC CCC TCT ACA G-3') designed by Thompson *et al.*, (2004b) was checked through an alignment including 16S rRNA gene sequences of *Vibrio* spp. and closely related type strains of *Vibrionaceae* using MEGA7 (Kumar *et al.*, 2016). Due to the low specific binding of the primer system to those 16S rRNA gene sequences, a second set of primers was designed to test a higher specificity for *Vibrio* spp. by comparing conserved regions unique in the 16S rRNA gene sequences of *Vibrio* type strains (Fig. 6). The primer sequences are as follows: Vibrio-744F (5'-CAG ATA CTG ACA CTC AGA TG-3') and Vibrio-849R (5'-CGG CTC AAG GCC ACA ACC T-3'). The numbers given in the primer names represent the primer binding positions according to the 16S rRNA gene sequence of the *rrnB* of *E. coli* (Brosius *et al.*, 1978).

3.1.9 Quantification of *Vibrio* spp. 16S rRNA gene targets by qPCR

The standard curve for qPCR quantification was obtained by PCR amplification of the 16S rRNA gene using the primer system 8F (5'-GAG TTT GAT CCT GGC TCA G-3') and 1492R (5'-TAC CTT GTT ACG ACT T-3') (Lane, 1991) from a cell lysate of *Vibrio coralliilyticus* LMG 20984^T. The DNA was obtained after three freeze-thaw cycles (-20 °C and 115 °C). To generate the standard, two 100 µL-PCR reactions were performed and the size of the PCR product was controlled by 1.4 % (w/v) agarose gel electrophoresis and ethidium bromide staining. The amplified DNA fragments were purified with a PCR purification kit (Qiagen) and quantified by the Pico Green (Molecular Probes) fluorescence assay. For the qPCR amplifications the *Vibrio* standard DNA was used in the range of 1×10^8 to 1×10^1 targets/µL. Primers 567F/680R amplify a DNA fragment of 114 bp, and its annealing temperature is 60.2 °C as done by Oberbeckmann *et al.*, (2018). Primers Vibrio-744F/Vibrio-849R amplify a DNA fragment of 106 bp and its annealing temperature is 52.8 °C. The ratio of *Vibrio* 16S rRNA gene targets / total bacterial 16S rRNA gene targets was also calculated, using the primer system Univ-F (5'-GTG STG CAY GGY TGT CGT CA-3') and Univ-R (5'-ACG TCR TCC MCA CCT TCC TC-3') (Carroll *et al.*, 2010) which amplifies a DNA fragments of 148 bp using an annealing temperature of 60 °C.

567F	- - - - - G G C G T A A A G C G C A T G C A G G T - - - - -
<i>Vibrio caribbeanicus</i> AEIU01000064	G G A A T T A C T G G G T T T G T T A A
<i>Vibrio coralliilyticus</i> ACZN01000020	G G A A T T A C T G G G T T T G T T A A
<i>Vibrio fortis</i> AJ514916	G G A A T T A C T G G G T T T G T T A A
<i>Vibrio harveyi</i> BCUF01000119	G G A A T T A C T G G G T T T G T T A A
<i>Vibrio japonicus</i> LC143378	G G A A T T A C T G G G T G T G T T A A
<i>Vibrio neocaledonicus</i> JQ934828	G G A A T T A C T G G G T T T G T T A A
<i>Vibrio owensii</i> JPRD01000038	G G A A T T A C T G G G T T T G T T A A
<i>Vibrio parahaemolyticus</i> BBQD01000032	G G A A T T A C T G G G T T T G T T A A
<i>Vibrio shilonii</i> ABCH01000080	G G A A T T A C T G G G T T C G T T A A
<i>Grimontia indica</i> ANFM02000053	G G A A T T A C T G C G G T C T G T T A A
<i>Salinivibrio sharmensis</i> AM279734	G G A A T T A C T G C G G T T T G T T A A
680R	- - - - - C T G T A G A G G G G G G T A G A A T T T C - - - - -
<i>Vibrio caribbeanicus</i> AEIU01000064	G A C T A G A G T A A G G T G T A G
<i>Vibrio coralliilyticus</i> ACZN01000020	G A C T A G A G T A A G G T G T A G
<i>Vibrio fortis</i> AJ514916	A A C T A G A G T A A G G T G T A G
<i>Vibrio harveyi</i> BCUF01000119	G A C T A G A G T A A G G T G T A G
<i>Vibrio japonicus</i> LC143378	G A C T A G A G T A A G G T G T A G
<i>Vibrio neocaledonicus</i> JQ934828	G A C T A G A G T A A G G T G T A G
<i>Vibrio owensii</i> JPRD01000038	G A C T A G A G T A A G G T G T A G
<i>Vibrio parahaemolyticus</i> BBQD01000032	G A C T A G A G T A A G G T G T A G
<i>Vibrio shilonii</i> ABCH01000080	G A C T A G A G T A A G G T G T A G
<i>Grimontia indica</i> ANFM02000053	G - C T A G A G T C T A G G T G T A G
<i>Salinivibrio sharmensis</i> AM279734	G G C T A G A G T C T A G G T G T A G
Vibrio-744F	- - - - - C A G A T A C T G A C A C T C A G A T G - - - - -
<i>Vibrio caribbeanicus</i> AEIU01000064	G C C C C C T G G A C G A A A G C G T G
<i>Vibrio coralliilyticus</i> ACZN01000020	G C C C C C T G G A C G A A A G C G T G
<i>Vibrio fortis</i> AJ514916	G C C C C C T G G A C G A A A G C G T G
<i>Vibrio harveyi</i> BCUF01000119	G C C C C C T G G A C G A A A G C G T G
<i>Vibrio japonicus</i> LC143378	G C C C C C T G G A C G A A A G C G T G
<i>Vibrio neocaledonicus</i> JQ934828	G C C C C C T G G A C G A A A G C G T G
<i>Vibrio owensii</i> JPRD01000038	G C C C C C T G G A C G A A A G C G T G
<i>Vibrio parahaemolyticus</i> BBQD01000032	G C C C C C T G G A C G A A A G C G T G
<i>Vibrio shilonii</i> ABCH01000080	G C C C C C T G G A C G A A A G C G T G
<i>Grimontia indica</i> ANFM02000053	G C C C C C T G G A . . A . G C G A A A G C G T G
<i>Salinivibrio sharmensis</i> AM279734	G C C C C C T G G A . . A . G C G A A A G C G T G
Vibrio-849R	- - - - - A G G T T G T G G C C T T G A G C C G - - - - -
<i>Vibrio caribbeanicus</i> AEIU01000064	G T C T A C T T G G T G G C T T T C G G A
<i>Vibrio coralliilyticus</i> ACZN01000020	G T C T A C T T G G T G G C T T T C G G A
<i>Vibrio fortis</i> AJ514916	G T C T A C T T G G T G G C T T T C G G A
<i>Vibrio harveyi</i> BCUF01000119	G T C T A C T T G G T G G C T T T C G G A
<i>Vibrio japonicus</i> LC143378	G T C T A C T T G G T G G C T T T C G G A
<i>Vibrio neocaledonicus</i> JQ934828	G T C T A C T T G G T G G C T T T C G G A
<i>Vibrio owensii</i> JPRD01000038	G T C T A C T T G G T G G C T T T C G G A
<i>Vibrio parahaemolyticus</i> BBQD01000032	G T C T A C T T G G T G G C T T T C G G A
<i>Vibrio shilonii</i> ABCH01000080	G T C T A C T T G G T G G C T T T C G G A
<i>Grimontia indica</i> ANFM02000053	G T C T A C T T G G . . C . . A . T T G G C T T T C G G A
<i>Salinivibrio sharmensis</i> AM279734	G T C T A C T T G G A . T T . A A G A . T T T G G C T T T C G G C

Fig. 6: Comparison of the binding regions of the primer sets used in this study. Binding regions to the DNA of the 16S rRNA gene of *Vibrio* spp. type strains and related type strain species of the family *Vibrionaceae*. The direction of all DNA sequences is 5' - 3'.

Each qPCR reaction was conducted in 96-well plates including duplicate reactions per DNA sample of MP, sediments, detritus, PA-, and FL-bacteria, the appropriate set of *Vibrio* standards, and DNA obtained from isolates classified as *Vibrio* sp., *Grimontia* sp., and *Salinivibrio* sp. (all family *Vibrionaceae*), used as positive and negative controls to test the specificity of the primers. The qPCR reactions included a “no template” negative control per primer set. The qPCR runs were performed in a total volume of 10 µL containing 1x of the Sso Fast EVA Green Supermix (Bio-Rad), 0.2 µM of each primer, and 1 µL of DNA template, in a CFX96 Real-Time System (Bio-Rad) under the following optimized conditions: 2 min at 98°C followed by 45 cycles of 5 seconds at 98°C and 5 seconds at the corresponding annealing temperature according to the primer set, while the melting curve was obtained in cycles of 5 seconds where the temperature increased 0.5 °C between 65 and 95 °C. All intra-tank replicates were analysed separately. DNA concentrations of the TC-DNA extracts were quantified using Pico Green with lambda DNA (Thermo Scientific) to generate a standard curve, in black 96-well plates (Greiner Bio-One) using an Infinite F200 Pro Fluorometer (Tecan; excitation 480 nm / emission 520 nm).

3.1.10 Clone library construction and screening

Specificity of primers 567F/680R and Vibrio-744F/Vibrio-849R was checked by cloning the products obtained by qPCR from MP, which first were reamplified in a PCR reaction with $1 \times$ Phusion GC Buffer (Thermo Scientific), $0.2 \mu\text{M}$ of each dNTP, $0.5 \mu\text{M}$ of each primer, and $0.02 \text{ U } \mu\text{L}^{-1}$ Phusion DNA polymerase (Thermo Scientific) to produce blunted PCR products. PCR conditions were: 98°C for 30 sec, 34 cycles of 98°C for 10 sec, 62°C (for primers 567F/680) or 54°C (for primers Vibrio-744F/Vibrio-849R) for 30 sec, and 72°C for 15 sec, and finally 72°C for 30 min. The PCR products were controlled in a 1.4 (w/v) agarose-gel electrophoresis, then the bands were excised and purified with a gel extraction kit (Qiagen) and the purified products were cloned into the pJET1.2/blunt Cloning Vector from the CloneJET PCR cloning kit (Thermo Scientific) following the manufacturer's instructions but in a final volume of $10 \mu\text{L}$. The transformation was carried out in α -select bronze competent cells (Bioline), which were grown on Luria-Bertani agar with ampicillin.

Screening of positive clones was done by colony-PCR using plasmid primers pJet1.2F (5'-CGA CTC ACT ATA GGG AGA GCG GC-3') and pJet1.2R (5'-AAG AAC ATC GAT TTT CCA TGG CAG-3') (Thermo Scientific) in a final volume of $10 \mu\text{L}$ including a colony of the clone, $1 \times$ DreamTaq Buffer (Thermo Scientific), $0.2 \mu\text{M}$ of each dNTP, $0.2 \mu\text{M}$ of each primer, and $0.02 \text{ U } \mu\text{L}^{-1}$ DreamTaq Polymerase (Thermo Scientific). PCR conditions were: 95°C for 3 min, 32 cycles of 95°C for 30 sec, 60°C for 30 sec, and 72°C for 2 min, and 72°C for 10 min. The size of PCR products was controlled by 1.4 (w/v) agarose-gel electrophoresis and the products were re-amplified in a final volume of $25 \mu\text{L}$ with the same conditions as described previously, only the number of cycles was reduced from 32 to 25. The size of PCR products were controlled once again by 1.4 (w/v) agarose-gel electrophoresis and sequenced with the primer pJet1.2F. Sequences were processed manually based on electropherograms using MEGA 7 (Kumar *et al.*, 2016), and phylogenetic assignments were done using the EzBioCloud type strain 16S rRNA gene database (Yoon *et al.*, 2017). The partial 16S rRNA gene sequences obtained in the analysis are listed at the appendix section, since due to their short length they could not be deposited in the GenBank.

3.1.11 Cultivation, isolation, and maintenance of bacteria

Abundant particle- and water-associated bacteria were cultivated under aerobic conditions. Collected MP, sediments, and detritus were rinsed immediately with $0.22 \mu\text{m}$ -filter sterilised and autoclaved ambient water to remove loosely attached bacteria. Then, particles were added to 1 mL of autoclaved 0.9% (w/v) NaCl and vortexed to detach bacterial cells. Total water-associated bacteria were cultured from water of one of the tanks, particle-associated bacteria were collected from 100 mL tank water by a sterile $5 \mu\text{m}$ Minisart filter and rewashed with 20 mL $0.22 \mu\text{m}$ filter-sterilised and autoclaved ASW. Free-living bacteria were cultured from the $> 5 \mu\text{m}$ pre-filtered water fraction (flow through of $5 \mu\text{m}$ Minisart filters). All cell suspensions were serially diluted (up to 10^{-6}) in 0.9% NaCl and $100 \mu\text{L}$ of each sample were plated on Marine Agar (MA; Roth). In addition, washed particles were placed directly on the surface of MA to culture further particle-associated bacteria directly from the particle

surfaces. All plates were incubated in dark at 25 °C for 2 weeks. Most abundant morphological different colonies were picked and purified using several transfer steps of single colonies. For long-term preservation two loops of fresh bacterial biomass was suspended in 1.4 mL u-bottom push cap tubes (Micronic, Netherlands) in 500 µL Gibco newborn calf serum (NBCS, ThermoFisher Scientific) and stored at -20 and -80 °C. A cell lysate from one loop of bacterial biomass suspended in 500 µL molecular grade water (Roth) was generated in parallel by three freeze-thaw cycles at -20 °C and 1.5 minutes at 100 °C.

3.1.12 Genotypic differentiation of isolates

Isolates were compared at the strain level by genomic fingerprinting using BOX-PCR. Cell lysates were used as template in two repetitive element PCR (rep)-PCRs: BOX-PCR with the primer BOX A1R (5'-CTA CGG CAA GGC GAC GCT GAC G-3') and (GTG)₅-PCR with the primer (GTG)₅ (5'-GTG GTG GTG GTG GTG-3'). PCR reactions were performed in a final volume of 15 µL including 1 X buffer, 200 µM of each dNTP, 1 µM of the respective primer, 0.4 mg mL⁻¹ BSA, 0.025 U Dream Taq DNA polymerase (all chemicals except primers from Fermentas / Thermo Scientific). Cycle conditions were: 95 °C for 3 min, 30 cycles of 94 °C for 30 sec, 53 °C for 1 min, and 72 °C for 8 min, and a final step at 72 °C for 16 min. Genomic fingerprint patterns were clustered using GelCompar II (Applied Maths) using the Pearson's correlation coefficient for comparison of the fingerprint patterns and UPGMA for clustering. Pattern differences were used to define genotypes.

3.1.13 Phylogenetic identification and phylotyping of isolates

Isolates with different BOX-PCR patterns were identified based on the partial 16S rRNA gene. Cell lysates were used as template for the amplification of the 16S rRNA gene with the primer system 8F (5'-AGA GTT TGA TCC TGG CTC AG-3') / 1492R (5'-ACG GCT ACC TTG TTA CGA CTT-3') (Lane, 1991). PCRs were performed in a total volume of 25 µL including 1x buffer, 200 µM of each dNTP, 0.2 µM of each primer, 0.04 mg mL⁻¹ BSA, and 0.02 U Dream Taq DNA polymerase (all chemicals except primers from Fermentas / Thermo Scientific). Cycle conditions were: 95 °C for 3 min, 34 cycles of 95 °C for 30 sec, 53.7 °C for 30 sec, and 72 °C for 1 min 30 sec, and finally 72 °C for 10 min. PCR products were sequenced with the Sanger method using the primer system 27F (5'-GAG TTT GAT CMT GGC TCA G-3') or E786F (5'-GAT TAG ATA CCC TGG TAG-3') by LGC Genomics (Berlin, Germany). DNA sequences were corrected manually using MEGA 7.0 (Kumar *et al.*, 2016) based on the electropherograms, removing ambiguous positions at the 5' and 3' ends of the sequences. A first identification of the phylogenetic affiliation of the strains was done through a BLAST analysis against the EzBioCloud database (Yoon *et al.*, 2017) resulting in 16S rRNA gene sequence similarities of closely related type strains included in the database.

The phylogenetic relationships among the isolates and to next related described species were determined by the generation of phylogenetic trees using ARB release 5.2 (Ludwig *et al.*, 2004) using the LTPs128 database of the "All Species Living Tree Project" (LTPs) (Yarza *et al.*, 2008). The 16S rRNA gene sequences and additional reference sequences not implemented

in the database were aligned using the SILVA Incremental Aligner (SINA version 1.2.11) (Pruesse *et al.*, 2012) and added to the database using the quick add mode of ARB. The resulting alignment of all selected sequences was controlled manually based on the secondary structure information of the 16S rRNA gene. Maximum-likelihood (ML) trees were calculated using RAxML v7.04 (Stamatakis, 2006) with GTR-GAMMA as evolutionary model and rapid bootstrap analysis based on 100 replications. Pairwise sequence similarities were calculated with the ARB neighbour-joining (NJ) tool, without considering evolutionary models. Isolates were differentiated into phylotypes, which represent sequences that shared a high 16S rRNA gene sequence similarity (at least above 98.65 %) and formed a distinct cluster in the generated phylogenetic tree. All 16S rRNA gene sequences of the isolates were deposited in GenBank/EMBL/DDBJ under accession numbers MG996609 to MG996729.

3.1.14 Statistical Analyses

The NMDS analyses based on Bray-Curtis similarity index and principal component analysis (PCA) were used to display differences between relative abundances patterns of the bacterial assemblages, as well as the contribution of the individual phyla, families, or taxa to the differences between samples. A ternary plot was calculated to illustrate the occurrence of abundant taxa (>1.0 % relative abundance) with respect to the sample. One-way ANOSIM was used to test statistical significant differences between the samples at a global scale. These analyses were performed in PAST version 3.11 (Hammer *et al.*, 2001). Due to the low number of sample replicates, pairwise multivariate analysis of variance (PERMANOVA) was done combined with the Monte Carlo correction to improve the accuracy of the p-value. The analyses were performed in PRIMER 7 with PERMANOVA+ (downloaded from <https://www.primer-e.com>) and based on 999 permutations and the sums of squares type: type III (partial) by Yina Cifuentes. One-way ANOSIM and PERMANOVA are based on Bray-Curtis similarity matrices. The alpha-diversity of bacterial assemblages were calculated with Chao 1, Shannon, evenness, and dominance indices. A ternary plot was calculated to illustrate the occurrence of abundant taxa (relative abundance ≥ 1.0 %) in the different bacterial assemblages. SigmaPLOT 12.5 (Systat Software Inc.) was used to generate BOX-plots and determine significant differences using one-way ANOVA and Tukey's pairwise multiple comparison tests. Statistical significance was accepted for $p < 0.05$.

3.2 Genome sequencing and genome-based analyses

3.2.1 Genome sequencing of selected strains

To obtain the complete genome sequence, genomic DNA (gDNA) was isolated using the NucleoSpin Microbial DNA Kit (Macherey-Nagel, Germany) according to the manufacturer's instructions, but reducing the elution volume to 50 μ L. From the gDNA, two sequencing libraries were prepared, one for sequencing on the MiSeq platform (Illumina Inc., Netherlands), and one for sequencing on the GridION platform (Oxford Nanopore

Technologies, UK). The former was constructed using the TruSeq DNA PCR-free Library Kit (Illumina Inc., Netherlands) and was run in a 2x 300 nt run using a 600 cycle MiSeq Reagent Kit v3 (Illumina Inc., Netherlands). For ONT sequencing, the Ligation Sequencing Kit SQK-LSK109 in combination was used to prepare the libraries, which was in turn run on a R9.4.1 flow cell. Basecalling of the raw ONT data was performed with GUPPY v3.1.5 (Wick *et al.*, 2019). For assembly, three assemblers were used: The CANU assembler v1.8 (Koren *et al.*, 2017) was used to assemble the ONT data, the resulting assembled contigs were subsequently polished using the Illumina data and the PILON polisher v1.22 (Walker *et al.*, 2014) for a total of 10 rounds. For the first 5 rounds, BWA MEM (Li, 2013) was used as a mapper, for the final 5 cycles, BOWTIE2 (Langmead and Salzberg, 2012) was applied. In addition, the Illumina data was assembled using NEWBLER v2.8 (Margulies *et al.*, 2005) and both data sets were assembled using UNICYCLER (Wick *et al.* 2017). All assemblies were compared with each other and checked for synteny using R2CAT (Husemann and Stoye, 2009). If no divergence was found, the UNICYCLER assembly was used for further analyses. In case of inconsistencies, all three assemblies were combined and manually curated using CONSED (Gordon and Green, 2013). Annotation of the finished genomes was performed using PROKKA v1.11 (Seemann, 2014). The sequencing of the genomes, as well as their analysis and annotation were performed by Dr. Christian Rückert, Dr. Tobias Busche, Katharina Hanuschka, from the working group of Prof. Dr. Jörn Kalinowski, from the Center for Biotechnology of the University of Bielefeld.

3.2.2 Analyses of genome sequences

The presence of prophages in the genomes was evaluated in the PHASTER server (Arndt *et al.*, 2016). The EGDAR platform (Blom *et al.*, 2016) was used to perform genome-based analyses, such as species assignments of the isolates through ANI calculations with genome sequences of type strains of next related species according to the 16S rRNA gene sequence-based similarity analysis. Pangenomes of genome-sequenced isolates obtained from MP and selected reference genomes of type strains were generated to study the core genomes and strain-specific genes associated to pathogenicity and the degradation of complex polymers, which were represented in circular plots.

Likewise, putative virulence-associated genes of selected *Vibrio* sp. strains were compared to homologs of nine known pathogenic and non-pathogenic strains of *Vibrionaceae*. The pathogenic strains included in the analysis were: *V. coralliilyticus* ATCC BAA-450^T, *V. coralliilyticus* OCN008, *V. cholerae* O1 biovar El Tor str. N16961, *V. parahaemolyticus* RIMD 2210633, *V. vulnificus* CMCP6, *V. vulnificus* YJ016. On the other hand, *V. fortis* Dalian14, *Aliivibrio fischeri* ES114 (formerly *V. fischeri*), and *V. diazotrophicus* NBRC 103148^T, have not been reported as pathogenic strains. Based on the putative virulence-associated genes reported for the strains *V. coralliilyticus* ATCC BAA-450^T (Kimes *et al.*, 2012) and *V. coralliilyticus* OCN008 (Ushijima *et al.*, 2014), the homologous genes of all strains were retrieved and their presence in the isolated strains was evaluated by using the Genome Browser function implemented in the EDGAR platform (Blom *et al.*, 2016). The support in the creation of the projects in the EDGAR platform, as well as the addition of the genomes to the database was

done by Dr. Jochen Blom from the working group of Prof. Dr. Alexander Goesmann from the Justus Liebig University Giessen.

3.3 Diversity of *Vibrio* spp. cultivated from the marine aquarium system

3.3.1 Amplification of housekeeping genes and genotyping of bacterial isolates

The cultivated *Vibrio* spp. community isolates from the aquarium system comprised 51 strains, from which 43 were selected for identification and phylotyping as described in the section 3.1.13. After a further selection based on the isolation source of the strains, a MLSA was performed on 31 *Vibrio* spp. isolates. The MLSA scheme included 5 housekeeping genes: *gyrB*, *pyrH*, *rctB*, *recA*, and *rpoD*, and the primers used to amplify and sequence the genes were those employed by Pascual *et al.*, (2010). PCR reactions were performed in a final volume of 25 µL including 1 X buffer, 200 µM of each dNTP, 0.5 µM of each forward and reverse primer, 0.02 U Dream Taq DNA polymerase (all chemicals except primers from Fermentas / Thermo Scientific). The cycle conditions were: 95 °C for 3 min, 30 cycles of 95 °C for 30 sec, 55 °C for 1 min 15 sec, and 72 °C for 1 min 15 sec, and a final step at 72 °C for 7 min. PCR products from housekeeping genes were examined by agarose-gel electrophoresis (1 %), ethidium bromide staining, and sequenced by LGC Genomics (Berlin, Germany).

The total cultivated *Vibrio* spp. community was screened to obtain the genomic fingerprints by two repetitive element PCR (rep)-PCR: BOX- and (GTG)₅-PCR. Conditions of the BOX-PCR are described in the section 3.1.12, which were identical for the (GTG)₅-PCR. In addition, two randomly amplified polymorphic DNA (RAPD)-PCRs with primers A and B, were done as described by Glaeser *et al.*, in 2013. Genomic fingerprints were analysed in GelCompar II (Applied Maths) with the Pearson's correlation coefficient for comparison of fingerprint patterns and UPGMA for clustering.

3.3.2 Phylogenetic analysis based on MLSA

All sequences were corrected manually based on electropherograms, nucleotide sequences were translated into amino acid sequences, and alignments were done using ClustalW implemented in MEGA7 (Kumar *et al.*, 2016). The MLSA included internal fragments of different lengths of the housekeeping genes: *gyrB* (792 bp), *pyrH* (480 bp), *recA* (681 bp), *rpoD* (777 bp), and *rctB* (645 bp), concatenated in the same order. Full-length reference genes obtained from *Vibrio* sp. type strains were retrieved from the EDGAR database (<https://edgar.computational.bio.uni-giessen.de>) (Blom *et al.*, 2016) and used to align sequences based on the correct open reading frames (ORF) for translation into amino acid sequences. Only type strains with public genomes containing sequences of all the studied genes were included in the MLSA: 70 *Vibrio* and 4 *Grimontia* species, since the latter genus is a member of *Vibrionaceae* and was also isolated from the marine system. Phylogenetic trees based on nucleotide sequences were constructed using the ML method and the General Time

Reversible model, with a discrete Gamma-distribution (+ G) with 5 rate categories and assuming that a certain fraction of sites are evolutionary invariable (+ I). Trees based on amino acid sequences were constructed with the Jones-Thornton-Taylor model (JTT) (Jones *et al.*, 1992) + G + I. All codon positions were considered and positions containing gaps and missing data were eliminated. In addition, for all single and concatenated genes, trees were constructed with the NJ method (Saitou and Nei, 1987) using the Kimura-2-parameter model (Kimura, 1980) (for nucleotide sequences) and the JTT matrix-based method (Jones *et al.*, 1992) (for amino acid sequences) to compare the phylogenetic relationships based on single genes. Bootstrap tests including 100 replications were used for all calculations.

3.4 Polyphasic characterization of new bacterial species

3.4.1 Isolation of the strains

The strain AFPH31^T was isolated from healthy tissues of the scleractinian coral *Pocillopora damicornis*, cultured in the CEMarin aquarium system at Justus Liebig University Giessen, Germany. For isolation, a healthy coral fragment was rinsed with autoclaved ASW and cut into small pieces with a sterile scalpel. Tissues were removed carefully from the skeleton, placed on MA, and incubated for 5 days at 28 °C in dark and aerobic conditions. The strains THAF1, THAF57, and THAF100 were isolated from the surface of a MP, a sandy sediment, and the total water fraction, respectively. After growth, the colonies were selected for further purification by continuous streaking and incubation following the protocol described in the section 3.1.11, as well as the long-term maintenance and DNA extraction.

3.4.2 Phylogenetic analyses and G+C content calculation

The phylogenetic analyses applied to those isolates that represented potential new species obtained from the marine system were performed as described in detail in the section 3.1.13. Besides the phylogenetic trees constructed with the ML method, additional trees were calculated with the maximum-parsimony (MaPa) method using DNAPARS v 3.6 (Felsenstein, 2005), and the NJ method using ARB NJ tool and Jukes-Cantor correction (Jukes and Cantor, 1969). When necessary, high molecular weight genomic DNA of the investigated strains was extracted according to Pitcher *et al.*, (1989) in order to calculate the DNA G+C content, determined with the DNA melting temperature method (Gonzalez and Saiz-Jimenez, 2002).

3.4.3 Morphological characterization and growth and degradation tests

All the characterization tests were performed in parallel for each of the investigated strains and their respective closest related type species and the type species of the analysed genera, which were grown under the same cultivation conditions to assure uniformity in the results. The modified Hucker method according to Gerhardt *et al.*, (1994) was used for Gram staining. To determine the cell morphology, cells on glass slides covered with 2 % (w/v)

washed and autoclaved agar (Becton Dickinson) were examined by light microscopy at 1000-fold magnification. Microscopy was done with the DM 5000 B microscope and images were taken with the camera DFC 3000 G and the Application Suit (LAS X) software (all Leica Microsystems, Germany).

Media and temperature growth and specific substrate degradation were tested by spot assays and bacterial growth was monitored after 2, 4, and 7 days of dark incubation. A loop of fresh biomass (3 days-old cultures) was suspended in autoclaved 0.9% (w/v) NaCl solution to a McFarland standard of 0.5. Cell suspensions were serially diluted up to 10^{-4} and 5 μL of each dilution were spotted on the respective agar plates. Media-dependent growth was tested on R2A (Oxoid), Nutrient agar (Nu, Oxoid), Tryptic Soy Agar (TSA, Becton Dickinson), Malt agar (Merck), glycine/arginine agar (G/A), PYE [0.3 % (w/v) yeast extract and 0.3 % (w/v) casein peptone, 15 g agar L^{-1} , pH 7.2], CASO agar (Carl Roth), K7 [0.1 % (w/v) of yeast extract, peptone, and glucose, 15 g L^{-1} agar, pH 6.8], medium 65 (M65, according to DSMZ), Nutrient broth (DEV, Merck), MacConkey agar (Oxoid), Nutrient agar (NA, Becton Dickinson), Luria Bertani (LB, Sigma-Aldrich), Marine agar (MA, Carl Roth), Columbia agar with sheep blood (Oxoid) and PYES agar [0.3 % (w/v) yeast extract, 0.3 % (w/v) casein peptone, 0.23 % disodiumsuccinate, 15 g agar L^{-1} , pH 7.2]. All media were prepared in pure water according the manufacturer's instructions and all of them, except for MA and Columbia agar, were also supplemented with 3 % (w/v) NaCl. Bacteria were cultivated in dark at 28 °C on all media except on Columbia agar, incubated at 37 °C. Temperature-dependent growth was tested on MA at 4, 8, 15, 21, 25, 28, 30, 37, 45, 50, and 55 °C in dark conditions. Anaerobic growth was tested on MA with Anaerocult A mini system pads (Merck) at 28 °C for 14 days.

Degradation of substrates was tested on modified Bennett agar prepared with ASW including 0.1 % (w/v) meat extract, 0.1 % (w/v) yeast extract, 0.2 % (w/v) casein-peptone, 1 % (w/v) glycerine, 15 g L^{-1} agar at pH 7.3 (Jones, 1949), and supplemented with 0.4 % adenine, 1 % casein, 0.5 % tyrosine, 0.4% starch, 0.4 % xanthin, 0.4 % hypoxanthin, 0.4 % xylan, 0.4 % gelatine, and 0.4 % glucose. To determine starch degradation, the colonies were covered with iodide solution (Lugol's solution), while for gelatine degradation, a 2 % (w/v) tannin solution was spread over the colonies. DNA degradation was tested using DNase test agar with methyl green (Difco, USA) prepared in ASW. Lipolytic activity was tested through hydrolysis of 1 % (w/v) Tween 20, 40, 60 and 80 in MA. In all these cases, clearing zones around and under the colonies after 7 days of dark incubation at 28 °C indicated substrate degradation.

Salinity-dependent growth was tested in marine broth (MB, Carl Roth) prepared with pure water and supplemented with NaCl to final NaCl concentrations of 1.0 to 12.0 % in 1 % intervals. Likewise, pH-dependent growth was tested in MB adjusted to pH values of pH 4.0 to 12.0 (in 0.5 pH unit intervals between pH 4.0 and 7.0 and 1.0 pH unit intervals between 8.0 and 12.0). The pH was adjusted using 1 M HCl and 1 M KOH and stabilized by the addition of 5 mM autoclaved potassium phosphate buffer (pH values 4.5 to 7.5), 5 mM autoclaved Tris-HCl buffer (pH values 8 to 10) and 5 mM CAPS buffer (for pH 11 and 12) adjusted to the same pH values. Both tests were performed in 96-well microtiter plates in a final volume of 200 μL .

3.4.4 Enzyme activity tests

Physiological tests were carried out using the API 20NE, API ZYM, or API 50CH test strips (bioMérieux) according to the manufacturer's instructions and the usage in the descriptions of the closest related strains. The panels were inoculated with 3 days-old colonies cultivated on MA at 28 °C and suspended in autoclaved 0.9 % NaCl solution and adjusted to a McFarland standard of 0.5 for API 20NE and 6 for API ZYM and API 50CH. For the API 50 CH tests, the bacterial suspensions were mixed with the CHB/E medium (bioMérieux) supplemented with 3 % (w/v) aquarium salts (Reef Crystals – Enriched Blend, Aquarium Systems, Inc.). Additional physiological tests as acid production, carbon substrate assimilation, and enzyme activity were analysed by using the test described by Kämpfer *et al.*, in 1991. The panels, 96-well microtiter plates, were inoculated with 3 days-old colonies grown on MA and suspended in 0.9 % NaCl adjusted to a McFarland standard of 0.5, from which 50 µL were added to each well. The strips and panels were analysed after 2, 4, 7 and 14 days of dark incubation at 28 °C. Cytochrome oxidase activity was tested with Microbiology Bactident oxidase test strips (Merck) and catalase activity by bubble production after dropping a 3 % (v/v) hydrogen peroxide solution onto a fresh colonies on MA.

3.4.5 Pigment extraction and analysis

The KOH method reported by Reichenbach in (1992) was used to test the production of flexirubin-type pigments by the tested strains. Cellular pigments of *Winogradskyella pocilloporae* AFPH31^T and its related strains were extracted from 3 days-old cultures grown on MA at 28 °C in dark by suspending a loop of the biomass in acetone / methanol (7:2, v/v). After incubation for 14 h in the dark at 4 °C, samples were centrifuged for 2 min at 5700 g at 4 °C. The absorption spectra of the supernatants were measured in 10 mm quartz cuvette using a NanoDrop 2000/2000 c spectrophotometer (Thermo Scientific).

3.4.6 Chemotaxonomy

The fatty acids profiles of the strains were obtained from biomass harvested after three days of incubation at 28 °C on MA (approximately late exponential growth phase). The extraction of fatty acids from total cell lysates and the analysis were performed as described previously (Kämpfer and Kroppenstedt, 1996) by the separation of fatty acid methyl esters using a gas chromatograph 5898A (Hewlett Packard). Fatty acid identification from automatically integrated peaks was performed with the Sherlock Microbial Identification System (MIDI) version 2.1 (TSBA version 4.1). The biomass of quinones and polar lipids were extracted after cultivation in PYE broth supplemented with 3 % (w/v) Tetra Marine SeaSalt (Tetra) at 28 °C and analysed by the integrated procedure described previously (Tindall, 1990a; Tindall, 1990b; Altenburger *et al.*, 1996). The biomass for polyamines was extracted in late exponential growth phase according to Busse and Auling (1988) and analysed by HPLC as reported by Busse *et al.*, in 1997, whose equipment is described in Stolz *et al.* (2007). The analyses of quinones, polar lipids, polyamines, and spermidines were performed by Prof. Dr. Hans-Jürgen Busse from the University of Veterinary Medicine Vienna.

CHAPTER IV

4. Results

4.1 The prokaryotic life on MP, natural particles, and water fractions in a marine system containing small-polyp stony corals

4.1.1 Bacterial colonisation of MP occurs within 24 hours

The progression of the bacterial colonisation on MP was evaluated after 24, 48, and 72 hours of incubation in the CEMarin aquarium system, as well as under optimal conditions in the laboratory after 24 hours of incubation in MB at 25 °C with strains of genera *Roseivivax* (member of the MRC) and *Vibrio* (Fig. 7). MP colonisation started within the first 24 hours after addition of the particles to the marine system with few cells on the MP surface that progressively increased. Under optimal conditions, the colonisation occurred faster as observed by the denser number of bacterial cells of both strains on MP surfaces after 24 hours.

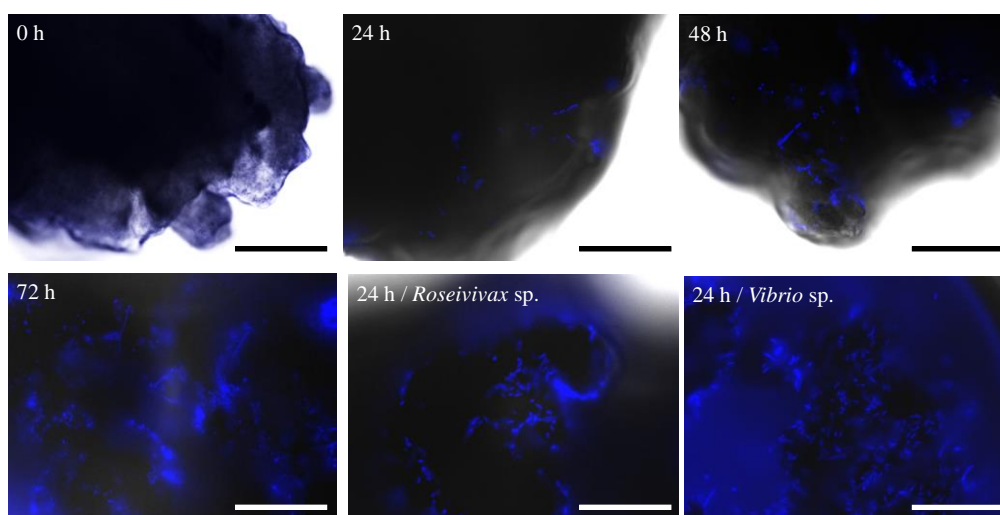


Fig. 7: Bacterial colonisation of MP in the system and under optimal conditions. MP were observed with an epifluorescence microscope after fixation in 2 % GDA and cellular DNA staining with a 1 µg mL⁻¹ DAPI solution. Bar = 25 µm.

4.1.2 SEM visualization indicated a specific colonisation of MP

The surface colonisation of MP, sandy sediments and detritus was visualized by SEM. Ethanol-sterilised MP were analysed right after addition to the system, revealing a microbe-free particle surfaces (Fig. 8A-C). Similar results were obtained for sterile sediment particles (data not shown). After one week of incubation, an early-stage biofilm formation was observed on MP with few, mainly rod-shaped bacterial cells containing stalk-like structures at one of the cell poles attached to the surface (Fig. 8D-F). After 12 weeks of incubation, changes in the MP surfaces were observed, from pristine MP to particles with a high level of deterioration. Likewise, morphologically diverse microbial communities were developed on MP, including

filamentous bacteria, often attached to diatoms, highly present on the surfaces as well (Fig. 8G-I). A denser bacterial biofilm was developed on sandy sediments, dominated by filamentous and spherical bacterial cells (Fig. 8J-L). Compared to MP, sandy sediments contained a large proportion of fungal-like cells including septate hyphae-like structures and spores pitting the surface (Fig. 8K). Broken diatoms, algal filaments, fungal hyphae, and few rod-shaped bacterial cells covered detritus particles (Fig. 8M-O). Bacteria on detritus particles clustered in patches, indistinctly distributed due to the high-porous surface of these aggregates.

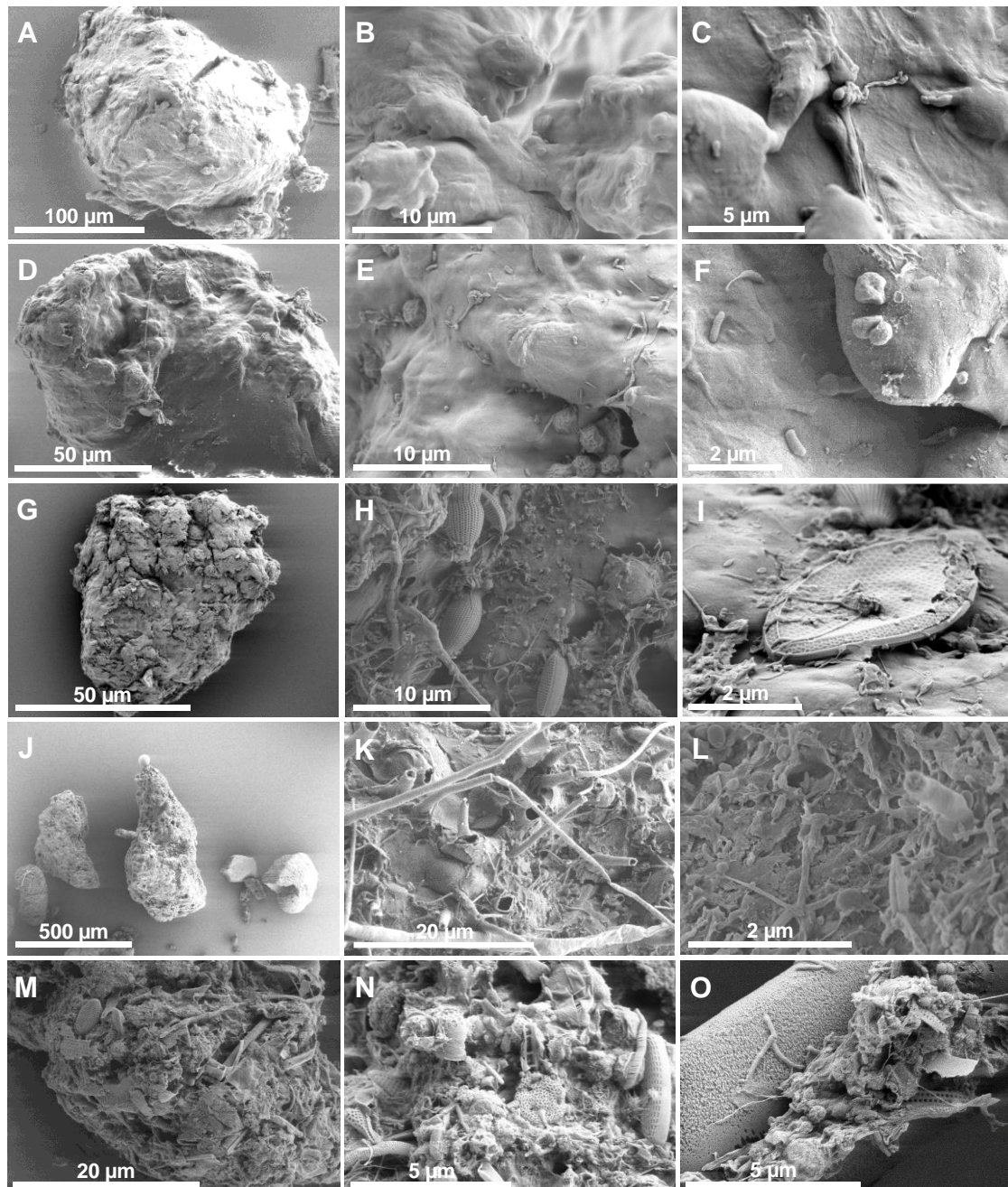


Fig. 8: Scanning electron micrographs of the particles. (A-C) surface-sterilised MP, microbial communities after one week (D-F) and twelve weeks of incubation of (G-I) MP, (J-L) sediments, and (M-O) detritus. Scale bars are given in each micrograph. Sizes: MP ~340 µm, sediments ~750 µm and detritus aggregates ~370 µm. The SEM microscopy was done in cooperation with Dr. Martin Hardt.

4.1.3 Bacterial community fingerprinting confirmed intra- and inter-tank stability of samples

Bacterial communities on MP, sandy sediments, and detritus were compared with the free-living bacterial communities present in the 0.22 to < 5 μm (particle-free) water fraction, by 16S rRNA gene based PCR-DGGE. Four replicates (1 to 4) of the particles and three replicates (1 to 3) of particle-free water fraction were investigated in parallel for three independent marine tanks (T2, T4, T6). Cluster and NMDS analyses illustrated MP-specific bacterial assemblages compared to those present on sandy sediments, detritus, and in the particle-free water fraction (Fig.9). Bacterial community fingerprinting patterns formed clearly separated clusters, which indicates intra- and inter-tank homogeneity of the samples (ANOSIM, $p = 0.0006$).

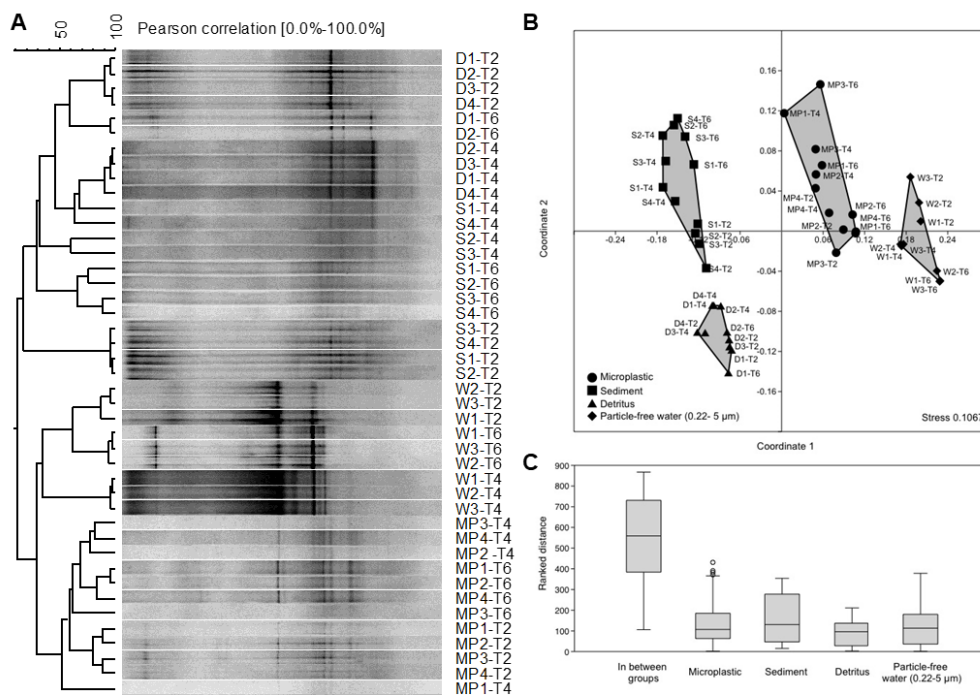


Fig. 9: Bacterial community fingerprinting analyses. (A) Clustering, (B) NMDS, and (C) ranked distance analyses of MP, sediments, detritus, and free-living bacterial community fingerprint patterns. Stress value is shown in the lower right corner of the NMDS plot. ANOSIM, $p = 0.0006$ (Bonferroni corrected). Microplastics (MP), sediment (S), detritus (D), free-living bacteria (W). Numbers following these letters represent the replicate. Tank (T), numbers following T represent the analysed tank.

Illumina 16S rRNA gene amplicon sequencing was subsequently performed with pooled DNA extracts from the intra-tank replicates. Amplicon sequencing revealed a total of 1,086,834 combined high-quality 16S rRNA gene amplicons with an average sequence length of 415 nt. After removing non-bacterial sequences, 1,044,756 sequences remained for bacterial community analysis (96.1% of the total obtained combined sequences). In total, 1,285 different phylogenetic groups (differentiated at the genus level) were detected: 330 to 501 for MP, 621 to 765 for Sed, 471 to 582 for Det, 474 to 553 for PA, and 433 to 637 for FL (Fig. 10).

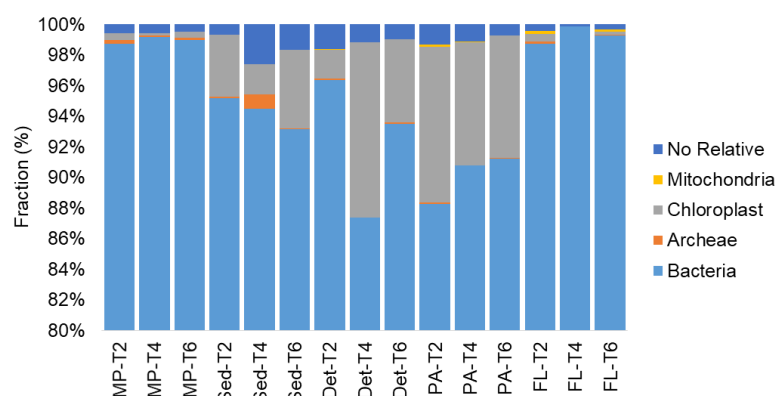


Fig. 10: Fractions of sequences per sample. Combined 16S rRNA genes sequences in Illumina amplicon data representing *Bacteria*, *Archaea*, chloroplast, mitochondria, and those which were not related to any taxa (no relative sequences).

4.1.4 Specificity of bacterial assemblages of MP

NMDS plots based on bacterial community patterns resolved at the genus level and compared using the Bray Curtis similarity index showed that the phylogenetic composition of bacterial communities developed on MP was stable among the studied tanks and distinct to those developed on sediments, detritus, and the surrounding water. In contrast to MP, bacterial assemblages developed on sediment particles (also added sterile to the system) were more similar to those present on detritus and the particle-associated water bacterial communities. All particle-associated bacterial assemblages showed strong differences to those of the free-living bacterial communities (Fig. 11A). NMDS analysis excluding the free-living bacteria illustrated more precisely differences among bacterial assemblages of sediments, detritus, and the particle-associated bacteria (Fig. 11B). It was also observed that MP-bacterial assemblages from the three independent tanks showed, in contrast to bacterial assemblages of the other samples, a very low variation, which indicates a specific and stable colonisation of MP surfaces in the marine system.

ANOSIM analysis showed at the global scale significant differences among the sample types ($p < 0.05$). Pairwise PERMANOVA analysis based on Monte Carlo permutations, optimized for samples with low replicate numbers, showed significant differences between MP-bacterial assemblages and the other sample types [p (MC) < 0.05], with exception of detritus- and particle-associated bacterial assemblages (Table 1). The environmental factors particle origin (anthropogenic vs natural), pre-colonisation (sterile vs pre-colonized), and particle location (floating vs sunken), showed a strong contribution to the separation of bacterial assemblages, while lifestyle (surface attached/biofilm-forming vs planktonic) mainly influenced the separation of the free-living water-bacterial communities (Fig. 10A-B). The factor “pre-colonisation” had a strong impact on the specificity of bacterial assemblages from MP but a low impact on those from sediments although both particle types were added sterile to the system.

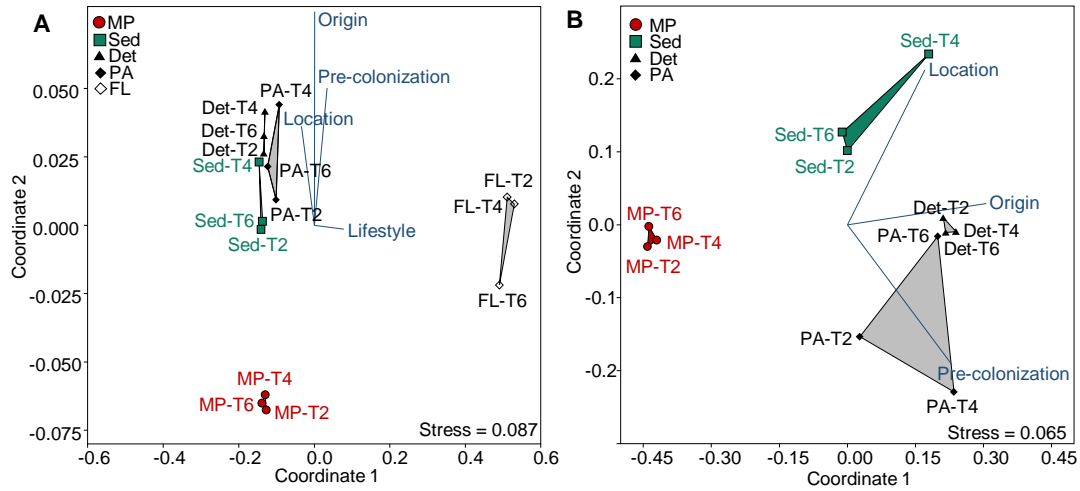


Fig. 11: NMDS of the composition of bacterial assemblages analysed by samples. (A) NMDS plot based on 16S rRNA gene amplicon data resolved at genus level including all the samples and (B) excluding the free-living bacterial assemblages. Plots were calculated with the Bray–Curtis similarity matrix including the influence of four different environmental factors. Stress values are indicated in the lower right corner of the plots. Tank (T), the number following T means the tank origin of the sample.

Table 1: Pairwise comparison using PERMANOVA based on Monte Carlo permutaions. Comparative analysis of bacterial assemblages of the different particles and water fractions based on Bray-Curtis similarity matrix. The *p* values were calculated based on type III sums of squares and 999 permutations. Monte Carlo permutations were calculated due to the low number of sample replicates. *p* < 0.05 indicated significant differences (bold). This statistical analysis was done by Yina Cifuentes.

Group 1	Group 2	PERMANOVA t	Unique p(perms)	Unique perms	Monte Carlo p values
MP	Sed	3.1314	0.099	10	0.008
MP	Det	3.5759	0.079	10	0.003
MP	PA	2.9514	0.12	10	0.014
MP	FL	3.9988	0.102	10	0.006
Sed	Det	2.2483	0.092	10	0.021
Sed	PA	2.108	0.102	10	0.033
Sed	FL	3.7366	0.088	10	0.005
Det	PA	1.5185	0.11	10	0.114
Det	FL	3.843	0.121	10	0.005
PA	FL	3.1495	0.1	10	0.006

4.1.5 Alpha diversity reveals similarities between particle-bacterial assemblages

The alpha-diversity of bacterial assemblages of the samples was compared based on the number of phylogenetic groups (genera) and numbers of sequences per phylogenetic group. MP-bacterial assemblages showed no significant differences with respect to community richness (Chao index) of bacterial assemblages associated with detritus and the particle-attached water bacteria, while sediment-bacterial assemblages were characterised by a significantly higher richness (Fig. 12A; *p* < 0.05). MP- and sediment-bacterial assemblages shared a similar high evenness similar to detritus and particle-attached water-bacterial

communities, with an equal distribution of phylogenetic groups (equal low dominance). In contrast, the free-living water-bacterial communities were characterised by a significantly lower evenness and a higher dominance due to the high abundance of few phylogenetic groups (Fig. 12B-C; $p < 0.01$). Bacterial assemblages of MP were similar to the overall community diversity to those developed or present on other particle types (Shannon index between 4.5 and 4.9). Only free-living water-bacterial communities showed a significantly lower diversity based on the dominance of few phylogenetic groups (Shannon index = 1.9; Fig. 12D; $p < 0.01$).

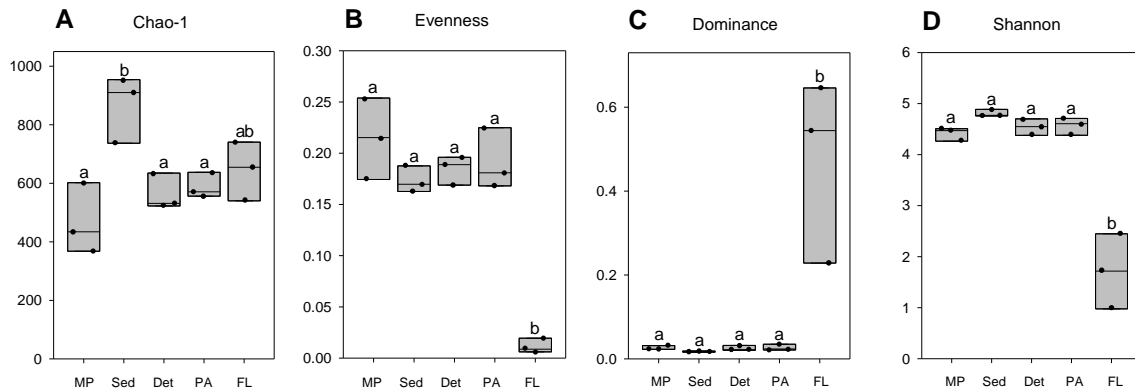


Fig. 12: Alpha diversity of bacterial assemblages. Differences in (A) richness, (B) evenness, (C) dominance, and (D) Shannon diversity, were calculated by using one-way ANOVA comparing the 5 samples. Black dots within bars represent values for biological replicates derived from three independent tanks. Letters indicate significant differences in the subsequent Tukey's pairwise multiple comparison test.

4.1.6 Specific families dominated the bacterial assemblages on MP

In total, 45 phyla including several candidate divisions were identified. *Proteobacteria* ($47.2 \pm 7.5\%$), *Bacteroidetes* ($17.6 \pm 5.6\%$), *Planctomycetes* ($15.9 \pm 5.8\%$), and *Cyanobacteria* ($6.3 \pm 3.9\%$) were the most dominant phyla of particle-assemblages (Fig. 13 and Table 2). Most abundant classes within *Proteobacteria* were *Alpha*- and *Gammaproteobacteria*. Particle-bacterial assemblages did not show significant differences for *Alpha*- and *Gammaproteobacteria*, *Bacteroidetes*, and *Cyanobacteria*, whereas *Planctomycetes* occurred in a significantly lower relative abundance on MP than on natural particles ($p < 0.05$) (Fig. 14A). In contrast to bacterial assemblages of particles, those of the free-living bacteria were dominated by *Bacteroidetes* ($65.4 \pm 20.9\%$) and *Proteobacteria* ($31.7 \pm 23.9\%$). At family level, MP-bacterial assemblages showed significant higher relative abundance of *Hyphomonadaceae* and *Erythrobacteraceae* (*Alphaproteobacteria*); *Alteromonadaceae* and Incertae Sedis group (*Gammaproteobacteria*); and *Flavobacteriaceae* and *Saprospiraceae* (*Bacteroidetes*). *Bacteroidetes* in the free-living bacterial assemblages was dominated by *Cryomorphaceae*, significantly less abundant on particles particularly on MP (Fig. 14B). Significant differences between the samples were calculated after one-way ANOVA and Tukey's pairwise multiple comparison test (Table 3). These results indicate a differential development of bacterial assemblages on the particles, especially on MP and sediments, even though both surface-sterilised particles were added to the system at the same time.

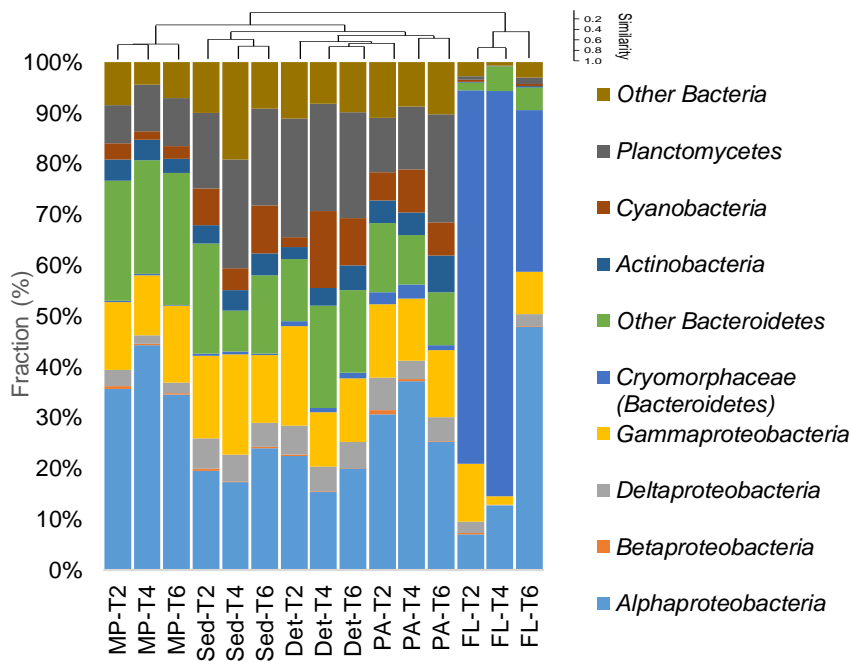


Fig. 13: Relative abundances of the dominant phyla associated to the samples. Main classes of *Proteobacteria* are depicted individually, as well as family *Cryomorphaceae* (*Bacteroidetes*).

Table 2: Relative abundances calculated for the most abundant phyla for each sample. Only those phyla with a relative abundance $\geq 0.3\%$ in at least one of the samples are shown.

Phylum	MP-T2	MP-T4	MP-T6	Sed-T2	Sed-T4	Sed-T6	Det-T2	Det-T4	Det-T6	PA-T2	PA-T4	PA-T6	FL-T2	FL-T4	FL-T6
<i>Proteobacteria</i>	53.0	58.3	52.5	43.4	45.7	44.4	48.7	31.7	38.4	53.1	53.9	43.9	21.3	14.6	59.1
<i>Bacteroidetes</i>	24.0	22.6	26.2	22.2	8.6	15.7	13.3	20.9	17.4	16.0	12.5	11.4	75.1	84.6	36.3
<i>Planctomycetes</i>	7.6	9.2	9.4	14.8	21.5	19.0	23.3	21.1	20.9	10.7	12.4	21.3	0.8	0.1	1.2
<i>Actinobacteria</i>	4.2	4.0	2.7	3.6	4.1	4.3	2.4	3.5	4.9	4.5	4.4	7.2	0.1	0.0	0.2
<i>Cyanobacteria</i>	3.2	1.7	2.6	7.3	4.2	9.4	1.9	15.2	9.3	5.5	8.5	6.6	0.4	0.0	0.5
<i>Firmicutes</i>	2.5	0.6	1.4	0.9	0.2	0.2	0.4	0.4	0.4	0.8	0.5	0.6	0.1	0.0	0.2
<i>Chloroflexi</i>	1.0	1.4	1.5	1.3	4.7	1.1	1.9	1.8	3.8	1.8	1.3	1.8	0.0	0.0	0.0
<i>Tenericutes</i>	2.0	0.4	1.2	0.0	0.0	0.0	0.1	0.1	0.1	0.2	0.3	0.0	0.1	0.0	0.1
<i>Acidobacteria</i>	0.6	0.5	0.6	1.0	2.9	1.8	0.8	0.2	0.5	0.3	0.2	0.8	0.0	0.0	0.0
<i>Parcubacteria</i>	0.5	0.3	0.5	1.7	1.3	1.2	0.4	0.2	0.1	0.3	0.3	0.2	0.4	0.2	0.5
<i>Verrucomicrobia</i>	0.5	0.3	0.3	0.7	1.4	0.6	2.4	1.6	1.3	2.7	2.2	2.3	0.3	0.0	0.4
<i>Chlamydiae</i>	0.3	0.1	0.2	0.3	0.5	0.2	0.7	1.8	0.8	1.1	1.8	0.8	0.3	0.2	0.6
<i>Saccharibacteria</i>	0.4	0.1	0.1	0.5	0.1	0.6	0.3	0.1	0.3	0.8	0.4	0.5	0.1	0.0	0.1
<i>Peregrinibacteria</i>	0.2	0.1	0.3	0.1	0.2	0.0	0.1	0.0	0.0	0.2	0.1	0.0	0.3	0.1	0.3
<i>Gemmatimonadetes</i>	0.1	0.1	0.1	0.4	1.0	0.3	0.2	0.1	0.1	0.0	0.0	0.1	0.0	0.0	0.0
<i>SBR1093</i>	0.0	0.1	0.1	1.3	1.0	0.4	2.2	0.8	1.2	1.2	0.9	1.9	0.0	0.0	0.0
<i>BRC1</i>	0.0	0.1	0.0	0.0	0.8	0.1	0.1	0.1	0.0	0.0	0.0	0.0	0.0	0.0	0.0
<i>Deinococcus-Thermus</i>	0.0	0.0	0.0	0.1	0.2	0.4	0.0	0.0	0.0	0.0	0.0	0.0	0.0	0.0	0.0
<i>Latescibacteria</i>	0.0	0.0	0.0	0.1	0.3	0.1	0.0	0.0	0.0	0.0	0.0	0.1	0.1	0.0	0.0

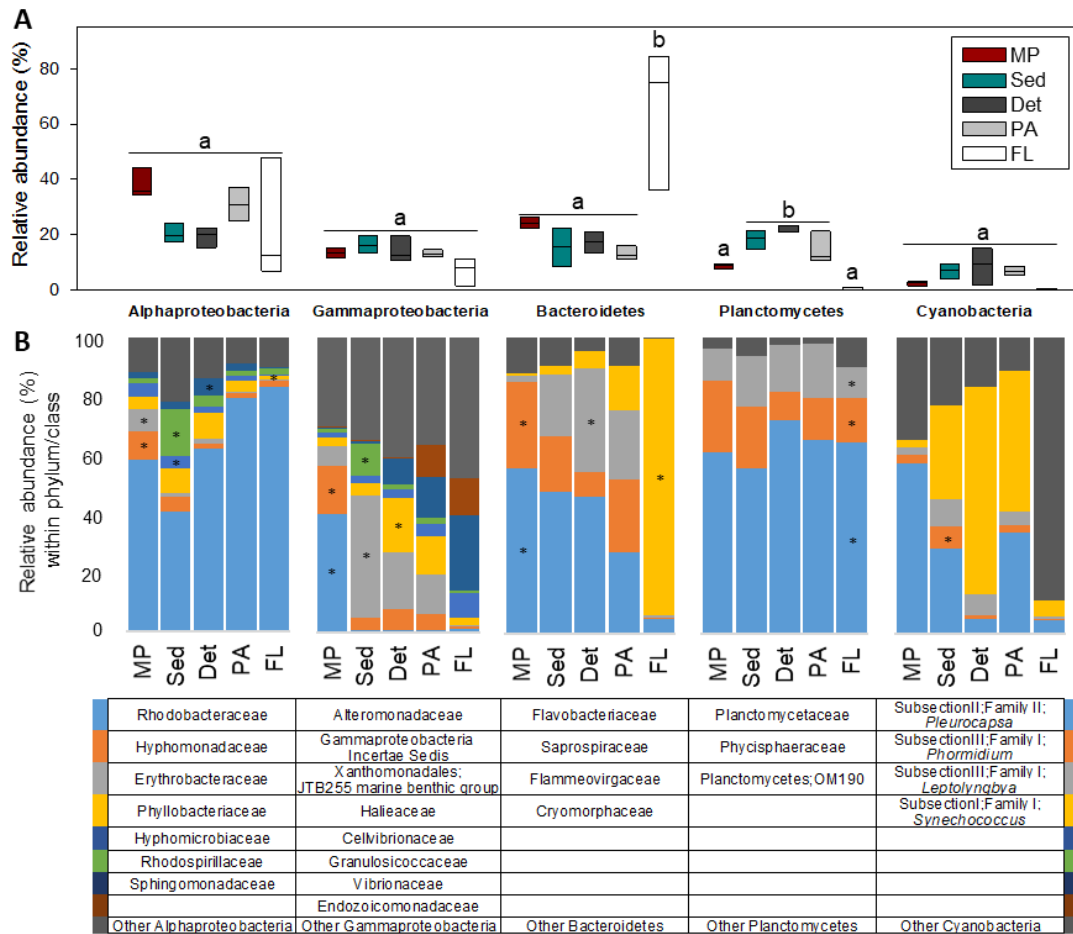


Fig. 14: Relative abundances of selected phyla and families in the samples. (A) Box-plot depicting relative abundances of the 5 most contributing phyla/classes, and (B) normalised relative abundances of the most contributing families within each phylum/class. Families and colours representing each one are shown in the table. When one single genus or one not yet-assigned clade comprises the abundant phylogenetic group, it is mentioned together with the taxonomy at higher levels. * represent significant differences between the samples ($p < 0.05$).

4.1.7 Bacterial assemblages of MP contain exclusive phylogenetic groups

In total, 83 phylogenetic groups were found with relative abundances $\geq 1\%$ in at least one replicate of the analysed samples. Hierarchical clustering and a heat map constructed based on the relative abundances of the phylogenetic groups illustrated the specificity of the MP-bacterial assemblages and showed the distribution of respective phylogenetic groups (genera) among sample types (Fig 15).

A ternary plot was generated to highlight the specific or shared occurrence of phylogenetic groups present in the bacterial assemblages of the studied samples (Fig. 16A). Significant differences of individual phylogenetic groups (genera) highlighted in the ternary plot were calculated with one-way ANOVA. Nine phylogenetic groups occurred with a significantly high relative abundance only on MP (MP-specialists). Among those, the most abundant (7.0-2.9 % relative abundance) were *Jejudonia* (Taxon-ID T1), *Roseivivax* (T3),

Marinobacter (T4), and *Erythrobacter* (T6). The high relative abundance of those phylogenetic groups was also responsible for the dominance of the respective families within *Alpha* and *Gammaproteobacteria*, and *Bacteroidetes* on MP. Other five phylogenetic groups of MP-specialists were uncultured *Rhodothermaceae* (T16), *Mycoplasma* (T17), *Marivita* (T21), uncultured *Alphaproteobacteria* (T22), and *Sulfitobacter* (T23), also occurred with a significantly higher relative abundance on MP (1.0-1.3 %) (Fig. 16B). Six additional phylogenetic groups occurred with a relative high abundance on MP (1.4-3.0 %), but also on other samples; namely *Lewinella* (T5), *Rubinimonas* (T8), *Winogradskyella* (T10), uncultured *Gammaproteobacteria* (T12), the OCS116 clade of *Rhizobiales* (T14), and uncultured *Hyphomonadaceae* (T15). Seven further phylogenetic groups occurred with a relative abundance of 1.1 to 6.0% on MP, but without significant differences to other particle types and water samples (Fig. 16A-B). On the other hand, sediments were colonised specifically by uncultured *Xanthomonadales* (T31) and *Rhodospirillaceae* (T48), *Andersenella* (T63), KI89A clade (T66), and *Granulosicoccus* (T94). Further phylogenetic groups abundant on sediments were uncultured *Rhodobacteraceae* (T2), also highly abundant on MP, OM190 (T28), *Muricauda* (T32), and *Blastopirellula* (T42).

Table 3: Significance values for pairwise comparisons between the samples. Significant differences at family level were calculated with one-way ANOVA and Tukey's pairwise multiple comparison test.

Alphaproteobacteria						Gammaproteobacteria						Bacteroidetes						Planctomycetes						Cyanobacteria						
	MP	Sed	Det	PA	FL		MP	Sed	Det	PA	FL		MP	Sed	Det	PA	FL		MP	Sed	Det	PA	FL		MP	Sed	Det	PA	FL	
Rhodobacteraceae	MP					Alteromonadaceae	MP					Flavobacteriaceae	MP					Planctomycetaceae	MP					Pleurocapsa	MP					
	Sed	-					Sed	<0.001					Sed	-					Sed	0.04					Sed	-				
	Det	-	-				Det	<0.001	-				Det	-	-				Det	<0.001	0.03				Det	-	-			
	PA	-	-	-			PA	<0.001	-	-			PA	0.02	-	-				PA	-	-	0.01			PA	-	-	-	
	FL	-	-	-	-			FL	<0.001	-	-		-	FL	0.01	-	-		-		FL	0.04	<0.001		<0.001	<0.001	FL	-	-	-
Hyphomonadaceae	MP					Incertae Sedis	MP					Saprospiraceae	MP					Physciaceae	MP					Phormidium	MP					
	Sed	<0.001					Sed	<0.001					Sed	0.02					Sed	0.04					Sed	0.04				
	Det	<0.001	-				Det	<0.001	-				Det	0	-				Det	-	0.04				Det	-	-			
	PA	<0.001	-	-			PA	<0.001	-	-			PA	0.03	-	-			PA	-	-	-			PA	-	-	-		
	FL	<0.001	-	-	-			FL	<0.001	-	-		-	FL	<0.001	-	-		-	FL	0.02	<0.001	0.02		0.01	FL	-	0.03	-	-
Erythrobacteraceae	MP					Benthic group	MP					Flammovirgaceae	MP					OM190	MP					Lepidolyngbya	MP					
	Sed	0					Sed	<0.001					Sed	<0.001					Sed	-					Sed	-				
	Det	0	-				Det	-	0				Det	<0.001	<0.001				Det	0.04	-				Det	-	-			
	PA	<0.001	-	-			PA	-	<0.001	-			PA	<0.001	-	<0.001			PA	-	-	-			PA	-	-	-		
	FL	<0.001	-	-	-			FL	-	<0.001	0.05		-	FL	-	<0.001	<0.001		<0.001	FL	-	0.02	0.01		0.03	FL	-	-	-	-
Phyllobacteriaceae	MP					Halobacteriaceae	MP					Cytophagaceae	MP					Synochococcus	MP					Synochococcus	MP					
	Sed	-					Sed	-					Sed	-					Sed	-					Sed	-				
	Det	-	-				Det	0.05	-				Det	-	-				Det	-	-				Det	-	-			
	PA	-	-	-			PA	-	-	-			PA	-	-	-			PA	-	-	-			PA	-	-	-		
	FL	0.01	0.01	0.01	-			FL	-	-	0.03		0.03	FL	<0.001	<0.001	<0.001		<0.001	FL	-	0.02	0.01		0.03	FL	-	-	-	-
Hyphomicrobiaceae	MP					Cellulirionaceae	MP					Granulosicoccaceae	MP					Vibrionaceae	MP					Endozoicomonadaceae	MP					
	Sed	-					Sed	-					Sed	0					Sed	-					Sed	-				
	Det	-	0.02				Det	-	-				Det	-	-				Det	-	-				Det	-	-			
	PA	-	-	-			PA	-	-	-			PA	-	-	-			PA	-	-	-			PA	-	-	-		
	FL	0.01	<0.001	-	-			FL	-	-	-		-	FL	-	-	-		-	FL	-	-	-		-	FL	-	-	-	-
Rhodospirillaceae	MP					Granulosicoccaceae	MP					Vibrionaceae	MP					Endozoicomonadaceae	MP					Endozoicomonadaceae	MP					
	Sed	<0.001					Sed	-					Sed	0					Sed	-					Sed	-				
	Det	-	<0.001				Det	-	0				Det	-	-				Det	-	-				Det	-	-			
	PA	-	<0.001	-			PA	-	0	-			PA	-	-	-			PA	-	-	-			PA	-	-	-		
	FL	-	<0.001	-	-			FL	-	<0.001	-		-	FL	-	<0.001	-		-	FL	-	-	-		-	FL	-	-	-	-
Sphingomonadaceae	MP					Vibrionaceae	MP					Endozoicomonadaceae	MP					Endozoicomonadaceae	MP					Endozoicomonadaceae	MP					
	Sed	-					Sed	-					Sed	-					Sed	-					Sed	-				
	Det	-	-				Det	-	-				Det	-	-				Det	-	-				Det	-	-			
	PA	-	-	-			PA	-	-	-			PA	-	-	-			PA	-	-	-			PA	-	-	-		
	FL	-	-	0.01	-			FL	-	-	-		-	FL	-	-	-		-	FL	-	-	-		-	FL	-	-	-	-
							MP						MP						MP						MP					
							Sed	-					Sed	-					Sed	-					Sed	-				
							Det	-	-				Det	-	-				Det	-	-				Det	-	-			
							PA	-	-	-			PA	-	-	-			PA	-	-	-			PA	-	-	-		
							FL	-	-	-	-			FL	-	-	-		-	FL	-	-	-		-	FL	-	-	-	-

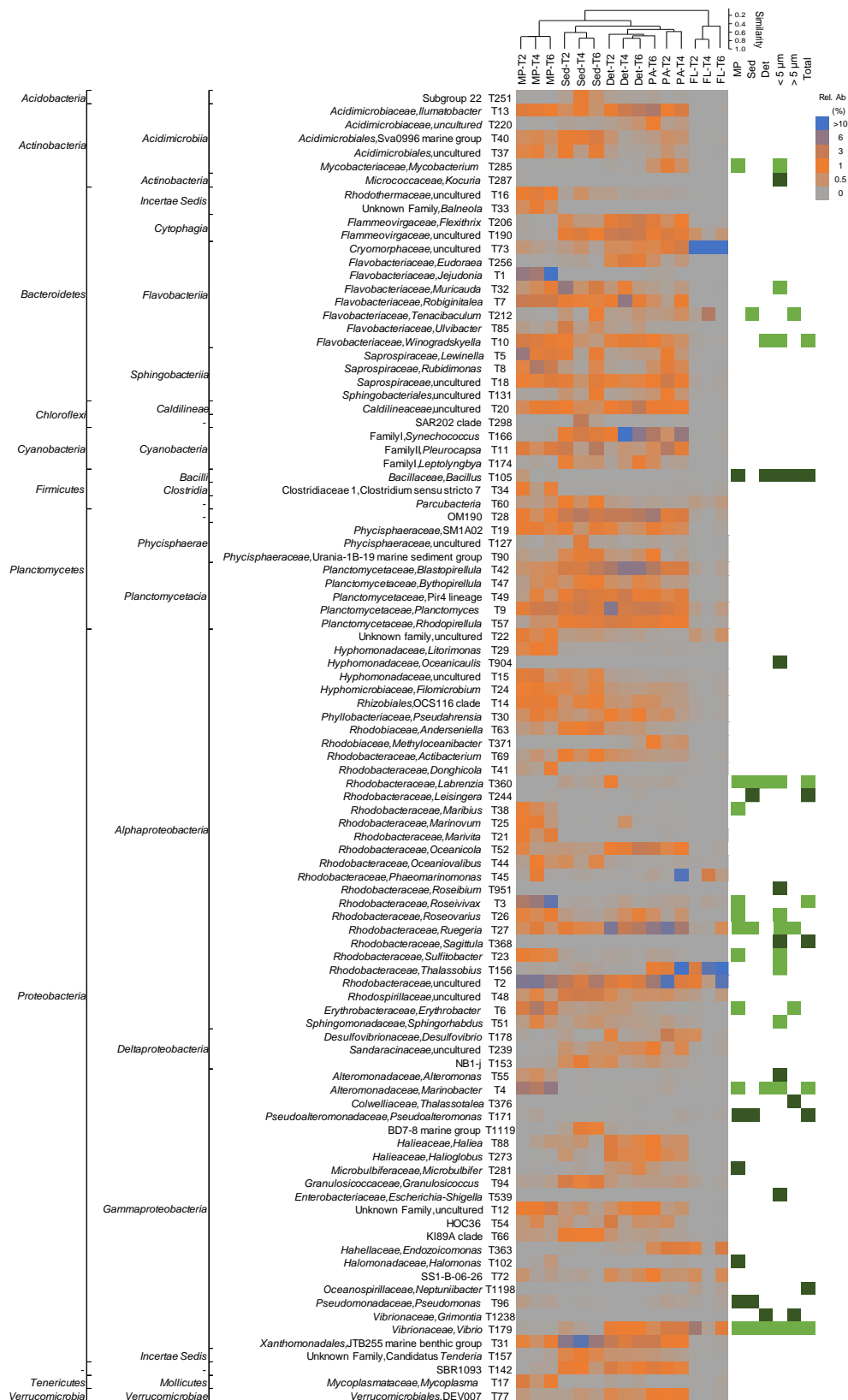


Fig. 15: Relative abundances of phylogenetic groups in the different samples and their classification at higher taxonomic levels. Green cells represent isolated genera from particles and water fractions and dark green cells those isolates from genera with relative abundances < 1 %. In total, 98 phylogenetic groups are shown: 83 occurred in at least one sample replicate with a relative abundance $\geq 1\%$ and 15 low abundant phylogenetic groups represented by the cultured bacteria.

Due to their close clustering, detritus and the particle-associated bacterial assemblages were merged for the ternary plot representation. Abundant phylogenetic groups in one or both of these bacterial assemblages, but unable to colonise efficiently MP and sediments, were *Ruegeria* (T27), *Phaeomarinomonas* (T45), *Oceanicola* (T52), *Desulfovibrio* (T178), *Flexithrix* (T206), and *Eudoraea* (T256). The free-living bacterial assemblages, contrary to those from particles, were dominated by only one phylogenetic group, uncultured *Cryomorphaceae* (T73; 61.7%). Five additional groups occurred with a mean relative abundance > 1 %, *Thalassobius* (T156; 15.1%), uncultured *Rhodobacteraceae* (T2; 3.6%), *Tenacibaculum* (T212; 2.4%), *Vibrio* (T179, 2.3%), and *Endozoicomonas* T363 (1.0%). *Thalassobius* and *Endozoicomonas* were also highly abundant in particle-associated bacterial assemblages (Fig. 16A). Interestingly, the relative abundance of sequences assigned to the genus *Vibrio* on MP and sandy sediments was low, 0.05 (\pm 0.01) % and 0.2 (\pm 0.1) %, respectively, while it was higher for detritus (1.2 ± 0.2 %) and the particulate and particle-free water fractions (1.8 ± 1.0 and 2.3 ± 2.5 %, respectively).

4.1.8 Quantification of *Vibrio* spp. based on qPCR

The absolute abundance of *Vibrio* spp. was quantified by qPCR due to their discussed presence on MP and their potential pathogenicity to the marine biota. Two different primer sets targeting the 16S rRNA gene of *Vibrio* spp. were used. With the primer set 567F/680R (Thompson *et al.*, 2004b) the average abundance of *Vibrio* spp. on MP was in the range of 10^3 16S rRNA gene copies/ng TC-DNA, with no significant differences compared to natural particles. Only the particle-free water fraction contained a significantly higher concentration of *Vibrio* spp. 16S rRNA gene targets per ng TC-DNA (one-way ANOVA; $p < 0.05$). In contrast, with the primer set Vibrio-744F/Vibrio-849R designed in this study to avoid the amplification of close-related *Vibrio* species, unspecific amplification products were not detected, indicating a higher specificity of this primer set. The average abundance of *Vibrio* spp. on MP was in the range of 10^4 16S rRNA gene copies/ng TC-DNA, significantly higher compared to the abundance on sediments (10^2 16S rRNA gene copies/ng TC-DNA), but in the same range as those of detritus and the particulate and particle-free water fractions (Fig. 17 and Table 4). The ratio *Vibrio* spp./total *Bacteria* 16S rRNA gene targets was for both primer sets slightly higher for MP than for sandy sediments, without significant differences. For MP, these ratios were, depending on the primer set, in the range of $0.06 \pm 0.05\%$ (567F/680R) to $0.07 \pm 0.05\%$ (Vibrio-744F/Vibrio-849R), slightly higher than the relative abundance obtained in the amplicon data.

The values obtained for the qPCR runs were for the primer system 567F/680R: efficiency = 97.5 %, $R^2 = 0.982$, slope = -3.382, γ -intercept = 37.639; for the primer system Vibrio-744F/Vibrio-849R: efficiency = 106.8 %, $R^2 = 0.966$, slope = -3.169, γ -intercept = 37.188; and for the primer system Univ-F/Univ-R: efficiency = 100.7 %, $R^2 = 0.959$, slope = -3.306, γ -intercept = 36.888.

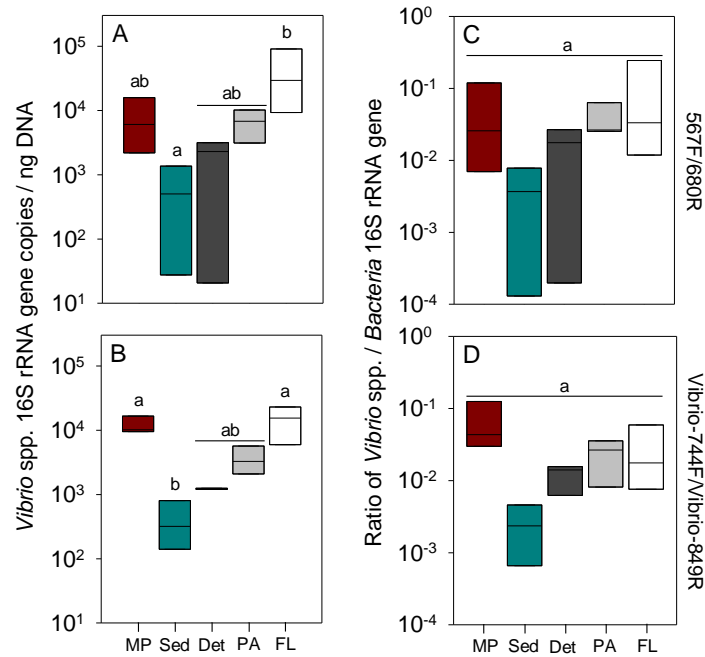


Fig. 17: Total abundance of *Vibrio* spp. calculated by qPCR. (A) Abundances were calculated using the primer sets 567F/680R and (B) Vibrio-744F/Vibrio-849R from particles and water fractions. *Bacteria* 16S rRNA gene copies/ng DNA were calculated with the primers Univ-F/Univ-R to determine the ratio (Fig. 17C-D). Values represent ranges of abundance obtained from biological replicates derived from the three independent tanks. Differences were calculated by using one-way ANOVA. Letters show significant differences obtained in the Tukey's pairwise multiple comparison test.

Table 4: Absolute quantification of *Vibrio* spp. and *Bacteria* 16S rRNA gene targets. Total abundances were determined by qPCR for the different bacterial assemblages of the samples.

Source	Primer set	16S rRNA gene copies / ng DNA	<i>Vibrio</i> 16S rRNA gene copies / <i>Bacteria</i> 16S rRNA gene copies
MP	567F/680R	8.0×10^3	0.05
Sed	567F/680R	6.3×10^2	0.004
Det	567F/680R	1.8×10^3	0.02
PA	567F/680R	6.7×10^3	0.04
FL	567F/680R	4.3×10^4	0.1
MP	Vibrio-744F/Vibrio-849R	1.2×10^4	0.07
Sed	Vibrio-744F/Vibrio-849R	4.2×10^2	0.003
Det	Vibrio-744F/Vibrio-849R	1.2×10^3	0.01
PA	Vibrio-744F/Vibrio-849R	3.7×10^3	0.02
FL	Vibrio-744F/Vibrio-849R	1.5×10^4	0.03
MP	Univ-F/Univ-R	2.3×10^5	
Sed	Univ-F/Univ-R	1.7×10^5	
Det	Univ-F/Univ-R	1.2×10^5	
PA	Univ-F/Univ-R	1.8×10^5	
FL	Univ-F/Univ-R	6.9×10^5	

4.1.9 Cloning and specificity of the *Vibrio* spp. primer sets

The specificity of the two primer sets used in the qPCR reactions was tested by cloning the qPCR-amplified fragments and the subsequent sequence analysis of the 16S rRNA gene fragments generated in the qPCR, which revealed differences among the detected *Vibrio* spp.

A total of 34 colonies obtained after cloning (17 per primer set) were randomly selected from the agar plates to sequence the inserted DNA fragments.

Clone libraries derived from the DNA fragments amplified with the primers 567F/680R were dominated by *Vibrio*-assigned sequences (59%), followed by *Grimontia* (29%), *Photobacterium* (6%), and *Enterobacter* (6%), all of them except of the last genus are members of *Vibrionaceae*. On the other hand, the clone libraries generated with the primer Vibrio-744F/Vibrio-849R were 100% dominated by *Vibrio*-assigned sequences (Table 5). This indicates that the primer set designed in this study has a higher specificity for the genus *Vibrio*. Employment of the primer set Vibrio-744F/Vibrio-849R might contribute to more accurate estimations of the abundance of *Vibrio* spp. or specific detection of this bacterial group in diverse samples, but not to study the diversity of this group, since most of the obtained cloned sequences were related to one *Vibrio* species (Fig. 18A-B).

Table 5: Taxonomic assignment of the clones. Sequences were generated with the DNA fragments produced by qPCR from MP using the primers sets 567F/680R and Vibrio-744F/Vibrio-849R.

Clon	Primer set	Closest related type strain	Similarity%	Acc. Number
C1-567F	567F/680R	<i>Vibrio sinaloensis</i> CAIM 797 ^T	99.12	DQ451211
C2-567F	567F/680R	<i>Vibrio sinaloensis</i> CAIM 797 ^T	99.12	DQ451211
C3-567F	567F/680R	<i>Enterobacter mori</i> LMG 25706 ^T	95.65	GL890774
C4-567F	567F/680R	<i>Grimontia celer</i> 96-237 ^T	97.37	LT160079
C6-567F	567F/680R	<i>Grimontia celer</i> 96-237 ^T	98.25	LT160079
C8-567F	567F/680R	<i>Vibrio sagamiensis</i> LC2-047 ^T	97.37	AB428909
C10-567F	567F/680R	<i>Vibrio sagamiensis</i> LC2-047 ^T	97.37	AB428909
C17-567F	567F/680R	<i>Vibrio sinaloensis</i> CAIM 797 ^T	100.00	DQ451211
C21-567F	567F/680R	<i>Vibrio pelagius</i> CECT 4202 ^T	100.00	AJ293802
C22-567F	567F/680R	<i>Photobacterium angustum</i> ATCC 25915 ^T	95.61	D25307
C28-567F	567F/680R	<i>Vibrio neocaledonicus</i> NC470 ^T	97.37	JQ934828
C29-567F	567F/680R	<i>Vibrio neocaledonicus</i> NC470 ^T	97.37	JQ934828
C35-567F	567F/680R	<i>Vibrio neocaledonicus</i> NC470 ^T	99.12	JQ934828
C36-567F	567F/680R	<i>Vibrio sinaloensis</i> CAIM 797 ^T	100.00	DQ451211
C39-567F	567F/680R	<i>Grimontia celer</i> 96-237 ^T	98.25	LT160079
C40-567F	567F/680R	<i>Grimontia celer</i> 96-237 ^T	98.25	LT160079
C50-567F	567F/680R	<i>Grimontia celer</i> 96-237 ^T	97.37	LT160079
C2-744F	Vibrio-744F/Vibrio849R	<i>Vibrio gazogenes</i> ATCC 29988 ^T	96.00	X74705
C3-744F	Vibrio-744F/Vibrio849R	<i>Vibrio gazogenes</i> ATCC 29988 ^T	97.17	X74705
C4-744F	Vibrio-744F/Vibrio849R	<i>Vibrio gazogenes</i> ATCC 29988 ^T	95.28	X74705
C5-744F	Vibrio-744F/Vibrio849R	<i>Vibrio gazogenes</i> ATCC 29988 ^T	97.17	X74705
C7-744F	Vibrio-744F/Vibrio849R	<i>Vibrio rarus</i> RW22 ^T	97.14	DQ914239
C8-744F	Vibrio-744F/Vibrio849R	<i>Vibrio gazogenes</i> ATCC 29988 ^T	98.11	X74705
C12-744F	Vibrio-744F/Vibrio849R	<i>Vibrio gazogenes</i> ATCC 29988 ^T	98.11	X74705
C15-744F	Vibrio-744F/Vibrio849R	<i>Vibrio gazogenes</i> ATCC 29988 ^T	96.23	X74705
C18-744F	Vibrio-744F/Vibrio849R	<i>Vibrio gazogenes</i> ATCC 29988 ^T	98.11	X74705
C22-744F	Vibrio-744F/Vibrio849R	<i>Vibrio gazogenes</i> ATCC 29988 ^T	98.11	X74705
C25-744F	Vibrio-744F/Vibrio849R	<i>Vibrio gazogenes</i> ATCC 29988 ^T	96.23	X74705
C28-744F	Vibrio-744F/Vibrio849R	<i>Vibrio gazogenes</i> ATCC 29988 ^T	95.28	X74705
C29-744F	Vibrio-744F/Vibrio849R	<i>Vibrio gazogenes</i> ATCC 29988 ^T	95.28	X74705
C32-744F	Vibrio-744F/Vibrio849R	<i>Vibrio gazogenes</i> ATCC 29988 ^T	97.17	X74705
C34-744F	Vibrio-744F/Vibrio849R	<i>Vibrio gazogenes</i> ATCC 29988 ^T	98.11	X74705
C41-744F	Vibrio-744F/Vibrio849R	<i>Vibrio palustris</i> EAod9 ^T	98.11	KU320862
C44-744F	Vibrio-744F/Vibrio849R	<i>Vibrio gazogenes</i> ATCC 29988 ^T	98.11	X74705

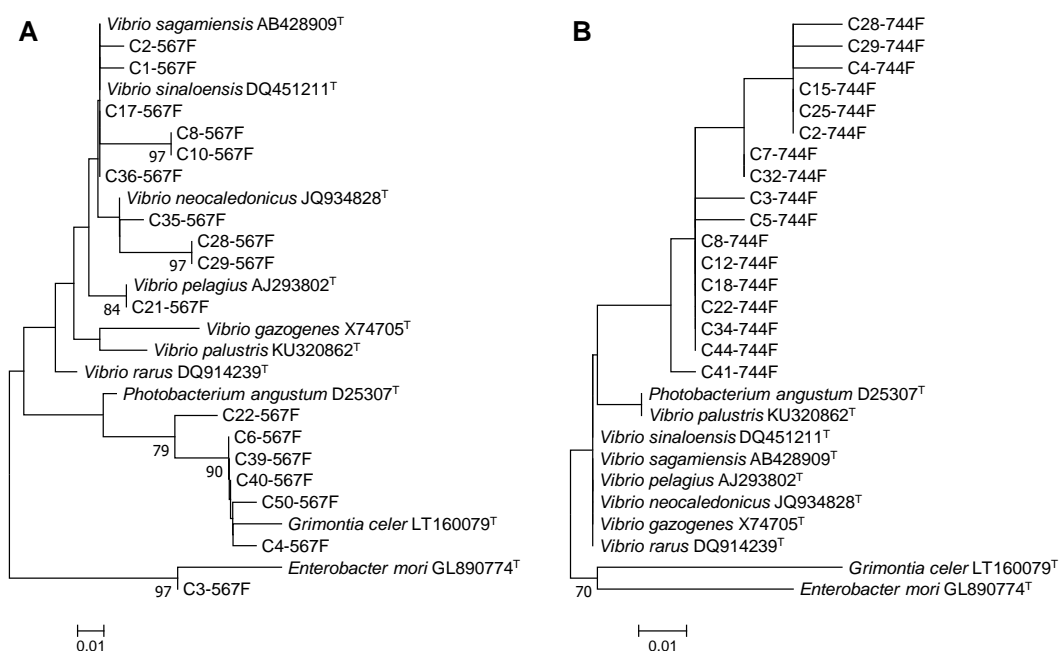


Fig. 18: Phylogenetic affiliation of cloned 16S rRNA gene sequences. NJ phylogenetic trees were calculated in MEGA7 (Kumar *et al.*, 2007) based on the cloned sequences generated with the primer set (A) 567F/680R and (B) Vibrio-744F/Vibrio-849R. The 16S rRNA gene sequences of the closest related type species of the clones were also analysed. Bootstrap values > 70 % based on 100 resamplings are shown at the nodes. Bar: 0.01 substitutions per nucleotide position.

4.1.10 Cultivation-dependent characterization of MP-specific bacteria

For a more detailed characterization of the properties and genetic traits of MP-colonizing bacteria, a cultivation-based approach was applied. In total, 172 heterotrophic isolates were obtained, 41 from MP, 29 from sediments, 17 from detritus, and 85 from the surrounding water (45 of the particle-free, 14 of the particulate, and 26 of the total water fraction). The isolates were differentiated based on partial 16S rRNA gene sequence into 56 phylotypes assigned to 30 genera of the *Alpha* and *Gammaproteobacteria*, *Bacteroidetes*, *Actinobacteria*, and *Firmicutes* (Table 6). All genera were also detected in the cultivation-independent analysis; 145 of the isolates were assigned to 15 genera with a relative abundance > 1% in the amplicon dataset (Fig. 15).

The diversity of bacteria cultured from MP was higher compared to the diversity of bacteria cultured from sediment and detritus particles. Bacteria of 22 phylotypes of 15 genera were isolated from MP, while only 11 phylotypes of 7 genera and 9 phylotypes of 6 genera were isolated from sediment and detritus particles, respectively. In contrast, a more diverse assemblage of bacteria was isolated from water samples, including 41 phylotypes of 26 genera (Table 6). Two genera, *Vibrio* and *Labrenzia*, were isolated from all type of samples. In addition, most of the MP-isolates were assigned to genera also isolated from water samples. Besides isolates of genera *Ruegeria*, *Marinobacter*, and *Bacillus*, obtained from MP, few isolates were also obtained from either sediments or detritus. However, isolates of those genera

obtained from MP represented distinct phylotypes indicating the MP specificity at intra-generic level (Table 6 and Fig. 19). Interestingly, isolates from MP represented three of the four genera, which showed a significantly high relative abundance on MP in the 16S rRNA gene amplicon approach: *Roseivivax* (T3), *Marinobacter* (T4), and *Erythrobacter* (T6), and one genus, *Sulfitobacter* (T23), whose abundant was lower but significantly higher on MP compared to the other samples (Fig. 16).

The highest intra-generic phylogenetic diversity was determined for isolates assigned to the genus *Vibrio* (n = 53), which were assigned to four stable phylotypes (V-1, V-2, V-4, and V-5) and the Harveyi clade (V-3) that contains several species that cannot be differentiated based on 16S rRNA gene sequence phylogeny. Six of the *Vibrio* sp. isolates were cultured from MP, the remaining 47 were cultured from water (30), detritus (12), and sediment particles (5). Only two *Vibrio* spp. phylotypes represented MP-colonizers. Isolates of those two phylotypes clustered with *V. coralliilyticus* and *V. fortis*, respectively. The phylogenetic relationships of all the isolates and their closest related strains are shown in the Fig. 20.

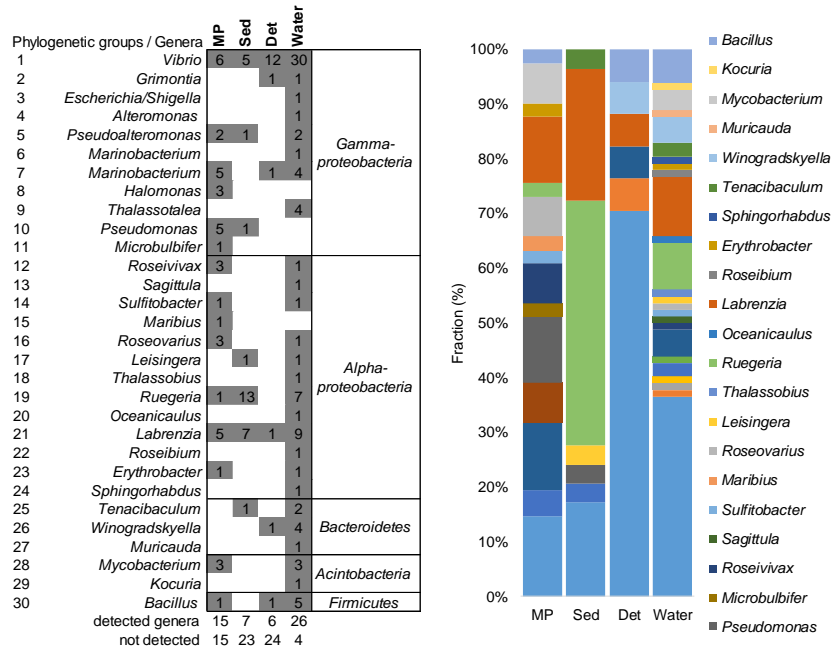
Table 6: Phylotype assignments of the isolated bacteria from the marine system. A BLAST using partial 16S rRNA gene sequences of the isolates was run against the EzBioCloud database to obtain their closest related type strains. Phylotype assignments were done based on 16S rRNA gene sequence similarities in cooperation with Dr. Stefanie Glaeser.

Isolate	Closest related type strain (determined by the EzBioCloud identifier)	16S rRNA gene similarity (%)	Accession Number	Phylo-type	MP	Sed	Det	Water
THAF119	<i>Vibrio coralliilyticus</i> ATCC BAA-450 ^T	99.5	ACZN01000020	V-1				x
THAF135	<i>Vibrio coralliilyticus</i> ATCC BAA-450 ^T	99.5	ACZN01000020	V-1				x
THAF191a	<i>Vibrio coralliilyticus</i> ATCC BAA-450 ^T	99.4	ACZN01000020	V-1	x			
THAF191b	<i>Vibrio coralliilyticus</i> ATCC BAA-450 ^T	99.5	ACZN01000020	V-1	x			
THAF194	<i>Vibrio coralliilyticus</i> ATCC BAA-450 ^T	99.5	ACZN01000020	V-1		x		
THAF231b	<i>Vibrio coralliilyticus</i> ATCC BAA-450 ^T	98.9	ACZN01000020	V-1				x
THAF4	<i>Vibrio coralliilyticus</i> ATCC BAA-450 ^T	99.4	ACZN01000020	V-1	x			
THAF62	<i>Vibrio coralliilyticus</i> ATCC BAA-450 ^T	99.5	ACZN01000020	V-1		x		
THAF64	<i>Vibrio coralliilyticus</i> ATCC BAA-450 ^T	99.5	ACZN01000020	V-1		x		
THAF212	<i>Vibrio coralliilyticus</i> ATCC BAA-450 ^T	99.5	ACZN01000020	V-1				x
THAF100	<i>Vibrio japonicus</i> JCM 31412 ^T	98.6	LC143378	V-2				x
THAF126	<i>Vibrio japonicus</i> JCM 31412 ^T	98.6	LC143378	V-2				x
THAF136	<i>Vibrio japonicus</i> JCM 31412 ^T	98.6	LC143378	V-2				x
THAF137	<i>Vibrio japonicus</i> JCM 31412 ^T	98.6	LC143378	V-2				x
THAF157	<i>Vibrio japonicus</i> JCM 31412 ^T	98.6	LC143378	V-2				x
THAF175	<i>Vibrio japonicus</i> JCM 31412 ^T	98.7	LC143378	V-2				x
THAF213	<i>Vibrio japonicus</i> JCM 31412 ^T	98.6	LC143378	V-2				x
THAF79	<i>Vibrio japonicus</i> JCM 31412 ^T	98.6	LC143378	V-2			x	
THAF174	<i>Vibrio japonicus</i> JCM 31412 ^T	98.6	LC143378	V-2				x
THAF177	<i>Vibrio japonicus</i> JCM 31412 ^T	98.7	LC143378	V-2				x
THAF178	<i>Vibrio japonicus</i> JCM 31412 ^T	98.7	LC143378	V-2				x
THAF18	<i>Vibrio harveyi</i> NBRC 15634 ^T	99.9	BCUF01000119	V-3			x	
THAF19a	<i>Vibrio harveyi</i> NBRC 15634 ^T	99.9	BCUF01000119	V-3			x	
THAF222a	<i>Vibrio harveyi</i> NBRC 15634 ^T	99.9	BCUF01000119	V-3		x		
THAF58	<i>Vibrio harveyi</i> NBRC 15634 ^T	99.8	BCUF01000119	V-3		x		
THAF86	<i>Vibrio harveyi</i> NBRC 15634 ^T	99.8	BCUF01000119	V-3			x	
THAF20	<i>Vibrio harveyi</i> NBRC 15634 ^T	99.9	BCUF01000119	V-3			x	
THAF22	<i>Vibrio harveyi</i> NBRC 15634 ^T	99.9	BCUF01000119	V-3			x	
THAF24	<i>Vibrio alginolyticus</i> NBRC 15630 ^T	99.8	CP006718	V-3			x	
THAF109	<i>Vibrio neocaledonicus</i> NC470 ^T	100.0	JQ934828	V-3				x
THAF145	<i>Vibrio neocaledonicus</i> NC470 ^T	99.5	JQ934828	V-3				x
THAF23	<i>Vibrio neocaledonicus</i> NC470 ^T	99.7	JQ934828	V-3			x	
THAF147	<i>Vibrio neocaledonicus</i> NC470 ^T	99.5	JQ934828	V-3				x
THAF151	<i>Vibrio neocaledonicus</i> NC470 ^T	100.0	JQ934828	V-3				x
THAF207b	<i>Vibrio owensii</i> LMG 25443 ^T	99.7	JPRD01000038	V-3				x
THAF234b	<i>Vibrio owensii</i> LMG 25443 ^T	99.9	JPRD01000038	V-3				x
THAF97	<i>Vibrio owensii</i> LMG 25443 ^T	99.7	JPRD01000038	V-3				x
THAF207a	<i>Vibrio owensii</i> LMG 25443 ^T	99.7	JPRD01000038	V-3				x
THAF234a	<i>Vibrio owensii</i> LMG 25443 ^T	99.9	JPRD01000038	V-3				x

THAF75	<i>Vibrio parahaemolyticus</i> NBRC 12711 ^T	99.6	BBQD01000032	V-3		x	
THAF210	<i>Vibrio parahaemolyticus</i> NBRC 12711 ^T	99.2	BBQD01000032	V-3		x	
THAF230	<i>Vibrio parahaemolyticus</i> NBRC 12711 ^T	99.7	BBQD01000032	V-3			x
THAF211	<i>Vibrio parahaemolyticus</i> NBRC 12711 ^T	99.7	BBQD01000032	V-3			x
THAF232	<i>Vibrio parahaemolyticus</i> NBRC 12711 ^T	99.7	BBQD01000032	V-3			x
THAF125	<i>Vibrio fortis</i> LMG 21557 ^T	99.7	AJ514916	V-4			x
THAF188a	<i>Vibrio fortis</i> LMG 21557 ^T	99.8	AJ514916	V-4	x		
THAF188b	<i>Vibrio fortis</i> LMG 21557 ^T	99.9	AJ514916	V-4	x		
THAF190c	<i>Vibrio fortis</i> LMG 21557 ^T	99.4	AJ514916	V-4	x		
THAF204	<i>Vibrio fortis</i> LMG 21557 ^T	99.9	AJ514916	V-4		x	
THAF88	<i>Vibrio fortis</i> LMG 21557 ^T	99.9	AJ514916	V-4		x	
THAF99	<i>Vibrio fortis</i> LMG 21557 ^T	99.9	AJ514916	V-4			x
THAF92	<i>Vibrio shilonii</i> AK1 ^T	99.7	ABCH01000080	V-5			x
THAF93	<i>Vibrio shilonii</i> AK1 ^T	99.8	ABCH01000080	V-5			x
THAF168	<i>Grimontia indica</i> AK16 ^T	99.5	ANFM02000053	G-1			x
THAF87	<i>Grimontia indica</i> AK16 ^T	99.3	ANFM02000053	G-1		x	
THAF131	<i>Escherichia coli</i> ATCC 11775 ^T	99.5	X80725	E-1			x
THAF114	<i>Thalassotalea loyana</i> CBMAI 722 ^T	100.0	AY643537	Tt-1			x
THAF156	<i>Alteromonas marina</i> SW-47 ^T	99.4	AF529060	A-1			x
THAF186	<i>Pseudoalteromonas luteoviolacea</i> DSM 6061 ^T	100.0	AUYB01000083	Pa-1			x
THAF6	<i>Pseudoalteromonas luteoviolacea</i> DSM 6061 ^T	100.0	AUYB01000083	Pa-1	x		
THAF180	<i>Pseudoalteromonas rubra</i> ATCC 29570 ^T	99.6	X82147	Pa-2			x
THAF3	<i>Pseudoalteromonas ruthenica</i> KMM 300 ^T	99.5	AF316891	Pa-3	x		
THAF14	<i>Pseudoalteromonas ruthenica</i> KMM 300 ^T	99.5	AF316891	Pa-3		x	
THAF106	<i>Neptuniibacter halophilus</i> antiso-13 ^T	94.4	GQ131677	Nep-1			x
THAF162	<i>Marinobacter algicola</i> DG893 ^T	97.8	ABCP01000031	Ma-1			x
THAF217	<i>Marinobacter algicola</i> DG893 ^T	98.5	ABCP01000031	Ma-2			x
THAF105	<i>Marinobacter halotolerans</i> CP12 ^T	98.2	LC009417	Ma-3			x
THAF26	<i>Marinobacter halotolerans</i> CP12 ^T	98.2	LC009417	Ma-3	x		
THAF190a	<i>Marinobacter shengliensis</i> SL013A34A2 ^T	99.1	KF307780	Ma-4	x		
THAF197a	<i>Marinobacter shengliensis</i> SL013A34A2 ^T	99.2	KF307780	Ma-4	x		
THAF39	<i>Marinobacter shengliensis</i> SL013A34A2 ^T	99.0	KF307780	Ma-4	x		
THAF107	<i>Marinobacter shengliensis</i> SL013A34A2 ^T	99.0	KF307780	Ma-4			x
THAF190b	<i>Marinobacter shengliensis</i> SL013A34A2 ^T	99.2	KF307780	Ma-4	x		
THAF19b	<i>Marinobacter xestospongiae</i> UST090418-1611 ^T	99.9	HQ203044	Ma-5		x	
THAF5a	<i>Halomonas denitrificans</i> M29 ^T	98.8	AM229317	H-1	x		
THAF5b	<i>Halomonas denitrificans</i> M29 ^T	98.8	AM229317	H-1	x		
THAF12	<i>Halomonas smvrnensis</i> AAD6 ^T	99.4	AJKS02000002	H-2	x		
THAF187a	<i>Pseudomonas oleovorans</i> subsp. <i>oleovorans</i> DSM 1045 ^T	98.8	NIUB01000072	P-1	x		
THAF42	<i>Pseudomonas oleovorans</i> subsp. <i>lubrificans</i> RS1 ^T	98.8	DQ842018	P-1	x		
THAF13	<i>Pseudomonas oleovorans</i> subsp. <i>lubrificans</i> RS1 ^T	98.8	DQ842018	P-1		x	
THAF187c	<i>Pseudomonas oleovorans</i> subsp. <i>lubrificans</i> RS1 ^T	98.8	DQ842018	P-1	x		
THAF7a	<i>Pseudomonas stutzeri</i> ATCC 17588 ^T	99.9	CP002881	P-2	x		
THAF7b	<i>Pseudomonas stutzeri</i> ATCC 17588 ^T	99.9	CP002881	P-2	x		
THAF38	<i>Microbulbifer variabilis</i> Ni-2088 ^T	99.1	AB167354	Mb-1	x		
THAF103	<i>Roseivivax halotolerans</i> DSM 15490 ^T	99.7	jgi.1085813	Ri-1			x
THAF30	<i>Roseivivax halotolerans</i> DSM 15490 ^T	99.7	jgi.1085813	Ri-1	x		
THAF197b	<i>Roseivivax lentus</i> DSM 29430 ^T	99.4	jgi.1096517	Ri-2	x		
THAF40	<i>Roseivivax lentus</i> DSM 29430 ^T	99.6	jgi.1096517	Ri-2	x		
THAF155	<i>Sagittula stellata</i> E-37 ^T	96.9	AAYA01000003	Sa-1			x
THAF167	<i>Sagittula stellata</i> E-37 ^T	97.0	AAYA01000003	Sa-1			x
THAF111	<i>Sagittula stellata</i> E-37 ^T	97.0	AAYA01000003	Sa-1			x
THAF141	<i>Sagittula stellata</i> E-37 ^T	97.0	AAYA01000003	Sa-1			x
THAF37	<i>Sulfitobacter dubius</i> DSM 16472 ^T	98.1	jgi.1055315	Su-1	x		
THAF158	<i>Sulfitobacter noctilucicola</i> NB-77 ^T	97.1	JASD01000008	Su-2			x
THAF1	<i>Maribius pontilimi</i> GH1-23 ^T	97.2	LT797154	M-1	x		
THAF143	<i>Roseovarius confluentis</i> SAG6 ^T	100.0	KX268605	Ro-1			x
THAF27	<i>Roseovarius confluentis</i> SAG6 ^T	99.5	KX268605	Ro-1	x		
THAF8	<i>Roseovarius confluentis</i> SAG6 ^T	99.2	KX268605	Ro-1	x		
THAF9	<i>Roseovarius confluentis</i> SAG6 ^T	100.0	KX268605	Ro-1	x		
THAF173a	<i>Leisingera caerulea</i> DSM 24564 ^T	98.2	KI421513	L-1			x
THAF202	<i>Leisingera caerulea</i> DSM 24564 ^T	98.2	KI421513	L-1		x	
THAF138	<i>Thalassobius activus</i> CECT 5113 ^T	97.7	CYTO01000011	Tb-1			x
THAF150	<i>Ruegeria arenilitoris</i> CECT 8715 ^T	99.7	FXYG01000008	Ru-2			x
THAF195a	<i>Ruegeria arenilitoris</i> CECT 8715 ^T	99.5	FXYG01000008	Ru-2		x	
THAF54	<i>Ruegeria arenilitoris</i> CECT 8715 ^T	99.7	FXYG01000008	Ru-2		x	
THAF121	<i>Ruegeria atlantica</i> CECT 4292 ^T	99.0	CYPU01000053	Ru-4			x
THAF33a	<i>Ruegeria atlantica</i> CECT 4292 ^T	98.9	CYPU01000053	Ru-4	x		
THAF200a	<i>Ruegeria conchae</i> TW15 ^T	99.7	AEYW01000009	Ru-3		x	
THAF201b	<i>Ruegeria conchae</i> TW15 ^T	99.5	AEYW01000009	Ru-3		x	
THAF203a	<i>Ruegeria conchae</i> TW15 ^T	99.3	AEYW01000009	Ru-3		x	
THAF67	<i>Ruegeria conchae</i> TW15 ^T	99.6	AEYW01000009	Ru-3		x	
THAF203b	<i>Ruegeria conchae</i> TW15 ^T	99.3	AEYW01000009	Ru-3		x	
THAF169	<i>Ruegeria conchae</i> TW15 ^T	99.6	AEYW01000009	Ru-3			x
THAF201a	<i>Ruegeria conchae</i> TW15 ^T	99.7	AEYW01000009	Ru-3		x	

THAF200b	<i>Ruegeria faecimaris</i> HD-28 ^T	98.0	GU057915	Ru-1	x	
THAF57	<i>Ruegeria faecimaris</i> HD-28 ^T	98.1	GU057915	Ru-1	x	
THAF60a	<i>Ruegeria faecimaris</i> HD-28 ^T	98.1	GU057915	Ru-1	x	
THAF60b	<i>Ruegeria faecimaris</i> HD-28 ^T	98.1	GU057915	Ru-1	x	
THAF71	<i>Ruegeria faecimaris</i> HD-28 ^T	98.1	GU057915	Ru-1	x	
THAF129	<i>Ruegeria intermedia</i> DSM 29341 ^T	99.4	jgi.1107789	Ru-6		x
THAF148	<i>Ruegeria mobilis</i> DSM 23403 ^T	99.1	jgi.1108012	Ru-5		x
THAF152	<i>Ruegeria mobilis</i> DSM 23403 ^T	99.4	jgi.1108012	Ru-5		x
THAF122	<i>Ruegeria mobilis</i> DSM 23403 ^T	99.1	jgi.1108012	Ru-5		x
THAF161	<i>Oceanicaulis alexandrii</i> DSM 11625 ^T	98.8	ATUP01000002	O-1		x
THAF183	<i>Labrenzia aggregata</i> IAM 12614 ^T	100.0	AAUW01000037	L-1		x
THAF187b	<i>Labrenzia aggregata</i> IAM 12614 ^T	99.7	AAUW01000037	L-1	x	
THAF35	<i>Labrenzia aggregata</i> IAM 12614 ^T	99.7	AAUW01000037	L-1	x	
THAF17	<i>Labrenzia aggregata</i> IAM 12614 ^T	99.7	AAUW01000037	L-1	x	
THAF193a	<i>Labrenzia aggregata</i> IAM 12614 ^T	99.7	AAUW01000037	L-1	x	
THAF196	<i>Labrenzia aggregata</i> IAM 12614 ^T	99.7	AAUW01000037	L-1	x	
THAF222b	<i>Labrenzia aggregata</i> IAM 12614 ^T	99.7	AAUW01000037	L-1	x	
THAF227	<i>Labrenzia aggregata</i> IAM 12614 ^T	99.7	AAUW01000037	L-1		x
THAF228b	<i>Labrenzia aggregata</i> IAM 12614 ^T	99.7	AAUW01000037	L-1		x
THAF231a	<i>Labrenzia aggregata</i> IAM 12614 ^T	99.7	AAUW01000037	L-1		x
THAF233a	<i>Labrenzia aggregata</i> IAM 12614 ^T	99.7	AAUW01000037	L-1		x
THAF233b	<i>Labrenzia aggregata</i> IAM 12614 ^T	99.7	AAUW01000037	L-1		x
THAF199b	<i>Labrenzia alba</i> CECT 5094 ^T	98.8	CXWA01000023	L-2	x	
THAF205	<i>Labrenzia alba</i> CECT 5094 ^T	99.0	CXWA01000023	L-2	x	
THAF82	<i>Labrenzia alba</i> CECT 5094 ^T	98.8	CXWA01000023	L-2		x
THAF153	<i>Labrenzia alba</i> CECT 5094 ^T	98.8	CXWA01000023	L-2		x
THAF16	<i>Labrenzia alba</i> CECT 5094 ^T	98.8	CXWA01000023	L-2	x	
THAF163	<i>Labrenzia alba</i> CECT 5094 ^T	98.8	CXWA01000023	L-2		x
THAF166	<i>Labrenzia alba</i> CECT 5094 ^T	98.8	CXWA01000023	L-2		x
THAF25	<i>Labrenzia alba</i> CECT 5094 ^T	98.8	CXWA01000023	L-2	x	
THAF31	<i>Labrenzia alba</i> CECT 5094 ^T	98.8	CXWA01000023	L-2	x	
THAF32	<i>Labrenzia alba</i> CECT 5094 ^T	98.8	CXWA01000023	L-2	x	
THAF159	<i>Roseibium hamelinense</i> ATCC BAA-252 ^T	98.4	jgi.1047187	R-1		x
THAF29	<i>Erythrobacter aquimaris</i> SW-110 ^T	99.4	AY461441	Er-1	x	
THAF118	<i>Erythrobacter flavus</i> SW-46 ^T	99.8	AF500004	Er-2		x
THAF215	<i>Sphingorhabdus flavimaris</i> SW-151 ^T	99.1	AY554010	Sp-1		x
THAF113	<i>Tenacibaculum litopenaei</i> B-I ^T	99.8	DQ822567	Te-1		x
THAF115	<i>Tenacibaculum litopenaei</i> B-I ^T	99.5	DQ822567	Te-1		x
THAF199a	<i>Tenacibaculum litopenaei</i> B-I ^T	99.8	DQ822567	Te-1	x	
THAF72	<i>Winogradskyella flava</i> SFD31 ^T	97.3	KX279346	W-1		x
THAF146	<i>Winogradskyella flava</i> SFD31 ^T	97.3	KX279346	W-1		x
THAF154	<i>Winogradskyella flava</i> SFD31 ^T	97.3	KX279346	W-1		x
THAF182	<i>Winogradskyella flava</i> SFD31 ^T	97.3	KX279346	W-1		x
THAF94	<i>Winogradskyella flava</i> SFD31 ^T	97.3	KX279346	W-1		x
THAF160	<i>Muricauda aquimarina</i> JCM 11811 ^T	98.7	RZMZ01000008	Mu-1		x
THAF130	<i>Mycobacterium bacteremicum</i> DSM 45578 ^T	98.9	MVHJ01000059	My-1		x
THAF139	<i>Mycobacterium bacteremicum</i> DSM 45578 ^T	98.9	MVHJ01000059	My-1		x
THAF192	<i>Mycobacterium poriferae</i> ATCC 35087 ^T	100.0	AF480589	My-2	x	
THAF198a	<i>Mycobacterium poriferae</i> ATCC 35087 ^T	100.0	AF480589	My-2	x	
THAF198b	<i>Mycobacterium poriferae</i> ATCC 35087 ^T	100.0	AF480589	My-2	x	
THAF128	<i>Kocuria palustris</i> DSM 11925 ^T	100.0	Y16263	K-1		x
THAF134	<i>Bacillus algalicola</i> KMM 3737 ^T	99.7	AY228462	B-1		x
THAF98	<i>Bacillus algalicola</i> KMM 3737 ^T	99.7	AY228462	B-1		x
THAF89	<i>Bacillus halmapalus</i> DSM 8723 ^T	99.2	KV917375	B-2		x
THAF216a	<i>Bacillus licheniformis</i> ATCC 14580 ^T	99.2	AE017333	B-3		x
THAF216b	<i>Bacillus licheniformis</i> ATCC 14580 ^T	99.4	AE017333	B-3		x
THAF120	<i>Bacillus simplex</i> NBRC 15720 ^T	100.0	BCVO01000086	B-4		x
THAF10	<i>Bacillus zhanjiangensis</i> JSM 099021 ^T	98.4	HM460884	B-5	x	

A



B

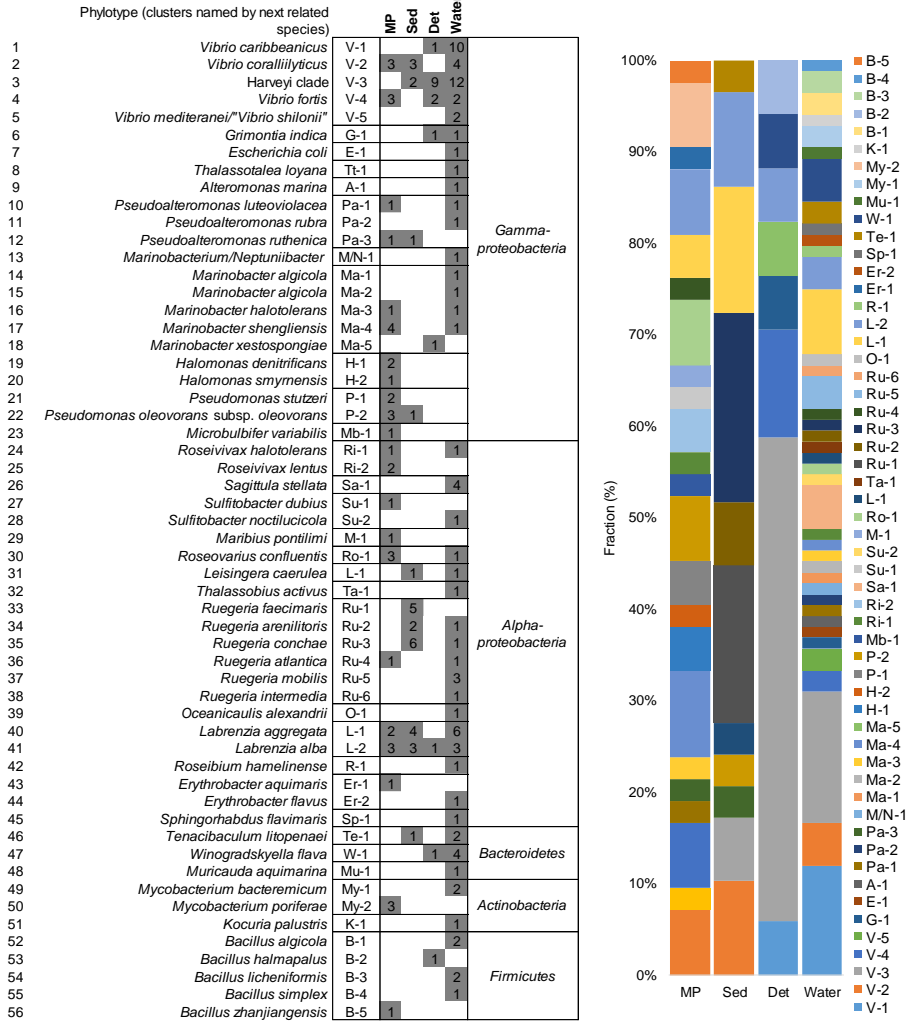
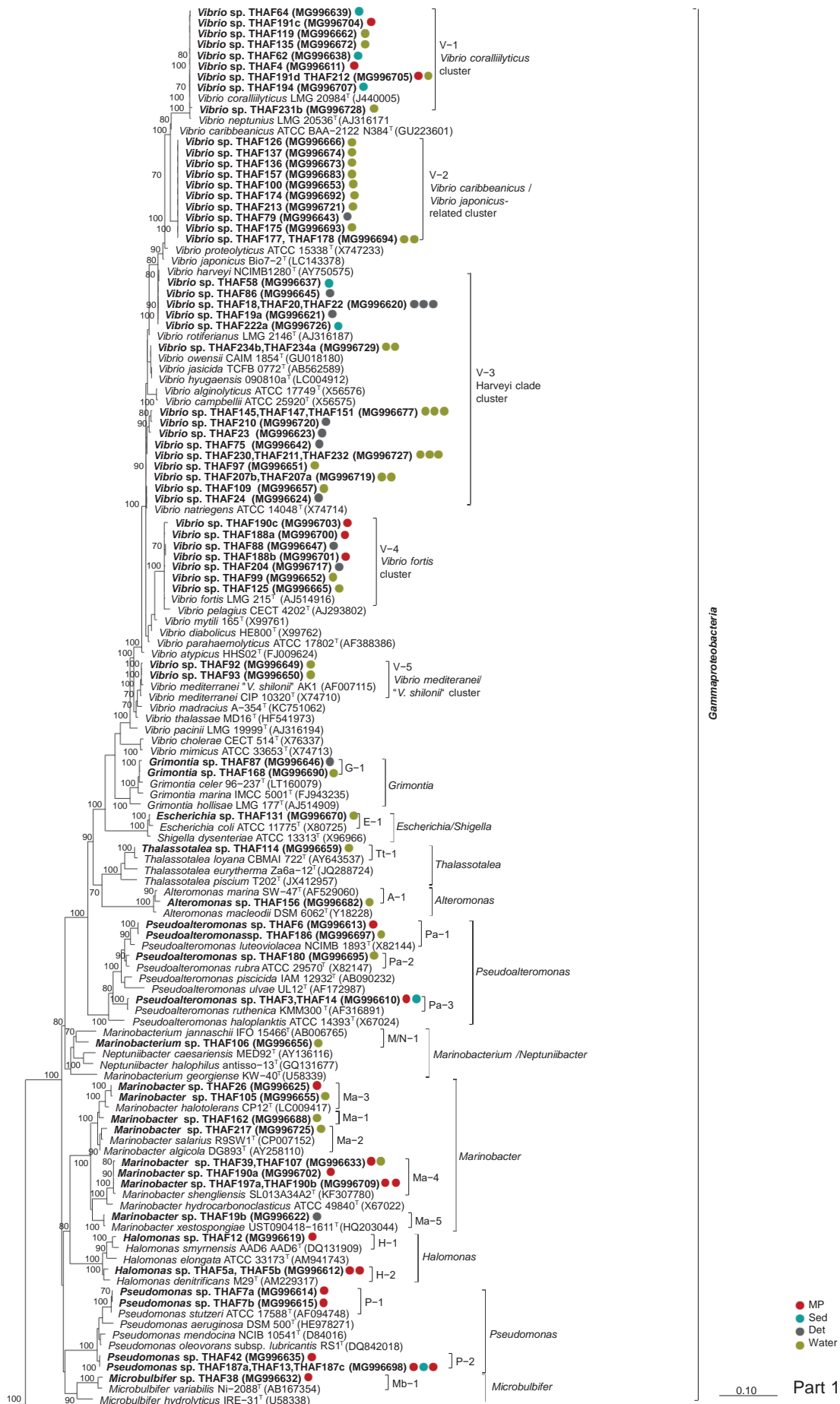
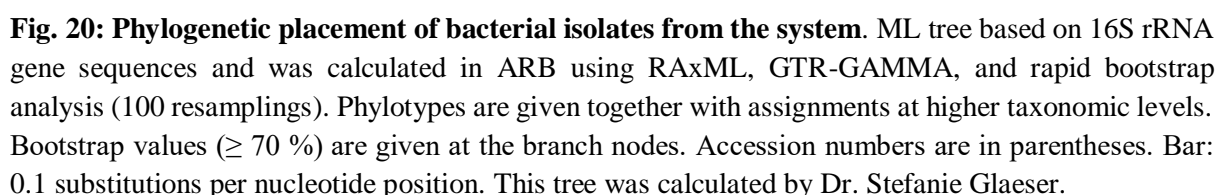


Fig. 19: Diversity of cultured bacteria per sample based on the phylotyping. The phylogenetic assignment at the level of genera (A) and phylotypes (B) were differentiated based on 16S rRNA gene sequence similarities and clustering in the phylogenetic tree.





4.2 Revealing the information contained in the genomes

4.2.1 Genome structure and the genetic potential of MP-colonizing bacteria

The complete genome of 26 isolates isolated from MP were sequenced to study their genetic potential. Six isolates could be assigned at the species level based on ANI values > 95-96% to type strains of species determined as next related based on pairwise 16S rRNA gene sequence similarities (> 98.65%). Those were THAF 3 (*Pseudoalteromonas ruthenica* KMM 300T, AOPM00000000 ANI: 97.9%), THAF7b (*Pseudomonas stutzeri* ATCC 17588T, CP002881, 96.5), THAF12 (*Halomonas smyrnensis* AAD6T, AJKS02000002, 98.2), THAF30 (*Roseivivax halotolerans* DSM 15490T, FOXV00000000, 97.6), THAF191c and THAF191d (*Vibrio coralliilyticus* ATCC BAA-450T, ACZN01000020, 99.5) (Table 7).

Table 7: Main characteristics of complete genomes of MP-colonizers. Information about prophages was obtained from the PHASTER server (Arndt et al., 2016) that, according to their completeness are classified in intact (int), incomplete (inc), or questionable (que). The table was done in cooperation with Dr. Stefanie Glaeser based on the information obtained by Dr. Christian Rückert, Dr. Tobias Busche, Katharina Hanuschka, and Prof. Dr. Jörn Kalinowski. The table continues in the next page.

Strain	Species	Replicon	Accession number	Size	G+C%	Prophage	Prophage proteins
THAF10	<i>Bacillus</i> sp.	Chromosome	CP045403	4,087,834	39.7	3 inc	7/9/8
THAF29	<i>Erythrobacter</i> sp.	Chromosome	CP045392	3,203,870	61.2	2 inc	8/8
THAF12	<i>Halomonas smyrnensis</i>	Chromosome	CP045399	3,799,380	67.5	1 int/1 inc	35/45
		Plasmid pTHAF12_a	CP045400	169,237		1 inc	17
		Plasmid pTHAF12_b	CP045401	47,894		-	-
		Plasmid pTHAF12_c	CP045402	23,068		1 inc	17
THAF5a	<i>Halomonas</i> sp.	Chromosome	CP045417	3,806,748	68.4	1 que	37
THAF187b	<i>Labrenzia</i> sp.	Chromosome	CP045344	6,069,958	59.0	1 int/1 inc	53/39
		Plasmid pTHAF187b_a	CP045345	538,462		-	-
		Plasmid pTHAF187b_b	CP045346	120,832		-	-
		Plasmid pTHAF187b_c	CP045347	93,994		-	-
		Plasmid pTHAF187b_d	CP045348	22,652		-	-
THAF35	<i>Labrenzia</i> sp.	Chromosome	CP045380	6,170,751	58.9	1 int/2 que	63/110/39
		Plasmid pTHAF35_a	CP045381	418,081		-	-
		Plasmid pTHAF35_b	CP045382	152,967		-	-
		Plasmid pTHAF35_c	CP045383	70,393		-	-
THAF1	<i>Maribius</i> sp.	Chromosome	CP045420	3,249,532	63.3	1 int/1 inc/1 que	19/13/20
		Plasmid pTHAF1_a	CP045421	90,721		-	-
THAF197a	<i>Marinobacter</i> sp.	Chromosome	CP045324	4,264,018	57.3	1 int/2 inc/1 que	53/25/11/32
THAF39	<i>Marinobacter</i> sp.	Chromosome	CP045367	4,256,935	57.3	1 int/2 inc/1 que	52/25/11/32
		Plasmid pTHAF39	CP045368	56,331		1 int	54
THAF38	<i>Microbulbifer</i> sp.	Chromosome	CP045369	4,683,451	50.2	2 int/2 que	48/29/19/44
		Plasmid pTHAF38_a	CP045370	102,668		-	-
		Plasmid pTHAF38_b	CP045371	2,647		-	-
THAF192	<i>Mycolicibacterium</i> sp.	Chromosome	CP045325	5,780,554	67.9	1 int	26
		Plasmid pTHAF192_a	CP045326	125,507		-	-
		Plasmid pTHAF192_b	CP045327	110,527		2 inc	9/8
THAF3	<i>Pseudoalteromonas ruthenica</i>	Chromosome	CP045418	3,231,996	47.6	1 int/1 inc	23/49
		Plasmid pTHAF3_a	CP045419	801,066		-	-
THAF187a	<i>Pseudomonas</i> sp.	Chromosome	CP045349	5,298,761	64.8	1 inc	11
THAF42	<i>Pseudomonas</i> sp.	Chromosome	CP045359	5,298,227	64.8	1 inc	11
THAF7b	<i>Pseudomonas stutzeri</i>	Chromosome	CP045416	4,522,538	63.3	3 inc	7/7/11

Strain	Species	Replicon	Accession number	Size	G+C%	Prophage	Prophage proteins
THAF197b	<i>Roseivivax</i> sp.	Chromosome	CP045318	3,794,303	64.1	1 inc/1 que	21/18
		Plasmid pTHAF197b_a	CP045319	234,384		1 inc	8
		Plasmid pTHAF197b_b	CP045320	91,442		1 inc	9
		Plasmid pTHAF197b_c	CP045321	84,228		1 inc	13
		Plasmid pTHAF197b_d	CP045322	30,727		-	-
		Plasmid pTHAF197b_e	CP045323	4,597		-	-
THAF30	<i>Roseivivax halotolerans</i>	Chromosome	CP045389	3,832,321	63.6	1 inc/1 que	19/15
		Plasmid pTHAF30_a	CP045390	73,873		1 inc	9
		Plasmid pTHAF30_b	CP045391	64,857		-	-
THAF40	<i>Roseivivax</i> sp.	Chromosome	CP045360	3,876,119	63.8	2 inc	21/11
		Plasmid pTHAF40_a	CP045361	219,612		1 que	19
		Plasmid pTHAF40_b	CP045362	81,963		-	-
		Plasmid pTHAF40_c	CP045363	65,946		-	-
		Plasmid pTHAF40_d	CP045364	34,238		-	-
		Plasmid pTHAF40_e	CP045365	15,149		-	-
		Plasmid pTHAF40_f	CP045366	4,597		-	-
THAF27	<i>Roseovarius</i> sp.	Chromosome	CP045393	4,195,115	64.1	2 inc	8/24
		Plasmid pTHAF27_a	CP045394	171,913		-	-
		Plasmid pTHAF27_b	CP045395	60,597		-	-
		Plasmid pTHAF27_c	CP045396	23,734		1 inc	12
		Plasmid pTHAF27_d	CP045397	5,571		-	-
		Plasmid pTHAF27_e	CP045398	4,597		-	-
THAF8	<i>Roseovarius</i> sp.	Chromosome	CP045410	4,049,107	64.1	3 inc	10/8/7
		Plasmid pTHAF8_a	CP045411	170,449		-	-
		Plasmid pTHAF8_b	CP045412	115,993		-	-
		Plasmid pTHAF8_c	CP045413	60,595		-	-
		Plasmid pTHAF8_d	CP045414	51,921		-	-
		Plasmid pTHAF8_e	CP045415	4,597		-	-
THAF9	<i>Roseovarius</i> sp.	Chromosome	CP045404	4,074,389	62.9	1 inc/1 que	7/17
		Plasmid pTHAF9_a	CP045405	182,030		-	-
		Plasmid pTHAF9_b	CP045406	135,260		1 inc	10
		Plasmid pTHAF9_c	CP045407	89,971		1 inc	10
		Plasmid pTHAF9_d	CP045408	51,098		-	-
		Plasmid pTHAF9_e	CP045409	27,503		-	-
THAF33	<i>Ruegeria</i> sp.	Chromosome	CP045384	3,455,485	58.1	1 que	20
		Plasmid pTHAF33_a	CP045385	811,101		1 inc	10
		Plasmid pTHAF33_b	CP045386	214,580		-	-
		Plasmid pTHAF33_c	CP045387	78,249		1 inc	10
		Plasmid pTHAF33_d	CP045388	73,543		-	-
THAF37	<i>Sulfitobacter</i> sp.	Chromosome	CP045372	3,447,997	63.3	1 inc	19
		Plasmid pTHAF37_a	CP045373	228,730		1 inc	10
		Plasmid pTHAF37_b	CP045374	181,132		-	-
		Plasmid pTHAF37_c	CP045375	106,274		1 inc	13
		Plasmid pTHAF37_d	CP045376	100,647		-	-
		Plasmid pTHAF37_e	CP045377	98,806		-	-
		Plasmid pTHAF37_f	CP045378	83,443		1 inc	13
		Plasmid pTHAF37_g	CP045379	17,241		-	-
		Chromosome	CP045338	3,313,709		1 int	43
THAF190c	<i>Vibrio</i> sp.	Chromid pTHAF190c_a	CP045339	1,722,714	44.7	-	-
		Plasmid pTHAF190c_b	CP045340	518,670		1 inc	10
		Plasmid pTHAF190c_c	CP045341	181,301		-	-
		Plasmid pTHAF190c_d	CP045342	99,578		-	-
		Plasmid pTHAF190c_e	CP045343	53,318		-	-
THAF191c	<i>Vibrio coralliilyticus</i>	Chromosome	CP046162	3,538,509	45.8	1 int	46
		Chromid pTHAF191c_b	CP046163	1,848,698		-	-
		Plasmid pTHAF191c_c	CP046164	396,310		1 int	12
		Plasmid pTHAF191c_d	CP046165	95,651		2 inc	18/71
THAF191d	<i>Vibrio coralliilyticus</i>	Chromosome	CP046065	3,537,514	45.8	1 int	46
		Chromid pTHAF191d_b	CP046066	1,847,800		-	-
		Plasmid pTHAF191d_c	CP046067	396,761		1 int	12
		Plasmid pTHAF191d_d	CP046068	95,651		3 inc	57/18/30

Nineteen isolates contained 1 to 6 plasmids in addition to the circular chromosomes. Three isolates from the genus *Vibrio* were isolated from MP, and a large plasmid was detected in their genomes, which were assigned as a second chromosome or chromid, according to the

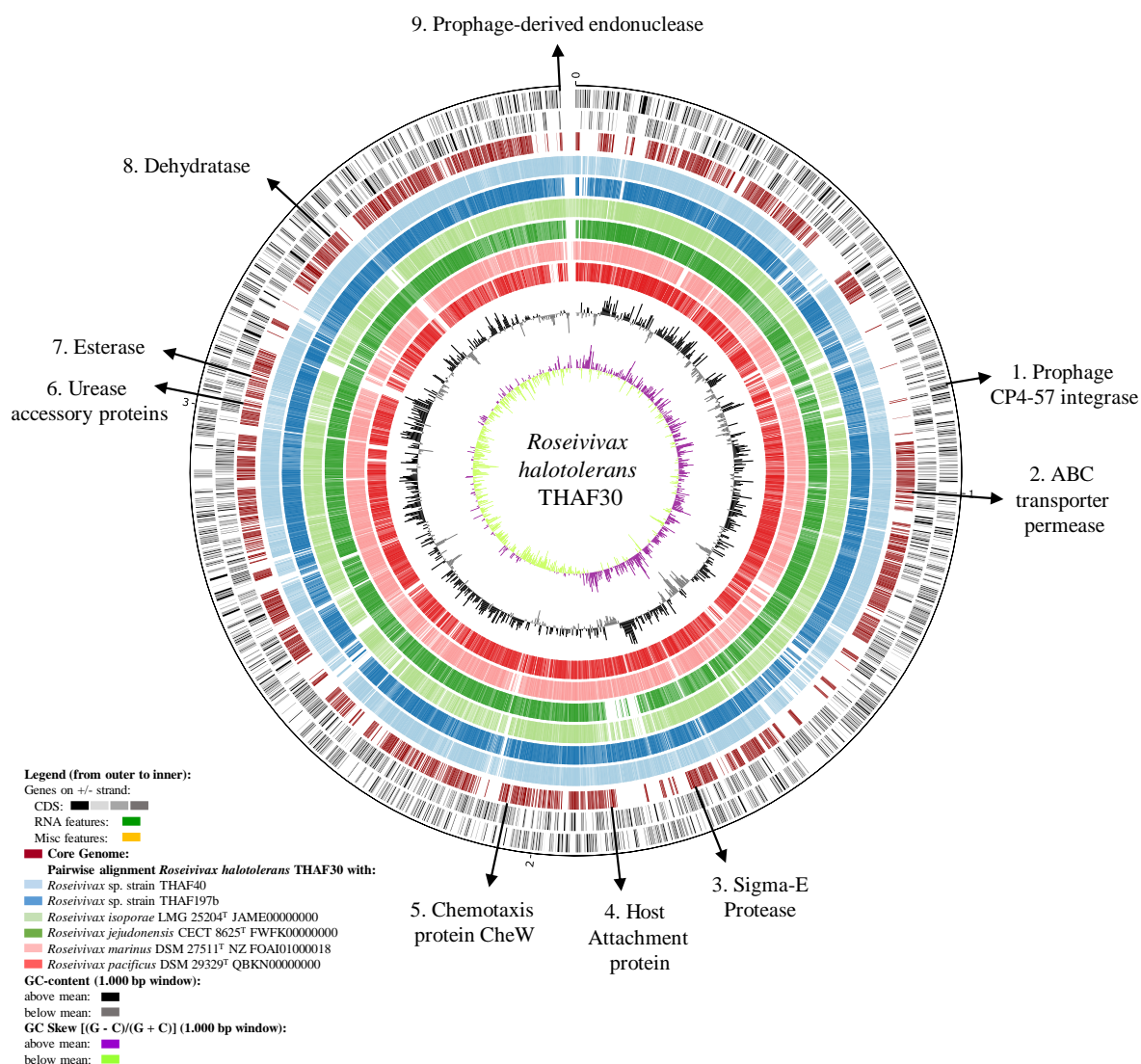
description given by Harrison *et al.*, in 2010, since several housekeeping genes, beside genetic elements typical for plasmids, were contained in these structures. Genomes of all the MP-colonizers contained prophages integrated in the chromosome or in certain plasmids (Table 7). Presence of prophages is important to determine since they are important genetic elements that directly affect, among others, the progression of biofilm formation (Nanda *et al.*, 2015).

In addition to the description of the structure of the genomes, isolates belonging to the genera *Roseivivax*, *Marinobacter*, *Erythrobacter* (abundant MP-colonizers), and *Vibrio*, abundantly isolated from MP were investigated in more detail. Core-genome comparisons per genus including the MP-colonizers and representative strains of the same or next related species (including pathogens) inhabiting marine ecosystems, were performed to detect shared genes potentially involved in the degradation of complex polymers and virulence.

Certain enzymes such as lipases, ureases, dehydratases, esterases, depolymerases, or hydrolases, which are normally associated to the degradation of diverse polymers were detected mainly in genomes of strains belonging to the genera *Roseivivax*, *Marinobacter*, and *Erythrobacter*. On the other hand, pathogenicity-associated genes coding for proteins involved in attachment, chemotaxis, quorum sensing, ABC transporters, type II and IV secretion systems, prophages, etc., were detected mainly in genomes from genera *Marinobacter* and *Vibrio*. Genes derived from prophages such as prophage-derived endonucleases, integrases, or regulatory proteins were found only in the genomes of the strains isolated from the marine system (Table 8). More detailed information of the genes shared among the analysed genomes are shown as circular plots in the Fig. 21 to 24.

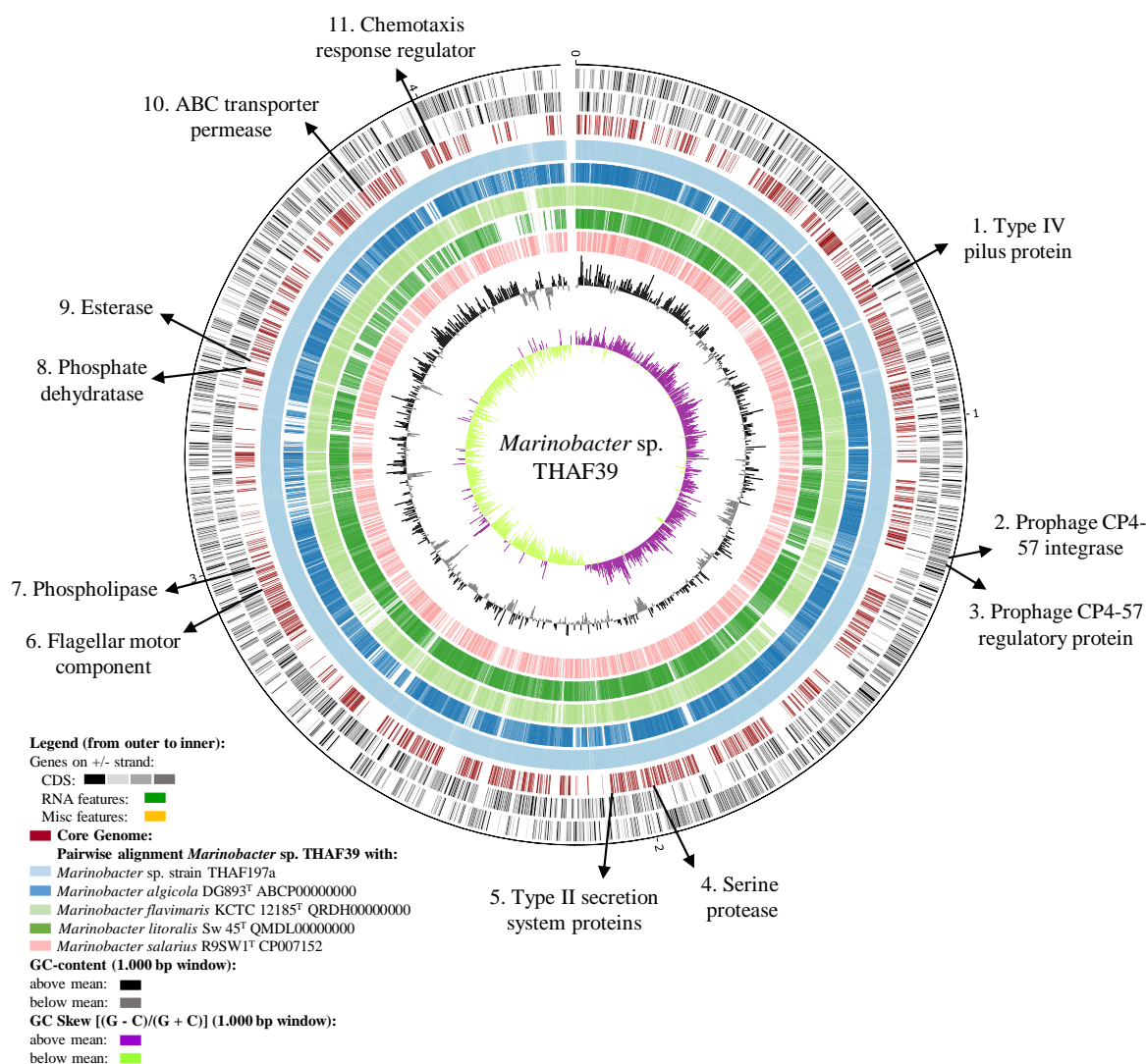
Table 8: Gene products potentially involved in polymer degradation and virulence. These genes were detected in the genomes of the selected MP-colonizers through comparisons with genomes of reference type strains using functions as Genome Browser or PanGenomes implemented in the EDGAR platform (Blom *et al.*, 2016). The respective locus tags of the genes are also listed. For more information see the circular plots (Fig. 21 to 24)

Gene product	<i>Roseivivax</i>	<i>Roseivivax</i> sp.	<i>Marinobacter</i>	<i>Marinobacter</i>	<i>Erythrobacter</i>	<i>Vibrio</i> sp.	<i>Vibrio</i>	<i>Vibrio</i>
	<i>halotolerans</i> THAF30	THAF40	THAF197b	sp. THAF39	sp. THAF197a	sp. THAF29	THAF190c	<i>coralliilyticus</i> THAF191c
(Lyso)phospholipase	FIU91_10560	FIU97_08230	FIU09_08125	FIU96_13885	FIU08_13975	FIU90_05655	-	-
Urease subunit alpha	FIU91_14815	FIU97_12825	FIU09_12505	-	-	-	-	-
Dehydratases	FIU91_16435	FIU97_01890	FIU09_01980	FIU96_15860	FIU08_15950	FIU90_15270	FIV04_14010	GGC03_01160
Esterases	FIU91_15095	FIU97_03250	FIU09_02990	FIU96_15950	FIU08_16040	FIU90_01105	FIV04_02045	GGC03_13545
Depolymerase	-	-	-	-	-	FIU90_03255	-	-
Alpha/beta hydrolase	FIU91_10500	FIU97_08285	FIU09_08180	FIU96_17425	FIU08_17520	FIU90_03010	FIV04_11445	GGC03_04075
Attachment protein	FIU91_09215	FIU97_09140	FIU09_09025	-	-	FIU90_00860	-	-
Chemotaxis proteins	FIU91_10085	FIU97_10230	FIU09_10245	FIU96_18565	FIU08_18660	-	FIV04_09845	GGC03_03655
ABC transporter permease	FIU91_04830	FIU97_04245	FIU09_03985	FIU96_17825	FIU08_17920	FIU90_10975	FIV04_09320	GGC03_10425
Flagellar motor components	-	-	-	FIU96_13660	FIU08_13750	-	FIV04_04160	GGC03_11805
Type II secretion system proteins	-	-	-	FIU96_10075	FIU08_10155	-	FIV04_00580	GGC03_00475
Type IV secretion system proteins	-	-	-	-	-	FIU90_13710	-	-
Type IV pilus protein	-	-	-	FIU96_03280	FIU08_03285	-	FIV04_13705	GGC03_15460
LuxQ system histidine kinase	-	-	-	-	-	-	FIV04_05480	GGC03_07495
LuxR transcriptional regulator	-	-	-	-	-	-	FIV04_06080	GGC03_06780
Prophage-derived endonuclease	FIU91_18920	FIU97_19755	-	-	-	-	-	-
Prophage CP4-57 integrase	FIU91_03930	FIU97_12900	FIU09_12580	FIU96_05840	FIU08_05915	FIU90_07650	-	GGC03_26560
Prophage CP4-57 regulatory protein (AlpA)	-	-	-	FIU96_05855	FIU08_05930	FIU90_07735	-	GGC03_02160
								GGC04_02165



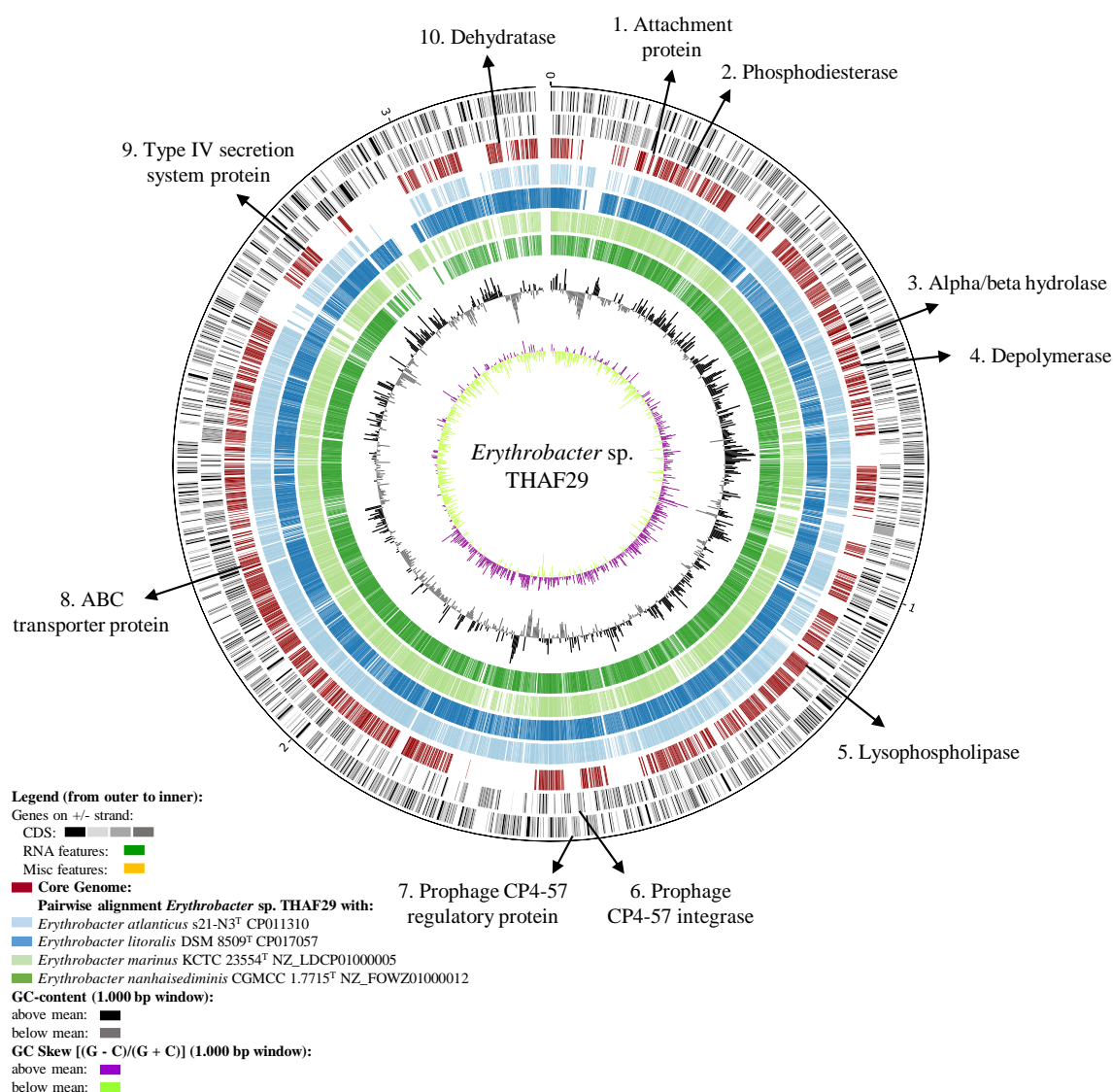
Gene product	<i>Roseivivax halotolerans</i> THAF30	<i>Roseivivax</i> sp. THAF40	<i>Roseivivax</i> sp. THAF197b	<i>Roseivivax isopora</i> LMG 25204 ^T JAME000000000	<i>Roseivivax jejudonensis</i> CECT 8625 ^T FWFK000000000	<i>Roseivivax marinus</i> DSM 27511 ^T NZ FOA101000018	<i>Roseivivax pacificus</i> DSM 29329 ^T QBKN000000000
1. Prophage CP4-57 integrase	FIU91_03930	FIU97_12900	FIV09_12580	-	-	-	-
2. ABC transporter permease	FIU91_04830	FIU97_04245	FIV09_03985	RISW2_17780	ROJ8625_03520	BMX29_RS01790	C8N44_106115
3. Sigma E-protease	FIU91_08250	FIU97_10745	FIV09_10760	RISW2_08030	ROJ8625_01421	BMX29_RS05140	C8N44_108103
4. Host attachment protein	FIU91_09215	FIU97_09140	FIV09_09025	RISW2_23755	ROJ8625_01073	BMX29_RS06025	C8N44_11668
5. Chemotaxis protein CheW	FIU91_10085	FIU97_10230	FIV09_10245	RISW2_07290	ROJ8625_01444	BMX29_RS05030	C8N44_13735
Urease accessory protein UreG	FIU91_14800	FIU97_12810	FIV09_12490	RISW2_18455	ROJ8625_00512	BMX29_RS02995	C8N44_11321
Urease accessory protein UreF	FIU91_14805	FIU97_12815	FIV09_12495	RISW2_18460	ROJ8625_00514	BMX29_RS03000	C8N44_11320
Urease accessory protein UreE	FIU91_14810	FIU97_12820	FIV09_12500	RISW2_18465	ROJ8625_00515	BMX29_RS03005	C8N44_11319
6. Urease subunit alpha	FIU91_14815	FIU97_12825	FIV09_12505	RISW2_18475	ROJ8625_00517	BMX29_RS03015	C8N44_11318
Urease subunit beta	FIU91_14840	FIU97_12835	FIV09_12515	RISW2_18490	ROJ8625_00520	BMX29_RS03030	C8N44_11315
Urease subunit gamma	FIU91_14850	FIU97_12840	FIV09_12520	RISW2_18500	ROJ8625_00522	BMX29_RS03040	C8N44_11313
Urease accessory protein ureD	FIU91_14855	FIU97_12845	FIV09_12525	RISW2_18505	ROJ8625_00523	BMX29_RS03045	C8N44_11312
7. Esterase	FIU91_15095	FIU97_03250	FIV09_02990	RISW2_15380	ROJ8625_02384	BMX29_RS14855	C8N44_13137
8. Dehydratase	FIU91_16435	FIU97_01890	FIV09_01980	RISW2_19600	ROJ8625_02678	BMX29_RS01410	C8N44_101311
9. Prophage-derived endonuclease	FIU91_18920	FIU97_19755	-	-	-	-	-

Fig. 21. Circular visualization of genomes of *Roseivivax* strains. The circular plot illustrates the genes shared by the analysed genomes (core genome = dark red). Position of potential genes involved in complex polymer degradation and virulence in the genomes are highlighted.



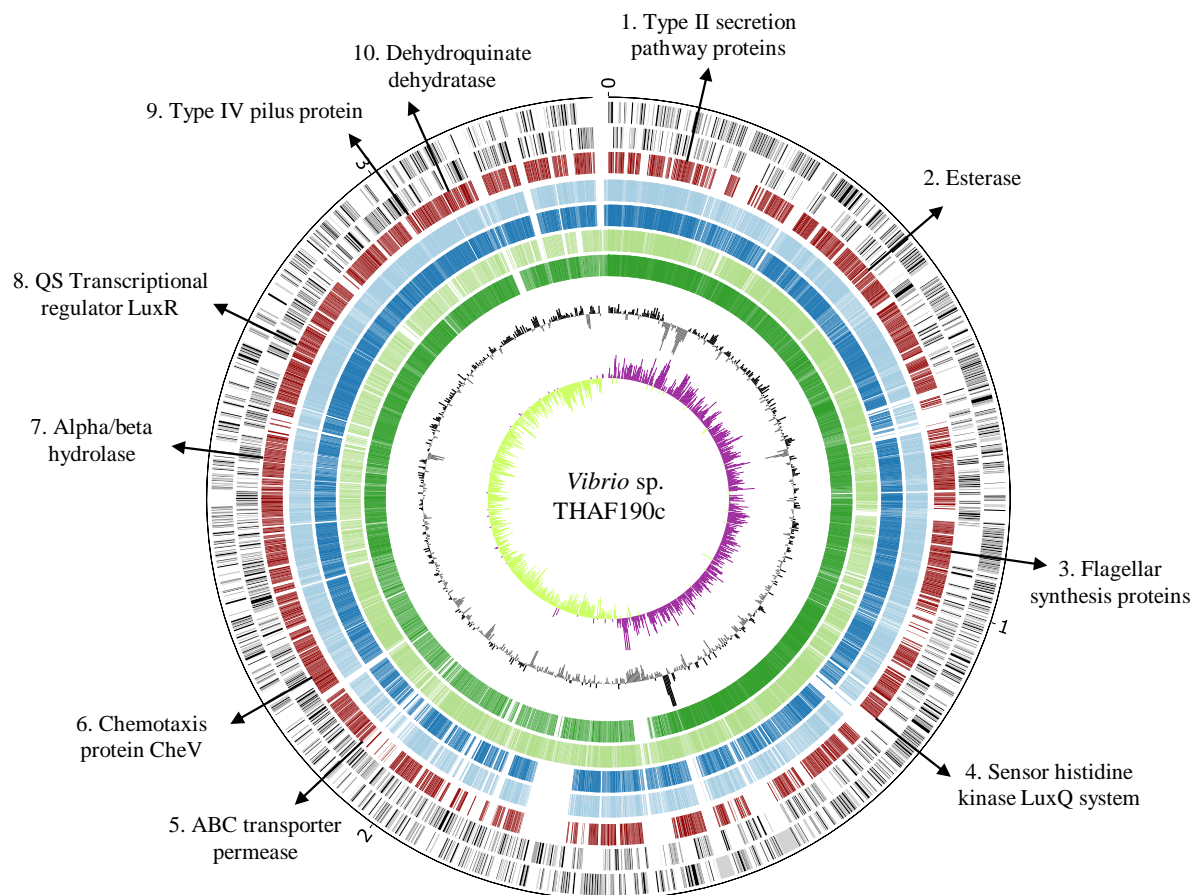
Gene product	<i>Marinobacter</i> sp. THAF39	<i>Marinobacter</i> sp. THAF197a	<i>Marinobacter</i> <i>algicola</i> DG893 ^T ABCP000000000	<i>Marinobacter</i> <i>flavimaris</i> KCTC 12185 ^T QRDH000000000	<i>Marinobacter litoralis</i> SW-45 ^T QMDL000000000	<i>Marinobacter salarius</i> R9SW1 ^T CP007152
1 Type IV pilus protein	FIU96_03280	FIV08_03285	MDG893_13229	DXI23_17125	DOQ08_03098	AU15_19820
2 Prophage CP4-57 integrase	FIU96_05840	FIV08_05915	-	-	-	-
3 Prophage CP4-57 regulatory protein	FIU96_05855	FIV08_05930	-	-	-	-
4 Serine protease	FIU96_09270	FIV08_09350	MDG893_06710	DXI23_04225	DOQ08_00925	AU15_07680
Type II secretion system protein J	FIU96_10075	FIV08_10155	MDG893_07590	DXI23_15275	DOQ08_01062	AU15_15860
Type II secretion system protein I	FIU96_10080	FIV08_10160	MDG893_07595	DXI23_15270	DOQ08_01063	AU15_15865
5 Type II secretion system protein H	FIU96_10085	FIV08_10165	MDG893_07600	DXI23_15265	DOQ08_01064	AU15_15870
Type II secretion system protein F	FIU96_10095	FIV08_10175	MDG893_07610	DXI23_15255	DOQ08_01066	AU15_15880
Type II secretion system protein E	FIU96_10100	FIV08_10180	MDG893_07615	DXI23_15250	DOQ08_01067	AU15_15885
6 Flagellar motor component	FIU96_13660	FIV08_13750	MDG893_01805	DXI23_00925	DOQ08_01379	AU15_00570
7 Phospholipase	FIU96_13885	FIV08_13975	MDG893_02025	DXI23_00725	DOQ08_01418	AU15_00340
8 Phosphate dehydratase	FIU96_15860	FIV08_15950	MDG893_03730	DXI23_11135	DOQ08_01704	AU15_11630
9 Esterase	FIU96_15950	FIV08_16040	MDG893_07090	DXI23_18960	DOQ08_01714	AU15_08160
10 ABC transporter permease	FIU96_17825	FIV08_17920	MDG893_19979	DXI23_12985	DOQ08_02608	AU15_01650
11 Chemotaxis response regulator	FIU96_18565	FIV08_18660	MDG893_18969	DXI23_14175	DOQ08_02472	AU15_05820

Fig. 22. Circular visualization of genomes of *Marinobacter* strains. The circular plot illustrates the genes shared by the analysed genomes (core genome = dark red). Position of potential genes involved in complex polymer degradation and virulence in the genomes are highlighted.



Gene product	<i>Erythrobacter</i> sp. THAF29	<i>Erythrobacter</i> <i>atlanticus</i> s21- N3 ^T CP011310	<i>Erythrobacter</i> <i>litoralis</i> DSM 8509 ^T CP017057	<i>Erythrobacter</i> <i>marinus</i> KCTC 23554 ^T NZ LDCP01000005	<i>Erythrobacter</i> <i>nanhaiediminis</i> CGMCC 1.7715 ^T NZ_FOWZ01000012
1 Attachment protein	FIU90_00860	CP97_03350	Ga0102493_111287	AB731_RS01040	BM173_RS03800
2 Phosphodiesterase	FIU90_01105	CP97_02970	Ga0102493_111200	AB731_RS01300	BM173_RS03535
3 Alpha/beta hydrolase	FIU90_03010	CP97_01555	Ga0102493_11819	AB731_RS02660	BM173_RS02120
4 Polyhydroxyalkanoate depolymerase	FIU90_03255	CP97_01250	Ga0102493_11771	AB731_RS03000	BM173_RS01250
5 Lysophospholipase	FIU90_05655	CP97_12345	Ga0102493_11245	AB731_RS05410	BM173_RS09600
6 Prophage CP4-57 integrase	FIU90_07650	-	-	-	-
7 Prophage CP4-57 regulatory protein	FIU90_07735	-	-	-	-
8 ABC transporter protein	FIU90_10975	CP97_09235	Ga0102493_112350	AB731_RS12080	BM173_RS07545
9 Type IV secretion system protein	FIU90_13710	CP97_13660	Ga0102493_111862	AB731_RS00415	BM173_RS05540
10 Dehydratase	FIU90_15270	CP97_04375	Ga0102493_111509	AB731_RS04285	BM173_RS04215

Fig. 23. Circular visualization of genomes of *Erythrobacter* strains. The circular plot illustrates the genes shared by the analysed genomes (core genome = dark red). Position of potential genes involved in complex polymer degradation and virulence in the genomes are highlighted.



Legend (from outer to inner):

Genes on +/- strand:

CDS:

RNA features:

Misc features:

Core Genome:

Pairwise alignment *Vibrio* sp. THAF190c with:

Vibrio coralliilyticus THAF191c

Vibrio coralliilyticus THAF191d

Vibrio coralliilyticus ATCC BAA 450^T ACZN000000000

Vibrio fortis Dalian14 JFFR000000000

GC-content (1,000 bp window):

above mean:

below mean:

GC Skew [(G - C)/(G + C)] (1,000 bp window):

above mean:

below mean:

Gene product	<i>Vibrio</i> sp. THAF190c	<i>Vibrio coralliilyticus</i> THAF191c	<i>Vibrio coralliilyticus</i> THAF191d	<i>Vibrio coralliilyticus</i> ATCC BAA 450 ^T ACZN000000000	<i>Vibrio fortis</i> Dalian14 JFFR000000000
Type II secretion pathway protein N	FIV04_00580	GGC03_00475	GGC04_00475	VIC_000122	VFDL14_15260
Type II secretion pathway protein M	FIV04_00575	GGC03_00470	GGC04_00470	VIC_000123	VFDL14_15255
Type II secretion pathway protein L	FIV04_00570	GGC03_00465	GGC04_00465	VIC_000124	VFDL14_15250
Type II secretion pathway protein K	FIV04_00565	GGC03_00460	GGC04_00460	VIC_000125	VFDL14_15245
Type II secretion pathway protein J	FIV04_00560	GGC03_00455	GGC04_00455	VIC_000126	VFDL14_15240
Type II secretion pathway protein I	FIV04_00555	GGC03_00450	GGC04_00450	VIC_000127	VFDL14_15235
Type II secretion pathway protein H	FIV04_00550	GGC03_00445	GGC04_00445	VIC_000128	VFDL14_15230
Type II secretion pathway protein G	FIV04_00545	GGC03_00440	GGC04_00440	VIC_000129	VFDL14_15225
Type II secretion pathway protein F	FIV04_00540	GGC03_00435	GGC04_00435	VIC_000130	VFDL14_15220
Type II secretion pathway protein E	FIV04_00535	GGC03_00430	GGC04_00430	VIC_000131	VFDL14_15215
Type II secretion pathway protein D	FIV04_00530	GGC03_00425	GGC04_00425	VIC_000132	VFDL14_15210
Type II secretion pathway protein C	FIV04_00525	GGC03_00420	GGC04_00420	VIC_000133	VFDL14_15205
Esterase	FIV04_02045	GGC03_13545	GGC04_13545	VIC_000767	VFDL14_09095
Flagellar synthesis protein FliB	FIV04_04185	GGC03_11825	GGC04_04345	VIC_001856	VFDL14_07700
Flagellar synthesis protein FliR	FIV04_04180	GGC03_11820	GGC04_04340	VIC_001857	VFDL14_07705
Flagellar synthesis protein FliQ	FIV04_04175	GGC03_11815	GGC04_04335	VIC_001858	VFDL14_07710
Flagellar synthesis protein FliP	FIV04_04170	GGC03_11810	GGC04_04330	VIC_001859	VFDL14_07715
Flagellar synthesis protein FliO	FIV04_04165	GGC03_04320	GGC04_04325	VIC_001861	VFDL14_07720
Flagellar motor switch protein FliN	FIV04_04160	GGC03_11805	GGC04_04320	VIC_001862	VFDL14_07725
Flagellar motor switch protein FliM	FIV04_04155	GGC03_04310	GGC04_04315	VIC_001863	VFDL14_07730
Flagellar synthesis protein FliL	FIV04_04150	GGC03_04305	GGC04_04310	VIC_001864	VFDL14_07735
Sensor histidine kinase LuxQ system	FIV04_05480	GGC03_07495	GGC04_10860	VIC_004549	VFDL14_06460
ABC transporter permease	FIV04_09320	GGC03_10425	GGC04_10420	VIC_004462	VFDL14_02840
Chemotaxis protein CheV	FIV04_09845	GGC03_03655	GGC04_05135	VIC_001701	VFDL14_02310
Alpha/beta hydrolase	FIV04_11445	GGC03_04075	GGC04_04080	VIC_001909	VFDL14_16725
QS Transcriptional regulator LuxR	FIV04_12235	GGC03_13975	GGC04_13975	VIC_000855	VFDL14_15895
Type IV pilus protein	FIV04_13705	GGC03_15460	GGC04_15475	VIC_000080	VFDL14_12145
Dehydroquinase dehydratase	FIV04_14010	GGC03_01160	GGC04_01165	VIC_004966	VFDL14_11835
Prophage CP4-57 integrase	-	GGC03_26560	GGC04_25385	-	-
Prophage CP4-57 regulatory protein	-	GGC03_02160	GGC04_02165	-	-

Fig. 24. Circular visualization of genomes of *Vibrio* strains. The circular plot illustrates the genes shared by the analysed genomes (core genome = dark red). Position of potential genes involved in complex polymer degradation and virulence in the genomes are highlighted.

4.2.2 Putative virulence-associated genes in *Vibrio* spp. genomes

The *Vibrio* spp. strains isolated from MP were investigated in more detail with respect to the presence of putative virulence-associated genes (n = 116) reported in known pathogenic strains of the family *Vibrionaceae*. The pathogenic strains included in the analysis were: *V. coralliilyticus* ATCC BAA-450^T, *V. coralliilyticus* OCN008 (known coral pathogens), *V. cholerae* O1 biovar El Tor str. N16961, *V. parahaemolyticus* RIMD 2210633, *V. vulnificus* CMCP6, and *V. vulnificus* YJ016. Likewise, strains *V. fortis* Dalian14, *Aliivibrio fischeri* ES114 (formerly *V. fischeri*), and *V. diazotrophicus* NBRC 103148^T, not reported as pathogenic strains were studied in parallel. The analysis revealed the presence of 91 genes or gene products for the strains THAF191c and THAF191d (*V. coralliilyticus*), while 70 were found for the strain THAF190c (closest related to *Vibrio fortis*). Most of the detected genes were related to flagella, motility, type IV pilus, ABC transport systems, quorum sensing systems including some of their autoinducers, chemotaxis proteins, type I, II, IV, and VI secretion system proteins, toxins, and enzymes. Genes related to accessory colonisation factors and vibriobactin synthesis and utilization were scarcely detected in the strains isolated from MP (Fig. 25).

Gene / product		1	2	3	4	5	6	7	8	9	10	11	12
Accessory colonization factor	<i>acfA</i>												
	<i>acfB</i>												
	<i>acfC</i>												
	<i>acfD</i>												
Flagella	<i>flaC</i>												
	<i>flaA</i>												
	<i>flgL</i>												
	<i>flgK</i>												
	<i>flgJ</i>												
	<i>flgI</i>												
	<i>flgH</i>												
	<i>flgG</i>												
	<i>flgF</i>												
	<i>flgE</i>												
	<i>flgD</i>												
	<i>flgC</i>												
	<i>flgB</i>												
	<i>flgN</i>												
Motility	<i>motA</i>												
	<i>motB</i>												
	<i>motY</i>												
	<i>motX</i>												
Type IV pilus	<i>pilA</i>												
	<i>pilB</i>												
	<i>pilC</i>												
	<i>pilD</i>												
ABC transport systems	<i>viuP</i>												
	<i>viuD</i>												
	<i>viuG</i>												
	<i>viuC</i>												
	<i>vctP</i>												
	<i>vctD</i>												
	<i>vctG</i>												
Vibriobactin biosynthesis and utilization	<i>vibB</i>												
	<i>vibE</i>												
	<i>vibC</i>												
	<i>vibA</i>												
	<i>vibH</i>												
	<i>vibD</i>												
	<i>viuB</i>												
Chemotaxis	<i>viuA</i>												
	<i>cheR</i>												
	<i>cheV</i>												
	<i>cheW</i>												
	<i>cheB</i>												
	<i>cheA</i>												
	<i>cheZ</i>												
	<i>cheY</i>												

Gene / product		1	2	3	4	5	6	7	8	9	10	11	12
Quorum Sensing	<i>luxS</i>												
	<i>lirR</i>												
	<i>hapR</i>												
	<i>luxR</i>												
	<i>fliA</i>												
	<i>sigE</i>												
	CAI-1 autoinducer synthase												
	Autoinducer sensor LuxN												
	Phosphorelay protein LuxU												
	Autoinducer sensor LuxQ												
Type I Secretion System Proteins	Anti-anti sigma regulatory factor												
	ABC transporter												
	ABC transporter												
	ABC transporter												
	ABC-type amino acid transporter												
	Amino acid ABC transporter												
	Excinuclease ABC												
	Nitrate ABC transporter												
	Outer membrane protein												
	Peptide ABC transporter												
	Peptide ABC transporter												
	ABC-type transport system												
	ABC transporter												
	Outer membrane protein												
	Sugar ABC transporter												
	Urea ABC transporter												
	Urea ABC transporter												
	Vitamin B12 ABC transporter												
Type II Secretion System Proteins	<i>epsN</i>												
	<i>epsM</i>												
	<i>epsL</i>												
	<i>epsK</i>												
	<i>epsJ</i>												
	<i>epsI</i>												
	<i>epsH</i>												
	<i>epsG</i>												
	<i>epsF</i>												
	<i>epsE</i>												
	<i>epsC</i>												
	General secretion pathway												
Type IV Secretion System Proteins	<i>mshG</i>												
	<i>mshQ</i>												
	<i>rcpC/cpaB</i>												
	<i>tadD</i>												
Type VI Secretion System Proteins	<i>tssF</i>												
	<i>impB</i>												
	Lipoprotein												
	FHA domain protein												
	ABC transporter binding protein												
Toxins and enzymes	<i>ace</i>												
	<i>ctxA</i>												
	<i>ctxB</i>												
	<i>vvhA</i>												
	<i>rtxA</i>												
	<i>rtxC</i>												
	<i>rtxB</i>												
	<i>rtxD</i>												
	<i>tlh</i>												
	<i>zot</i>												
	<i>toxR</i> -like												
	<i>toxR</i>												
	<i>rseP</i>												
	<i>degS</i>												
	<i>hap/vvp</i>												
	<i>nanH</i>												
	Stomatin-like												
	Hemolysin												

Present

Absent

Figure 25. Presence and absence of putative virulence-associated genes in *Vibrio* strains. (1) *Vibrio* sp. THAF190c, (2) *V. coralliilyticus* THAF191c, (3) *V. coralliilyticus* THAF191d, (4) *V. coralliilyticus* ATCC BAA-450^T, (5) *V. coralliilyticus* OCN008, (6) *V. fortis* Dalian14, (7) *V. cholerae* O1 biovar El Tor str. N16961, (8) *V. parahaemolyticus* RIMD 2210633, (9) *V. vulnificus* CMCP6, (10) *V. vulnificus* YJ016 (11) *A. fischeri* ES114, (12) *V. diazotrophicus* NBRC 103148^T.

4.3 The genus *Vibrio* as a key member of the marine system

The genus *Vibrio* was selected to perform a deep analysis due to its ubiquity in marine environments, present a wide range of marine habitats and playing key roles in the health of ecosystems as coral reefs, where numerous members of the genus participate in coral diseases. The isolation of *Vibrio* spp. was performed as described in the section 3.1.11, allowing the cultivation of several strains from all the analysed sample types. As the taxonomy of the group is challenging, a MLSA approach, as well as core genome-based phylogeny was applied to the isolates to determine the diversity of *Vibrio* spp. in the marine system.

4.3.1 High diversity of *Vibrio* spp. phylotypes detected in the marine system

A total of 53 *Vibrio* spp. isolates were cultured from the different particles and water fractions of the studied marine system: six isolates from MP, five from sediments, 12 from detritus, and 30 from the surrounding aquarium water. Isolates from the water were either cultured from the particulate-water fraction (5 isolates), the particle-free water fraction (15 isolates), or the total water fraction (10 isolates). Phylogenetic assignment based on partial 16S rRNA gene sequences, placed the isolates into 5 phylogenetic groups (V-1 to V-5) within the genus *Vibrio* (Table 9).

Four out of the five groups formed distinct clusters in the ML tree calculated based on nearly full length 16S rRNA gene sequences and shared a high 16S rRNA gene sequence similarity among each other (> 99 %). Those groups were assigned as phylotypes, named according to a respective *Vibrio* species if the type strain of a species was placed within the cluster. The differentiation of the phylotype clusters was supported by high bootstrap values (70-100 %) in the ML tree (Fig. 26) and the presence of the same clusters in a NJ tree calculated in parallel (data not shown). Ten isolates were assigned to phylotype V-1 including MP (n=3), sediment (3), and water (4) isolates. The V-1 isolates clustered together with the type strain of *V. coralliilyticus* (99.9 to 100 % pairwise 16S rRNA gene sequence similarities). Eleven isolates were assigned to phylotype V-2 including water (10) and detritus (1) isolates. The isolates of V-2 shared identical 16S rRNA gene sequences and showed highest phylogenetic relationship to the type strains of the species *Vibrio caribbeanicus* (97.9 - 98.4 %) and *Vibrio japonicus* (98.4 - 98.5 %). The type strains of those species were not placed within the V-2 cluster but on separate branches next to it. The phylotype V-2 was therefore named as *V. caribbeanicus* / *V. japonicus*-related cluster. The phylotype V-4 contained 7 isolates cultured from MP (3), detritus (2), and water (2) and clustered with the type strain of *Vibrio fortis* (*V. fortis* cluster). V-4 isolates shared 99.4 to 100 % 16S rRNA gene sequence similarity among each other and with the type strain of *V. fortis*. Two isolates from the non-pre-treated water (total water fraction) clustered together with type strains of *V. mediterranei* / "*V. shilonii*" and formed the V-5 (*V. mediterranei* / "*V. shilonii*") phylotype. These isolates shared 99.8 % 16S rRNA gene sequence similarity among each other and 99.6 % with the type strains of *V. mediterranei* / "*V. shilonii*".

The remaining 23 *Vibrio* spp. isolates from sediments (2), detritus (9), and water (12) were placed within the so-called Harveyi clade and assigned as Harveyi clade cluster V-3. *Vibrio* spp. of this clade cannot be clearly differentiated based only on the 16S rRNA gene sequence phylogeny. Seven of the V-3 isolates (two from sediments and five from detritus) formed a distinct sub-cluster with the type strain of *Vibrio harveyi* (phylotype V-3.1). The isolates shared identical 16S rRNA gene sequences among each other and with the type strain of *V. harveyi*. The remaining isolates placed into the Harveyi clade shared 98.0 to 100% 16S rRNA gene sequence similarities among each other and with type strains of species of the clade.

Table 9: Overview of *Vibrio* spp. phylotypes and number of isolates per sample. Intra-phylotype pairwise sequence similarities based on partial 16S rRNA gene sequences and partial concatenated nucleotide and amino acid sequences of five protein-coding genes are depicted. Similarity values represent ranges of pairwise sequence similarities among phylotype isolates and values given in brackets are ranges of pairwise sequence similarities of the phylotype isolates to next related type strain placed within a phylotype cluster. In addition, the similarity value to the next related type strain beside the phylotype cluster is given. This table was done in cooperation with Dr. Stefanie Glaeser.

Phylo- type	Phylotype assignment based on 16S rRNA gene and MLSA phylogeny	Range of pairwise 16S rRNA gene sequence similarities	MLSA Intra-phylotype pairwise sequence (nucleotide sequence)	MLSA Intra-phylotype pairwise sequence (amino acid sequence)	MP	Sed	Det	FL	PA	Total water	Total number of isolates
V-1	<i>Vibrio coralliilyticus</i> cluster	99.4 - 100 % (99.9 - 100 % to <i>Vibrio coralliilyticus</i>)	99.5 - 99.9 % (98.8 - 98.9 % <i>Vibrio coralliilyticus</i>) (-)	99.6 - 100 % (99.8 - 99.9 % <i>Vibrio coralliilyticus</i>) (Next outside the cluster < 96 %)	3	3		3	1		10
V-2	<i>Vibrio caribbeanicus</i> / <i>Vibrio japonicus</i> - related cluster	100% (97.9 - 98.4 % to <i>Vibrio caribbeanicus</i> / 98.4 - 98.5 % to <i>Vibrio japonicus</i>)	99.9 - 100 % (-) (Next outside the cluster: < 90 % <i>Vibrio caribbeanicus</i>)	100% (-) (Next outside the cluster: 95.2 % <i>Vibrio coralliilyticus</i>)			1	5		5	11
V-3.1	<i>Vibrio harveyi</i> cluster	100% (100 % to <i>Vibrio harveyi</i>)	99.9 - 100 % (99.3 % <i>Vibrio harveyi</i>) (Next outside the cluster: < 90 %)	100% (100 % <i>Vibrio harveyi</i>) (Next outside the cluster: < 98.6 %)		2	5				7
V-3.2	<i>Vibrio owensii</i> cluster	98.0 - 100 % (98.0 - 100 % Harveyi clade species type strains)	99.1 - 100 % (98.5 - 99 % <i>Vibrio owensii</i>) (Next outside the cluster < 95%)	99.9 - 100 % (99.9 - 100 % <i>Vibrio owensii</i>) (Next outside the cluster < 98.6%)			2	4	3	1	10
V-3.3	<i>Vibrio alginolyticus</i> cluster	98.0 - 100 % (98.0 - 100 % Harveyi clade species type strains)	99.9 - 100 % (99.6 % <i>Vibrio alginolyticus</i> (Next outside the cluster 95.5% <i>Vibrio diabolicus</i>)	99.0 - 100 % (99.9 - 100 % <i>Vibrio alginolyticus</i>) (Next outside the cluster 99.6 - 99.7 % <i>Vibrio diabolicus</i>)			2	3		1	6
V-4	<i>Vibrio fortis</i> cluster	99.4 - 100 % (99.4 - 100 % to <i>Vibrio fortis</i>)	98.3 - 99.9 % (98.2 - 99 % <i>Vibrio fortis</i>) (-)	100% (100 % <i>Vibrio fortis</i>) (-)	3		2		1	1	7
V-5	<i>Vibrio mediterranei</i> / “ <i>Vibrio shilonii</i> ” cluster	99.8% (99.6 % to <i>Vibrio mediterranei</i> / “ <i>Vibrio shilonii</i> ”)	100% (98.6 - 99.5 % <i>Vibrio mediterranei</i> / “ <i>Vibrio shilonii</i> ”) (94.9 % <i>Vibrio barjaei</i>)	100% (99.8 - 100 % <i>Vibrio mediterranei</i> / “ <i>Vibrio shilonii</i> ”) (98.9 % <i>Vibrio barjaei</i>)						2	2

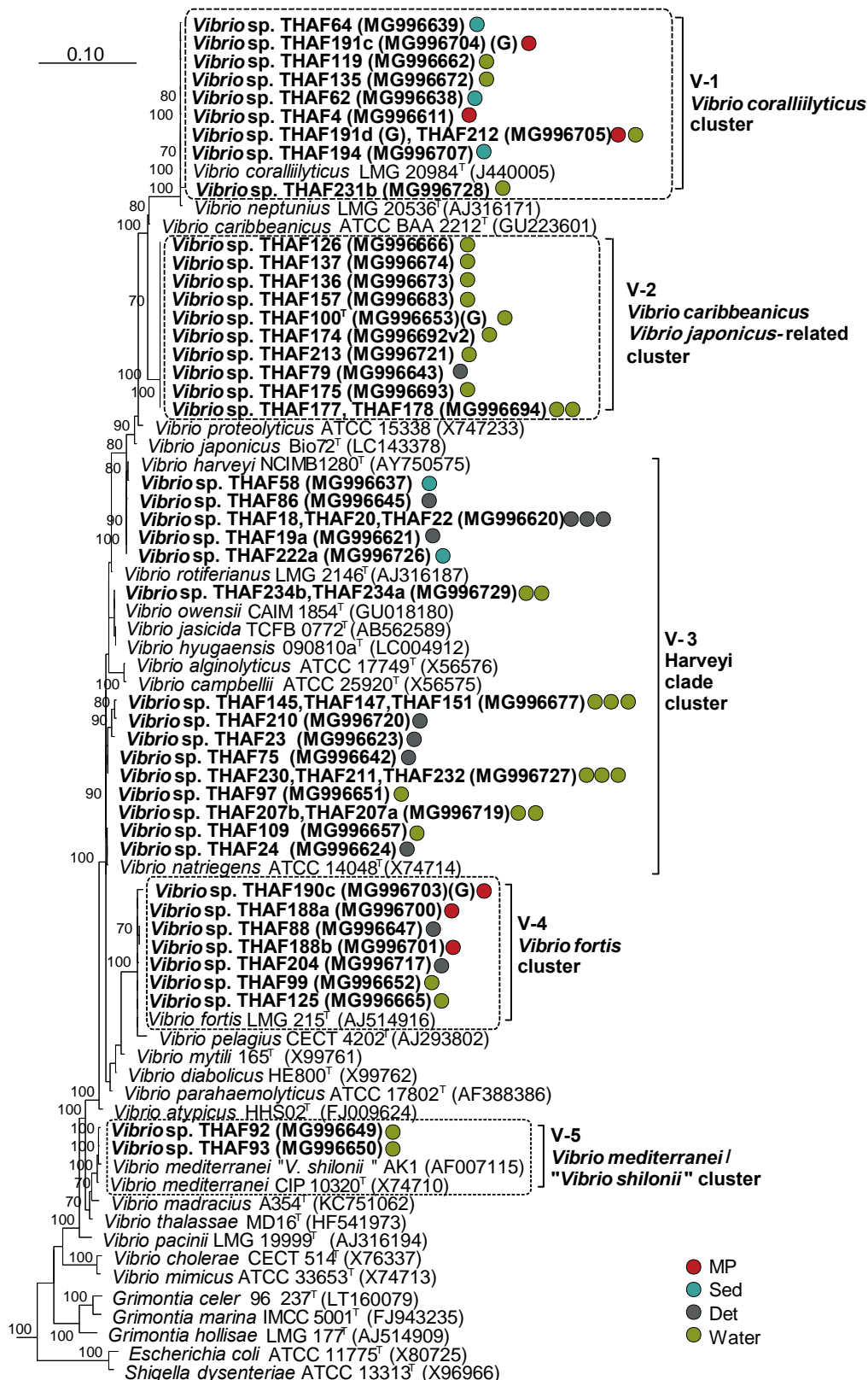


Fig. 26: Phylogenetic placement of the *Vibrio* spp. isolated from the marine system. ML tree calculated in ARB using RAxML, GTR-GAMMA, and rapid bootstrap analysis (100 resamplings). Bootstrap values (> 70 %) are given at the branch nodes. The GenBank accession numbers are given in parentheses. The type strains of *Escherichia coli* and *Shigella dysenteriae* were used as out-group. Bar, number of substitutions per nucleotide positions. This tree was calculated by Dr. Stefanie Glaeser.

4.3.2 MLSA-based phylogeny of *Vibrio* spp. isolates

V. japonicus could not be included in the five gene-based MLSA approach, since no genome sequence was available. Instead, partial sequences of the genes *recA*, *pyrH*, and *gyrB* of the type strain are available and were used for MLSA. The analysis based on concatenated sequences of these three genes (1953 nt / 651 aa) showed that in both trees, strains belonging to phylotype V-2 were placed distantly from *V. japonicus* and closer to *V. caribbeanicus* (data not shown). For this reason, the type strain of *V. japonicus* was excluded from the MLSA phylogeny based on concatenated partial nucleotide and amino acid sequences of genes *recA*, *pyrH*, *rpoD*, *gyrB*, and *rctB* (3757 nt / 1120 aa).

These trees confirmed the phylogenetic assignment of the phylotypes V-1, V-2, V-4, and V-5, obtained by 16S rRNA gene sequence phylogeny. In addition, the Harveyi clade (V-3 cluster) isolates could be distinguished into three sub clusters (phylotypes). The *V. harveyi* phylotype V-3.1, obtained already in the 16S rRNA gene sequence-based phylogeny, and two further phylotypes. Six of the remaining V-3 isolates (one isolated from detritus and five from water) formed a distinct sub-cluster with the type strain of *V. owensii* (*V. owensii* phylotype V-3.2). The remaining four Harveyi clade isolates (two isolated from detritus and two from water) formed a distinct sub-cluster with the type strain of *V. alginolyticus* (*V. alginolyticus* phylotype V-3.2). The topology of the nucleotide- and amino acid-based trees was highly conserved and all clusters including the isolated strains were supported by high bootstrap values ($\geq 70\%$) (Fig. 27A-B).

The isolates of six out of seven phylotypes (all except V-2) formed defined and stable clusters including the type strains of the species naming the phylotype in the nucleotide- and amino acid-based phylogenetic trees. This was also confirmed by phylogenetic trees calculated with the NJ method (data not shown). The *V. caribbeanicus* / *V. japonicus*-related phylotype V-2 was, based on the MLSA, distinct to all current *Vibrio* species. In the nucleotide-based MLSA tree, the phylotype was placed in a distinct branch next to the type strain of *V. caribbeanicus* (Fig. 27A). No clustering with that or other type strains was obtained for the V-2 cluster in the amino acid-based MLSA tree (Fig. 27B). Similar clustering of the isolated *Vibrio* spp. and type strains was observed in trees constructed based on individual genes (Fig. 28-32). However, not all the clusters were stable and several strains were misplaced in clusters formed by defined *Vibrio* clades. Due to the short sequences and the more conservative character of the amino acid sequences, it was observed that several clusters could not be resolved, especially for the Harveyi clade strains in the trees based on single genes *recA* and *pyrH*. The accession numbers of the gene sequences used for the MLSA are listed in the Table 10.

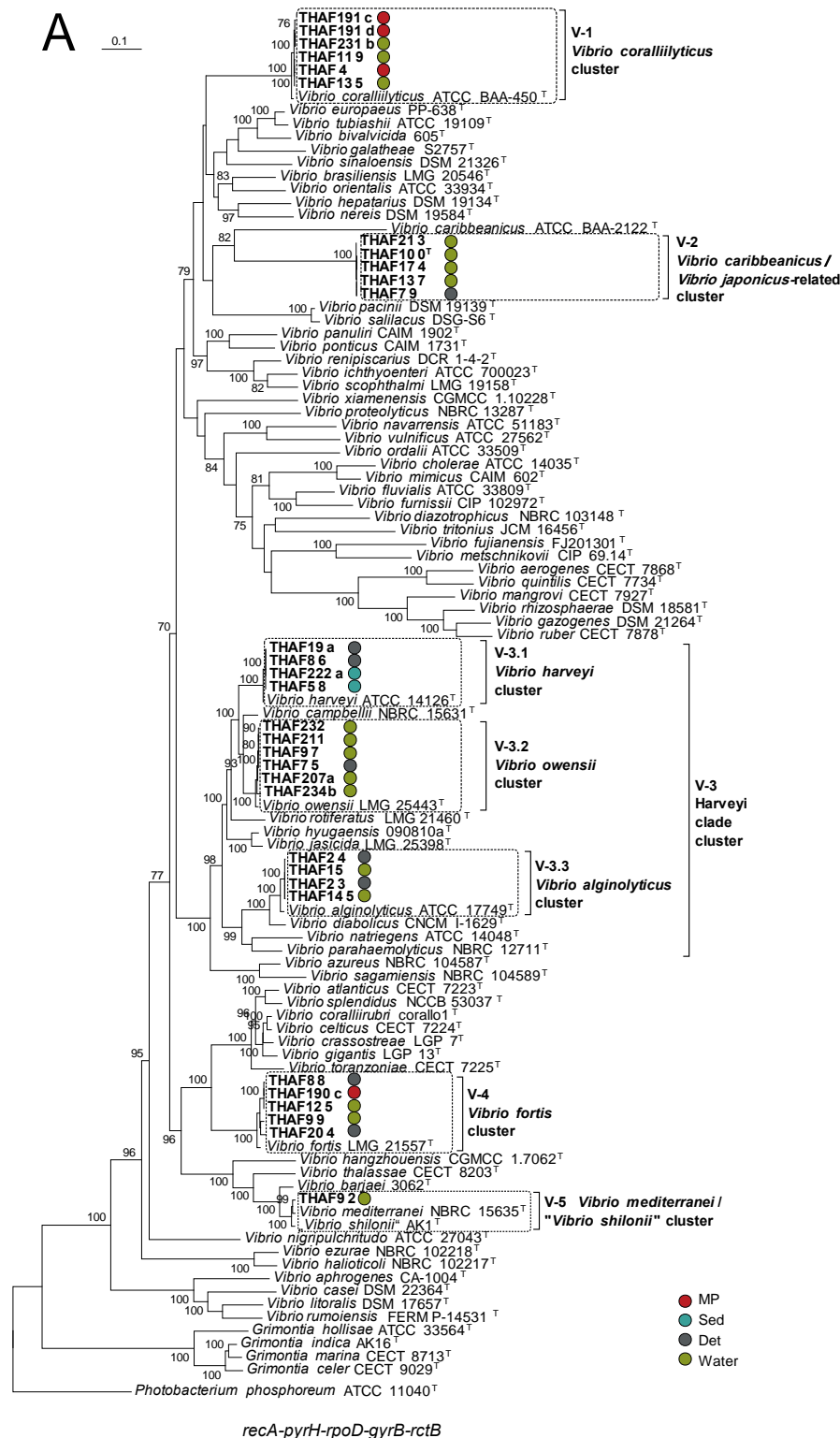
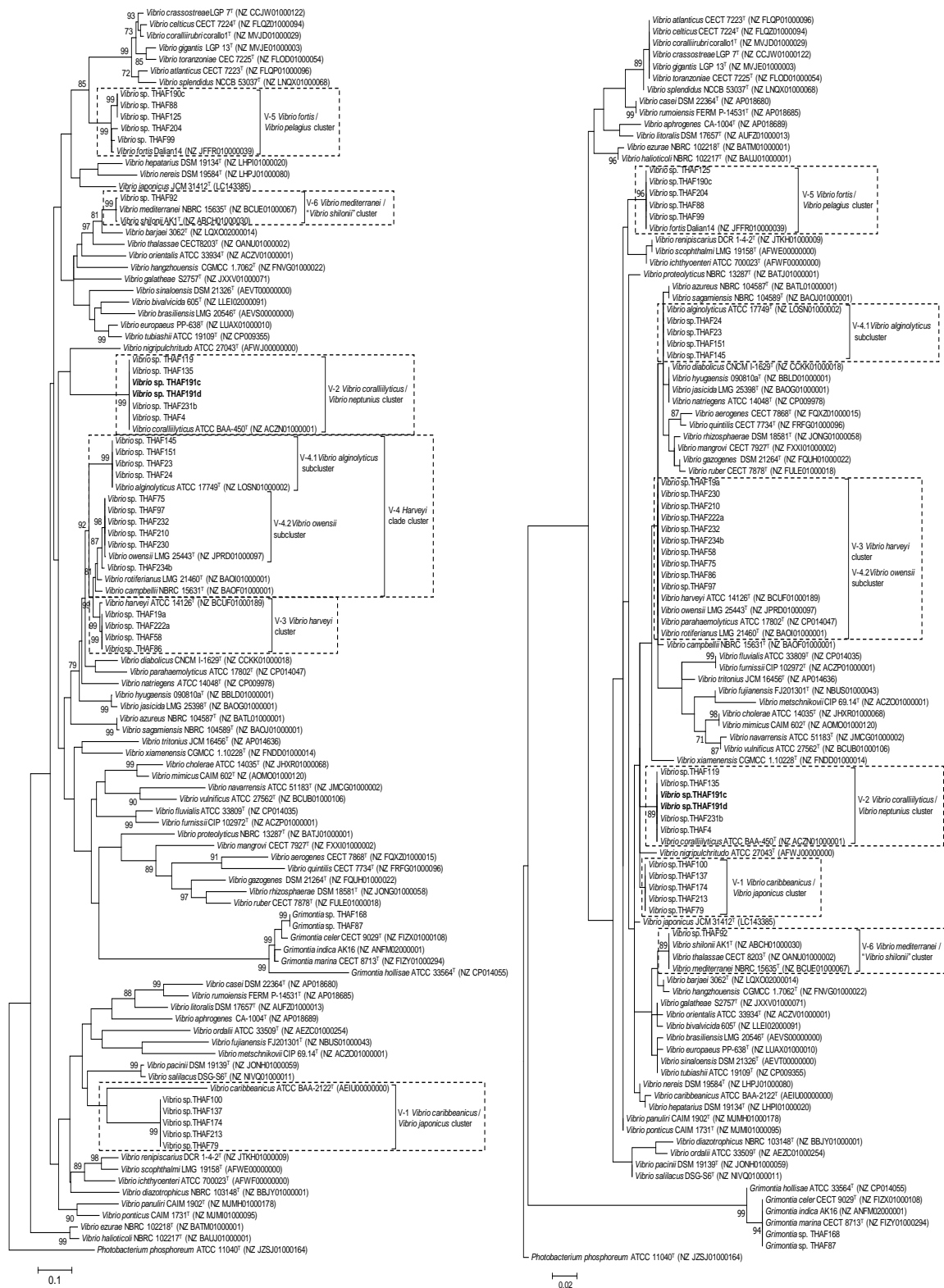


Fig. 27A. Phylogenetic placement of *Vibrio* spp. based on MLSA with five 5 genes. The tree was calculated based on concatenated partial sequences of *recA*, *pyrH*, *rpoD*, *gyrB*, and *rctB* at nucleotide level using the ML algorithm and the GTR evolutionary model (nucleotide sequences) in MEGA7. Bootstrap values (> 70 %) based on 100 resamplings are shown at branch nodes. *Photobacterium phosphoreum* ATCC 11040^T was used as out-group. Bars, number of substitutions per nucleotide or amino acid sequence positions. This tree was done by Angel Franco and edited by Dr. Stefanie Glaeser.



Fig. 27B. Phylogenetic placement of *Vibrio* spp. based on MLSA with five 5 genes. The tree was calculated based on concatenated partial sequences of *recA*, *pyrH*, *rpoD*, *gyrB*, and *rctB* at amino acid level using the ML algorithm and the JTT evolutionary model (amino acid sequences) in MEGA7. Bootstrap values (> 70 %) based on 100 resamplings are shown at branch nodes. *Photobacterium phosphoreum* ATCC 11040^T was used as out-group. Bars, number of substitutions per nucleotide or amino acid sequence positions. This tree was done by Angel Franco and edited by Dr. Stefanie Glaeser.



recA

RecA

Fig. 28: Phylogenetic placement of *Vibrio* spp. based on partial sequences of *recA*. The ML trees were done using nucleotide and amino acid sequences of the gene. GenBank accession numbers of the genomes are in parentheses. Bootstrap values (≥ 70 %) based on 100 resamplings are shown at the branch nodes. *Photobacterium phosphoreum* ATCC 11040^T was used as out-group. Length of the alignment 682 nt / 227 aa. Bar, number of substitutions per nucleotide positions.



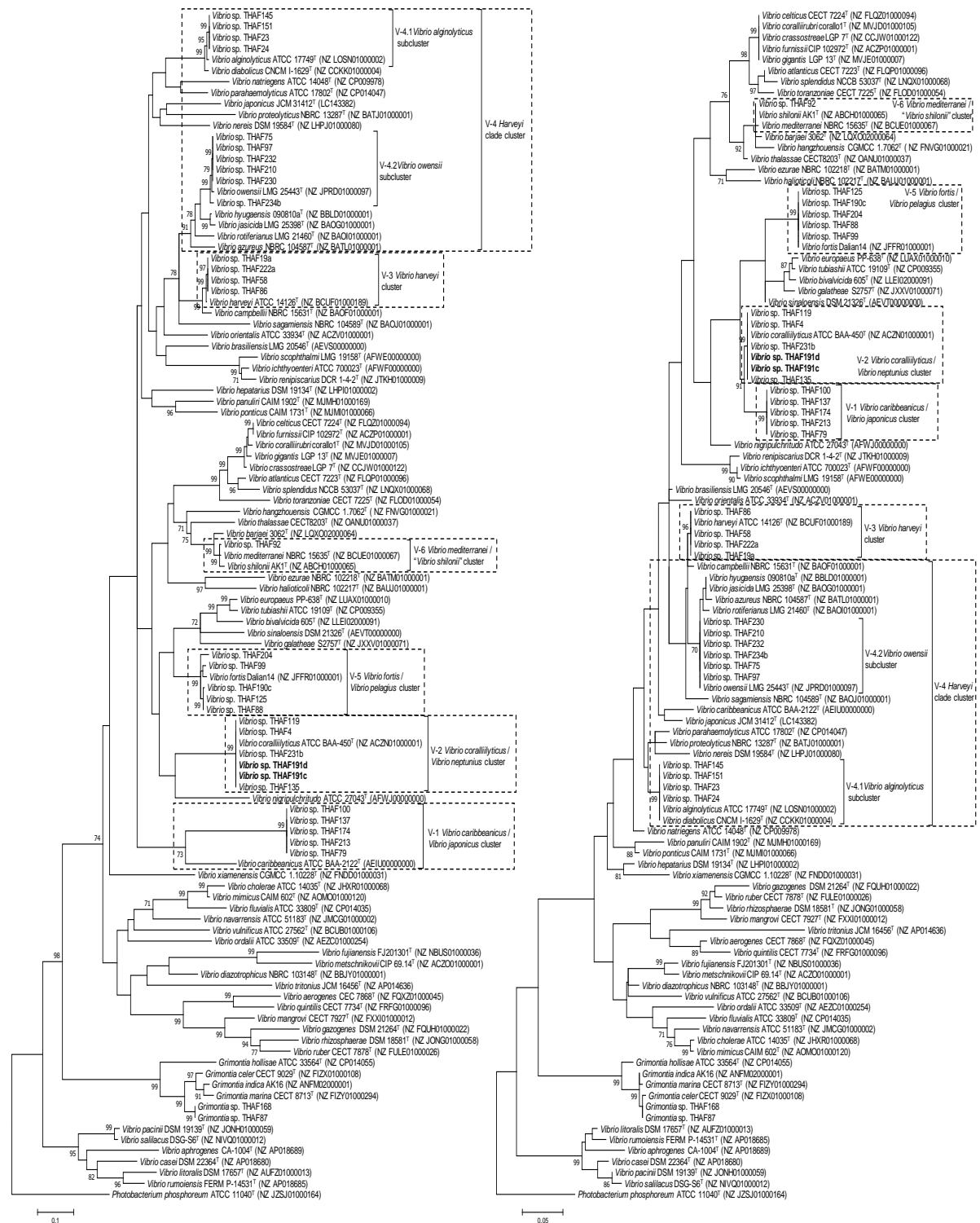
pyrH

PyrH

Fig. 29: Phylogenetic placement of *Vibrio* spp. based on partial sequences of *pyrH*. The ML trees were done using nucleotide and amino acid sequences of the gene. GenBank accession numbers of the genomes are in parentheses ($\geq 70\%$) based on 100 resamplings are shown at the branch nodes. *Photobacterium phosphoreum* ATCC 11040^T was used as out-group. Length of the alignment 480 nt / 160 aa. Bar, number of substitutions per nucleotide positions.



Fig. 30: Phylogenetic placement of *Vibrio* spp. based on partial sequences of *rpoD*. The ML trees were done using nucleotide and amino acid sequences of the gene. GenBank accession numbers of the genomes are in parentheses. Bootstrap values (≥ 70 %) based on 100 resamplings are shown at the branch nodes. *Photobacterium phosphoreum* ATCC 11040^T was used as out-group. Length of the alignment 771 nt / 257 aa. Bar, number of substitutions per nucleotide positions.



gyrB

GyrB

Fig. 31: Phylogenetic placement of *Vibrio* spp. based on partial sequences of *gyrB*. The ML trees were done using nucleotide and amino acid sequences of the gene. GenBank accession numbers of the genomes are in parentheses. Bootstrap values (≥ 70 %) based on 100 resamplings are shown at the branch nodes. *Photobacterium phosphoreum* ATCC 11040^T was used as out-group. Length of the alignment 783 nt / 261 aa. Bar, number of substitutions per nucleotide positions.



Fig. 32: Phylogenetic placement of *Vibrio* spp. based on partial sequences of *rctB*. The ML trees were done using nucleotide and amino acid sequences of the gene. GenBank accession numbers of the genomes are in parentheses. Bootstrap values ($\geq 70\%$) based on 100 resamplings are shown at the branch nodes. *Photobacterium phosphoreum* ATCC 11040^T was used as out-group. Length of the alignment 642 nt / 214 aa. Bar, number of substitutions per nucleotide positions.

Table 10: Accession numbers of the gene sequences employed in the MLSA.

Strain	16S rRNA	<i>recA</i>	<i>pyrH</i>	<i>rpoD</i>	<i>gyrB</i>	<i>rctB</i>
THAF4	MG996611	MN610898	MN610929	MN610960	MN610991	MN611022
THAF18	MG996620	-	-	-	-	-
THAF19a	MG996621	MN610899	MN610930	MN610961	MN610992	MN611023
THAF20	-	-	-	-	-	-
THAF22	-	-	-	-	-	-
THAF23	MG996623	MN610900	MN610931	MN610962	MN610993	MN611024
THAF24	MG996624	MN610901	MN610932	MN610963	MN610994	MN611025
THAF58	MG996637	MN610902	MN610933	MN610964	MN610995	MN611026
THAF62	MG996638	-	-	-	-	-
THAF64	MG996639	-	-	-	-	-
THAF75	MG996642	MN610903	MN610934	MN610965	MN610996	MN611027
THAF79	MG996643	MN610904	MN610935	MN610966	MN610997	MN611028
THAF86	MG996645	MN610905	MN610936	MN610967	MN610998	MN611029
THAF88	MG996647	MN610906	MN610937	MN610968	MN610999	MN611030
THAF92	MG996649	MN610907	MN610938	MN610969	MN611000	MN611031
THAF93	MG996650	-	-	-	-	-
THAF97	MG996651	MN610908	MN610939	MN610970	MN611001	MN611032
THAF99	MG996652	MN610909	MN610940	MN610971	MN611002	MN611033
THAF100	MG996653	MN610910	MN610941	MN610972	MN611003	MN611034
THAF109	MG996657	MN610911	MN610942	MN610973	MN611004	MN611035
THAF119	MG996662	MN610912	MN610943	MN610974	MN611005	MN611036
THAF125	MG996665	MN610913	MN610944	MN610975	MN611006	MN611037
THAF126	MG996666	-	-	-	-	-
THAF135	MG996672	MN610914	MN610945	MN610976	MN611007	MN611038
THAF136	MG996673	-	-	-	-	-
THAF137	MG996674	MN610915	MN610946	MN610977	MN611008	MN611039
THAF145	MG996677	MN610916	MN610947	MN610978	MN611009	MN611040
THAF147	-	-	-	-	-	-
THAF151	-	-	-	-	-	-
THAF157	MG996683	-	-	-	-	-
THAF174	MG996692	MN610917	MN610948	MN610979	MN611010	MN611041
THAF175	MG996693	-	-	-	-	-
THAF177	MG996694	-	-	-	-	-
THAF178	-	-	-	-	-	-
THAF188a	MG996700	-	-	-	-	-
THAF188b	MG996701	-	-	-	-	-
THAF190c	MG996703	MN610918	MN610949	MN610980	MN611011	MN611042
THAF191a	MG996704	MN610919	MN610950	MN610981	MN611012	MN611043
THAF191b	MG996705	MN610920	MN610951	MN610982	MN611013	MN611044
THAF194	MG996707	-	-	-	-	-
THAF204	MG996717	MN610921	MN610952	MN610983	MN611014	MN611045
THAF207a	-	-	-	-	-	-
THAF207b	MG996719	-	-	-	-	-
THAF210	MG996720	MN610922	MN610953	MN610984	MN611015	MN611046
THAF211	-	-	-	-	-	-
THAF212	-	-	-	-	-	-
THAF213	MG996721	MN610923	MN610954	MN610985	MN611016	MN611047
THAF222a	MG996726	MN610924	MN610955	MN610986	MN611017	MN611048
THAF230	MG996727	MN610925	MN610956	MN610987	MN611018	MN611049
THAF231b	MG996728	MN610926	MN610957	MN610988	MN611019	MN611050
THAF232	-	MN610927	MN610958	MN610989	MN611020	MN611051
THAF234a	-	-	-	-	-	-
THAF234b	MG996729	MN610928	MN610959	MN610990	MN611021	MN611052

4.3.3 Different distribution of *Vibrio* spp. phylotypes in the marine system

Seriation analysis showed the presence and absence of the seven detected phylotypes in the habitats of the marine system. The water contained, with six out of seven phylotypes, the highest diversity of *Vibrio* spp. In contrast, only two *Vibrio* phylotypes were isolated from MP and sediment particles. Representatives of the *V. coralliilyticus* phylotype (V-1) were isolated from both surfaces, while representatives of the *V. fortis* phylotype (V-4) only from MP and the *V. harveyi* phylotype (V-3.1) only from sediment particles. These three phylotypes were also isolated from detritus, water, or both. (Fig. 33).

	MP	Sediment	Detritus	Water
V-1	■	■	■	■
V-3.1	■	■	■	■
V-4	■	■	■	■
V-2	■	■	■	■
V-3.2	■	■	■	■
V-3.3	■	■	■	■
V-5	■	■	■	■

Fig. 33: Seriation analysis of phylotypes based on an absence-presence (0/1) matrix. This analysis illustrates the presence of *Vibrio* phylotypes in the different habitats of the marine system. The analysis and figure were done by Dr. Stefanie Glaeser.

4.3.4 Genotypic differentiation and specific occurrence of *Vibrio* spp. genotypes

UPGMA clustering based on a Pearson correlation matrix and the genomic fingerprint patterns, grouped the *Vibrio* spp. isolates into clusters similar to the phylotype clusters obtained by the 16S rRNA gene and MLSA-based phylogeny. In total, isolates were differentiated into 27 genotypes and between two to six different genotypes were obtained for each phylotype. The lowest intra-phylotype diversity was obtained for isolates of the phylotype V-2, all except one isolate shared the same genotype (Fig. 34).

Seriation analysis based on an absence-presence (0/1) matrix of the individual genotypes per sample, showed that the highest genotype diversity was recovered from detritus and water samples. Only few genotypes were cultured from MP and sediments (Fig. 35). Almost all isolates from MP represented different genotypes, only two isolates shared the same genotype (V-4-1), and two genotypes were MP-specific (V-1-1 and V-1-4). Similarly, the five sediment-derived isolates represented four genotypes, from which two were sediment-specific. Five out of ten and 11 out of 16 genotypes cultured from detritus and water were only detected from the respective sample. The genotyping illustrates that the diversity of *Vibrio* spp. at strain level within the studied aquarium system is higher than indicated by the 16S rRNA gene and

MLSA approaches. For a statistical estimation of a niche specificity the number of studied isolates was unfortunately still too low.

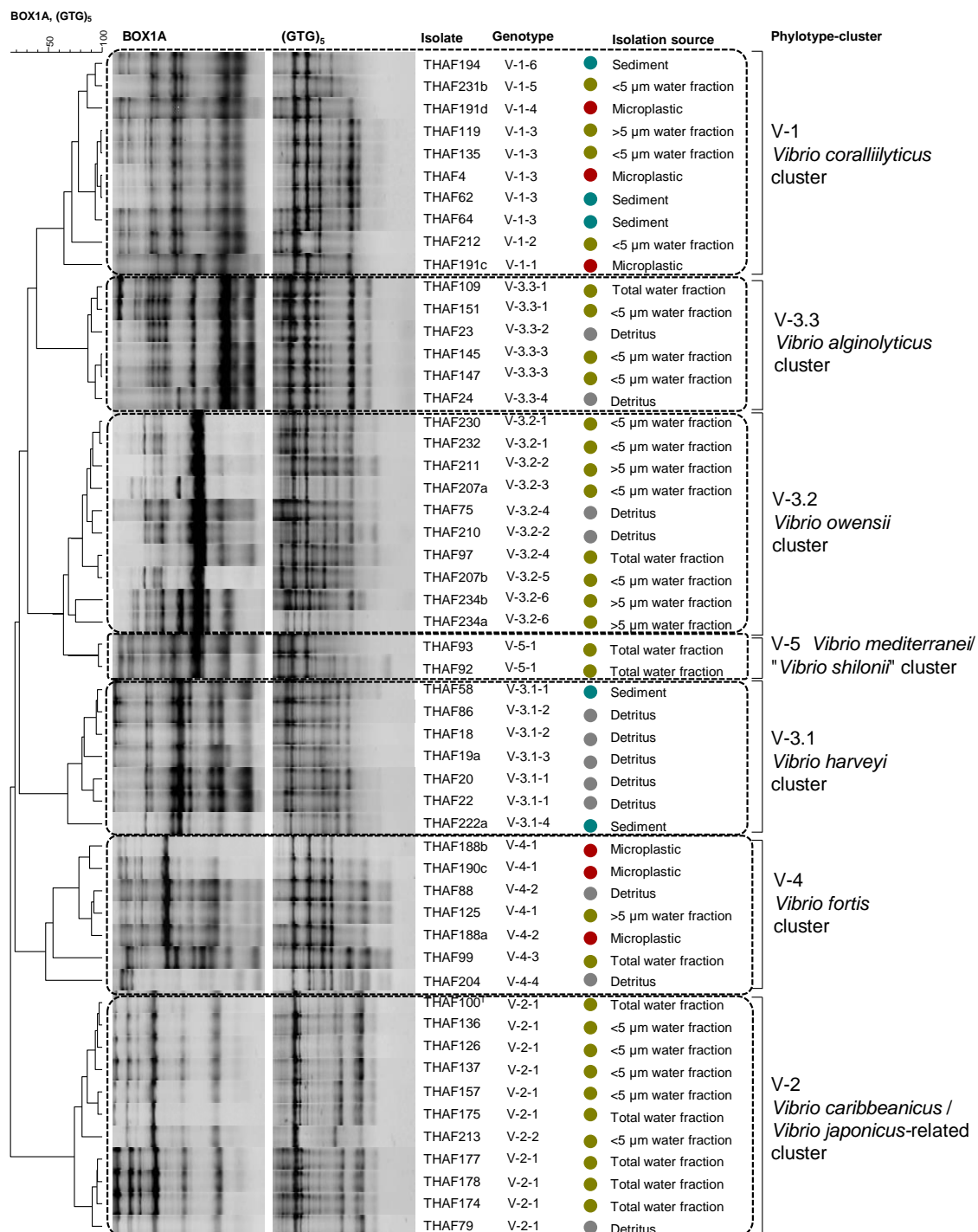


Fig. 34: Genotyping of *Vibrio* spp. isolates based on their genomic fingerprint patterns. The genomic fingerprints were obtained by BOX and (GTG)₅-PCRs. Cluster analysis was performed in GelCompar II version 4.5 (Applied Maths) using UPGMA clustering, based on dissimilarity matrices generated by the Pearson correlation for the two fingerprint patterns, which were subsequently merged. The genotyping was obtained by Angel Franco and the figure edited by Dr. Stefanie Glaeser.

	MP	Sediment	Detritus	Water
V-1-1	■			
V-1-4	■			
V-1-6		■		
V-3.1-4		■		
V-4-2	■		■	
V-1-3	■	■		■
V-3.1-1		■	■	
V-4-1	■			■
V-4-4			■	
V-3.3-2			■	
V-3.1-2			■	
V-3.1-3			■	
V-3.3-4			■	
V-3.2-2			■	■
V-2-1			■	■
V-3.2-4			■	■
V-2-2				■
V-3.2-5				■
V-3.2-6				■
V-3.3-1				■
V-1-5				■
V-3.3-3				■
V-4-3				■
V-3.2-1				■
V-5-1				■
V-1-2				■
V-3.2-3				■

Fig: 35: Seriation analysis of genotypes based on an absence-presence (0/1) matrix. This analysis illustrates the presence of *Vibrio* genotypes in the different samples of the marine system. The analysis and figure were done by Dr. Stefanie Glaeser.

4.3.5 Analysis of the genome of the strain THAF100

As observed in the MLSA, the members of the phylotype V-2 did not cluster with any valid species within the genus *Vibrio*. Therefore, one representative of the phylotype, the strain THAF100, was selected for further polyphasic characterisation and its full genome sequence of the strain THAF100 was generated. The ANI values calculated between the strains THAF100 and the type strains of *V. caribbeanicus* and *V. coralliilyticus*, the closest related species as determined in the nucleotide and amino acid-based MLSA were low, with 70.8 % and 74.8 %, respectively. The type strains of those two species also shared a similar low ANI value among each other (70.9 %).

The genome has a size of 4.5 Mbp with a G+C content of 42.7 %, 4,111 assigned genes, and 3,880 of these are protein-coding. The genome was structured into one chromosome of

3,138,671 bp (CP045350.1) and three plasmids with sizes of 1,317,907 bp (pTHAF100_a; CP045351.1), 39,604 bp (pTHAF100_b; CP045352.1) and 4,831 bp (pTHAF100_c; CP045353.1). The plasmid assignment was performed based on plasmid typical genetic elements; for instance, the plasmid-type replication system. The large plasmid pTHAF100_a, might also represent the second chromosome described for other full genome sequenced *Vibrio* spp., or a chromid or megaplasmid, which has been already reported (Harrison *et al.*, 2010; Kirkup *et al.*, 2010). All ribosomal RNA gene operons were located on the chromosome. The strain contained nine rRNA operons including 16S rRNA gene sequences with slight differences in two of the three rRNA operons.

The genomes of THAF100, and type strains of *V. coralliilyticus* and *V. caribbeanicus* shared 2,453 paralogous genes but also a high number of singletons or genes just shared with one of the other strains. The genome of THAF100 contained 917 singleton genes and shared 205 and 448 paralogous genes only with the type strains of *V. caribbeanicus* and *V. coralliilyticus*, respectively. Those two genomes also shared with 287 genes a similar amount of paralogous genes only among each other and carried 1,078 and 1,832 individual gene, respectively Fig. 36A. The genomic subset distributions between the same 3 genomes indicated that for the chromosome I the 54 % of 6795 CDS represent singletons, 28.9 % belong to the core, and 17.1 % are dispensable; while for the chromid (large plasmid) the 54.5 % of 6663 CDS represent singletons, only 8% belong to the core, and 37.6 5 % are dispensable (Fig. 36B).

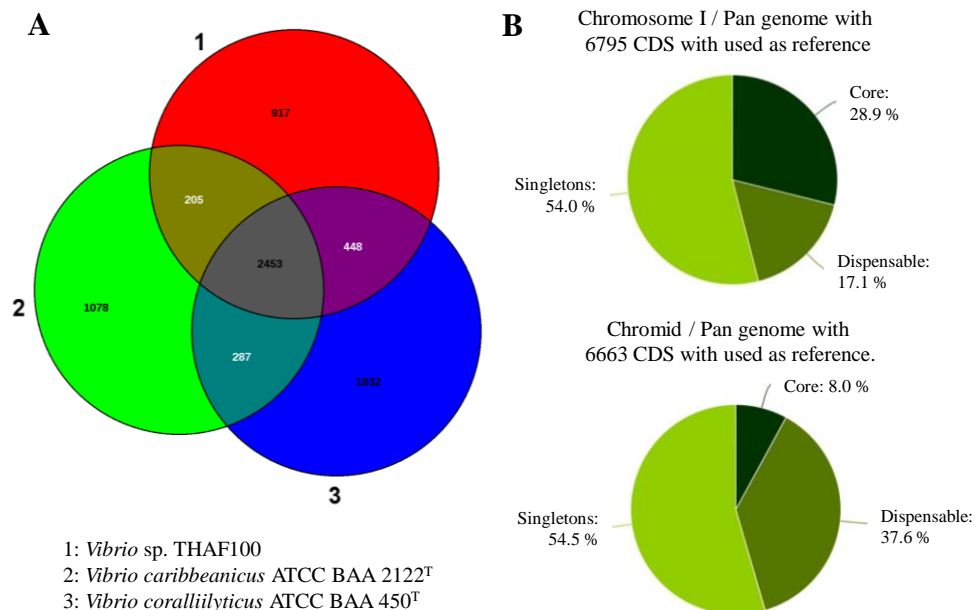


Fig. 36: Distribution of genes in the genome of strain the THAF100. (A) Venn diagram indicating the identical paralogous and singleton genes in the genomes of THAF100, *V. coralliilyticus* ATCC BAA-450^T, and *V. caribbeanicus* ATCC BAA-2122^T. (B) Pie charts indicating the genomic subset distributions of the chromosome I and the chromid (chromosome II) of the analysed strains. The analysis was done by Dr. Stefanie Glaeser.

The presence of phages in the genome of the strain THAF100 was evaluated through the PHASTER server. No phages were detected on the chromosome I, pTHAF100_a

(chromid), and plasmid pTHAF100_c. However, one apparently complete intact plasmid phage was located on plasmid pTHAF100_b. The identified phage was the plasmid-like phage VP882 characterised from a pandemic *V. parahaemolyticus* strain (Lan *et al.*, 2009). The phage contained 59 proteins and covered almost the entirety of the plasmid (39.4 Kb from the 39.6 Kb of the plasmid).

The phylogenetic placement of THAF100 into the genus *Vibrio* was confirmed based on core genome-based phylogenetic trees calculated at nucleotide and amino acid sequence levels (Fig. 37 and 38). Both trees confirmed the close phylogenetic relationship of strain THAF100 to the type strains of *V. coralliilyticus* and *V. caribbeanicus*. On the other hand, the type strains of *V. sinaloensis* and *V. brasiliensis*, both with higher 16S rRNA gene sequence similarities compared to *V. coralliilyticus* (96.8 %), were placed distant from the strain THAF100 in separated subclusters.

4.3.6 Presence of putative pathogenicity-related genes in *Vibrio* sp. THAF100

Based on the 16S rRNA gene, MLSA, and core genome-based phylogenetic analyses, the closest related species of strain THAF100 is the coral pathogenic species *V. coralliilyticus*, which suggests that the novel species or at least the studied type strain may be pathogenic as well. A pangenome analysis of the strains THAF100, *V. coralliilyticus* ATCC BAA-450^T, *V. caribbeanicus* ATCC BAA-2122^T, and *V. coralliilyticus* OCN008 (another coral pathogenic strain) was done to identify pathogenicity-related genes present in strain THAF100 (Fig. 39).

The analysis of the pangenome of the four compared strains indicated that several pathogenicity-related genes were only detected in the genome of the strain THAF100. For instance, the presence of fimbrial assembly proteins (locus tags FIV01_RS01130-RS01140), permeases (FIV01_RS04105), components of toxin-antitoxin systems including genes coding for the toxins RelE2 (FIV01_RS06200) or HigB-2 (FIV01_RS13385), and the antitoxin HipB (FIV01_RS03265). Likewise, quorum sensing-related genes that codify for Acyl-protein LuxE synthase (FIV01_RS00090), homoserine lactone efflux proteins (FIV01_RS01990), and sensory histidine kinase-like DcuS from the two-component sensor-regulator system (DcuS-DcuR) (FIV01_RS00665) were also detected only in the genome of the strain THAF100. Transposable genetic elements related to the transposon Tn7 (FIV01_RS02105-RS02125), as well as phage-related genes (FIV01_RS09550), represented additional differential genetic traits between the strain THAF100 and the reference strains.

The strain THAF100 shared genes with the coral pathogens *V. coralliilyticus* ATCC BAA-450^T and *V. coralliilyticus* OCN008, as well as with *V. caribbeanicus* ATCC BAA-2122^T, reported as non-pathogenic (Huang *et al.*, 2018). For instance, a cluster of flagellar biosynthesis proteins (FIV01_RS10605-RS10725), type II secretion system proteins (FIV01_RS00515-RS00570), quorum sensing receptors LuxR and LuxQ (FIV01_RS12310, FIV01_RS05710), chemotaxis proteins (FIV01_RS09775), or ABC transporter permease (FIV01_RS06260). Additional exclusive and shared genes found in the genome of the strain THAF100 are depicted in Fig. 39.

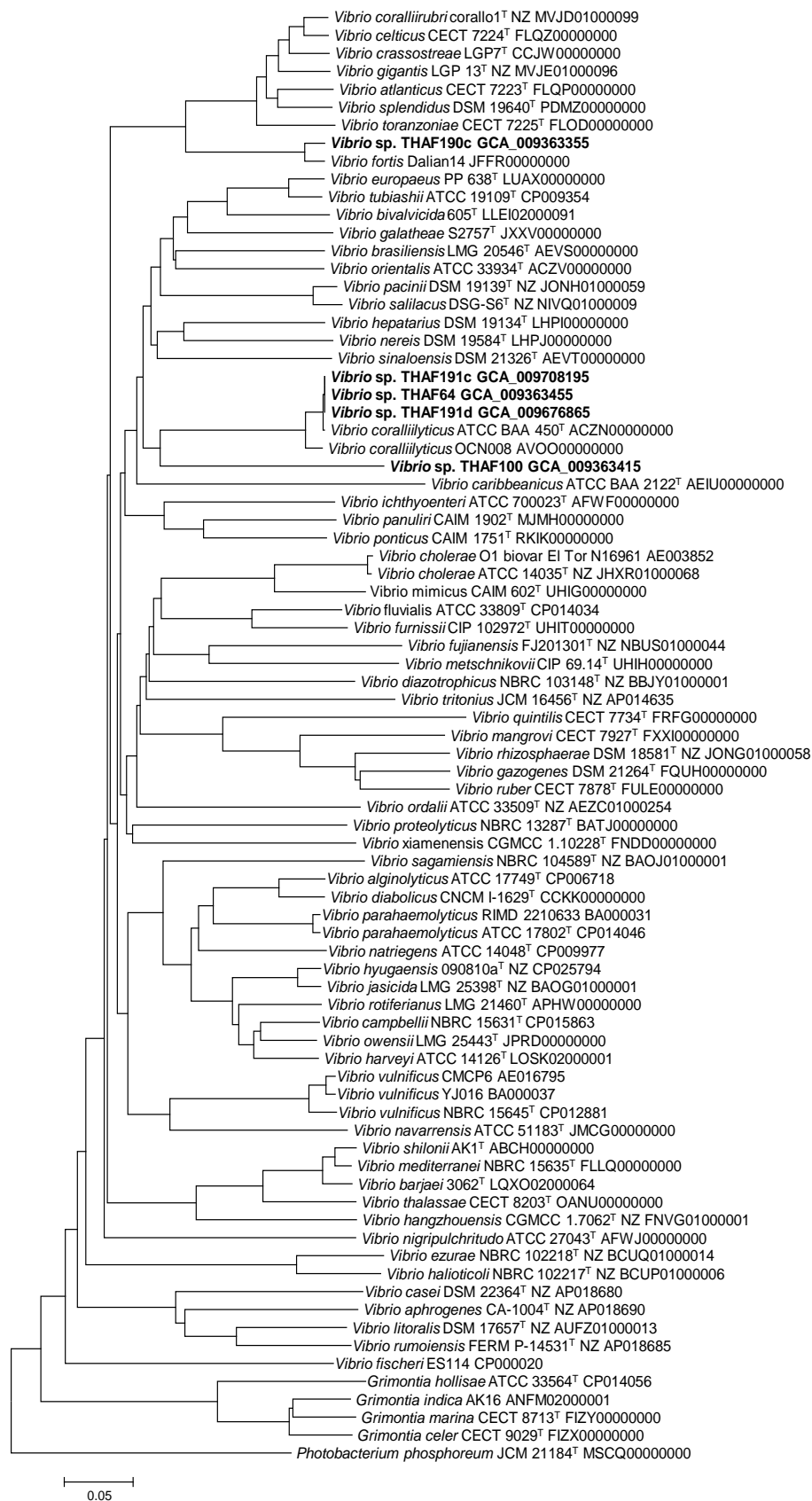


Fig. 37: Core genome phylogenetic tree based on nucleotide sequences. The tree was constructed with the NJ method in the EDGAR platform. Multiple alignments of 733 genes were generated using MUSCLE for 81 genomes. In total, 757,751 bp per genome were included in the analysis. The genome sequence of *Photobacterium phosphoreum* ATCC 11040^T was used as outgroup.

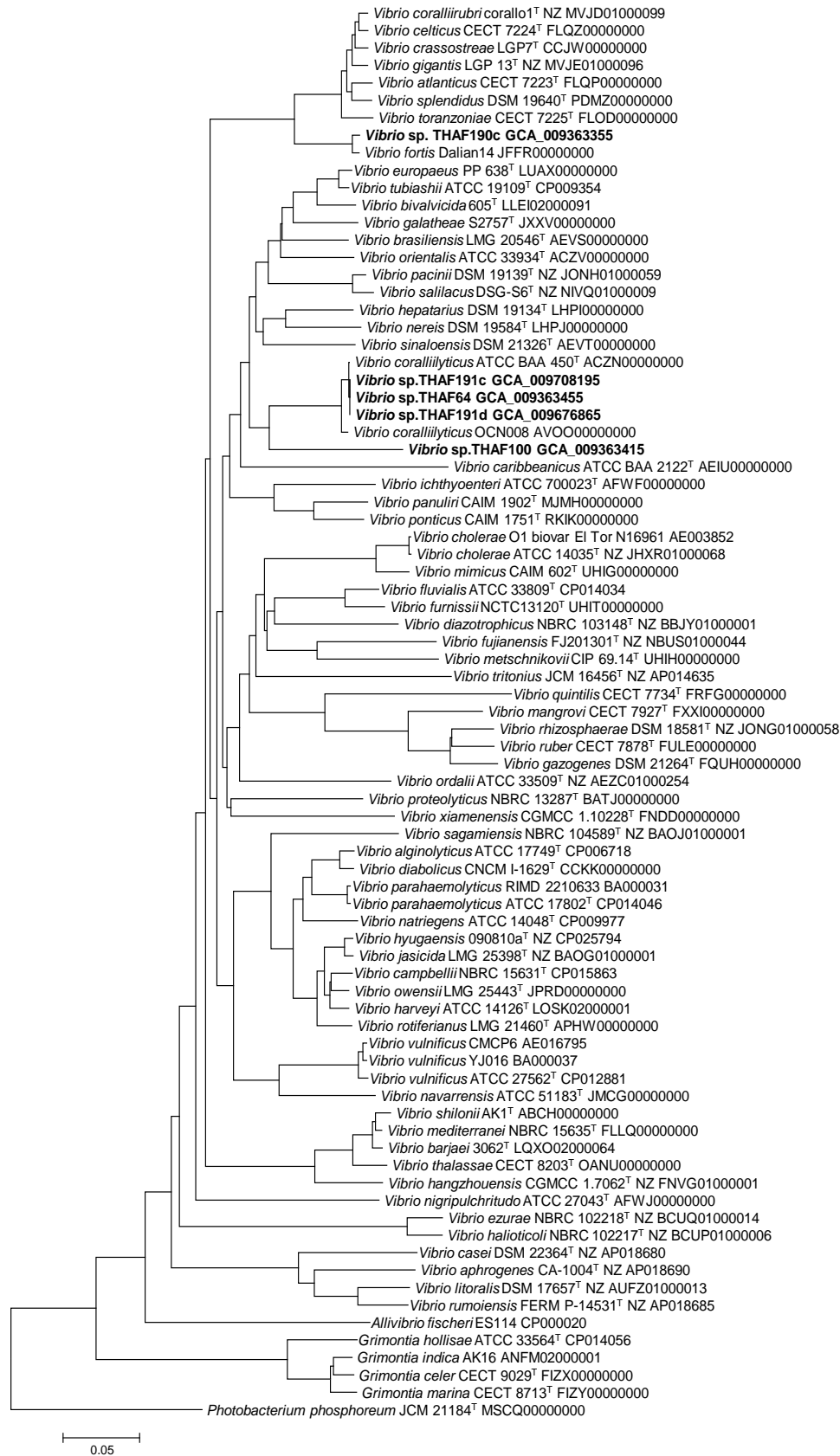


Fig. 38: Core genome phylogenetic trees based on amino acid sequences. The tree was constructed with the NJ method in the EDGAR platform. Multiple alignments of 733 genes were generated using MUSCLE for 81 genomes. In total, 265,277 residues per genome were included in the analysis. The genome sequence of *Photobacterium phosphoreum* ATCC 11040^T was used as outgroup.

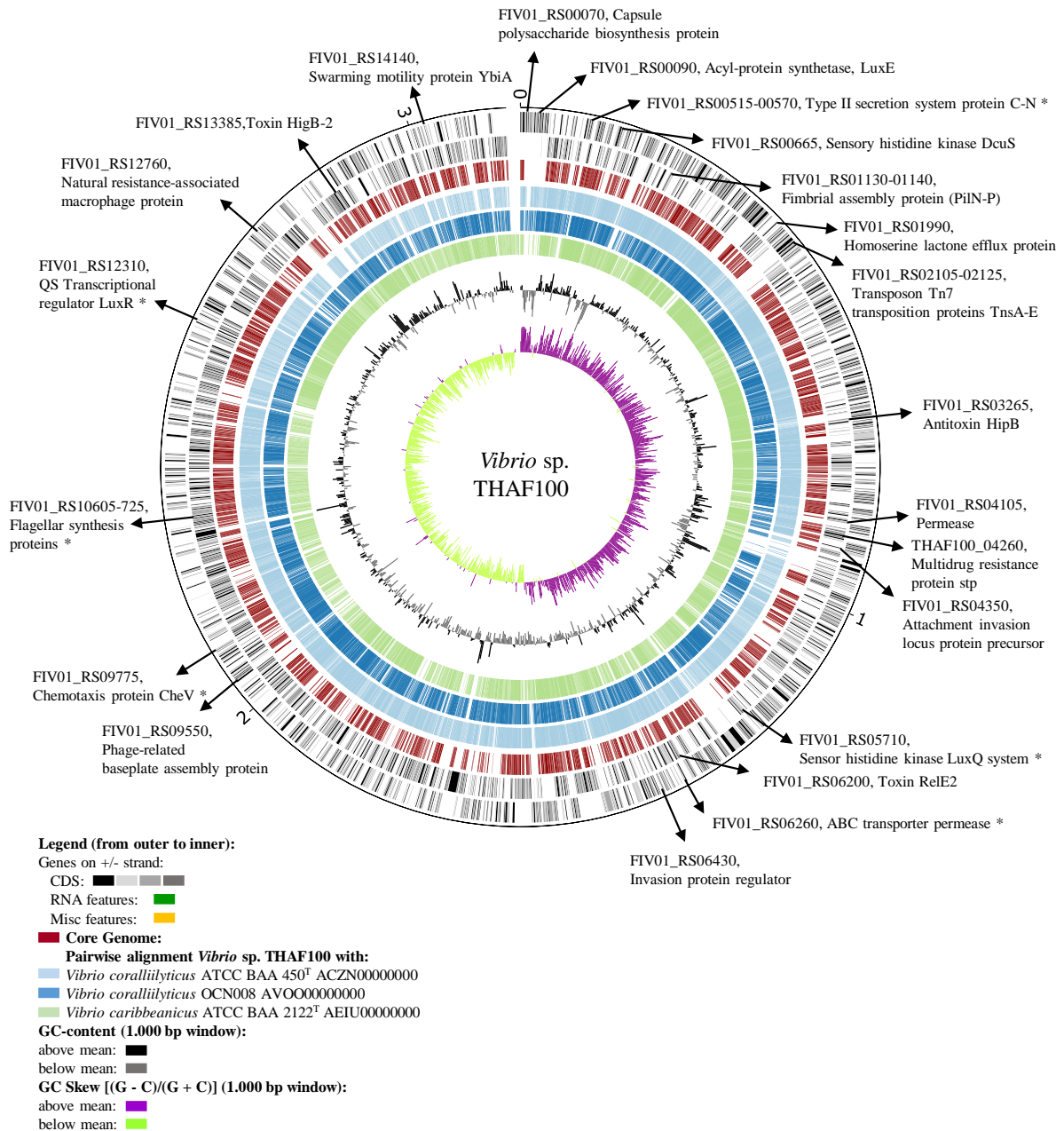


Fig. 39: Gene products associated to pathogenicity detected in the strain THAF100. The circular plot was generated in the EDGAR platform including the genomes of the strains *V. coralliilyticus* ATCC BAA-450^T, *V. caribbeanicus* ATCC BAA-2122^T, and *V. coralliilyticus* OCN008. (*) represent those genes detected in the four strains, all the others were only detected in the strain THAF100. Locus tags of the genes of the strain THAF100 are indicated next to the gene products.

4.4 The CEMarin microcosm system harbours new bacterial species

As mention in the section 4.1.10, the cultivable community isolated from the marine system comprised 172 isolates. Several of these isolates might represent new bacterial species since their 16S rRNA gene sequence similarities were below the proposed threshold for species

demarcation of prokaryotes (98.65 %) (Kim *et al.*, 2014). Hence, a polyphasic characterisation was performed on four strains: AFPH31, THAF1, THAF57, and THAF100.

4.4.1 *Winogradskyella pocilloporae* sp. nov. isolated from healthy tissues of the coral *Pocillopora damicornis*

4.4.1.1 Phylogenetic analysis

The cell lysate of the strain AFPH31^T was used as DNA template to amplify the 16S rRNA gene, whose final sequence (Acc. Number MG571571) represented a continuous stretch of 1433 nucleotides spanning gene termini 28 to 1460, according to the *E. coli rrnB* numbering (Brossius *et al.*, 1978). BLAST analyses against the EzBioCloud database indicated that strain AFPH31^T shared highest 16S rRNA gene sequence similarity with the type strain of *Winogradskyella eximia* LMG 22474^T (96.6 %), followed by *Winogradskyella wandonensis* WD-2-2^T (96.4 %) and *Winogradskyella damuponensis* F081-2^T (96.4 %). Sequence similarities to all other *Winogradskyella* type strains were in the range of 94.5 – 96.3 %.

The phylogenetic analyses based on the 16S rRNA gene sequences confirmed the placement of strain AFPH31^T within the monophyletic genus *Winogradskyella*. In the ML tree, strain clustered next to the type strains of *Winogradskyella maritima* and *Winogradskyella exilis*, which was however, not supported by high bootstrap values (Fig. 40). A direct clustering with *Winogradskyella* species type strains was not obtained in the phylogenetic tree calculated based on the MaPa and NJ methods. The placement of strain AFPH31^T varied between the phylogenetic trees and was also not supported by high bootstrap values. The DNA G+C content of strain AFPH31^T was determined by the DNA melting temperature method established by Gonzalez and Saiz-Jimenez (2002) as described previously (Glaeser *et al.*, 2013). The G+C content of strain AFPH31^T was 36.8 mol%, a value slightly above the range reported for other *Winogradskyella* species, reported in 30.0 to 36.4 % (Bernardet *et al.*, 2002; Nedashkovskaya *et al.*, 2005; Ivanova *et al.*, 2017; Park *et al.*, 2017; Yoon *et al.*, 2017).

4.4.1.2 Morphological and physiological characterisation

A detailed characterisation of the strain AFPH31^T was performed in parallel with cultures of *W. eximia* LMG 22474^T and *W. thalassocola* LMG 22492^T always under the same cultivation conditions. Colonies of the strain AFPH31^T were orange-yellow-pigmented, creamy in texture, and round shaped with smooth edges. Cells were rod-shaped, Gram-stain-negative, not motile, with a size of 2.0 (±0.2) × 0.9 (±0.2) µm. The strains were compared with respect to their cellular pigment content. The maximum absorption of cellular pigments extracted in acetone/methanol (7:2, v/v) were at 452 and 476nm for strain AFPH31^T, at 452 and 477 nm for *W. eximia* LMG 22474^T, and at 453 and 480 nm for *W. thalassocola* LMG 22492^T (Fig. 41). These values of absorption of cellular pigments are similar to those reported for other *Winogradskyella* type strains (Ivanova *et al.*, 2010; Zhang *et al.*, 2016).

The strain AFPH31^T and the reference strains grew well at 25 °C on MA and slightly on R2A and TSA only when the medium was supplemented with 3% (w/v) NaCl. In contrast, none grew on Nu, malt agar, G/A agar, PYE, CASO, K7, M65, DEV, NA, LB, MacConkey agar, Columbia agar and PYES neither with 3% (w/v) NaCl nor without salt addition. For strain AFPH31^T, good growth was observed after 2 days in a range between 15 and 37 °C; *W. eximia* LMG 22474^T and *W. thalassocola* LMG 22492^T grew in a range between 4 and 30 °C.

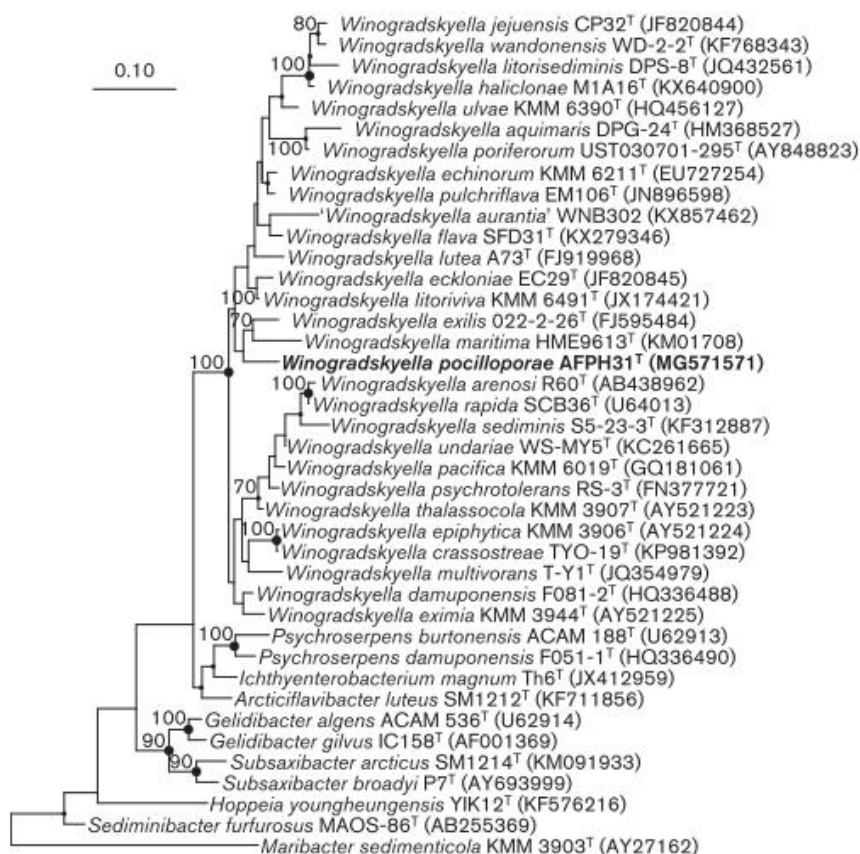


Fig. 40: Phylogenetic placement of strain AFPH31^T within the genus *Winogradskyella*. The 16S rRNA gene-based tree was generated in ARB with the ML method (RAxML, GTR-GAMMA, rapid bootstrap analysis) using the sequence termini 96 and 1417 (numbering according to Brosius *et al.*, 1978) and 100 replications. Bootstrap values > 70 % are depicted at the nodes. Filled circles mark nodes that were also present in the MaPa and NJ trees; while large circles represent those nodes, which were also supported by a high bootstrap value in those trees. Type strains of *Sediminibacter furfurosus* and *Maribacter sedimenticola* were used as outgroups. Bar: 0.1 substitutions per nucleotide position. This tree was calculated by Dr. Stefanie Glaeser.

Differences regarding the tolerance to TS prepared with ASW and supplemented with NaCl were observed. Strain AFPH31^T and *W. eximia* LMG 22474^T grew in the presence of 0.5–8.5% (w/v) NaCl, while *W. thalassocola* LMG 22492^T grew only in the range of 0.5–7.5 % (w/v) NaCl in the medium. Likewise, the strains differed in their pH range of growth, strain AFPH31^T grew between pH 5.5 and 9.0, while *W. eximia* LMG 22474^T and *W. thalassocola* LMG 22492^T grew only at pH 5.0–9.0. None of the strains grew under anaerobic conditions after 14 days of incubation on MA. Cells of AFPH31^T were positive for cytochrome oxidase

and catalase activity, but negative for flexirubin-type pigment production. None of the tested strains hydrolysed cellulose, casein or DNA, but only strain AFPH31^T hydrolysed starch. Strain AFPH31^T and *W. thalassocola* LMG 22492^T hydrolysed Tweens 40 and 60, but not Tweens 20 and 80, while *W. eximia* LMG 22474^T did not hydrolyse Tween compounds (Table 11).

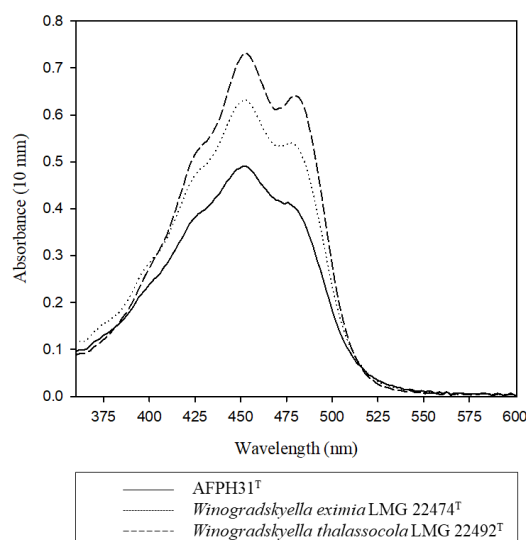


Fig. 41: Absorption spectra of cellular pigments of *Winogradskyella* strains. Pigments were extracted with acetone/methanol (7:2, v/v) and analysed with a spectrophotometer.

Physiological tests were performed with the API 20 NE and API ZYM tests (bioMérieux) and the test panel design by Kämpfer *et al.*, (1991). API 20 NE test gave positive results for activity of aesculin hydrolase for all strains and positive for gelatine hydrolase only for *W. eximia* LMG 22474^T. Negative results were obtained for the remaining tests of the panel for the three tested strains. The activity of 7 out of 19 tested enzymes examined with the API ZYM test was positive for strain AFPH31^T, differing in the activities of the enzymes leucine arylamidase, valine arylamidase and cystine arylamidase (Table 11). Results of the test panel indicated that strain AFPH31^T was positive for 5 of 21 acid production tests, 4 of 55 carbon source assimilation tests, and 7 out of 12 enzyme activity tests (Table 12). Strains AFPH31^T, *W. eximia* LMG 22474^T and *W. thalassocola* LMG 22492^T differed in the acid production of α -D-lactose and α -D-glucose, in the assimilation of p-arbutin, D-galactose, D-mannose, α -D-melibiose, sucrose, i-inositol, D-mannitol, adipate, glutarate, DL-lactate, L-malate, mesaconate, suberate, and L-tryptophan, and in the enzyme activity of *p*NP- β -D-glucopyranoside, *p*NP-phenyl-phosphonate, *p*NP-phosphoryl-choline, and L-proline-pNA.

4.4.1.3 Chemotaxonomic characterisation

Seven lipids were detected in the polar lipid profile. The major compounds were phosphatidylethanolamine and two unidentified lipids (L2, L3) lacking a functional group. In addition, moderate to minor amounts of two unidentified aminolipids (AL1, AL2) and two unidentified lipids (L1, L4) lacking a functional group were also detected (Fig. 42). The major cellular fatty acids of strain AFPH31^T were iso-C_{15:0} (22.0 %), iso-C_{15:1} G (16.9 %), iso-C_{17:0}

3-OH (14.9 %) and C_{15:0} (11.9%), similar to the fatty acids profile of *W. eximia* LMG 22474^T (Nedashkovskaya *et al.*, 2005). Differences between the fatty acid profiles of strain AFPH31^T and the other member of the genus *Winogradskyella* are listed in Table 13. The overall polyamine content was rather low, containing exclusively *sym*-homospermidine [2.9 µmol (g dry weight)⁻¹]. This might be explained by the use of a growth medium supplemented with sea salt, which has been demonstrated to influence inversely the internal polyamine content in the cells (Auling *et al.*, 1991) as previously reported for *W. haliclonae* (Schellenberg *et al.*, 2017). Like all members of *Flavobacteriaceae*, the strain AFPH31^T contained MK-6, which is the characteristic respiratory quinone of the family (Bernardet *et al.*, 2002).

Based on phylogenetic, phenotypic and chemotaxonomic results, the strain AFPH31^T (=CCM 8816^T =CIP 111546^T) represents a novel species of the genus *Winogradskyella*, for which the name *Winogradskyella pocilloporae* is proposed.

Table 11: Phenotypic characteristics that differentiate the strain AFPH31^T. Strains: 1, *Winogradskyella pocilloporae* sp. nov. AFPH31^T; 2, *W. eximia* LMG 22474^T; 3, *W. thalassocola* LMG 22492^T; 4, *W. wandonensis* WD-2-2^T; 5, *W. damuponensis* F081-2^T; 6, *W. litoriviva* KMM 6491^T; 7, *W. sediminis* S5-23-3^T. Strains 1, 2, and 3 were investigated in parallel under the same conditions. A, strictly aerobic; F, facultative anaerobic; +, positive; -, negative; W, weakly positive; NA, not available. Values in brackets were taken from Nedashkovskaya *et al.*, (2005 and 2012) for strains 2 and 3. Data for strains 4, 5, 6 and 7 were taken from Park *et al.*, (2017), Lee *et al.*, (2007), Nedashkovskaya *et al.*, (2015), and Zhang *et al.*, (2016), respectively.

Characteristic	1	2	3	4	5	6	7
Pigmentation	Orange-yellow	Yellow	Yellow	Orange-yellow	Yellow	Yellow	Yellow
Gliding motility	-	+	+	-	+	+	+
Type of metabolism	A	A (A)	A (A)	A	A	F	A
Temperature range of growth (°C)	15-37	4-30 (4-33)	4-30 (4-33)	15-40	4-35	4-34	1-30
NaCl range of growth (% w/v)	0.5-8.5	0.5-8.5 (1.0-5.0)	0.5-7.5 (1.0-8.0)	0.5-5.0	1.0-5.0	0.5-7.0	2.0-6.0
pH range of growth	5.5-9.0	5.0-9.0 (NA)	5.0-9.0 (NA)	6.0-8.0	6.0-9.5	5.5-10.0	6.0-8.0
Hydrolysis of							
Hypoxanthin	w	+	+	-	NA	NA	NA
Tyrosin	-	+	w	+	NA	+	NA
Starch	+	-	-	-	-	+	+
Tween 20	-	-	-	+	+	-	NA
Tween 40	+	-	+	+	+	+	NA
Tween 60	+	-	+	+	NA	NA	NA
Tween 80	-	-	-	+	+	+	NA
API 20 NE							
Gelatin hydrolase	-	+	-	+	+	+	+
Enzyme activities (API ZYM)							
Leucine arylamidase	w	+	+	+	+	+	+
Valine arylamidase	w	+	+	+	+	+	+
Cystine arylamidase	-	+	+	+	+	+	-
DNA G+C content (mol%)	36.8	(36.1)	(34.6)	36.4	32.3	31.3	36.1

Table 12: Physiological characterisation of the strain AFPH31^T obtained with the test panel. Positive results obtained for the strain AFPH31^T compared to the other tested strains. Strains: 1, *Winogradskyella pocilloporae* sp. nov. AFPH31^T; 2, *W. eximia* LGM 22474^T; 3, *W. thalassocola* LMG 22492^T. +, Positive; -, negative.

Characteristic	1	2	3
Acid production from			
L-arabinose	+	+	+
D-maltose	+	+	+
D-xylose	+	+	+
aesculin	+	+	+
α -D-glucose	+	-	-
Assimilation of			
I-inositol	+	-	-
D-mannitol	+	+	-
L-aspartate	+	+	+
L-tryptophan	+	-	-
Enzyme activity			
pNP- α -D glucopyranoside	+	+	+
Bis-pNP-phosphate	+	+	+
pNP-phenyl-phosphonate	+	-	+
pNP-phosphoryl-choline	+	-	-
pNP-phosphate-disodium salt	+	+	+
L-alanine-pNA	+	+	+
L-glutamate- γ -Carboxy pNA	+	+	+

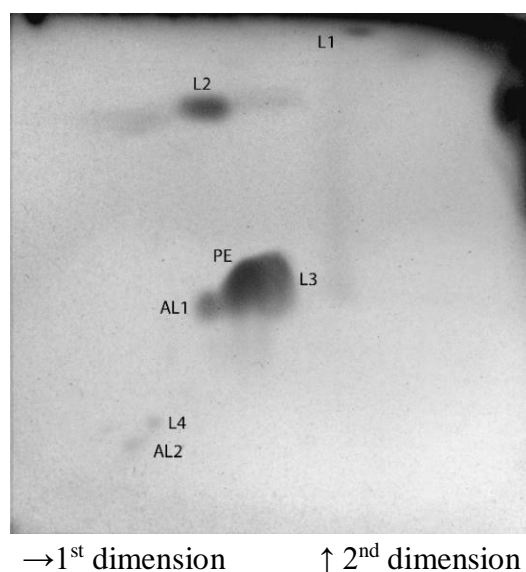


Fig. 42: Polar lipid profile of the strain AFPH31^T. Staining was done with 5 % ethanolic molybdatophosphoric acid (w/v). PE, phosphatidylethanolamine; AL1, AL2, unidentified aminolipids; L1 - 4, unidentified lipids lacking a functional group. This chromatography was done by Prof. Dr. Hans-Jürgen Busse.

Table 13: Fatty acid composition of strain AFPH31^T and its closest related type strains. Strains: 1, *Winogradskyella pocilloporae* sp. nov. AFPH31^T; 2, *W. eximia* LGM 22474^T; 3, *W. thalassocola* LMG 22492^T; 4, *W. wandonensis* WD-2-2^T; 5, *W. damuponensis* F081-2^T; 6, *W. litoriviva* KMM 6491^T; 7, *W. sediminis* S5-23-3^T. Strains 1 and 2 were investigated in parallel under the same conditions. Values show the percentage of the total fatty acids. Values for strains 2 (brackets) and 3 were taken from Nedashkovskaya *et al.*, (2005 and 2012). Data for strains 4, 5, 6 and 7 were taken from Park *et al.*, (2017), Lee *et al.*, (2007), Nedashkovskaya *et al.*, (2015), and Zhang *et al.*, (2016), respectively. -, not detected; TR, trace amount (< 1 %).

Fatty acid	1	2	3	4	5	6	7
Straight-chain							
C _{15:0}	11.9	10.4 (6.7)	7.9	-	5.3	6.4	3.7
Branched							
iso-C _{14:0}	-	-(1.4)	2.6	TR	1.3	-	-
iso-C _{15:0}	22.0	25.5 (25.6)	8.7	15.9	25.3	19.4	24.4
iso-C _{15:1} G	16.9	16.5 (10.4)	11.4	21.8	14.4	15.5	19.5
iso-C _{16:0}	4.4	3.0 (5.7)	TR	1.4	1.9	TR	-
iso-C _{16:1} H	4.7	6.1 (4.7)	2.7	-	2.2	-	-
iso-C _{16:1} G	-	-	-	1.9	-	-	-
anteiso-C _{15:0}	-	6.3 (7.0)	4.9	1.3	7.8	9.5	6.2
anteiso-C _{15:1} A	-	2.7 (1.4)	1.6	1.6	3.9	4.8	1.7
anteiso-C _{17:1}	-	-(2.3)	-	-	-	-	-
Unsaturated							
C _{15:1} ω6c	3.3	3.2 (-)	6.5	-	1.9	1.4	1.5
C _{15:1} ω8c	-	-	-	-	-	1.7	-
C _{17:1} ω6c	3.6	- (-)	TR	TR	1.1	-	-
iso-C _{17:1} ω9c	3.2	- (-)	TR	-	-	-	1.2
Hydroxy							
C _{15:0} 2-OH	-	-(1.0)	1.8	1.2	2.0	-	1.2
C _{17:0} 2-OH	-	-(1.0)	TR	TR	2.6	-	1.4
C _{15:0} 3-OH	-	- (-)	2.5	TR	1.2	TR	1.3
C _{16:0} 3-OH	-	- (-)	1.0	1.8	TR	TR	TR
iso-C _{16:0} 2-OH	-	-	-	-	-	1.2	-
iso-C _{15:0} 3-OH	6.0	6.0 (2.6)	11.9	7.8	7.6	9.6	12.9
iso-C _{16:0} 3-OH	4.4	9.8 (3.2)	18.1	8.1	6.7	4.6	4.0
iso-C _{17:0} 3-OH	14.9	6.6 (6.7)	5.4	21.5	9.3	8.4	10.5
anteiso-C _{17:0} 3-OH	-	-	-	-	-	4.7	-
Unknown 13.565	1.6	-(5.6)	4.8	-	-	-	1.4
Summed feature 3*	3.2	3.9 (6.1)	4.2	9.8	2.0	5.8	5.0
Summed feature 9*	-	-	-	-	2.4	-	-

* Summed features are groups of two or more fatty acids that could not be separated with the MIDI system. Summed feature 3 comprised C_{16:1} ω7c and/or iso-C_{15:0} 2-OH; summed feature 9 comprised C₁₀-methyl and/or iso-C_{17:1} ω9c.

4.4.1.4 Description of *Winogradskyella pocilloporae* sp. nov.

Winogradskyella pocilloporae (po.cil.lo.po'rae. N.L. gen. n. *pocilloporae* of *Pocillopora*, isolated from the coral *Pocillopora damicornis*).

Cells are Gram-stain-negative, non-flagellated, non-gliding and rod-shaped, 2.0 (±0.2) μm long and 0.9 (±0.2) μm wide. Colonies grown after 3 days on MA at 25 °C are circular, slightly convex, with smooth borders, shiny and orange-yellow pigmented. The optimal

temperature for growth is 25 °C; growth occurs between 15 and 37 °C. Best growth on MA and moderate on R2A and TSA only when media was supplemented with 3% (w/v) NaCl. Growth at pH 5.5–9.0 (optimal from pH 6.0 to 8.5). Growth in the salt-tolerance test occurred from 0.5 to 8.5% NaCl (w/v), optimal growth from 1.0 to 4.5% NaCl. Growth does not occur under anaerobic conditions on MA. Yellow water-soluble pigments extracted with acetone/methanol (7:2, v/v) with absorption maxima at 452 and 476 nm are produced but flexirubin-type pigments are not produced. Catalase- and cytochrome oxidase-positive. Hypoxanthin, starch, xanthin, aesculin, Tweens 40, and 60 are hydrolysed, but cellulose, casein, adenine, tyrosine, xylan, gelatin, urea, DNA, Tweens 20, and 80 are not. Acid is produced from α -D-glucose, L- arabinose, maltose, and D-xylose, but not from lactose, sucrose, D-mannitol, dulcitol/dulcitol, D-salicin, adonite/adonitol, i-inositol, D-sorbitol, raffinose, α -L-rhamnose, trehalose, cellobiose, 1-O-methyl-D-glucosidepyranosid, *meso*-erythritol, melibiose, D-arabitol, and D-mannose. Positive for the assimilation of i-inositol, D-mannitol, L-aspartate, and L- tryptophan, but negative for *N*-acetyl-D-galactosamine, *N*-acetyl-D-glucosamine, L-arabinose, p-arbutin, cellobiose, D-fructose, D-galactose, D-gluconate, α -D-glucose, maltose, D-mannose, α -L-rhamnose, D-ribose, D-sucrose, D-salicin, trehalose, D-xylose, adonite, maltite, D-sorbitol, putrescine, sodium acetate, propionate, cis-aconitate, trans-aconitate, adipate, 4-aminobutyrate, azetalic acid, citrate, fumarate, glutarate, DL-3-hydroxybutyrate, itaconate, DL-lactate, L-malate, mesaconate, 2-oxoglutarate, pyruvate, suberate, L- alanine, β -alanine, L-aspartate, L-histidine, L-leucine, L-ornithine (hydrochloride), L-phenylalanine, L-proline, L-serine, 3-hydroxybenzoate, 4-hydroxybenzoate, and DL-3-phenylacetate; positive for the enzyme activity of *p*NP- α -D-glucopyranoside, Bis-*p*NP-phosphate, *p*NP-phenyl-phosphonate, *p*NP-phosphoryl-choline, *p*NP-phosphate-disodium salt, L-alanine-pNA, and L-glutamate- γ -carboxy pNA, and negative for *p*NP- β -D-galactopyranoside, *p*NP- β -D-glucuronoside, *p*NP- β -D-glucopyranoside, *p*NP- β -D-xylopyranoside, and L-proline-pNA. In assays with the API ZYM system, activity of enzymes alkaline phosphatase, esterase (C4), esterase lipase (C8), leucine arylamidase, valine arylamidase, acid phosphatase and naphthol-AS-BI-phosphohydrolase are positive, but negative for enzyme activity of lipase (C14), cystine arylamidase, trypsin, α -chymotrypsin, α -galactosidase, β -galactosidase, β -glucuronidase, α -glucosidase, β -glucosidase, *N*-acetyl- β -glucosaminidase, α -mannosidase, and α -fucosidase. According to the API 20 NE test system, positive for hydrolysis of aesculin, but negative for the reduction of nitrate to nitrite, indole production, glucose fermentation, arginine dihydrolase, urease, hydrolysis of gelatin, β -galactosidase and the assimilation of glucose, L-arabinose, D-mannose, maltose, *N*-acetyl-glucosamine, malate, potassium gluconate, capric acid, adipic acid, malic acid, trisodium citrate, and phenylacetic acid. The fatty acid profile of total cell hydrolysates consists of several branched and hydroxylated fatty acids with similar abundances including iso-C_{15:0}, iso-C_{15:1} G, iso-C_{17:0} 3-OH, and C_{15:0}. The major polyamine is *sym*-homospermidine and the major respiratory quinone is menaquinone MK-6. The polar lipid profile comprises the major lipids phosphatidylethanolamine and two unidentified lipids lacking a functional group (L2, L3). Moderate to minor amounts of two unidentified aminolipids (AL1, AL2) and two unidentified lipids lacking an amino group (L1, L4), a phosphate group and a sugar moiety are detectable, as well. The genomic G+C content of the type strain is 36.8mol% (Tm).

The type strain, AFPH31^T (=CCM 8816^T=CIP 111546^T), was isolated from internal tissues of the scleractinian coral *Pocillopora damicornis*, which was cultured in a marine aquarium system at Justus Liebig University Giessen, Germany.

4.4.2 *Pseudomaribius plastisphaeris* sp. nov. a new moderately halophilic species isolated from the surface of a polyethylene microplastic particle incubated in a marine aquarium system

4.4.2.1 Phylogenetic analysis

The 16S rRNA gene sequence of the strain THAF1 (Acc. number MG571573) represented a continuous stretch of 1362 nucleotides spanning gene termini 31 to 1392, according to the *E. coli* *rrnB* numbering (Brossius *et al.*, 1978). A first identification of the phylogenetic affiliation of strain THAF1 by BLAST analysis against the EzBioCloud database indicated that the similarity to the 16S rRNA gene sequences of closely related type strains included in the database was clearly below the threshold proposed for species differentiation (98.65 %). Closest related type strains were those of the species *Maribius pontilimi* (97.2 %), *Pseudomaribius aestuariivivens* (96.8 %), *Palleronia abyssalis* (95.8 %), *Maribius salinus* (95.7 %), *Palleronia soli* (95.6 %), *Maribius pelagius* (95.6 %), and *Palleronia marisminoris* (95.1 %). Despite the 16S rRNA gene-based pairwise sequence similarity analysis showed highest similarity to the type strain of *M. pontilimi* (97.2 %), in the phylogenetic trees, the strain THAF1 clustered with the type strain of *P. aestuariivivens* in the ML tree (Fig. 43). Type species of the genera *Palleronia* and *Maribius* formed distinct and separated clusters next to the cluster of strain THAF1.

Most of the cultured members of the *Roseobacter* clade are characterised by large genomes with high DNA G+C content (60 ± 4 mol %) (Luo and Moran, 2014). The DNA G+C content for strain THAF1 obtained from the genome sequence data was 63.3 mol %, in accordance with the standard values of the *Roseobacter* clade, but lower than all those reported for type strains of the described species of genera *Pseudomaribius*, *Maribius*, and *Palleronia* 64.2 mol % and 70.0 mol % (Martínez-Checa *et al.*, 2005; Choi *et al.*, 2007).

4.4.2.2 Morphological and physiological characterisation

Colonies of the strain THAF1 were pale-orange, 2 mm in diameter, round-shaped, and dry in appearance. Cells were Gram-stain negative, non-motile, short rod-shaped with a mean size of $1.6 (\pm 0.2)$ µm in length and $0.9 (\pm 0.1)$ µm in width, and grew strictly under aerobic conditions. The strain was positive for catalase and cytochrome C oxidase activity but negative for production of flexirubin-type pigments.

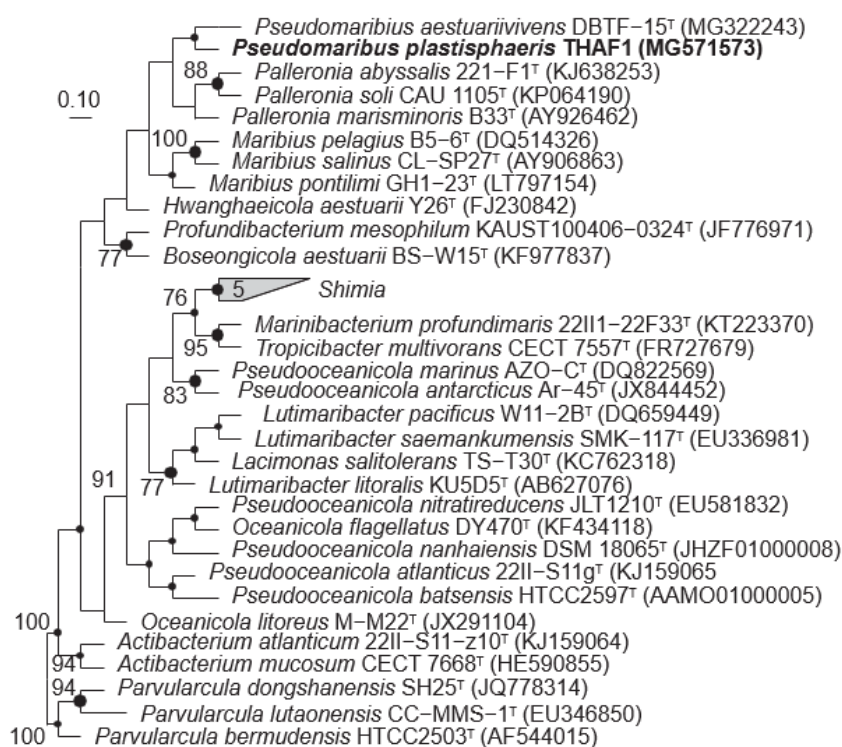


Fig. 43: Phylogenetic placement of strain THAF1 with members of the *Roseobacter* clade. The phylogenetic tree based on nearly full-length 16S rRNA gene sequences was constructed in ARB with the MaPa method using DNAPARS v 3.6 and based on sequence termini 81 and 1469 (numbering according to Brosius *et al.* 1978) and 100 replications (bootstrap support). Bootstrap values >70 % are showed at nodes. Filled circles mark nodes that were also present in the ML and NJ trees; large circles represent nodes, which were additionally supported by high bootstrap values in the ML and NJ trees. Type strains of *Parvularcula dongshanensis*, *Parvularcula lutaonensis*, and *Parvularcula bermudensis* were used as outgroup. Bar: 0.10 substitutions per nucleotide positions. This tree was calculated by Dr. Stefanie Glaeser.

Phenotypic characterization assays were performed in parallel with the strains THAF1, *P. aestuariivivens* KACC 19431^T, *P. abyssalis* LMG 27977^T, and *P. marisminoris* LMG 22959^T, grown under the same cultivation conditions on MA at 28°C for 3 days. The reference strains were selected based on the clustering of the strain THAF1 to the genera *Pseudomaribius* and *Palleronia* observed in the phylogenetic tree (Fig. 43). Strain THAF1 grew well only on MA and slightly on M65 medium supplemented with 3% (w/v) NaCl. The reference strains grew well on MA as well, but only *P. abyssalis* LMG 27977^T and *P. marisminoris* LMG 22959^T on PYES supplemented with 3% (w/v) aquarium salts (Reef Crystals – Enriched Blend, Aquarium Systems, Inc.) and on M65 supplemented with 3 % (w/v) NaCl. Growth of the four strains occurred between 15 and 37 °C. Gelatine was hydrolysed only by strain THAF1, while hypoxanthin by strains THAF1 and *P. marisminoris* LMG 22959^T, which was the only strain that hydrolysed tyrosine and xanthin. None of the four strains hydrolysed adenine, casein, starch, xylan, and glucose. Lipolytic activity was observed for strain THAF1 by the hydrolysis of Tween 60, *P. abyssalis* LMG 27977^T by the hydrolysis of Tween 20 and 60. *P. marisminoris* LMG 22959^T hydrolysed weakly Tween 20. DNase activity was observed for the strains THAF1 and *P. marisminoris* LMG 22959^T. Differences in pH-tolerance were also detected,

strain THAF1 grew in a broad pH range from pH 4.5 to 10.0, while *P. aestuarii* KACC 19431^T between pH 5.0 and 9.0, *P. abyssalis* LMG 27977^T between pH 4.5 and 8.0, and *P. marisminoris* LMG 22959^T between pH 4.5 and 9.0. Strains THAF1 and *P. marisminoris* LMG 22959^T grew in presence of 1.0 to 12.0 % (w/v) NaCl, whereas *P. abyssalis* LMG 27977^T grew in a range of 1.0 to 11.0 % (w/v) NaCl, and *P. aestuarii* KACC 19431^T in presence of 1.0 to 8.0 % (w/v) NaCl (Table 14).

Table 14: Phenotypic characteristics that distinguish the strain THAF1. Strains: 1, *Pseudomaribius plastisphaeris* sp. nov. THAF1; 2, *P. aestuarii* KACC 19431^T; 3, *P. abyssalis* LMG 27977^T; 4, *P. marisminoris* LMG 22959^T; 5, *P. soli* CAU 1105^T; 6, *M. pontilimi* GH1-23^T; 7, *M. pelagius* B5-6^T; 8, *M. salinus* CL-SP27^T. Strains 1, 2, 3, and 4 were investigated in parallel under the same cultivation conditions. +, Positive; -, negative; w, weakly positive; NA, not available. Values in brackets were taken from Park *et al.*, (2018) for strain 2, Albuquerque *et al.*, (2015) for strain 3 and some for strain 4, as well as from Martínez-Checa *et al.*, (2005). Data of strains 5 and 6 were taken from Kim *et al.*, (2005) and Lee (2018), respectively, and of strains 7 and 8 from Choi *et al.*, (2007).

Characteristic	1	2	3	4	5	6	7	8
Cell morphology	Short rod	Ovoid / rod	Cocci / pleomorphic	Rod	Short rod	Rod	Rod	Rod
Pigmentation	Pale-orange	Greyish-yellow	Red	Pink	Beige	Light-brown	Beige	Beige
Cytochrome C oxidase	+	+	+	-	-	+	+	+
Temperature range of growth (°C)	Aug-37	15-30 (10-37)	15-37 (15-37)	8-37 (20-37)	20-40	10-30	10-40	10-35
NaCl range of growth (% w/v)	1.0-12.0	1.0-8.0 (0.5-5.0)	1.0-11.0 (0.0-13.0)	1.0-12.0 (0.5-15.0)	1.0-11.0	0.5-5.0	2.0-15.0	1.0-10.0
pH range of growth	4.5-10.0	5.0-9.0 (6.0-8.0)	4.5-8.0 (6.0-8.0)	4.5-9.0 (5.0-10.0)	4.5-11.0	6.0-10.0	6.0-9.0	7.0-8.0
Hydrolysis of								
DNA	w	- (NA)	- (-)	+	NA	NA	-	-
Tyrosin	-	- (-)	- (NA)	+	NA	NA	NA	NA
Hypoxanthin	+	- (-)	- (NA)	+	NA	NA	NA	NA
Gelatine	+	- (-)	- (-)	- (-)	-	-	-	-
Xanthin	-	- (-)	- (NA)	+	NA	NA	NA	NA
Tween 20	-	- (-)	+	w	NA	NA	NA	NA
Tween 60	+	- (-)	+	-	NA	NA	NA	NA
Enzyme activity (API ZYM)								
Valine arylamidase	+	+	+	+	-	w	-	-
Cystine arylamidase	+	- (-)	- (-)	-	-	-	-	-
Naphthol-AS-BI-phosphohydrolase	+	+	+	-	+	+	-	-
α-galactosidase	+	- (-)	- (-)	-	-	+	-	-
α-glucosidase	+	- (-)	+	+	-	-	-	-
Assimilation of (API 50 CH)								
Glycerol	-	- (NA)	+	-	-	+	+	-
D-arabinose	-	- (NA)	-	+	-	-	NA	NA
D-ribose	+	-	+	-	-	NA	+	-
D-xylose	-	-	-	+	-	+	+	+
L-rhamnose	-	-	-	+	-	+	-	-
D-lyxose	-	- (NA)	-	+	-	NA	NA	NA
L-fucose	-	- (NA)	+	+	-	NA	NA	NA
Potassium 5-ketogluconate	-	+	-	-	+	NA	NA	NA
DNA G+C content (mol %)	63.3	(68.7)	(64.7)	(64.2)	64.3	66.7	66.7	70

The activity of 19 enzymes of the four strains were evaluated with the API ZYM test strips (bioMérieux). Positive results were obtained for 10 enzymes for strain THAF1, 5 of them

(valine arylamidase, cystine arylamidase, naphthol-AS-BI-phosphohydrolase, α -galactosidase, and α -glucosidase) differed from the activity of the reference strains *P. aestuarii* KACC 19431^T, *P. abyssalis* LMG 27977^T, and *P. marisminoris* LMG 22959^T. In addition, strains THAF1, *P. aestuarii* KACC 19431^T, *P. abyssalis* LMG 27977^T, and *P. marisminoris* LMG 22959^T differed in 8 out of 49 carbohydrates assimilation tests of the API 50 CH test strips (Table 14).

Results obtained from the physiological test panel proposed by Kämpfer *et al.*, (1991), indicated that strain THAF1 was positive for 2 out of 21 acid production tests, 1 out of 55 carbon source assimilation tests, and 5 out of 12 enzyme activity tests (Table 15). In total, strains THAF1, *P. aestuarii* KACC 19431^T, *P. abyssalis* LMG 27977^T, and *P. marisminoris* LMG 22959^T, did not reveal differences in the acid production tests, but in the assimilation of L-arabinose, D-ribose, D-sorbitol, cis-aconitate, trans-aconitate, adipate, DL-lactate, L-malate, pyruvate, L-histidine, and L-tryptophan; and in the activity of the enzymes bis-*p*-nitrophenyl (*p*NP)-phenyl-phosphonate and *p*NP-phosphate-disodium salt.

Table 15: Physiological characterisation of the strain THAF1 obtained with the test panel. Positive results obtained for the strain THAF1 compared to the reference strains. Strains: 1, *Pseudomonas* *plastisphaera* sp. nov. THAF1; 2, *P. aestuarii* KACC 19431^T; 3, *P. abyssalis* LMG 27977^T; 4, *P. marisminoris* LMG 22959^T. +, positive; -, negative.

Characteristic	1	2	3	4
Acid production from				
L-arabinose	+	+	+	+
aesculin	+	+	+	+
Assimilation of				
D-ribose	+	-	+	-
Enzyme activity				
<i>p</i> NP- α -D glucopyranoside	+	+	+	+
<i>p</i> NP- β -D-glucopyranoside	+	+	+	+
Bis- <i>p</i> NP-phosphate	+	+	+	+
<i>p</i> NP-phosphate-disodium salt	+	-	+	-
L-alanine- <i>p</i> NA	+	+	+	+

4.4.2.3 Chemotaxonomic characterisation

Cellular fatty acids of strain THAF1 were C_{18:1} ω 7c (61.1 %), cyclo C_{19:0} ω 8c (20.0 %), 11-Methyl C_{18:1} ω 7c (8.0 %), C_{18:0} (7.5 %), and C_{16:0} (3.4 %), roughly similar to the profiles reported for the closest related type strains. (Table 16). Differences were the absence of the summed feature 7 in THAF1, present in type strains of the species *M. pontilimi* (4.0 %) and *P. aestuarii* (1.4 %). Furthermore, the presence of C_{17:0} (6.4 %), C_{10:0} 3-OH (2.3 %), C_{17:1} ω 8c (2.0 %), and C_{17:1} ω 6c (1.4 %), present in the type strain of *P. aestuarii* but absent in the strain THAF1. The polar lipid profile consisted of 10 lipids including phosphatidylglycerol (PG), diphosphatidylglycerol (DPG), phosphatidylcholine (PC), three unidentified aminolipids (AL1, AL2, AL3), one unidentified phospholipid (PL1), two unidentified lipids without specific staining (L1, L2), and one unidentified glycolipid (GL1)

(Fig. 44). This profile reflected certain differences with those reported for the genera *Pseudomaribius*, *Palleronia*, and *Maribius*. Main differences were the presence of three unidentified aminolipids instead of one, the absence of one phosphoglycolipid, which was present in all *Maribius* species, and the absence of glycolipid in the type strain of species *P. soli*, *P. aestuariivivens* and all *Maribius* species. Strain THAF1 as other members of the *Roseobacter* clade, contained ubiquinone Q-10 as the only respiratory quinone. The polyamine content of the three reference genera have not been determined so far, but Hamana and Takeuchi (1998) reported that the two representatives of the *Roseobacter* clade, *Roseobacter litoralis* and *Roseobacter denitrificans* contain exclusively spermidine, as determined for the strain THAF1 [11.3 μmol (g dry weight)⁻¹], although traces of putrescine [1.1 μmol (g dry weight)⁻¹] and spermine [(0.05 μmol (g dry weight)⁻¹] were also found.

Table 16: Cellular fatty acid composition of strain THAF1 and its closest related type strains.

Strains: 1, *Pseudomaribius plastisphaeri* sp. nov. THAF1; 2, *P. aestuariivivens* KACC 19431^T; 3, *P. abyssalis* LMG 27977^T; 4, *P. marisminoris* LMG 22959^T; 5, *P. soli* CAU 1105^T; 6, *M. pontilimi* GH1-23^T; 7, *M. pelagius* B5-6^T; 8, *M. salinus* CL-SP27^T. Strains 1, 2, 3, and 4 were investigated in parallel and their biomass were obtained under same growth conditions. Values show the percentage of the total fatty acids. Only values higher than 1% are shown. -, not detected. Values in brackets were taken from Park *et al.*, (2018) for strain 2, Albuquerque *et al.*, (2015) for strain 3, and from Martínez-Checa *et al.*, (2005) for strain 4. Data of strains 5 and 6 were taken from Kim *et al.*, (2005) and Lee (2018), respectively, and of strains 7 and 8 from Choi *et al.*, (2007).

Fatty acid	1	2	3	4	5	6	7	8
Straight-chain								
C _{12:0}	-	-	-	-	1.1	-	-	-
C _{16:0}	3.4	(1.9)	6.4 (5.9)	(4.3)	5.1	4.7	-	4.6
C _{17:0}	-	(6.4)	-	-	7.5	-	-	1.3
C _{18:0}	7.5	3.5 (3.0)	3.3 (2.7)	(3.4)	9.7	7.2	2.7	5.4
Hydroxy								
C _{10:0} 3-OH	-	3.2 (2.3)	(2.0)	(5.0)	2.2	-	3.8	3.5
C _{12:0} 3-OH	-	-	2.4 (2.9)	-	-	-	-	-
Unsaturated								
C _{17:1} ω6c	-	(1.4)	-	-	-	-	-	-
C _{17:1} ω8c	-	(2.0)	-	-	1.5	-	-	-
C _{18:1} ω7c	61.1	93.3 (70.7)	76.8 (54.6)	90.4 (69.0)	62.9	51	54.2	65.3
C _{18:3} ω6c (6,9,12)	-	-	-	-	-	-	-	1.7
11-Methyl C _{18:1} ω7c	8.0	(5.4)	-	-	5.3	6.8	-	3.4
Cyclo C _{19:0} ω8c	20.0	(3.7)	11.2 (26.5)	9.6 (12.8)	-	22.3	21	8.2
C _{19:1} ω6c/ECL 18.846/Cyclo C _{19:0} ω10c	-	-	-	-	-	-	2.4	1.7
Unknown 11.799	-	-	(2.6)	-	-	-	2.8	2.3
Summed feature 7*	-	(1.4)	-	-	-	4.0	-	-

* Summed feature 7 comprised cyclo C_{19:0}ω10c and / or C_{19:1}ω6c and / or C_{19:1}ω7c which could not be separated with the MIDI system.

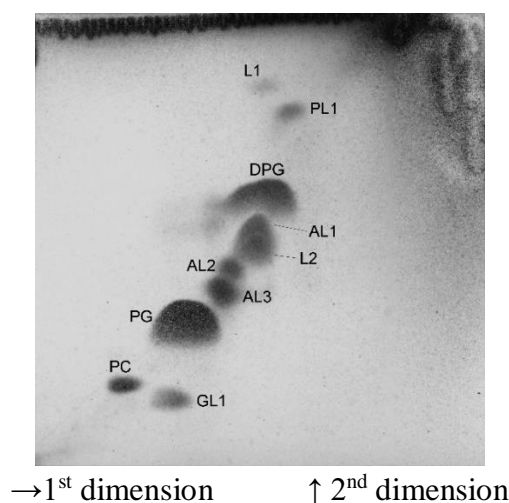


Fig. 44: Thin-layer chromatography of the polar lipid profile of the strain THAF1. Staining was done with 5 % ethanolic molybdotophosphoric acid (w/v). PG, phosphatidylglycerol; DPG, diphosphatidylglycerol; PC, phosphatidylcholine; AL1-AL3, unidentified aminolipids; PL1, unidentified phospholipid; L1, L2, unidentified lipids; GL1, unidentified glycolipid. This chromatography was done by Prof. Dr. Hans-Jürgen Busse.

Based on the phylogenetic, phenotypic, and chemotaxonomic differences found between the strain THAF1 and the described species belonging to the genera *Pseudomaribius*, *Palleronia*, and *Maribius*, this polyphasic characterization suggests that the strain THAF1 (=DSM 106077 =CCM 8817 =CIP 111544) represents a novel species within the family *Rhodobacteraceae*, for which the name *Pseudomaribius plastisphaeris* sp. nov., is proposed.

4.4.2.4 Description of *Pseudomaribius plastisphaeris* sp. nov.

Pseudomaribius plastisphaeris (plas.ti.sphe'ris. L. fem. n. *sphaera* a sphere; N.L. gen. n. *plastisphaeris* of the plastisphere, the surface of microplastics colonised by microbes.

After 3 days of dark incubation on MA at 28 °C, colonies are small (~ 2 mm in diameter), pale-orange, round-shaped, opaque, and dry in appearance. Cells are Gram-stain negative, rod-shaped with 1.6 (±0.2) µm long and 0.9 (±0.1) µm wide, non-motile, and strictly aerobic. Good growth occurs on MA and moderate on M65 medium supplemented with 3% (w/v) NaCl, and between 15 and 37 °C (optimum 21-30 °C), in presence of 1.0 to 12.0 % NaCl (optimum 2.0-8.0 %), and at pH 4.5-10.0 (optimum pH 5.0-9.0). Hypoxanthin, gelatine, aesculin, Tweens 60, and DNA are hydrolysed, but adenine, casein, tyrosine, starch, xanthin, xylan, glucose, Tweens 20, 40, and 80 are not. Cells are positive for catalase and cytochrome C oxidase and do not produce flexirubin-type pigments. Cells produce acid from L-arabinose, but not from α-D-glucose, α-D-lactose, D-saccharose, D-mannitol, dulcitol/dulcitol, D-salicin, adonite/adonitol, i-inositol, D-sorbitol, α-D-raffinose, α-L-rhamnose, D-maltose, D-xylose, D-trehalose, D-cellobiose, 1-O-methyl-D-glucosidepyranosid, *meso*-erythritol, α-D-melibiose, D-arabitol and D-mannose. Cells can assimilate L-arabinose, D-ribose, and D-fucose but not N-acetyl-D-galactosamine, N-acetyl-D-glucosamine, p-arbutin, D-cellobiose, D-fructose, D-

galactose, D-gluconate, α -D-glucose, D-maltose, D-mannose, α -D-melibiose, α -L-rhamnose, D-saccharose, D-salicin, D-trehalose, D-xylose, adonite, i-inositol, maltite, D-mannitol, D-sorbitol, putrescine, sodium acetate, propionate, cis-aconitate, trans-aconitate, adipate, 4-aminobutyrate, azetetic acid, citrate, fumarate, glutarate, DL-3-hydroxybutyrate, itaconate, DL-lactate, L-malate, mesaconate, 2-oxoglutarate, pyruvate, suberate, L-alanine, β -alanine, L-aspartate, L-histidine, L-leucine, L-ornithine (hydrochloride), L-phenylalanine, L-proline, L-serine, L-tryptophan, 3-hydroxybenzoate, 4-hydroxybenzoate, DL-3-phenylacetate, glycerol, erythritol, D-arabinose, L-xylose, methyl- β D-xylopyranoside, D-sorbose, dulcitol, methyl- α D-mannopyranoside, methyl- α D-glucopyranoside, amygdalin, D-lactose, inuline, D-melezitose, D-raffinose, amidon, glycogene, xylitol, gentiobiose, D-turanose, D-lyxose, D-tagatose, L-fucose, D-arabitol, L-arabitol, potassium gluconate, potassium 2-ketogluconate, and potassium 5-ketogluconate. Positive for the enzyme activity of *p*NP- α -D glucopyranoside, *p*NP- β -D-glucopyranoside, Bis-*p*NP-phosphate, *p*NP-phosphate-disodium salt, and L-alanine-pNA, but negative for *p*NP- β -D-galactopyranoside, *p*NP- β -D-glucuronoside, *p*NP- β -D-xylopyranoside, *p*NP-phenyl-phosphonate, *p*NP-phosphoryl-choline, L-glutamate- γ -Carboxy pNA, and L-proline-pNA. Enzymes tested with the API ZYM system are positive for alkaline phosphatase, esterase (C4), esterase lipase (C8), leucine arylamidase, valine arylamidase, cystine arylamidase, acid phosphatase, naphthol-AS-BI-phosphohydrolase, α -galactosidase, and α -glucosidase, but negative for lipase (C14), trypsin, α -chymotrypsin, β -galactosidase, β -glucuronidase, β -glucosidase, N-acetyl- β -glucosaminidase, α -mannosidase and α -fucosidase. Major polyamine is spermidine and major quinone is ubiquinone Q-10. The diamino acid of the peptidoglycan is *meso*-diaminopimelic acid. Major polar lipids are phosphatidylglycerol and diphosphatidylglycerol. Phosphatidylcholine, three unidentified aminolipids, one unidentified phospholipid, two lipids lacking a functional group and one glycolipid are present in moderate or minor amounts. Major fatty acids are C_{18:1} ω 7c and cyclo C_{19:0} ω 8c. The genomic DNA G+C content obtained from the genome sequence data is 63.3 mol %.

The type strain THAF1 (=DSM 106077 =CCM 8817 =CIP 111544) was isolated from the surface of a polyethylene microplastic particle incubated in a marine aquarium system located at the Justus Liebig University Giessen, Germany.

4.4.3 *Ruegeria sedimentorum* sp. nov., a moderately halophilic bacterium isolated from the surface of a sandy sediment

4.4.3.1 Phylogenetic analysis

The 16S rRNA gene sequence of the strain THAF57 (Acc. Number MG996636) had a length of 1362 nucleotides, covering the gene termini 29 to 1390, according to the *E. coli* *rrnB* numbering (Brossius *et al.*, 1978). A BLAST analysis against the EzBioCloud database indicated the closest related type strains of the isolate THAF57: *Ruegeria faecimaris* (98.1 % sequence similarity), *Ruegeria profundus* (98.0 %), *Ruegeria arenilitoris* (97.9 %), *Ruegeria conchae* (97.9 %), *Ruegeria denitrificans* (97.3 %), and *Ruegeria lacuscaerulensis* (97.1 %), within *Rhodobacteraceae*.

The strain THAF57 clustered, independent of the applied method (ML, MaPA, or NJ), with the type strain of *Ruegeria faecimaris* (Fig. 45). However this cluster was not supported by high bootstrap values in all the treeing methods and its placement was not consistent among the calculated trees. The strain THAF57 was separated from the type species of *Ruegeria atlantica*, *Ruegeria conchae*, *Ruegeria profundus*, *Ruegeria arenilitoris*, and *Ruegeria lacuscaerulensis*, the core species of the genus (Arahal *et al.*, 2018).

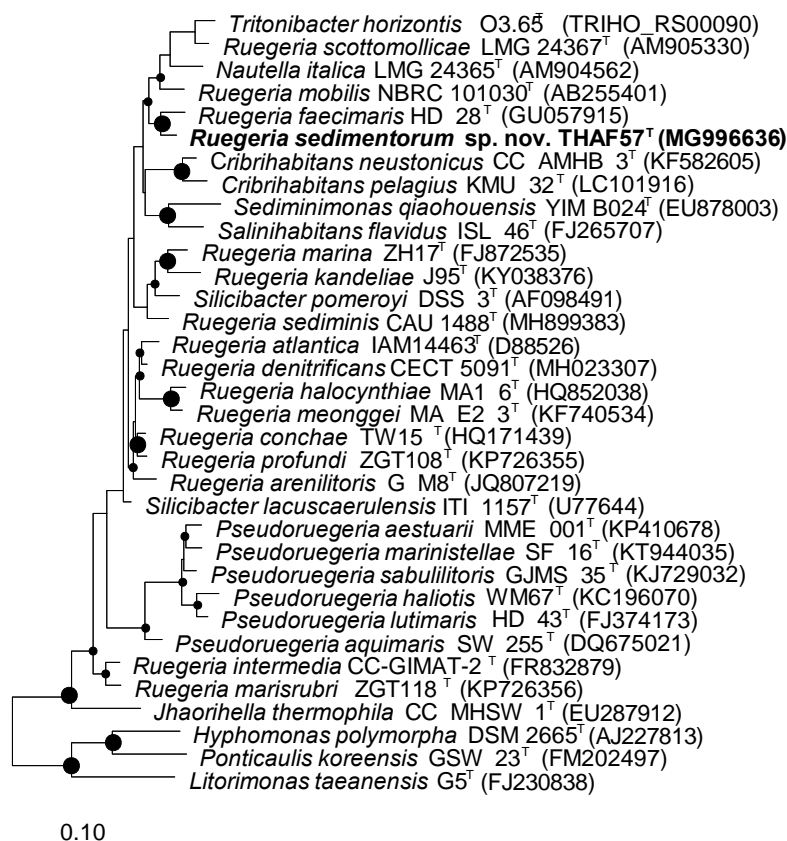


Fig. 45: Phylogenetic placement of strain THAF57 with members of *Rhodobacteraceae*. The phylogenetic consensus tree was generated in ARB based on parallel calculations of ML, MaPA, and NJ trees. The tree is based on nucleotide sequences of gene termini 56 to 1453 (numbering according to Brosius *et al.* 1978). Large circles mark nodes which were present in all three phylogenetic trees, small circles nodes which were present in two out of three trees and non-marked nodes were only present in one of the calculated trees. Sequences of three type strains of *Hyphomonadaceae* were used as outgroup. Bar: 0.1 substitutions per nucleotide positions. This tree was calculated by Dr. Stefanie Glaeser.

4.4.3.2 Morphological and physiological characterisation

The colonies of the strain THAF57 were of about 3 mm in diameter, of beige colour, circular, convex, and with entire borders. Cells were rods with 2.9 (± 0.3) μm length \times 0.8 (± 0.2) μm width, Gram-stain negative, strictly aerobic, non-motile.

The strains THAF57, *R. faecimaris* CCUG 58878^T, and *R. atlantica* CIP 105975^T, were analysed in parallel during the physiological characterization. All strains were positive for

cytochrome oxidase and catalase activity, but negative for the presence of flexirubin-type pigments. Only the strain THAF57 was able to hydrolyse tyrosine and xanthin, while hypoxanthin was hydrolysed by THAF57 and *R. faecimaris* CCUG 58878^T, and gelatine only by the last one. None of the strains hydrolysed adenine, casein, starch, xylan, and glucose. DNase activity was detected in strains THAF57 (weakly) and *R. atlantica* CIP 105975^T but not in *R. faecimaris* CCUG 58878^T. Strains THAF57 and *R. atlantica* CIP 105975^T did not show lipase activity, while *R. faecimaris* CCUG 58878^T hydrolysed Tween 40 and 60 (Table 17).

Table 17: Differential characteristics of the strain THAF57 and its related species. Strains: 1, *Ruegeria sedimentorum* sp. nov. THAF57; 2, *R. faecimaris* CCUG 58878^T; 3, *R. atlantica* CIP 105975^T; 4, *R. profundus* ZGT108^T; 5, *R. arenilitoris* G-M8^T; 6, *R. conchae* TW15^T; 7, *R. denitrificans* CECT 5091^T. Strains 1, 2, and 3 were investigated in parallel under the same conditions. +, Positive; -, negative; w, weakly positive; NA, not available. Values in brackets taken from Oh *et al.*, (2011) for strain 2, Ruger and Höfle, 1992 and Oh *et al.*, (2011) for strain 3. For strains 4, 5, 6, and 7 taken from Zhang *et al.*, (2017), Park and Yoon (2012), Lee *et al.*, (2012), and Arahall *et al.*, (2018), respectively.

Characteristic	1	2	3	4	5	6	7
Cell morphology	Rod	Rod	Rod	Rod	Rod	Rod	Coccobacilli
Pigmentation	Beige	Greyish-yellow	Non-pigmented	Creamy	Greyish-yellow	Yellow	Non-pigmented
Motility	-	- (-)	- (-)	-	+	-	-
Anaerobic growth	-	- (-)	- (-)	-	+	-	-
Temperature range of growth (°C)	15-37	15-30 (4-37)	15-30 (20-30)	15-42	4-45	10-37	15-26
NaCl range of growth (% w/v)	1.0-12.0	1.0-10.0 (1.0-7.0)	1.0-10.0 (3.0-10.0)	2.9-11.1	0.5-6.0	1.0-5.0	1.5-6.0
pH range of growth	4.5-10.0	5.0-10.0 (5.0-8.0)	5.0-10.0 (6.0-11.0)	5.5-9.0	5.5-8.0	7.0-10.0	6.0-9.0
Hydrolysis of							
Tyrosine	+	- (+)	- (NA)	NA	+	NA	NA
Xanthin	+	- (-)	- (+)	NA	-	NA	NA
Hypoxanthin	+	+	- (NA)	NA	+	NA	NA
Gelatin	-	+	- (-)	-	-	-	-
DNA	w	- (NA)	+	NA	NA	NA	-
Tween 40	-	+	- (NA)	NA	-	NA	NA
Tween 60	-	+	- (NA)	NA	-	NA	NA
Enzyme activity (API ZYM)							
Acid phosphatase	-	+	- (-)	w	-	+	+
Acid production from							
D-Maltose	+	- (+)	- (-)	NA	-	+	NA
D-Cellobiose	+	- (-)	+	NA	w	-	NA
Assimilation of							
N-acetyl-D-glucosamine	+	- (NA)	- (NA)	-	NA	-	+
(α-) D-Glucose	+	- (+)	+	-	+	+	+
D-Ribose	+	- (NA)	- (-)	NA	NA	+	+
DL-Lactate	+	- (NA)	- (+)	NA	NA	NA	+
β-Alanine	+	+	- (+)	NA	NA	NA	+

Growth of the strains on different media was highly restricted, since all of them grew well only on MA and only strains THAF57 and *R. atlantica* CIP 105975^T grew also on PYES supplemented with 3 % (w/v) of aquarium salts (Reef Crystals – Enriched Blend, Aquarium Systems, Inc.). Growth of the strain THAF57 was observed between 15 and 37 °C, while the reference strains grew between 15 and 30 °C. Strain THAF57 grew in presence of 1.0-12.0 %

(w/v) NaCl, and the reference strains between 1-10 % (w/v) NaCl. The strains differed in their growth range at different pH as well, since strain THAF57 grew between pH 4.5 and 10.0, and the reference strains between pH 5.0-10.0 (Table 17).

According to the API ZYM test, the three strains showed positive results for the enzymatic activity of 5 out of 19 enzymes (alkaline phosphatase, esterase (C4), esterase lipase (C8), leucine arylamidase, and naphthol-AS-BI-phosphohydrolase), and solely *R. faecimaris* CCUG 58878^T was positive for acid phosphatase. Additional physiological tests performed with the panel designed by Kämpfer *et al.*, (1991) indicated that the strain THAF57 was positive for 5 of 21 acid production tests (D-salicin, L-arabinose, D-maltose, D-cellobiose, and α -D-melibiose), 6 of 55 carbon source assimilation tests (*N*-acetyl-D-glucosamine, α -D-glucose, D-ribose, DL-lactate, pyruvate, and β -alanine), and 9 out of 12 enzyme activity tests (*p*NP- β -D-galactopyranoside, *p*NP- α -D glucopyranoside, *p*NP- β -D-glucopyranoside, Bis-*p*NP-phosphate, *p*NP-phenyl-phosphonate, *p*NP-phosphoryl-choline, L-alanine-*p*NA, L-glutamate- γ -Carboxy *p*NA, and L-proline-*p*NA). Differences observed in the results of this panel among the three tested strains are summarised in the Table 18.

Table 18: Physiological characterisation of the strain THAF57 obtained with the test panel. Differences in the physiological characteristics obtained among the strains. Strains: 1, *Ruegeria sedimentorum* sp. nov. THAF57; 2, *R. faecimaris* CCUG 58878^T; 3, *R. atlantica* CIP 105975^T. +, positive; -, negative.

Characteristic	1	2	3
Acid production from			
D-maltose	+	+	-
D-xylose	-	+	+
D-cellobiose	+	-	+
D-mannose	-	+	-
Assimilation of			
N-acetyl-D-glucosamine	+	-	-
(α -) D-glucose	+	-	+
D-ribose	+	-	-
trans-aconitate	-	+	-
glutarate	-	+	-
DL-3-hydroxybutyrate	-	+	-
DL-lactate	+	-	-
L-malate	-	-	+
β -alanine	+	+	-
L-histidine	-	+	-
L-phenylalanine	-	+	-
L-tryptophan	-	+	-
Enzyme activity			
<i>p</i> NP- β -D-galactopyranoside	+	+	-
<i>p</i> NP- α -D glucopyranoside	+	-	-
L-proline- <i>p</i> NA	+	-	-

4.4.3.3 Chemotaxonomic characterisation

Predominant cellular fatty acids of strain the THAF57 were C_{18:1 ω 7c} (56.9 %), 11 methyl C_{18:1 ω 7c} (15.7 %), C_{16:0} 2-OH (7.9 %), and C_{12:0} 3-OH (5.7 %), comparable to the fatty

acids profile of the reference strains. However, differences were found with *R. faecimaris* CCUG 58878^T, since the predominant fatty acid was basically C_{18:1}ω7c (73.6. %) and 11 methyl C_{18:1}ω7c, the second most abundant in the strain THAF57, was underrepresented (2.1). On the contrary, the profile of *R. atlantica* CIP 105975^T was highly similar to the profile of the strain THAF57, dominated by C_{18:1}ω7c (63.5 %) and 11 methyl C_{18:1}ω7c (11.3 %) (Table 19).

Table 19: Cellular fatty acids profile of the strain THAF57 and its related species. Strains: 1, *Ruegeria sedimentorum* sp. nov. THAF57; 2, *R. faecimaris* CCUG 58878^T; 3, *R. atlantica* CIP 105975^T; 4, *R. profundus* ZGT108^T; 5, *R. arenilitoris* G-M8^T; 6, *R. conchae* TW15^T; 7, *R. denitrificans* CECT 5091^T. Strains 1, 2, and 3 were investigated in parallel under the same conditions. Values show the percentage of the total fatty acids. -, not detected; TR, trace amount (< 1 %). Values in brackets were taken from Oh *et al.*, (2011) for strain 2, Ruger and Höfle, 1992 and Oh *et al.*, (2011) for strain 3. Data of strains 4, 5, 6, and 7 were taken from Zhang *et al.*, (2017), Park and Yoon (2012), Lee *et al.*, (2012), and Arahal *et al.*, (2018), respectively.

Fatty acid	1	2	3	4	5	6	7
Straight-chain							
C _{10:0}	3.5	3.1 (3.1)	2.6 (2.6)	3.3	2.9	3.2	2.3
C _{12:0}	3.7	3.4 (3.4)	3.2 (3.1)	1.8	3.4	3.6	2.9
C _{16:0}	4.7	5.2 (4.4)	4.7 (3.6)	4.7	3.7	5.5	2.9
C _{18:0}	1.9	1.4 (0.7)	1.1 (0.6)	1.3	0.6	2.7	1.2
Unsaturated							
C _{17:1} ω7c	-	- (-)	TR (-)	-	TR	-	-
C _{17:1} ω8c	-	- (-)	- (-)	TR	-	TR	-
C _{18:1} ω7c	56.9	59.2 (73.6)	47.3 (63.5)	-	51.3	-	-
C _{18:1} ω9c	-	- (-)	- (-)	TR	-	TR	-
C _{20:1} ω7c	-	- (-)	- (0.3)	TR	-	-	-
Hydroxy							
C _{10:0} 3-OH	-	- (TR)	TR (TR)	1.0	TR	-	TR
C _{12:0} 3-OH	5.7	4.8 (4.8)	5.5 (5.2)	6.4	5.6	5.2	5.8
C _{16:0} 2-OH	7.9	5.5 (3.9)	7.4 (6.9)	11.9	7.4	5.5	8.1
C _{18:1} 2-OH	-	- (1.1)	- (1.2)	1.4	1.1	TR	-
iso-C _{17:0} 3-OH	-	- (-)	- (-)	-	-	-	1.2
Branched							
anteiso-C _{15:0}	-	- (-)	- (-)	-	-	TR	-
11 methyl C _{18:1} ω7c	15.7	17.5 (2.1)	27.3 (11.3)	9.4	17.6	15.2	3.5
Cyclo C _{19:0} ω8c	-	- (-)	- (-)	1.3	4.7	-	-
Unknown ECL 11.799*	-	- (TR)	- (TR)	-	TR	-	-
Summed feature 8	-	- (-)	- (-)	50.7	-	56.3	70.3

* ECL, equivalent chain-length. Summed feature are groups of two or more fatty acids that could not be separated with the MIDI system. Summed feature 8 consisted of C_{18:1}ω7c and/or C_{18:1}ω6c.

Like almost all species of *Rhodobacteraceae* (and even all members of *Alphaproteobacteria*), the major respiratory quinone of the strain THAF57 was ubiquinone Q-10 (95.8 %) (Pujalte *et al.*, 2013). Minor amounts of Q-9 (3.6 %) and Q-11 (0.6 %) were detected as well. The polar lipid profile indicated the presence of phosphatidylglycerol, diphosphatidylglycerol, phosphatidylcholine and several unidentified lipids including a phospholipid (PL1), an aminolipid (AL1), and three lipids lacking a functional group (L1-L3). (Fig. 46). The majority of *Ruegeria* species have been reported to contain phosphatidylethanolamine in their polar lipid profiles. However, the next related species of the

strain THAF57, *R. faecimaris*, as well as a more distantly related species *R. intermedia* were shown to lack this compound in their polar lipid profile (Oh *et al.*, 2011; Kämpfer *et al.*, 2013). Hence, the presence of phosphatidylethanolamine is not a characteristic for the genus. The polyamine pattern of the strain THAF57 consisted of $[4.9 \mu\text{mol (g dry weight)}^{-1}]$ spermidine, $[0.3 \mu\text{mol (g dry weight)}^{-1}]$ putrescine, $[0.1 \mu\text{mol (g dry weight)}^{-1}]$ cadaverine, and $[0.1 \mu\text{mol (g dry weight)}^{-1}]$ 1,3-diaminopropane. A similar polyamine pattern with the major component spermidine was also reported for *Ruegeria intermedia* (Kämpfer *et al.*, 2013). Though so far only strain THAF57 and *Ruegeria intermedia* CC-GIMAT-2^T have been studied for their polyamine pattern, it can be supposed that a polyamine pattern with the major compound spermidine is a characteristic trait of the species of the genus *Ruegeria*.

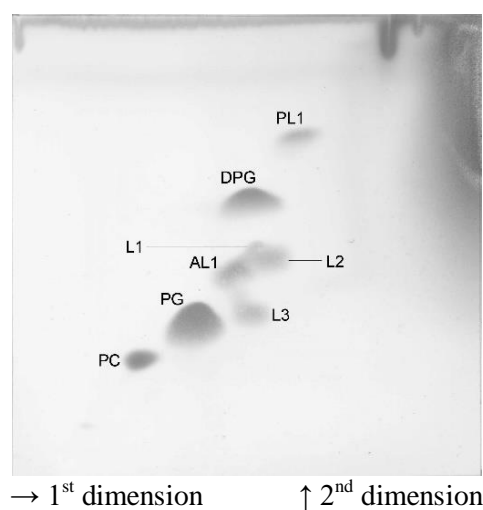


Fig. 46: Polar lipid profile of the strain THAF57. Staining done with 5 % ethanolic molybdotophosphoric acid (w/v) and development at 140 °C. DPG, diphosphatidylglycerol; PG, phosphatidylglycerol; PC, phosphatidylcholine; L1-3, unidentified lipid lacking a functional group; AL1, unidentified aminolipid; PL1, unidentified phospholipid. This chromatography was done by Prof. Dr. Hans-Jürgen Busse.

Based on the differences at the level of phylogeny, physiology, and chemotaxonomy showed by the strain THAF57 (=DSM 106802 =CIP 111611) with respect to the reference type strains included in the analyses, it is considered that the strain represents a novel species within the genus *Ruegeria*, for which the name *Ruegeria sedimentorum* is proposed.

4.4.3.4 Description of *Ruegeria sedimentorum* sp. nov.

Ruegeria sedimentorum (se.di.men.to'rum L. gen. pl. n. *sedimentorum*, of sediments, referring to the isolation source.

Colonies on MA after 3 days of incubation are ~ 3 mm in diameter, beige, circular, convex, with entire borders, and do not produce flexirubin-type pigments. Cells are rod-shaped, Gram-stain negative, aerobic, non-motile, $2.9 (\pm 0.3) \mu\text{m}$ length \times $0.8 (\pm 0.2) \mu\text{m}$ width, positive for cytochrome oxidase and catalase activity. Best growth on MA although also grows moderately on PYES supplemented with 3 % (w/v) of aquarium salts (no growth without added

salts). Mesophilic, growth between 15 and 37 °C (optimum 28 °C), but not at lower or higher temperatures. Moderate halophile, growth in presence of 1.0-12.0 % (w/v) NaCl (optimum 2.0-9.0 %), as well as in a pH range of 4.5 and 10.0 (optimum pH 5.0-7.0). Positive for hydrolysis of tyrosine, xanthin, hypoxanthin, aesculin, and DNA (weak). Do not hydrolyze adenine, casein, starch, xylan, glucose, Tween 20, 40, 60, and 80. According to the API ZYM system, alkaline phosphatase, esterase (C4), esterase lipase (C8), leucine arylamidase, and naphthol-AS-BI-phosphohydrolase are present, but lipase (C14), valine arylamidase, cystine arylamidase, trypsin, α -chymotrypsin, acid phosphatase, α -galactosidase, β -galactosidase, β -glucuronidase, α -glucosidase, β -glucosidase, *N*-acetyl- β -glucosaminidase, α -mannosidase and α -fucosidase are absent. Cells produce acid from D-salicin, L-arabinose, D-maltose, D-cellobiose, and α -D-melibiose, but not from α -D-glucose, α -D-lactose, D-saccharose, D-mannitol, dulcitol/dulcitol, adonite/adonitol, i-inositol, D-sorbitol, α -D-raffinose, α -L-rhamnose, D-xylose, D-trehalose, 1-O-methyl-D-glucosidepyranosid, *meso*-erythritol, D-arabitol, and D-mannose. Cells assimilate *N*-acetyl-D-glucosamine, α -D-glucose, D-ribose, DL-lactate, pyruvate, and β -alanine, but not *N*-acetyl-D-galactosamine L-arabinose, p-arbutin, D-cellobiose, D-fructose, D-galactose, D-gluconate, D-maltose, D-mannose, α -D-melibiose, α -L-rhamnose, D-saccharose, D-salicin, D-trehalose, D-xylose, adonite, i-inositol, maltite, D-mannitol, D-sorbitol, putrescine, sodium acetate, propionate, cis-aconitate, trans-aconitate, adipate, 4-aminobutyrate, azetalic acid, citrate, fumarate, glutarate, DL-3-hydroxybutyrate, itaconate, L-malate, mesaconate, 2-oxoglutarate, suberate, L-alanine, L-aspartate, L-histidine, L-leucine, L-ornithine (hydrochloride), L-phenylalanine, L-proline, L-serine, L-tryptophan, 3-hydroxybenzoate, 4-hydroxybenzoate, DL-3-phenylacetate. Activity of enzymes *p*NP- β -D-galactopyranoside, *p*NP- α -D glucopyranoside, *p*NP- β -D-glucopyranoside, Bis-*p*NP-phosphate, *p*NP-phenyl-phosphonate, *p*NP-phosphoryl-choline, L-alanine-*p*NA, L-glutamate- γ -Carboxy *p*NA, and L-proline-*p*NA is positive, while for enzymes *p*NP- β -D-glucuronoside, *p*NP- β -D-xylopyranoside, and *p*NP-phosphate-disodium salt is negative. Cellular fatty acid profile was dominated by C_{18:1} ω 7c and 11 methyl C_{18:1} ω 7c, and C_{16:0} 2-OH and C_{12:0} 3-OH as minor components. The major respiratory quinone is ubiquinone Q-10. The polar lipid profile comprises the major lipids phosphatidylglycerol, diphosphatidylglycerol, phosphatidylcholine, and several unidentified lipids including a phospholipid (PL1), an aminolipid (AL1) and three lipids lacking a functional group (L1-L3). The major polyamine is spermidine.

The type strain THAF57 (=DSM 106802 =CIP 111611) was isolated from the surface of a sandy sediment particle obtained from one aquaria system containing stony-coral fragments at the animal facility of the Justus Liebig University Giessen, Germany.

4.4.4 *Vibrio aquimaris* sp. nov. a novel member of *Vibrionaceae* with putative pathogenicity-related genes, isolated from the water of a marine aquarium system

4.4.4.1 Phylogenetic analysis

The detailed phylogenetic analyses of the *Vibrio* spp. isolates based on the 16S rRNA gene sequences, MLSA using the concatenated nucleotide and amino acid sequences of five

housekeeping genes, as well as the core-genome-based phylogeny were already described in the sections 4.3.1, 4.3.2, and 4.3.5. These analyses indicated that the eleven isolates belonging to the phylotype V-2 cannot be assigned to a current described *Vibrio* species. One representative of the phylotype V-2, the strain THAF100, was selected as the type strain of this group to be used in the polyphasic characterisation of the novel species. A BLAST analysis based on the nearly full-length 16S rRNA gene of the strain THAF100 against the EzBioCloud database indicated that the closest related species were *Vibrio japonicus* (16S rRNA gene sequence similarity, 98.5 %) and *Vibrio caribbeanicus* (98.4 %), followed by *Vibrio sinaloensis* (98.2 %), and *Vibrio brasiliensis* (98.1 %). A clustering with the type strain of any of these species was obtained neither in the 16S rRNA gene nor in the MLSA-based phylogenetic trees (Fig. 26, 27A-B, 37, and 38).

4.4.4.2 Morphological and physiological characterisation

The strain THAF100 showed phenotypic properties that define the genus *Vibrio*. For instance, motile, rod-shaped, and Gram-staining negative cells, positive for cytochrome C oxidase and catalase activity, aerobic or facultative anaerobic. Additional phenotypic traits of strain THAF100 were compared with those published for the type species of *V. coralliilyticus* (analysed in parallel together with the strain THAF100), *V. caribbeanicus*, and *V. japonicus*, from Ben-Haim *et al.*, (2003), Hoffmann *et al.*, (2012), and Doi *et al.* (2017), respectively.

The strain THAF100 and *V. coralliilyticus* LMG 20984^T were able to hydrolyse tyrosine, hypoxanthin, casein, and gelatine. DNase and lipase activities were positive by the degradation of DNA and Tween 40, 60, and 80. Good growth of both strains was registered on media R2A, glycine/arginine, PYE, CASO, LB, all supplemented with 3 % (w/v) NaCl, PYES supplemented with 3 % (w/v) aquarium salts (Reef Crystals – Enriched Blend, Aquarium Systems, Inc.), as well as on MA and blood agar without any salt addition. Weak growth was observed on NU and K7 supplemented with 3 % (w/v) NaCl. *V. coralliilyticus* LMG 20984^T grew well on DEV without salt addition, while growth of strain THAF100 was weak. No growth of the strain THAF100 was observed on TS, CASO, and LB without salt addition. The strains did not grow neither on the salt-supplemented nor on the original version of Malt extract, M65, and McConkey media. Good growth of both strains was observed between 15 and 37 °C, and weak at 8 °C. The strains THAF100 grew in presence of 1.0-11.0 % (w/v) NaCl and between pH 4.5 and 10.0, while *V. coralliilyticus* LMG 20984^T grew in presence of 1.0-10.0 % (w/v) NaCl and between pH 4.0 and 10.0 (Table 20).

The API ZYM panels indicated enzymatic activity of alkaline phosphatase, esterase (C4), esterase lipase (C8), lipase (C14), leucine arylamidase, and acid phosphatase by the tested strains. Only THAF100 was positive for *N*-acetyl- β -glucosaminidase and *N*-acetyl- β -glucosaminidase. The API 50CH system using API 50 CHB/E medium supplemented with 3 % (w/v) aquarium salts (Reef Crystals – Enriched Blend, Aquarium Systems, Inc.) indicated that both strains assimilate D-glucose, D-fructose, D-mannose, aesculin, D-maltose, D-saccharose, amidon, glycogene, and weakly potassium 2-ketogluconate. Physiological tests with the API 20 NE system were positive for aesculin dihydrolase for the strain THAF100,

while the API 20 E system indicated negative results for activity of β -galactosidase, tryptophan deaminase, and indole production (Table 20). According to the panel designed by Kämpfer *et al.* (1991), the strain THAF100 was positive for 3 of 21 acid production tests, 16 of 55 carbon source assimilation tests, and 7 of 12 enzyme activity tests. Differences obtained in this test between the strain THAF100 and *V. coralliilyticus* LMG 20984^T are listed in the Table 21.

Table 20: Phenotypic characteristics differentiating the strain THAF100. Strains: 1, *Vibrio aquimaris* sp. nov. THAF100; 2, *V. coralliilyticus* LMG 20984^T; 3, *V. caribbeanicus* N384^T; 4, *V. japonicus* JCM 31412^T. Strains 1 and 2 were studied in parallel under the same cultivation conditions. Data for strains 2 (in brackets), 3, and 4 were taken from Ben-Haim *et al.*, (2003), Hoffmann *et al.*, (2012), and Doi *et al.* (2017), respectively. * done according to Kämpfer *et al.*, 1991.

Characteristic	1	2	3	4
Pigmentation	Beige	Cream	Cream	Cream
Temperature range of growth (°C)	8-37	8-37 (until 35)	10-35	10-37
NaCl range of growth (% w/v)	1.0-11.0	1.0-9.0 (0.5-8.0)	0.5-8.0	0.5-9.0
pH range of growth	4.5-10.0	4.0-10.0 (NA)	6.0-10.0	7.0-12.0
Anaerobic growth	+	+	+	+
Nitrate reduction	-	+	-	-
Indole production	-	+	+	+
Hydrolysis of				
Tyrosine	+	+	NA	NA
Xanthin	-	+	NA	NA
Hypoxanthin	+	+	NA	NA
Gelatin	+	+	-	-
Starch	-	+	-	+
Aesculin	+	+	-	-
Blood	-	+	NA	NA
Tween 40	+	+	-	NA
Tween 60	+	+	NA	NA
Tween 80	+	+	-	NA
Enzyme activity				
Catalase	+	+	-	-
Gelatinase	-	+	NA	-
Tryptophan deaminase	-	+	-	+
Lipase (C14)	+	+	-	-
Valine arylamidase	-	-	-	+
Trypsin	-	-	-	+
N-Acetyl- β -glucosaminidase	+	-	-	-
α -Galactosidase	-	-	-	+
β -Glucuronidase	-	-	-	+
Arginine dehydrolase	-	+	+	+
Lysine decarboxylase	-	-	-	+
Fermentation of				
Glucose	+	+	-	+
Amygdalin	-	-	-	+
D-Arabinose	-	-	-	+
D-Mannose	+	+	+	-
D-Melibiose	-	-	-	+
D-Mannitol	-	+	+	+
Assimilation of				
D-Galactose	-	+	-	+
D-Maltose	+	+	+	NA
L-Malate	+	+	-	NA
D-Cellobiose	-	-	-	+
D-Ribose	-	+	+	+
D-Trehalose	-	+	+	+
DNA G+C content (mol%)	42.7	45.6	41.6	46.8

Table 21: Acid production and assimilation of different carbon sources and enzyme activity determined using a 96-well panel designed by Kämpfer *et al.*, 1991. Strains: 1, *Vibrio aquimaris* sp. nov. THAF100; 2, *Vibrio coralliilyticus* LMG 20984^T. -, negative reaction; +, positive reaction.

Characteristic	1	2
Acid production from		
L-arabinose	+	+
D-xylose	+	+
D-mannose	+	+
Assimilation of		
N-acetyl-D-galactosamine	+	+
D-fructose	+	+
D-galactose	-	+
(D-) gluconate	-	+
(α -) D-glucose	+	+
D-maltose	+	+
D-mannose	+	+
D-ribose	-	+
D- saccharose	-	+
(D-) salicin	-	+
D-trehalose	-	+
L-leucine	-	+
L-phenylalanine	-	+
D-trehalose	-	+
adonite	-	+
malite	-	+
(sodium) acetate	+	+
propionate	+	+
cis-aconitat	-	+
citrate	-	+
fumarate	+	+
DL-lactate	+	+
L-malate	+	+
2-oxoglutarate	+	+
L-alanine	+	+
L-aspartate	+	+
L-histidine	-	+
L-leucine	-	+
L-ornithine (hydrochloride)	+	+
L-phenylalanine	-	+
L-proline	+	+
L-serine	+	+
Enzyme activity		
pNP- β -D-galactopyranoside	-	+
pNP- α -D glucopyranoside	-	+
pNP- β -D-glucopyranoside	-	+
pNP- β -D-xylopyranoside	+	-
Bis-pNP-phosphate	+	+
pNP-phenyl-phosphonate	+	+
CRS-control	-	+
pNP-phosphoryl-choline	+	+
L-alanine-pNA	+	+
L-glutamate- γ -Carboxy pNA	+	+
L-proline-pNA	+	+

4.4.4.3 Chemotaxonomic characterisation

The fatty acids profile of strain THAF100 and its close related strains was similar, reflecting the characteristic composition of the genus *Vibrio* with C_{12:0}, C_{14:0}, C_{16:0}, summed feature 3 (C_{16:1} ω7c and/or C_{16:1} ω6c), C_{18:1} ω7c, and/or C_{18:1} ω6c. Predominant fatty acids of the strain THAF100 were those in the summed feature 3 (C_{16:1} ω7c and/or C_{16:1} ω6c) (33.3 %), C_{16:0} (12.6 %), C_{18:1} ω7c (11.4 %), C_{15:0} (8.7 %). The fatty acid profile of the strain THAF100 differed from its related strains in the presence of C_{15:0}, C_{17:1} ω8c, C_{17:0}, C_{17:1} ω6c, and C_{13:0}, more abundant or above the trace values registered for the reference strains (Table 22).

Table 22: Cellular fatty acids composition of strain THAF100 and its related type strains. Strains: 1, *Vibrio aquimaris* sp. nov. THAF100; 2, *V. coralliilyticus* LMG 20984^T; 3, *V. caribbeanicus* N384^T; 4, *V. japonicus* JCM 31412^T. Strains 1 and 2 were investigated in parallel. Values represent the percentage of total cellular fatty acids. Values of strains 2 (in brackets), 3, and 4 were taken from Ben-Haim *et al.*, (2003), Hoffmann *et al.*, (2012), and Doi *et al.*, (2017), respectively. Cellular fatty acid compositions were obtained after cultivation of bacteria on TSA (strain 2), TSA containing 1 % NaCl (w/v) (3), and TSA containing 1.5 % NaCl (w/v) (4). –, Not detected; TR, trace amount (< 1 %). Biomass of the strain THAF100 was obtained after the cultivation on MA since the strain did not grow neither on TSA nor on TSA supplemented with NaCl.

Fatty acid	1	2	3	4
Straight-chain				
C _{12:0}	3.4	3.1 (2.2)	4.8	3.8
C _{13:0}	1.6	- (-)	TR	-
C _{14:0}	6.6	5.3 (6.5)	2.6	4.5
C _{15:0}	8.7	1.3	2.2	-
C _{16:0}	12.6	17.1 (14.1)	20.8	21.9
C _{17:0}	2.8	1.2 (2.0)	1.7	1.5
C _{18:0}	-	1.9 (-)	TR	-
Unsaturated				
C _{16:1} ω 7c alcohol	1.1	- (-)	-	TR
C _{17:1} ω 6c	2.5	- (-)	TR	TR
C _{17:1} ω 8c	6.4	(1.3)	1.7	1.9
C _{18:1} ω 6c	-	5.5 (-)	-	-
C _{18:1} ω 7c	11.4	24.7 (18.2)	10.4	17.3
Hydroxy				
C _{12:0} 3-OH	2.6	2.6 (2.7)	2.4	4.3
iso-C _{14:0} 3-OH	-	- (-)	TR	-
C _{15:0} 2-OH	-	- (-)	-	1.2
iso-C _{15:0} 3-OH	-	(1.7)	TR	-
Branched				
iso-C _{13:0}	-	(2.6)	2.1	TR
iso-C _{14:0}	-	- (TR)	TR	4.5
iso-C _{15:0}	-	(2.8)	1.6	TR
anteiso-C _{15:0}	-	- (-)	TR	TR
iso-C _{16:0}	-	- (-)	1	TR
iso-C _{17:0}	-	(3.2)	3	TR
iso-C _{18:0}	-	-	-	-
Summed feature 1 ^a	2	- (-)	-	1.2
Summed feature 2 ^b	4.1	3.7 (-)	-	6.4
Summed feature 3 ^c	33.3	34.1 (-)	35.6	27.7

Summed features are groups of two or more fatty acids that could not be separated with the MIDI system. ^a C_{15:1} iso H and/or C_{13:0}-3OH; ^b C_{12:0}, ALDE, C_{14:0}-3OH, C_{16:1} iso I, unknown 10.928 ; ^c C_{16:1} ω7c and/or C_{16:1} ω6c.

The genome of the strain THAF100 has a size of 4.5 Mbp with a G+C content of 42.7 %, which fits in the range of the G+C content reported for the genus (38-51 mol%) (Hoffmann *et al.*, 2012). The genome was structured into one chromosome (CP045350.1) and three plasmids (pTHAF100_a; CP045351.1, pTHAF100_b; CP045352.1, and pTHAF100_c; CP045353.1). Based on the differences obtained during the polyphasic characterisation, including 16S rRNA gene, MLSA, and genome-based analyses, genotyping, morphologic, phenotypic, and chemotaxonomic characterisation, it was shown that the strain THAF100 represents a novel species within the genus *Vibrio*, different from its related species. The name *Vibrio aquimaris* is proposed with THAF100 (=DSM 109633) as the type strain.

4.4.4.4 Description of *Vibrio aquimaris* sp. nov.

Vibrio aquimaris (a.qui.ma'ris. L. n. *aqua* from water; L. gen. n. *maris* of a sea; N.L. gen. n. *aquimaris* of the water of the sea).

Cells are rod-shaped, 2.5 (± 0.4) μm length \times 0.8 (± 0.1) μm width, Gram-stain negative, motile, aerobic, and facultative anaerobic. Colonies on MA after 3 days of incubation are ~ 3 mm in diameter, beige, circular, convex, with entire borders. Best growth occurs on MA, also on CASO, glycine/arginine, LB, PYE, R2A (all supplemented with 3 % (w/v) NaCl), PYES supplemented with 3 % (w/v) aquarium salts, and Columbia agar. The species is mesophilic with growth between 8 and 37 °C (optimum 28 °C) and moderate halophilic with growth in the presence of 1.0-11.0 % (w/v) NaCl (optimum 2.0-9.0 %). It has a wide pH range of growth, pH 4.5 to pH 10.0 (optimum pH 4.5-7.0). Positive for cytochrome oxidase and catalase activity, negative for citrate utilization, nitrate reduction, production of indole, hydrogen sulfide, and acetoin (Voges–Proskauer). Tyrosine, casein, gelatine, hypoxanthin (weakly), aesculin, DNA, Tween 40, 60, and 80 are hydrolysed, but adenine, starch, xanthin, xylan, cellulose, and blood are not. Activity of enzymes alkaline phosphatase, esterase (C4), esterase lipase (C8), lipase (C14), leucine arylamidase, acid phosphatase, naphthol-AS-BI-phosphohydrolase, and N-acetyl- β -glucosaminidase are positive, but negative for valine arylamidase, cystine arylamidase, trypsin, α -chymotrypsin, α -galactosidase, β -galactosidase, β -glucuronidase, α -glucosidase, β -glucosidase, α -mannosidase, and α -fucosidase. Acid is produced from L-arabinose, D-xylose, D-mannose, D-fructose, D-maltose, D-saccharose, amidon, glycogene, and potassium 2-ketogluconate, but not from dulcitol/dulcitol, adonite/adonitol, 1-O-methyl-D-glucosidepyranosid, glycerol, erythritol, D-arabinose, L-xylose, D-adonitol, methyl- β -D-xylopyranoside, D-galactose, D-glucose, D-sorbose, L-rhamnose, inositol, D-mannitol, D-sorbitol, methyl- α -D-mannopyranoside, methyl- α -D-glucopyranoside, N-acetylglucosamine, amygdalin, arbutin, salicin, D-cellobiose, D-lactose, D-melibiose, D-trehalose, inuline, D-melezitose, D-raffinose, xylitol, gentiobiose, D-turanose, D-lyxose, D-tagatose, D-fucose, L-fucose, D-arabitol, L-arabitol, potassium gluconate, and potassium 5-ketogluconate. Cells assimilate N-acetyl-D-glucosamine, D-fructose, α -D-glucose, sodium acetate, propionate, fumarate, DL-lactate, L-malate, 2-oxoglutarate, L-alanine, L-aspartate, L-ornithine (hydrochloride), L-proline, and L-serine, but not maltite, putrescine, cis-aconitate, trans-aconitate, adipate, 4-aminobutyrate, azetalic acid, citrate, glutarate, DL-3-hydroxybutyrate, itaconate, mesaconate, pyruvate, suberate, β -alanine, L-histidine, L-leucine, L-phenylalanine, L-tryptophan, 3-hydroxybenzoate, 4-hydroxybenzoate, and DL-3-phenylacetate. Positive for enzyme activity of *p*NP- β -D-xylopyranoside, bis-*p*NP-phosphate, *p*NP-phenyl-phosphonate,

*p*NP-phosphoryl-choline, L-alanine-pNA, L-glutamate- γ -Carboxy pNA, and L-proline-pNA, while *p*NP- β -D-galactopyranoside, *p*NP- β -D-glucuronoside, *p*NP- α -D glucopyranoside, *p*NP- β -D-glucopyranoside, *p*NP-phosphate-disodium salt, arginine dihydrolase, urease, lysine decarboxylase, tryptophan deaminase, and ornithine decarboxylase are negative. Major fatty acids are summed feature 3 (C_{16:1} ω 7c and/or C_{16:1} ω 6c), C_{16:0}, and C_{18:1} ω 7c. The genomic G+C content of the type strain is 42.7 mol % (complete genome sequence). The genome of the type strain is organized in chromosome I (3,138,671 bp), a large plasmid (1,317,907 bp) also intended as second chromoson or chromide, and two further smaller plasmids (39,604 and 4,831 bp).

The type strain THAF100 (=DSM 109633) was isolated from the water column of a marine aquaria system containing stony-coral fragments at the animal facility of Justus Liebig University Giessen, Germany.

CHAPTER V

5. Discussion

5.1 Bacterial assemblages developed on MP differed from those on natural particles

It is widely known that plastic surfaces are new hotspots for habitat use by a huge variety of prokaryotic and eukaryotic organisms. The bacterial MP colonisation is affected by environmental factors as nutrient availability, water salinity, geographic location, and season (Amaral-Zettler *et al.*, 2015; De Tender *et al.*, 2015; Oberbeckmann *et al.*, 2016; Oberbeckmann *et al.*, 2018). Here, bacterial communities that colonise the plastisphere were analysed through cultivation-dependent and independent techniques, as well as the potential implications of members of these communities on coral health.

The comparison of bacterial assemblages developed in the marine system indicated a specific and uniform colonisation of MP. This was confirmed by the low variance of community profiles obtained from MP that differed from the high variance observed for sterile sandy sediments, detritus, and the particulate and particle-free water fractions. The specific bacterial colonisation of MP has been widely observed in open waters (Zettler *et al.*, 2013; Oberbeckmann *et al.*, 2014; McCormick *et al.*, 2014; Amaral-Zettler *et al.*, 2015; De Tender *et al.*, 2015; Debroas *et al.*, 2017; Dussud *et al.*, 2018a; Oberbeckmann *et al.*, 2018; Miao *et al.*, 2019). In these studies, members of families such as *Rhodobacteraceae*, *Alteromonadaceae*, *Flavobacteraceae*, *Erythrobacteraceae*, *Hyphomonadaceae*, *Pseudoalteromonadaceae*, and the JTB255 marine benthic group were described as the most abundant bacterial colonizers of plastic debris. These families were also reported as members of a core bacteriome on plastic surfaces (De Tender *et al.*, 2017a), also detected on MP incubated in the CEMarin aquarium system.

The SEM micrographs revealed bacterial cells able to produce adhesion structures as stalks or prosthecae, mainly used for attachment to MP surfaces. Some bacteria that produce polar holdfast structures are members of the MRC (*Rhodobacteraceae*), families *Hyphomonadaceae* and *Caulobacteraceae*, and the *Blastocaulis-Planctomyces* group (Dang and Lovell, 2016). Other structures as pili, flagella, fimbriae, or curli, also facilitate attachment and give advantages to the cells over other bacteria competing for space during early colonisation stages, as increased nutrient uptake, genetic transfer, enzymatic activity, or biofilm formation regulated by quorum sensing (Buchan *et al.* 2005; Dang *et al.* 2008; Dang and Lovell, 2016).

Interestingly, the MP incubated in the system were abundantly colonised by genera belonging to the MRC, mainly *Roseivivax*, *Marivita*, and *Sulfitobacter*, and to a lesser extent *Roseovarius* and *Ruegeria* (all *Rhodobacteraceae*). Those are known primary surface colonisers that use attachment structures and were detected in both the cultivation-dependent and –independent approaches. *Flavobacteriaceae* and *Saprospiraceae*, the second and third

most abundant families on the studied MP, were also found on PE-debris collected from different marine regions (De Tender *et al.*, 2017b). Oberbeckmann *et al.* (2016) even found *Flavobacteriaceae* to be the most abundant family on PET, indicating in some extend polymer-specific colonisation by certain groups. *Alteromonadaceae* and *Hyphomonadaceae*, the fourth and fifth most abundant families on MP, were also discriminant on plastic litter in the North and Baltic Sea (De Tender *et al.*, 2015; Oberbeckmann *et al.*, 2018). Members of *Hyphomonadaceae* are also primary surface colonisers and able to produce holdfast structures that provide a more efficient nutrient uptake on surfaces, favouring their growth in nutrient-poor habitats as already detected on MP (Zettler *et al.*, 2013; Dang and Lowell, 2016; Oberbeckmann *et al.*, 2018; Ogonowski *et al.*, 2018). The high abundance of *Erythrobacteraceae* (mainly *Erythrobacter* sp.) on MP, also observed by Dussud *et al.*, (2018b) and Oberbeckmann *et al.* (2018), might be explained by specific physiological features related to habitat adaptation. For instance, the production of bacteriochlorophyll *a* and carotenoids that protect *Erythrobacter* cells from UV radiation (Setiyono *et al.*, 2019). This contributes to their survival on MP floating in the sea surface, protecting the cells of the radiation but also using light as energy source. These characteristics of the most abundant groups found on MP from the system, could explain their high relative abundance after twelve weeks of incubation.

Harrison *et al.* (2014) indicated that bacterial communities were formed on LDPE-MP within seven days and became significantly less diverse over time. In the marine system the bacterial assemblages were still significantly different after twelve weeks of incubation, which suggests that during the first stages of colonisation, the bacterial communities of the marine system were, likely, even more diverse. This also suggests that the colonisation process is shaped by the events occurring in the early stages of colonisation, favouring the primary surface colonisers over time, where microbial succession leads to more stable bacterial assemblages in terms of structure and composition. This behaviour of the bacterial succession was observed recently by Pinto *et al.* (2019) even in biofilms developed on plastics of different materials. Nevertheless, to understand the temporal fluctuations of bacterial assemblages until the development of a stable biofilm, it is necessary to investigate MP colonisation stages directly after the addition of sterile particles to the aquaria system in short time lapses.

The SEM micrographs also illustrated an abundant presence of diatoms and other algae on MP. Algae and even corals produce exudates that are rich in dissolved neutral sugars, which stimulate fast-growing bacteria (Nelson *et al.*, 2013). Likely, these exudates and other nutrients product of the photosynthetic activity of the algae, accumulated on the surfaces of MP incubated in the system and induced an overgrowth of certain bacterial groups. Members of the MRC, and genera as *Vibrio*, *Marinobacter*, etc. exploit rapidly the presence of DOC (Nelson *et al.*, 2013). Therefore, the abundant presence of genera as *Roseivivax*, *Marivita*, and *Sulfitobacter* on MP, could have been influenced by those exudates in the marine system. Likewise, antimicrobial activity was registered for *Roseivivax* and *Sulfitobacter* by Bibi *et al.* (2018), which probably favoured the selective growth of other MRC members during the early stages of MP colonisation. *Marivita* was found associated to algae-dominated coral reefs (Cárdenas, 2016), being another example of the influence of algae in shaping the structure of communities with predominant bacteria acting as opportunistic copiotrophs.

The specificity of the bacterial colonisation of MP observed in this study, including numerous taxa detected in the core bacteriome associated to plastics in open waters of different locations (De Tender *et al.*, 2017a), argues against the bottle effect in this particular experiment. This effect has been discussed as an experimental disturbing side effect in confined incubation experiments with marine and freshwater bacterioplankton (Pernthaler and Amann, 2005). The results obtained in this study suggest that the conditions used during the experiment, in addition to the wildlife inhabiting in the CEMarin aquarium system, emulated to a great extent a realistic marine environment, reducing possible biases proper of studies carried out under laboratory conditions. In previous studies, the bottle effect was reflected in the overall decrease of the community richness and diversity in incubation experiments (Ogonowski *et al.*, 2018; Keszy *et al.*, 2019). However, the observed differences between the bacterial community composition of MP and the natural particles incubated in the CEMarin system under identical experimental conditions, cannot be ascribed to bottle effects of confined systems or planned manipulation. Despite, bottle effects cannot be completely ruled out from controlled experiments.

5.2 Potential bacterial degradation of PE-MP

Some studies have pointed out that PE is resistant to biodegradation due to highly stable covalent bonds, high molecular weight of the molecules, lack of readily oxidisable and/or hydrolysable groups in the polymer backbone, etc. (Hadad *et al.*, 2005; Gautam *et al.*, 2007). However, the bacterial biodegradation of PE has been already described, showing physical damage and molecular weight loss of PE films, which was caused by bacteria and the activity of different enzymes (Hadad *et al.*, 2005; Yang *et al.*, 2014).

Jejudonia, *Roseivivax*, *Marinobacter*, *Erythrobacter*, and *Sulfitobacter*, some of the most abundant genera only found on MP surfaces, belong to families *Flavobacteriaceae*, *Rhodobacteraceae*, *Alteromonadaceae*, and *Erythrobacteraceae*. Interestingly, these families contain genera with members known to degrade complex polymer substrates as hydrocarbonoclastic strains of *Marinobacter* or *Erythrobacter* (Kirchman, 2002; Dang and Lovell, 2016; Oberbeckmann *et al.*, 2016; Curren and Leong, 2018; Dussud *et al.*, 2018a; Dussud *et al.*, 2018b). Several enzymes as depolymerases, cutinases, lipases, serine proteases, endopeptidases, esterases, proteinases, ureases, dehydratases, or hydrolases are involved in the breakdown of complex polymers and have been detected in members of the mentioned families (Tokiwa *et al.*, 2009; Chronopoulou *et al.*, 2015; Pathak and Navneet 2017; Morohoshi *et al.*, 2018; Urbanek *et al.*, 2018; Butbunchu and Pathon-Aree, 2019; Jacquin *et al.*, 2019).

It is not yet confirmed if *Jejudonia* sp., the most abundant genus on MP contains the genes coding for the mentioned enzymes. The presence of *Jejudonia* sp. on plastics has been unprecedented and little is known about the genus, which comprises only one species isolated from brackish waters (Park *et al.*, 2013). Unfortunately, representatives of the genus were not

obtained in the cultivation procedure and its genome is not yet available, which could have contributed in the identification of specific genes that might be involved in surface attachment processes or polymer degradation that would unveil its abundant presence exclusively on MP in the marine system. Particular conditions of the MP, which likely influenced the successful colonisation of *Jejudonia* sp. members, as well as its potential hydrocarbonoclastic metabolism, should be studied in future studies. On the other hand, most of the genes that codify for the mentioned enzymes were detected in the genomes of strains of genera *Roseivivax*, *Marinobacter*, and *Erythrobacter* isolated from the MP incubated in the system and analysed in this study. This suggests that these bacterial strains have the metabolic potential to induce chemical changes in the polymer chains of the PE-MP. Similarly, these bacteria may use the PE-MP constituents or accumulated compounds, as polycyclic aromatic hydrocarbons (PAH), as nutrient sources, which may explain the selective colonisation of the sterile MP instead of the natural particles in the system.

The use of different polymers as major energy and carbon source was documented by Yoshida *et al.* (2016). PET was degraded and assimilated by bacteria capable of hydrolysing PET into two benign monomers. Likewise, esterases were involved in PET biodegradation by *Nocardia* sp. (Sharon and Sharon, 2012). A discriminant family present on PET particles found in the ocean was *Cryomorphaceae*, whose members have dioxigenases and haloacid dehalogenases that suggest a role of these microbes in the respiratory degradation of recalcitrant compounds (Riedel *et al.*, 2012). In the CEMarin system, this family was highly abundant in the free-living bacterioplankton community but absent on MP, suggesting a differential colonisation of PET and PE surfaces by members of *Cryomorphaceae*, probably due to the different chemical structure of these polymers.

The presence of potential plastic-degrading enzymes was detected to a lesser extent in *Vibrio* spp. genomes compared to the genomes of the other analysed genera. Dehydratases, esterases, and hydrolases were the detected enzymes in the *Vibrio* spp. genomes. Foulon *et al.* suggested in 2016, that *Vibrio* spp. are secondary colonisers that exploit the prior formation of aggregates including numerous bacteria. This is consistent with the fact that *Vibrio* has not been reported as a common abundant genus on plastic debris. There is only one study indicating that the genus *Vibrio* dominated the bacterial community on plastics, specifically only on one out of three polypropylene samples recovered from the ocean (Zettler *et al.*, 2013). This evidence suggests that *Vibrio* spp. are not polymer-degrading bacteria and its presence on plastic is rather explained by the exploitation of formed biofilms and the surface transformations caused by those primary colonisers than to the degradation and uptake of nutrients derived from polymers. So far, there is no evidence indicating that *Vibrio* spp. possess enzymes involved in polymer degradation. This does not imply that *Vibrio* spp. are not able to colonise plastic surfaces, which is a widely discussed topic originated by the variable abundance of the genus on plastic debris reported in different studies and its relevance due to its potential to trigger numerous diseases in marine animals and humans (Kirstein *et al.*, 2016).

Polycyclic aromatic hydrocarbon-degrading genera, such as *Erythrobacter* were recently reported on MP in oil polluted locations (Zhuang *et al.*, 2015; Curren and Leong,

2019). This suggests plastic debris and MP, independently of their composition, might be a source of strains with potential applications in bioremediation. *In silico* approaches as genome sequencing and identification of putative genes coding for hydrocarbon degrading enzymes might also contribute to the identification of bacteria with other biotechnological applications in the degradation of complex polymers.

5.3 MP as a refuge of potential pathogens for the marine biota

The role of MP as vector of non-native and potential pathogenic bacteria that might be dispersed along marine ecosystems affecting the health of the marine biota has been widely discussed in the past years (Zettler *et al.*, 2013; Reisser *et al.*, 2014; Wagner *et al.*, 2014; Keswani *et al.*, 2016; Kirstein *et al.*, 2016; Oberbeckmann *et al.*, 2016). This becomes more relevant as evidence indicates that plastics fragments of different sizes are ingested by a wide range of marine animals including corals (Andrady *et al.*, 2011; Carson, 2013; Cole *et al.*, 2013; Wright *et al.*, 2013; Hall *et al.*, 2015). In this context, MP ingestion or exposure might represent a huge risk for the health of marine animals, simulating the Trojan horse effect described with pollutants by Park *et al.* (2010), but in this situation by transferring and delivering non-native and potential pathogenic bacteria to animal internal tissues.

As mentioned before, algal and coral exudates stimulated fast-growing bacteria and selected for minor shifts in the coral reef bacterioplankton, which harbour bacteria of families that contain relatively few virulence factors as *Hyphomonadaceae* and *Erythrobacteraceae* (Nelson *et al.*, 2013). These exudates might have accumulated on MP in the system and selected for communities with virulence factor-carrying bacteria as members of the MRC, or genera as *Marinobacter*, *Erythrobacter*, or *Vibrio*, which have been reported as causative agents of several coral diseases (Buchan *et al.*, 2005; Wagner-Döbler and Biebl, 2006; Sekar *et al.*, 2008; Cárdenas *et al.*, 2012; Kimes *et al.*, 2012; Sweet and Bythell, 2012; Kemp *et al.*, 2018). For instance, components of the type VI secretion system, a key virulence factor, were overexpressed by a *Marinobacter* strain and although this does not assure the pathogen character of the genus (Vaysse *et al.*, 2009), it might explain the high abundances of *Marinobacter* in the microbiome of corals affected with black band disease (BBD), white plague disease (WPD), White Syndrome (PWS) and Brown Band Disease (BrB) (Sunagawa *et al.*, 2009; Sweet and Bythell, 2012; Meyer *et al.*, 2016). *Mycoplasma* sp. was also abundant only on MP and it has been found in bleached and healthy corals (Quintanilla *et al.*, 2018). The genus harbours several pathogenic species and is considered an emerging pathogen in wildlife due the limited biosynthetic capabilities and the expression of virulence factors as haemolysins, proteases, lipases, and proteins involved in attachment to obtain nutrients (Papazisi *et al.*, 2003; Citti and Blanchard, 2013). In addition to the representatives of the mentioned families and genera detected on the MP of the CEMarin system, there are other taxa that contain putative pathogens, which were also found on MP sampled in open waters of different locations. Some of these genera are *Aeromonas*, *Arcobacter*, *Campylobacteraceae*, *Leptolyngbya*, *Phormidium*,

Pseudomonas, *Tenacibaculum*, etc., which affect fish, shrimps, and of course corals (McCormick *et al.*, 2014; Oberbeckmann *et al.*, 2016; Dussud *et al.*, 2018b).

Although the factors that trigger pathogenic events that led to diseases in these animals remain partially unclear, this study provides additional evidence supporting the hypothesis about MP as vector of potential pathogenic bacteria. On MP, bacteria might accumulate and reach higher densities if compared to those in the water column. Environmental stressors related to climate change as increased nutrients, DOC, high water temperatures, and low water pH, induced an integration of more genes encoding virulence pathways within the coral microbiome, increasing the abundance of virulence genes in the holobiont. This process also induced a transition from one “healthy-associated coral community” to a community characterised by microbes often present on diseased corals (Vega-Thurber *et al.*, 2009). Therefore, it would be expected that bacterial communities on plastic debris, subjected to these stressing conditions, shift from the natural structure of marine-surface associated communities to communities that harbour potential pathogens. In these “new” communities, genes involved in virulence, stress resistance, sulfur and nitrogen metabolism, motility, and chemotaxis would be expressed as a consequence of climate change stressing factors as reported by Kimes *et al.*, in 2012, for the coral pathogen *Vibrio coralliilyticus*.

5.4 The genus *Vibrio* is an important member of the bacterial community of the marine system

The presence and the abundance of the genus *Vibrio* on MP has been controversial in different studies (Zettler *et al.*, 2013; Kirstein *et al.*, 2016; Oberbeckmann *et al.*, 2018). In the marine system, even though that based on the 16S rRNA amplicon sequencing, the genus *Vibrio* was underrepresented on MP, the cultivation-dependent approach indicated that *Vibrio* was the most abundant genus of the cultivated community. This is explained since members of the genus *Vibrio* have a versatile metabolism favouring the use of a wide range of nitrogen and carbon sources, which makes this genus one of the most diverse and important marine heterotrophic bacteria easy to isolate in the laboratory (Thompson *et al.*, 2004; Sawabe *et al.*, 2013).

The phylogeny of the genus *Vibrio* is challenging due to the close taxonomic similarities between the species, which makes necessary the use of phenotypic and genotypic traits in order to differentiate closely related strains. The MLSA approach conducted in this study based on the concatenated sequences of five housekeeping genes (*recA*, *pyrH*, *rpoD*, *gyrB*, and *rctB*), revealed that the isolates and the respective type strains of individual phylotypes shared sequence similarities in the range of the intra-species similarities and above the MLSA-based cut-off values proposed by Pascual *et al.* (2010). This indicates that the MLSA scheme implemented in this study, resolved accurately the phylogenetic relationships of the isolates and assigned them into seven different phylotypes: *V. coralliilyticus*, *V. fortis*, *V. alginolyticus*,

V. harveyi, *V. owensii*, *V. mediterranei*, and *V. aquimaris*, the latter belonging to the new *Vibrio* species described here.

In several studies all these phylotypes, except *V. aquimaris*, have been isolated mainly from seawater but also associated to healthy or diseased animals, being reported as potential pathogens (Cano-Gomez *et al.*, 2011; Séré *et al.*, 2015; Rubio-Portillo *et al.*, 2016; Wang *et al.*, 2016; Kemp *et al.*, 2018; Rubio-Portillo *et al.*, 2018). Only few reports have indicated the presence of *Vibrio* spp. on plastic particles using high-resolution cultivation-dependent approaches. *V. coralliilyticus*, *V. alginolyticus*, and *V. harveyi* were detected on plastic particles (Schmidt *et al.*, 2014; Kirstein *et al.*, 2016; Dussud *et al.*, 2018b) but none on sandy sediments. Therefore, this study represents the first report of *Vibrio* spp. isolated from sandy sediments, as well as the first report of *V. fortis* obtained from plastic particles. This evidence supports the hypothesis about MP as a vector of potential pathogenic *Vibrio* spp., which will be discussed in more depth in the next sections.

The genotyping indicated that the diversity of *Vibrio* spp. at strain level within the studied marine system was higher than indicated by the 16S rRNA gene and MLSA-based approaches. For a statistical estimation of habitat specificity the number of studied isolates was unfortunately still too low. Through genotyping it was possible to observe a considerable heterogeneity at the strain level within the *Vibrio* phylotypes as found by Rubio-Portillo *et al.* (2018) during the identification of genotypes of pathogenic *Vibrio* species associated with corals from different geographical locations in the Mediterranean Sea. However, the factors that induce this diversity are still unclear. Environmental pressures, competition among strains, accumulation of neutral allelic variations, and horizontal gene transfer have been discussed as causes leading to ecologically distinct populations with adaptive mutations that might explain genotype diversity (Thompson *et al.*, 2005b). According to these authors, the genotype diversity and habitat-specific differences in the marine system may reflect a starting point of specialization of (sub) populations to either a planktonic or surface-associated life style. The expression of certain phenotypes as colonisation factors or attachment proteins could have favoured the transition of cells from a planktonic to a particle-associated lifestyle, thriving in new habitats, for example in the cases of MP- and sediment-associated genotypes of the *V. coralliilyticus*, *V. harveyi*, and *V. fortis* phylotypes. This might indicate, to some extent, habitat specialisation of certain genotypes within the system.

5.5 MP carried *Vibrio* spp. with putative pathogenic genes

The genus *Vibrio* includes several pathogenic species often associated to coral diseases (Vezzulli *et al.*, 2010; Kimes *et al.*, 2012; Kemp *et al.*, 2018). For this reason, this genus has drawn the attention of this study to evaluate the connection between its presence on MP and the impairment of the coral health after MP exposure and ingestion, observed by Reichert *et al.* (2018) in corals incubated in the CEMarin system.

The numerous putative virulence-associated genes detected in three MP-associated *Vibrio* spp.: *V. fortis* (THAF190c) and *V. coralliilyticus* (THAF191c and THAF191d) were mainly detected on genomes of the coral pathogens *V. coralliilyticus* ATCC BAA-450^T and *V. coralliilyticus* OCN008. Strains of this species are known pathogens of oysters, fish, corals, and other animals causing enteritis, vibriosis, bleaching, and several coral-specific diseases (Ben-Haim *et al.*, 2003; Ushijima *et al.*, 2014; Wang *et al.*, 2016; Ushijima *et al.*, 2018).

The mechanisms used by several *Vibrio* spp. to cause diseases to corals lie in the virulence-related pathogenic factors, which are strictly regulated by quorum sensing systems and environmental conditions (Jung *et al.*, 2015; Liu *et al.*, 2018). One of the best examples of this virulence regulation is the coral pathogen *V. coralliilyticus*. It has been shown that the expression of virulence factors is upregulated at water temperatures above 27 °C (Kimes *et al.*, 2012; Ushijima *et al.*, 2014). Some of the most relevant genes detected on genomes of the three analysed strains belong to quorum sensing systems, such as *luxS*, *litR*, *hapR*, *fliA*, *sigE*, as well as homologues of the HapR system of the virulent *Vibrio cholerae*, the CAI-1 autoinducer synthase, and the protein LuxU. These genes are involved in the regulation of virulence factors as invasion, adhesion, motility, biofilm formation, production and secretion of siderophores, enzymes or toxins, etc. (Dang and Lovell, 2016; Payne *et al.*, 2016; Liu *et al.*, 2018). Similarly, genes coding for proteins associated to flagella, type IV pilus, ABC transporters, and secretion systems, which play key roles in pathogenic *Vibrio* species where also detected in the *Vibrio* strains (Kimes *et al.*, 2012; Tercero-Alburo *et al.*, 2014; Ushijima *et al.*, 2014; Payne *et al.*, 2016; Mewborn *et al.*, 2017).

The bacterial secretion systems are widely used by pathogenic *Vibrio* spp. to translocate virulence factors, toxins, and enzymes into the host cells (Kimes *et al.*, 2012; Chernyatina and Low, 2019). As expected, several genes coding for proteins involved in type I, II, IV, and VI secretion systems were mainly detected in the strains THAF191c and THAF191d (*V. coralliilyticus*) and in less extent in THAF190c (*V. fortis*). Genes coding for toxins and enzymes, such as *rseP* (Zinc metallo-protease), *degS* (Serine endoprotease), *tlh* (thermolabile haemolysin), *hap/vvp* (metallo-proteases), and others coding for stomatin-like, and haemolysin enzymes, all involved in pathogenicity (Kimes *et al.*, 2012, Ushijima *et al.*, 2014) were also detected on the genomes of the three strains. The *toxR* gene, also detected in the MP-derived *Vibrio* spp., is an important transcriptional activator of virulence factors in *Vibrio* spp., since a mutation of this gene in *V. coralliilyticus* strain OCN014 reduced the infectivity of the strain (Ushijima *et al.*, 2016). By last, several prophages that could encode virulence factors, were detected integrated on the chromosomes or plasmids of the MP-associated *Vibrio* spp. These prophages might provide competitive advantages to these strains especially in the promotion of host virulence, control of biofilm formation, antibiotic resistance, and horizontal gene transfer (Nanda *et al.*, 2015; Castillo *et al.*, 2018).

This evidence indicates that beside the presence of *Vibrio* spp. on MP, those strains also contained putative pathogenic genes. Bacteria on MP (and other surfaces) form biofilms, where high cell densities are reached, those required to activate quorum sensing systems and thus virulence factors (Rodrigues *et al.*, 2018). This makes MP a reservoir of active potential

pathogens that may trigger diseases in animals if the MP come into contact with animal tissues. In addition, as warmer water temperatures are becoming more frequent in all latitudes as consequence of the climate change, it is expected that virulence-associated genes are upregulated, increasing the occurrence of *Vibrio*-induced diseases and bleaching episodes in corals. However, it is necessary to take into account that the virulence level vary even within members of the same species, supporting the hypothesis that there are several (still unknown) virulence-related genes that affect the overall coral health (Rubio-Portillo *et al.* 2018).

5.6 *Vibrio aquimaris* THAF100 also contain putative pathogenic genes

Although the strain THAF100 was not isolated from MP but from the water column of the marine system, it was also interesting for this study since 16S rRNA gene and MLSA-based analyses suggested that the strain represents a novel species within the genus *Vibrio*. The ANI values calculated for the strain THAF100 with the type strains of *V. caribbeanicus* and *V. coralliilyticus* were 70.8 % and 74.8 %, respectively. These values were clearly below the proposed cut-off value for species designation of 95 - 96 % (Goris *et al.*, 2007; Richter and Rosselló-Mora, 2009), which suggests that the strain THAF100 is indeed a potential novel species of the genus *Vibrio*.

The genome of the strain THAF100 consisted of one chromosome, one large plasmid, and two additional plasmids. The assigned “large plasmid” might also represent a second chromosome, which is described for other full genome sequenced *Vibrio* spp. (Okada *et al.*, 2005; Thompson *et al.*, 2009) or a “chromid” or “megaplasmid” according to previous studies (Harrison *et al.*, 2010; Kirkup *et al.*, 2010). The phage identified in the plasmid pTHAF100_b, was the plasmid-like phage VP882 characterised from a pandemic *V. parahaemolyticus* strain, which does not integrate into the host chromosome. Interestingly, this phage contains transcriptional regulators of quorum sensing that might regulate physiological of virulence-related traits in the host (Lan *et al.*, 2009), which might confer pathogenicity-related traits to the strain THAF100. The strain contained nine rRNA operons as reported for several other bacteria (Ludwig, 2010). The genome structure and the number of ribosomal operons of the strain THAF100 were similar to those obtained for other *Vibrio* spp. genomes (Ruby *et al.*, 2005; Thompson *et al.*, 2009; Kimes *et al.*, 2012).

The strain THAF100 showed specific genetic traits, some of them related to pathogenicity that were not detected in the other analysed strains *V. coralliilyticus* ATCC BAA-450^T, *V. coralliilyticus* OCN008, and *V. caribbeanicus* ATCC BAA 2122^T. For instance, the presence of fimbrial assembly proteins decisive in motility and adhesion to eukaryotic hosts, invasion protein regulator, attachment invasion proteins, or permeases, all contributing to pathogenesis (Rodrigues *et al.*, 2018). Homologs of toxin-antitoxin systems described in *Vibrio cholerae* were also detected with toxins as RelE2 or HigB-2 that inhibit cell growth, and antitoxin HipB that inhibits the activity of the toxin, which are involved in bacterial persistence during stressing conditions and antibiotic tolerance (Christensen-Dalsgaard and Gerdes, 2004;

Budde *et al.*, 2007; Wen *et al.*, 2014). In addition, transposable genetic elements related to the transposon Tn7, as well as phage-related genes represented additional differential genetic traits between the strain THAF100 and the reference strains. These elements play pivotal roles in genetic exchange and gene expression contributing to mutations, deletions, insertions, and adaptations, as well as in the mediation of toxicity of *Vibrio* spp. by controlling toxin production (Thompson *et al.*, 2004; Austin *et al.*, 2006).

The strain THAF100 also shared some genes with the reference strains. For instance a cluster of flagellar biosynthesis proteins that influence pathogenicity through motility or Type II secretion system proteins which translocate virulence factors, already discussed in the last section (Nørstebø *et al.*, 2017). Quorum sensing receptors as LuxR and LuxQ responsible for the induction and repression of several pathogenicity genes, as well as chemotaxis proteins, which play important roles in initial steps of infection mainly in the location of hosts or avoiding hostile environments (Lorenz *et al.*, 2017; Ushijima and Häse, 2018). ABC transporter permease involved in resistance in bacteria were also detected in on the genomes of the compared strains (McDaniel *et al.*, 2016).

Ten of the isolates assigned to the same phylotype as THAF100 (V-2) were cultivated from the water column and only one from detritus, suggesting that the studied MP and sandy sediments were not a suitable habitat for the members of this phylotype. However, neither attachment, colonisation, nor biofilm formation on MP or sediments were proved yet for the strain THAF100. Despite this, here it was shown that *V. aquimaris* strain THAF100 is also a potential pathogen, not only due to its taxonomic proximity to the coral pathogen *V. coralliilyticus* revealed by the employed phylogenetic analyses, but also by the diverse putative pathogenic genes detected on its genome. As virulence might vary even within members of the same phylotype, it is not clear if the potential pathogenicity of the strain THAF100 is a feature of the investigated strain or a general trait of the proposed new species.

All the evidence presented in this study supports the hypothesis focused on plastic debris (micro and macroplastics) as key players involved in coral disease outbreaks observed in reefs worldwide showing diverse responses after exposure (Lamb *et al.*, 2018; Reichert *et al.*, 2018). Under this hypothesis, plastic debris promote the invasion and infection of coral (and other animal) tissues by non-native and potential bacterial pathogens present on plastics. Although these bacterial communities do not belong to the microbiome of the coral holobiont, after plastic exposure or ingestion, they might colonise and thrive in coral tissues. By doing this, plastic-associated bacterial communities displace native members of the microbiome, altering its composition and causing a disruption of its normal functioning, compromising the health of the holobiont, which also deals with adverse environmental conditions as high SST, OA, water pollution, overfishing, increased nutrients, habitat destruction, etc. Under those stress conditions, the bacterial component of the microbiome may tend to express more virulence genes, increasing the abundance of their products as toxins and enzymes that eventually lead to diseases due to the shift from a healthy bacterial community to one characterised by microbes often present in diseased corals. However, the presence of the pathogenicity-related genes in the MP-associated strain predicted virulence but did not prove

it, for which it is necessary to conduct further ecotoxicology experiments to validate the hypothesis.

5.7 Conclusions and perspectives

This thesis contributed with evidence that strengthen the current understanding about bacterial assemblages present on MP, natural particles, and the water of marine systems and how MP constitute different habitats for marine bacteria, acting as vectors that carry and distribute non-native bacteria and potential pathogens in marine ecosystems. The thesis also explored the potential negative effects of MP-associated bacteria on coral health, represented among others, by bleaching or tissue necrosis in corals cultivated in the CEMarin aquarium system, observed previously after MP exposure and ingestion by corals.

The findings of this thesis further support previous studies that stated that plastic fragments in marine environments are colonised by specific bacterial communities, which are distinct from those present in the bacterioplankton of the surrounding water or colonising natural particles. The bacterial assemblages on MP incubated in the marine system were dominated by families *Rhodobacteraceae*, *Hyphomonadaceae*, *Erythrobacteraceae*, *Alteromonadaceae*, *Flavobacteriaceae*, *Saprospiraceae*, and *Planctomycetaceae*, which also support the recently suggested specific bacteriome associated to plastic debris. The cultivation-independent analysis indicated high abundances of genera *Jejundonia*, *Roseivivax*, *Marinobacter*, and *Erythrobacter* only on MP and not present in any other sample.

Representatives of the most abundant genera detected through the 16S rRNA gene amplicon sequencing from the diverse samples were also detected in the cultivation-dependent approach. The genomes of the most abundant bacteria isolated from MP were sequenced in order to study their genetic traits, an interesting approach that had not been evaluated in previous studies, which were rather focused on the description cultivation-independent-based techniques. Numerous genes coding for enzymes as depolymerases, lipases, esterases, serine proteases, dehydratases, or hydrolases, all involved in the degradation of complex polymers were detected on the genomes of genera as *Roseivivax*, *Marinobacter*, and *Erythrobacter*, and to a lesser extent in *Vibrio*. These strains might have an impact in biotechnological applications for the remediation of polluted marine ecosystems.

Vibrio was the most abundant cultivated genus, whose diversity was evaluated by MLSA using five housekeeping genes. The applied MLSA scheme demonstrated to be a robust method to resolve the phylogenetic relationships among members of the genus *Vibrio*, which was later confirmed by core-genome-based phylogeny. Through genome comparison analyses with known coral pathogenic *Vibrio* sp. strains, a broad range of pathogenicity genes coding for proteins involved in motility, type I, II, IV, and VI secretion systems, ABC transport systems, toxins, enzymes, autoinducers and regulators of quorum sensing and chemotaxis systems, were detected in the MP-associated *Vibrio* sp. strains, which may induce diseases to corals. Some of those genes were also detected to a lesser extent on genomes of the other

isolates, which suggests that *Roseivivax*, *Marinobacter*, and *Erythrobacter* strains might also be potential pathogens present on MP.

Moreover, through the cultivation process, four bacterial strains isolated from the marine system were proposed as new species: *Winogradskyella pocilloporae*, *Pseudomaribius plastisphaeri*, *Ruegeria sedimentorum*, and *Vibrio aquimaris*. This highlights the importance of implementing cultivation-dependent approaches in microbiological studies, as well as the CEMarin aquarium system as source of new bacterial species. The cultivation approach allowed the establishment of a strain collection that can be used in further analyses and open a wide variety of research questions.

This thesis provided interesting and significant insights and evidence that supports the idea that MP-associated bacteria might be involved in the development of coral diseases. However, it is still not possible to conclude whether the MP *per se* or the bacteria that colonised and inhabited the MP were responsible of the health impairment observed in different coral species exposed to MP (Reichert *et al.*, 2018). In order to provide more conclusive answers to these observations, the isolated heterotrophic bacteria from the different samples of the marine system represent a starting point to evaluate bacterial groups with relevant importance in the induction of coral diseases. To investigate this, the strains can be subjected to ecotoxicology experiments with corals by using MP as vectors to assess the scope and the effects of the interaction with the coral host from diverse approaches, such as tissue colonisation, infection mechanisms, quorum sensing signalling, expression of virulence factors, etc. The expression of these and other genes needs to be evaluated under global warming conditions, especially under heat stress, with the isolated strains of genera *Roseivivax*, *Marinobacter*, *Erythrobacter*, but especially with those belonging to *Vibrio*, due to the temperature-dependent regulation of these genes as occur with *V. coralliilyticus*. *V. aquimaris* strain THAF100 was closely related to the type species of *V. coralliilyticus*, suggesting that this new species may constitute a new coral pathogen, whose gene regulation must be also studied. All these studies will provide more scientific evidence needed to identify, mitigate, and control the factors that induce the current massive disease outbreaks and loss of coral reefs.

Previous studies have identified hydrocarbonoclastic bacteria on plastics. Therefore, the potential biodegradation of complex polymers could be tested by doing experiments cultivating strains of the most abundant genera isolated from plastics in media including hydrocarbons or plastic films of different composition and the respective monitoring to determine the potential degradation rates. This could improve the current understanding on polymer-degradation pathways used by bacteria, as well as a method to identify strains with potential applications in bioremediation and other biotechnological applications.

References

- Ainsworth, T. D., Krause, L., Bridge, T., Torda, G., Raina, J.-B., Zakrzewski, M., et al., (2015). The coral core microbiome identifies rare bacterial taxa as ubiquitous endosymbionts. *ISME J* 9, 2261–2274.
- Ainsworth, T. D., and Gates, R. D. (2016). Coral's microbial sentinels. *Science* 352, 1518–1519.
- Ainsworth, T. D., Thurber, R. V., and Gates, R. D. (2009). The future of coral reefs: a microbial perspective. *Trends Ecol. Evol.* 25, 233–240.
- Alagely, A., Krediet, C. J., Ritchie, K. B., and Teplitski, M. (2011). Signaling-mediated cross-talk modulates swarming and biofilm formation in a coral pathogen *Serratia marcescens*. *ISME J.* 5, 1609–1620.
- Albuquerque, L., França, L., Taborda, M., La Cono, V., Yakimov, M., and da Costa, M. S. (2015). *Palleronia abyssalis* sp. nov., isolated from the deep Mediterranean Sea and the emended description of the genus *Palleronia* and of the species *Palleronia marisminoris*. *Antonie Van Leeuwenhoek* 107, 633–642.
- Allen, A. S., Seymour, A. C., and Rittschof, D. (2017). Chemoreception drives plastic consumption in a hard coral. *Mar. Pollut. Bull.* 124, 198–205.
- Altenburger, P., Kämpfer, P., Makristathis, A., Lubitz, W., and Busse, H. J. (1996). Classification of bacteria isolated from a medieval wall painting. *J. Biotechnol.* 47, 39–52.
- Andrady, A. L. (2011). Microplastics in the marine environment. *Mar Pollut Bull* 62, 1596–1605.
- Arahal, D. R., Lucena, T., Rodrigo-Torres, L., Pujalte, M. J. (2018). *Ruegeria denitrificans* sp. nov., a marine bacterium in the family *Rhodobacteraceae* with the potential ability for cyanophycin synthesis. *Int. J. Syst. Evol. Microbiol.* 68, 2515–2522.
- Arahal, D. R., Macián, M. C., Garay, E., Pujalte, M. J. (2005). *Thalassobius mediterraneus* gen. nov., sp. nov., and reclassification of *Ruegeria gelatinovorans* as *Thalassobius gelatinovorans* comb. nov. *Int. J. Syst. Evol. Microbiol.* 55, 2371–2376.
- Arndt, D., Grant, J. R., Marcu, A., Sajed, T., Pon, A., Liang, Y., et al. (2016). PHASTER: a better, faster version of the PHAST phage search tool. *Nucleic Acids Res.* 44, 16–21.
- Auling, G., Busse, H. J., Pilz, F., Webb, L., Kneifel, H., and Claus, D. (1991). Rapid differentiation, by polyamine analysis, of *Xanthomonas* strains from phytopathogenic pseudomonads and other members of the class *Proteobacteria* interacting with plants. *Int. J. Syst. Bacteriol.* 41, 223–228.
- Austin, B., and Zhang, X.-H. (2006). *Vibrio harveyi*: a significant pathogen of marine vertebrates and invertebrates. *Lett. Appl. Microbiol.* 43, 119–124.
- Baek, J., Kim, J.-H., Sukhoom, A., and Kim, W. (2020). *Ruegeria sediminis* sp. nov., isolated from tidal flat sediment. *Int. J. Syst. Evol. Microbiol.*
- Baker-Austin, C., Trinanès, J.A., Taylor, N.G.H., Hartnell, R., Siitonen, A., Martínez-Urtaza, J. (2012). Emerging *Vibrio* risk at high latitudes in response to ocean warming. *Nat. Clim. Change.* 3, 73–77.
- Ben-Haim, Y., Zicherman-Keren, M., and Rosenberg, E. (2003). Temperature-regulated bleaching and lysis of the coral *Pocillopora damicornis* by the novel pathogen *Vibrio coralliilyticus*. *Appl Environ Microbiol* 69, 4236–4242.
- Bernardet, J. F., Nakagawa, Y., Holmes, B. (2002). Proposed minimal standards for describing new taxa of the family *Flavobacteriaceae* and emended description of the family. *Int. J. Syst. Evol. Microbiol.* 52, 1049–1070.

- Bibi, F., Naseer, M. I., Hassan, A. M., Yasir, M., Al-Ghamdi, A. A. K., and Azhar, E. I. (2018). Diversity and antagonistic potential of bacteria isolated from marine grass *Halodule uninervis*. *3 Biotech* 8, 48.
- Bižić-Ionescu, M., Zeder, M., Ionescu, D., Orlić, S., Fuchs, B. M., Grossart, H. P., et al., (2014). Comparison of bacterial communities on limnic versus coastal marine particles reveals profound differences in colonisation. *Environ. Microbiol.* 17, 3500–3514.
- Blackall, L. L., Wilson, B., and van Oppen, M. J. H. (2015). Coral - the world's most diverse symbiotic ecosystem. *Mol Ecol* 24, 5330–5347.
- Blom, J., Kreis, J., Spänig, S., Juhre, T., Bertelli, C., Ernst, C., et al. (2016). EDGAR 2.0: an enhanced software platform for comparative gene content analyses. *Nucleic Acids Res.* 44, 22–28.
- Boettcher, K. J., Geaghan, K. K., Maloy, A. P., Barber, B. J. (2005). *Roseovarius crassostreae* sp. nov., a member of the *Roseobacter* clade and the apparent cause of juvenile oyster disease (JOD) in cultured eastern oysters. *Int. J. Syst. Evol. Microbiol.* 55:1531–1537.
- Boström-Einarsson, L., Bonin, M. C., Munday, P. L., and Jones, G. P. (2018). Loss of live coral compromises predator-avoidance behaviour in coral reef damselfish. *Sci. Rep.* 8, 7795.
- Bourne, D. G., Morrow, K. M., and Webster, N. S. (2016). Insights into the coral microbiome: underpinning the health and resilience of reef ecosystems. *Annu. Rev. Microbiol.* 70, 317–340.
- Brinkhoff, T., and Muyzer, G. (1997). Increased species diversity and extended habitat range of sulfur-oxidizing *Thiomicrospira* spp. *Appl Environ Microbiol.* 63, 3789–3796.
- Brosius, J., Palmer, M., and Kennedy, P. (1978). Complete nucleotide sequence of a 16S ribosomal RNA gene from *Escherichia coli*. *Proc. Natl. Acad. Sci.* 75, 4801–4805.
- Brown, B. E., Dunne, R. P., Goodson, M. S., and Douglas, A. E. (2000). Bleaching patterns in reef corals. *Nature* 404, 142–143.
- Browne, M. A., Galloway, T., and Thompson, R. (2007). Microplastic - an emerging contaminant of potential concern? *Integr. Environ. Assess. Manag.* 3, 559–566.
- Browne, M. A., Niven, S. J., Galloway, T. S., Rowland, S. J., and Thompson, R. C. (2013). Microplastic moves pollutants and additives to worms, reducing functions linked to health and biodiversity. *Curr. Biol.* 23, 2388–2392.
- Bruto, M., Labreuche, Y., James, A., Piel, D., Chenivresse, S., Petton, B., et al. (2018). Ancestral gene acquisition as the key to virulence potential in environmental *Vibrio* populations. *ISME J.* 12, 2954–2966.
- Buchan, A., González, J. M., and Moran, M. A. (2005). Overview of the marine *Roseobacter* lineage. *Appl. Environ. Microbiol.* 71, 5665–5677.
- Budde, P. P., Davis, B. M., Yuan, J., and Waldor, M. K. (2007). Characterization of a *higBA* toxin-antitoxin locus in *Vibrio cholerae*. *J. Bacteriol.* 189, 491–500.
- Burriesci, M. S., Raab, T. K., and Pringle, J. R. (2012). Evidence that glucose is the major transferred metabolite in dinoflagellate-cnidarian symbiosis. *J. Exp. Biol.* 215, 3467–3477.
- Burmølle, M., Ren, D., Bjørnsholt, T., and Sørensen, S. J. (2014). Interactions in multispecies biofilms: do they actually matter? *Trends. Microbiol.* 22, 84–91.
- Busse, H. J., and Auling, G. (1988). Polyamine pattern as a chemotaxonomic marker within the *Proteobacteria*. *Syst. Appl. Microbiol.* 11, 1–8.
- Busse, H. J., Bunka, S., Hensel, A., and Lubitz, W. (1997). Discrimination of members of the family *Pasteurellaceae* based on polyamine patterns. *Int. J. Syst. Bacteriol.* 47, 698–708.
- Camacho, C., Coulouris, G., Avagyan, V., Ma, N., Papadopoulos, J., Bealer, K., et al., (2009). BLAST+: architecture and applications. *BMC Bioinformatics* 10, 421.
- Cano-Gomez, A., Høj, L., Owens, L., Andreakis, N. (2011). Multilocus sequence analysis provides basis for fast and reliable identification of *Vibrio harveyi*-related species and reveals previous misidentification of important marine pathogens. *Syst. Appl. Microbiol.* 34, 561–565.

- Capra, E. J. and Laub, M. T. (2012). Evolution of two-component signal transduction systems. *Annu. Rev. Microbiol.* 66, 325–347.
- Cárdenas, A. (2016). Bacterial response to elevated dissolved organic carbon in coral reef ecosystems. Universität Bremen.
- Cárdenas, A., Rodríguez-R, L. M., Pizarro, V., Cadavid, L. F., and Arévalo-Ferro, C. (2011). Shifts in bacterial communities of two Caribbean reef-building coral species affected by white plague disease. *ISME J.* 6, 502–512.
- Carpenter, E. J., and Smith, K. L. (1972). Plastics on the Sargasso Sea surface. *Science* 175, 1240–1241.
- Carroll, I. M., Maharshak, N., Ringel, Y., Katibian, D., Lundqvist, A., Sartor, R. B., et al., (2018). Fecal and mucosa-associated intestinal microbiota in patients with diarrhea-predominant irritable bowel syndrome. *Dig. Dis. Sci.* 63, 1890–1899.
- Carson, H. S. (2013). The incidence of plastic ingestion by fishes: From the prey's perspective. *Mar. Pollut. Bull.* 74, 170–174.
- Castillo, D., Kauffman, K., Hussain, F., Kalatzis, P., Rørbo, N., Polz, M. F., et al. (2018). Widespread distribution of prophage-encoded virulence factors in marine *Vibrio* communities. *Sci. Rep.* 8, 9973.
- Cervino, J. M., Thompson, F. L., Gomez-Gil, B., Lorence, E. A., Goreau, T. J., Hayes, R. L., et al., (2008). The *Vibrio* core group induces yellow band disease in Caribbean and Indo-Pacific reef-building corals. *J Appl Microbiol* 105, 1658–1671.
- Chambers, J. R. and Sauer, K. (2013). Small RNAs and their role in biofilm formation. *Trends. Microbiol.* 21, 39–49.
- Chapron, L., Peru, E., Engler, A., Ghiglione, J. F., Meistertzheim, A. L., Meistertzheim, A. L., et al. (2018). Macro- and microplastics affect cold-water corals growth, feeding and behaviour. *Sci. Rep.* 8, 15299.
- Chernyatina, A. A., and Low, H. H. (2019). Core architecture of a bacterial type II secretion system. *Nat. Commun.* 10, 5437.
- Chimetto, L.A., Brocchi, M., Thompson, C.C., Martins, R.C.R., Ramos, H.R., Thompson, F.L. (2008) *Vibrios* dominate as culturable nitrogen-fixing bacteria of the Brazilian coral *Mussismilia hispida*. *Syst Appl Microbiol* 31, 312–319.
- Choi, D. H., Cho, J. C., Lanoil, B. D., Giovannoni, S. J., and Cho, B. C. (2007). *Maribius salinus* gen. nov., sp. nov., isolated from a solar saltern and *Maribius pelagius* sp. nov., cultured from the Sargasso Sea, belonging to the *Roseobacter* clade. *Int. J. Syst. Evol. Microbiol.* 57, 270–275.
- Christensen-Dalsgaard, M., and Gerdes, K. (2006). Two *higBA* loci in the *Vibrio cholerae* superintegron encode mRNA cleaving enzymes and can stabilize plasmids. *Mol. Microbiol.* 62, 397–411.
- Chronopoulou, P. M., Sanni, G. O., Silas-Olu, D. I., van der Meer, J. R., Timmis, K. N., Brussaard, C. P. D., et al. (2015). Generalist hydrocarbon-degrading bacterial communities in the oil-polluted water column of the North Sea. *Microb. Biotechnol.* 8, 434–447.
- Chung, H. C., Lee, O. O., Huang, Y.-L., Mok, S. Y., Kolter, R., and Qian, P.-Y. (2010). Bacterial community succession and chemical profiles of subtidal biofilms in relation to larval settlement of the polychaete *Hydroides elegans*. *ISME J* 4, 817–28.
- Citti, C., and Blanchard, A. (2013). Mycoplasmas and their host: Emerging and re-emerging minimal pathogens. *Trends Microbiol.* 21, 196–203.
- Claessen, D., Rozen, D. E., Kuipers, O. P., Søgaaard-Andersen, L., and van Wezel, G. P. (2014). Bacterial solutions to multicellularity: a tale of biofilms, filaments and fruiting bodies. *Nat. Rev. Microbiol.* 12, 115–124.
- Cole, M., Lindeque, P., Halsband, C., and Galloway, T. S. (2011). Microplastics as contaminants in the marine environment: A review. *Mar. Pollut. Bull.* 62, 2588–2597.

- Cole, M., Lindeque, P., Fileman, E., Halsband, C., Goodhead, R., Moger, J., et al., (2013). Microplastic ingestion by zooplankton. *Environ. Sci. Technol.* 47, 6646–6655.
- Colton, J. J., Burns, B., and Knapp, F. (1974). Plastic particles in surface waters of the Northwestern Atlantic. *Science* 185, 491–497.
- Colwell, R. R. (2006). A global and historical perspective of the genus *Vibrio*. In: Thompson, F. L., Austin, B., Swings, J. (Eds.), *The biology of Vibrios*, ASM Press, pp. 3–11.
- Cooper, T. F., De’ath, G., Fabricius, K. E., and Lough, J. M. (2008). Declining coral calcification in massive *Porites* in two nearshore regions of the northern Great Barrier Reef. *Glob Chang Biol* 14, 529–538.
- Curren, E., and Leong, S. C. Y. (2019). Profiles of bacterial assemblages from microplastics of tropical coastal environments. *Sci. Total Environ.* 655, 313–320.
- Dang, H., and Lovell, C. R. (2000). Bacterial primary colonisation and early succession on surfaces in marine waters as determined by amplified rRNA gene restriction analysis and sequence analysis of 16S rRNA genes. *Appl. Environ. Microbiol.* 66, 467–475.
- Dang, H., and Lovell, C. R. (2016). Microbial surface colonisation and biofilm development in marine environments. *Microbiol. Mol. Biol. Rev.* 80, 91–138.
- Dang, H. Y., Li, T. G., Chen, M. N., Huang, G. Q. (2008). Cross-ocean distribution of *Rhodobacterales* bacteria as primary surface colonisers in temperate coastal marine waters. *Appl. Environ. Microbiol.* 74, 52–60.
- Davey, M. E., O’Toole, G. A. (2000). Microbial biofilms: from ecology to molecular genetics. *Microbiol. Mol. Biol. Rev.* 64, 847–867.
- Delacuvellerie, A., Cyriaque, V., Gobert, S., Benali, S., and Wattiez, R. (2019). The plastisphere in marine ecosystem hosts potential specific microbial degraders including *Alcanivorax borkumensis* as a key player for the low-density polyethylene degradation. *J. Hazard. Mater.* 380, 120899.
- De Tender, C. A., Devriese, L. I., Haegeman, A., Maes, S., Ruttink, T., and Dawyndt, P. (2015). Bacterial community profiling of plastic litter in the Belgian part of the North Sea. *Environ. Sci. Technol.* 49, 9629–9638.
- De Tender, C., Devriese, L. I., Haegeman, A., Maes, S., Vangeyte, J., Cattrijsse, A., et al. (2017a). Temporal dynamics of bacterial and fungal colonisation on plastic debris in the North Sea. *Environ. Sci. Technol.* 51, 7350–7360.
- De Tender, C. A., Schlundt, C., Devriese, L. I., Mincer, T. J., Zettler, E. R., and Amaral-Zettler, L. A. (2017b). A review of microscopy and comparative molecular-based methods to characterise “Plastisphere” communities. *Anal. Methods* 9, 2132–2143.
- Ding, J.-Y., Shiu, J.-H., Chen, W.-M., Chiang, Y.-R., and Tang, S.-L. (2016). Genomic insight into the host-endosymbiont relationship of *Endozoicomonas montiporae* CL-33(T) with its coral host. *Front. Microbiol.* 7:251.
- Doi, H., Osawa, I., Adachi, H., Kawada, M. (2017). *Vibrio japonicus* sp. nov., a novel member of the Nereis clade in the genus *Vibrio* isolated from the coast of Japan. *PLoS One* 12, e0172164.
- Doney, S. C., Fabry, V. J., Feely, R. A., and Kleypas, J. A. (2009). Ocean acidification: the other CO₂ problem. *Ann. Rev. Mar. Sci.* 1, 169–192.
- Doropoulos, C., Ward, S., Diaz-Pulido, G., Hoegh-Guldberg, O., and Mumby, P. J. (2012). Ocean acidification reduces coral recruitment by disrupting intimate larval-algal settlement interactions. *Ecol. Lett.* 15, 338–346.
- Duncan, E. M., Broderick, A. C., Fuller, W. J., Galloway, T. S., Godfrey, M. H., Hamann, M., et al., (2019). Microplastic ingestion ubiquitous in marine turtles. *Glob. Chang. Biol.* 25, 744–752.
- Dussud, C., Hudec, C., George, M., Fabre, P., Higgs, P., Bruzaud, S., et al., (2018a). Colonisation of non-biodegradable and biodegradable plastics by marine microorganisms. *Front. Microbiol.* 9, 1–13.

- Dussud, C., Meistertzheim, A. L., Conan, P., Pujo-Pay, M., George, M., Fabre, P., et al., (2018b). Evidence of niche partitioning among bacteria living on plastics, organic particles and surrounding seawaters. *Environ. Pollut.* 236, 807–816.
- ElAhwany, A. M. D., Ghozlan, H. A., Elsharif, H. A., and Sabry, S. A. (2013). Phylogenetic diversity and antimicrobial activity of marine bacteria associated with the soft coral *Sarcophyton glaucum*. *J Basic Microbiol* 55, 2–10.
- Engler, R. E. (2012). The complex interaction between marine debris and toxic chemicals in the ocean. *Environ. Sci. Technol.* 46, 12302–12315.
- Felsenstein, J. (2005). PHYLIP (Phylogeny Inference Package) version 3.6. Distributed by the author. Department of Genome Sciences, University of Washington, Seattle.
- Flemming, H.-C., Wingender, J., Szewzyk, U., Steinberg, P., Rice, S. A., and Kjelleberg, S. (2016). Biofilms: an emergent form of bacterial life. *Nat. Rev. Microbiol.* 14, 563–575.
- Franco, A., Busse, H.-J., Schubert, P., Wilke, T., Kämpfer, P., and Glaeser, S. P. (2018). *Winogradskyella pocilloporae* sp. nov. isolated from healthy tissue of the coral *Pocillopora damicornis*. *Int. J. Syst. Evol. Microbiol.* 68, 1689–1696.
- Franco, A., Cadavid, L. F., and Arévalo-Ferro, C. (2019). Biofilms and extracts from bacteria producing “quorum sensing” signaling molecules promote chemotaxis and settlement behaviors in *Hydractinia symbiolongicarpus* (Cnidaria: Hydrozoa) larvae. *Acta Biológica Colomb.* 24, 150–162.
- Frère, L., Maignien, L., Chalopin, M., Huvet, A., Rinnert, E., Morrison, H., et al., (2018). Microplastic bacterial communities in the Bay of Brest: Influence of polymer type and size. *Environ. Pollut.* 242, 614–625.
- Gall, S. C., and Thompson, R. C. (2015). The impact of debris on marine life. *Mar. Pollut. Bull.* 92, 170–179.
- Galloway, T. S., Cole, M., and Lewis, C. (2017). Interactions of microplastic debris throughout the marine ecosystem. *Nat. Ecol. Evol.* 1, 1–8.
- Garcia, G. D., Gregoracci, G. B., Santos, E. D. O., Meirelles, P. M., Silva, G. G. Z., Edwards, R., et al., (2013). Metagenomic analysis of healthy and white plague-affected *Mussismilia braziliensis* corals. *Microb. Ecol.* 65, 1076–1086.
- Gautam, R., Bassi, A. S., and Yanful, E. K. (2007). A review of biodegradation of synthetic plastic and foams. *Appl. Biochem. Biotechnol.* 141, 85–108.
- Gerhardt, P., Murray, R. G. E., Wood, W. A., Krieg, N. R. (1994). *Methods for General and Molecular Bacteriology*. Washington, DC: American Society for Microbiology.
- Glaeser, S. P., Galatis, H., Martin, K., and Kämpfer, P. (2013). *Niabella hirudinis* and *Niabella drilacis* sp. nov., isolated from the medicinal leech *Hirudo verbana*. *Int. J. Syst. Evol. Microbiol.*, 3487–3493.
- Glaeser, S. P., Grossart, H. P., and Glaeser, J. (2010). Singlet oxygen, a neglected but important environmental factor: Short-term and long-term effects on bacterioplankton composition in a humic lake. *Environ. Microbiol.* 12, 3124–3136.
- Gonzalez, J. M., and Saiz-Jimenez, C. (2002). A fluorimetric method for the estimation of G+C mol % content in microorganism by thermal denaturation temperature. *Environ. Microbiol.* 4, 770–773.
- Gordon, D., and Green, P. (2013) Consed: a graphical editor for next-generation sequencing. *Bioinformatics* 29, 2936–2937.
- Goris, J., Konstantinidis, K. T., Klappenbach, J. A., Coenye, T., Vandamme, P., and Tiedje, J. M. (2007). DNA-DNA hybridization values and their relationship to whole-genome sequence similarities. *Int. J. Syst. Evol. Microbiol.* 57, 81–91.
- Hadad, D., Geresh, S., and Sivan, A. (2005). Biodegradation of polyethylene by the thermophilic bacterium *Brevibacillus borstelensis*. *J. Appl. Microbiol.* 98, 1093–1100.

- Hall, N. M., Berry, K. L. E., Rintoul, L., and Hoogenboom, M. O. (2015). Microplastic ingestion by scleractinian corals. *Mar. Biol.* 162, 725–732.
- Hamana, K., and Takeuchi, M. (1998). Polyamine profiles as chemotaxonomic marker within alpha, beta, gamma, delta and epsilon subclasses of class *Proteobacteria*: distribution of 2-hydroxyputrescine and homospermidine. *Microbiol. Cult. Coll.* 14:1-14.
- Hammer, Ø., Harper, D. A. T., and Ryan, P. D. (2001). PAST: paleontological statistics software package for education and data analysis. *Palaeontol. Electron.* 4, 1-9
- Hankins, C., Duffy, A., and Drisco, K. (2018). Scleractinian coral microplastic ingestion: Potential calcification effects, size limits, and retention. *Mar. Pollut. Bull.* 135, 587–593.
- Hansen, J., Sato, M., Ruedy, R., Lo, K., Lea, D. W., and Medina-Elizade, M. (2006). Global temperature change. *Proc. Natl. Acad. Sci. U. S. A.* 103, 14288–14293.
- Harris, D. L., Rovere, A., Casella, E., Power, H., Canavesio, R., Collin, A., et al. (2018). Coral reef structural complexity provides important coastal protection from waves under rising sea levels. *Sci. Adv.* 4, eaao4350.
- Harrison, P. W., Lower, R. P. J., Kim, N. K. D., and Young, J. P. W. (2010). Introducing the bacterial “chromid”: Not a chromosome, not a plasmid. *Trends Microbiol.* 18, 141–148.
- Harrison, J. P., Schratzberger, M., Sapp, M., and Osborn, A. (2014). Rapid bacterial colonisation of low-density polyethylene microplastics in coastal sediment microcosms. *BMC Microbiol.* 14, 232.
- Heidelberg, J. F., Heidelberg, K. B., Colwell, R. R. (2002) Bacteria of the gamma-subclass *Proteobacteria* associated with zooplankton in Chesapeake Bay. *Appl. Environ. Microbiol.* 68, 5498–5507.
- Heindl, J. E., Wang, Y., Heckel, B. C., Mohari, B., Feirer, N., and Fuqua, C. (2014). Mechanisms and regulation of surface interactions and biofilm formation in *Agrobacterium*. *Front. Plant. Sci.* 5, 176.
- Hernandez-Agreda, A., Leggat, W., Bongaerts, P., and Ainsworth, T. D. (2016). The microbial signature provides insight into the mechanistic basis of coral success across reef habitats. *MBio* 7, e00560-16.
- Hoffmann, M., Monday, S. R., Allard, M. W., Strain, E. A., Whittaker, P., Naum, M., et al., (2012). *Vibrio caribbeanicus* sp. nov., isolated from the marine sponge *Scleritoderma cyanea*. *Int. J. Syst. Evol. Microbiol.* 62, 1736–1743
- Hoegh-Guldberg, O., and Bruno, J. F. (2010). The impact of climate change on the world’s marine ecosystems. *Science* 328, 1523–1528.
- Hoegh-Guldberg, O., Mumby, P. J., Hooten, A. J., S., S. R., Greenfield, P., Gomez, E., et al. (2007). Coral reefs under rapid climate change and ocean acidification. *Science*. 318, 1737–1742.
- Hughes, T. P., Baird, a H., Bellwood, D. R., Card, M., Connolly, S. R., Folke, C., et al., (2003). Climate change, human impacts, and the resilience of coral reefs. *Science* 301, 929–33.
- Huo, Y.-Y., Xu, X.-W., Li, X., Liu, C., Cui, H.-L., Wang, C.-S., et al. (2011). *Ruegeria marina* sp. nov., isolated from marine sediment. *Int. J. Syst. Evol. Microbiol.* 61, 347–350.
- Husemann, P., and Stoye, J. (2009) r2cat: Synteny plots and comparative assembly. *Bioinformatics* 26, 570–571.
- Ivanova, E. P., Christen, R., Gorshkova, N. M., Zhukova, N. V, Kurilenko, V. V, Crawford, R. J., et al., (201). *Winogradskyella exilis* sp. nov., isolated from the starfish *Stellaster equestris*, and emended description of the genus *Winogradskyella*. 60, 1577–1580.
- Jackson, J. B. C., Kirby, M. X., Berger, W. H., Bjorndal, K. A., Botsford, L. W., Bourque, B. J., et al., (2001). Historical overfishing and the recent collapse of coastal ecosystems. *Science* 293, 629–637.

- Jacquín, J., Cheng, J., Odobel, C., Pandin, C., Conan, P., Pujo-Pay, M., et al. (2019). Microbial ecotoxicology of marine plastic debris: A review on colonisation and biodegradation by the “plastisphere.” *Front. Microbiol.* 10, 865.
- Jambeck, J. R., Geyer, R., Wilcox, C., Siegler, T., Perryman, M., Andrady, A., et al., (2015). Plastic waste inputs from land into the ocean. *Science* 347, 786–771.
- Jansen, E., Overpeck, J., Briffa, K.R., Duplessy, J.-C., Joos, F., Masson-Delmotte, V. et al., (2007). “Palaeoclimate,” in *Climate Change 2007: the physical science basis*, ed. S. Solomon, D. Qin, M. Manning, Z. Chen, M. Marquis, K.B. Averyt, et al., (Cambridge University Press, Cambridge), pp. 433–498
- Jones, K. L. (1949). Fresh isolates of actinomycetes in which the presence of sporogenous aerial mycelia is a fluctuating characteristic. *J. Bacteriol.* 57, 141–145.
- Jones, D. T., Taylor, W. R., Thornton, J. M. (1992). The rapid generation of mutation data matrices from protein sequences. *Comp. Appl. Biosc.* 8, 275–282.
- Jukes, T. H., and Cantor, C. R. (1969). Evolution of protein molecules. In: Munro, H. N. (Ed), *Mammalian Protein Metabolism*. Academic Press. pp. 21–132.
- Jung, S. A., Chapman, C. A., and Ng, W. L. (2015). Quadruple quorum-sensing inputs control *Vibrio cholera* virulence and maintain system robustness. *PLoS Pathog.* 11:e1004837.
- Kämpfer, P., Arun, A. B., Rekha, P. D., Busse, H. J., Young, C. C., and Glaeser, S. P. (2013). *Ruegeria intermedia* sp. nov., a moderately thermophilic bacterium isolated from a coastal hot spring. *Int. J. Syst. Evol. Microbiol.* 63, 2538–2544.
- Kämpfer, P., and Kroppenstedt, R. M. (1996). Numerical analysis of fatty acid patterns of coryneform bacteria and related taxa. *Can. J. Microbiol.* 42, 989–1005.
- Kämpfer, P., Steiof, M., and Dott, W. (1991). Microbiological characterization of a fuel-oil contaminated site including numerical identification of heterotrophic water and soil bacteria. *Microb. Ecol.* 21:227–251.
- Karjalainen, M., Reinikainen, M., Spoof, L., Meriluoto, J. A. O., Sivonen, K., and Viitasalo, M. (2005). Trophic transfer of cyanobacterial toxins from zooplankton to planktivores: Consequences for pike larvae and mysid shrimps. *Environ. Toxicol.* 20, 354–362.
- Kemp, K. M., Westrich, J. R., Alabady, M. S., Edwards, M. L., and Lipp, E. K. (2018). Abundance and multilocus sequence analysis of *Vibrio* bacteria associated with diseased elkhorn coral (*Acropora palmata*) of the Florida Keys. *Appl. Environ. Microbiol.* 84, e01035-17.
- Kesy, K., Oberbeckmann, S., Kreikemeyer, B., and Labrenz, M. (2019). Spatial environmental heterogeneity determines young biofilm assemblages on microplastics in Baltic Sea mesocosms. *Front. Microbiol.* 10, 1665.
- Keswani, A., Oliver, D. M., Gutierrez, T., and Quilliam, R. S. (2016). Microbial hitchhikers on marine plastic debris: Human exposure risks at bathing waters and beach environments. *Mar. Environ. Res.* 118, 10-19.
- Kim, H. S., Park, S. J., Lee, K. H. (2009). Role of NtrC-regulated exopolysaccharides in the biofilm formation and pathogenic interaction of *Vibrio vulnificus*. *Mol. Microbiol.* 74, 436–453.
- Kim, J., Kim, D. Y., Yang, K. H., Kim, S., and Lee, S. S. (2019). *Ruegeria lutea* sp. nov., isolated from marine sediment, Masan Bay, South Korea. *Int. J. Syst. Evol. Microbiol.* 69, 2854-2861.
- Kim, J.-H., Kim, W., Lee, J.-S., Kim, Y., and Lee, K. C. (2015). *Palleronia soli* sp. nov., isolated from a soil sample on reclaimed tidal land, and emended description of the genus *Palleronia*. *Int. J. Syst. Evol. Microbiol.* 65, 2516–2521.
- Kim, M., Oh, H. S., Park, S. C., and Chun, J. (2014). Towards a taxonomic coherence between average nucleotide identity and 16S rRNA gene sequence similarity for species demarcation of prokaryotes. *Int. J. Syst. Evol. Microbiol.* 64, 346–351.

- Kim, Y. O., Park, S., Nam, B. H., Jung, Y. T., Kim, D. G., and Yoon, J. H. (2014). *Ruegeria meonggei* sp. nov., an alphaproteobacterium isolated from ascidian *Halocynthia roretzi*. *Antonie van Leeuwenhoek, Int. J. Gen. Mol. Microbiol.* 105, 551–558.
- Kim, Y. O., Park, S., Nam, B. H., Kang, S. J., Hur, Y. B., Lee, S. J., et al. (2012). *Ruegeria halocynthiae* sp. nov., isolated from the sea squirt *Halocynthia roretzi*. *Int. J. Syst. Evol. Microbiol.* 62, 925–930.
- Kimes, N. E., Grim, C. J., Johnson, W. R., Hasan, N. A., Tall, B. D., Kothary, M. H., et al., (2012). Temperature regulation of virulence factors in the pathogen *Vibrio coralliilyticus*. *ISME J* 6, 835–846.
- Kimura, M. (1980). A simple method for estimating evolutionary rate of base substitutions through comparative studies of nucleotide sequences. *J. Mol. Evol.* 16, 111–120.
- Kirkup, B. C., Chang, L., Chang, S., Gevers, D., and Polz, M. F. (2010). *Vibrio* chromosomes share common history. *BMC Microbiol.* 10, 2–13.
- Kirstein, I. V., Kirmizi, S., Wichels, A., Garin-Fernandez, A., Erler, R., Löder, M., et al., (2016). Dangerous hitchhikers? Evidence for potentially pathogenic *Vibrio* spp. on microplastic particles. *Mar. Environ. Res.* 120, 1–8.
- Klindworth, A., Pruesse, E., Schweer, T., Peplies, J., Quast, C., Horn, M., et al., (2013). Evaluation of general 16S ribosomal RNA gene PCR primers for classical and next-generation sequencing-based diversity studies. *Nucleic Acids Res.* 41:e1.
- Koelmans, A. A., Bakir, A., Burton, G. A., and Janssen, C. R. (2016). Microplastic as a vector for chemicals in the aquatic environment: critical review and model-supported reinterpretation of empirical studies. *Environ. Sci. Technol.* 50, 3315–3326.
- Koren, S., Walenz, B. P., Berlin, K., Miller, J. R., Bergman, N. H., and Phillippy, A. M. (2017). Canu: scalable and accurate long-read assembly via adaptive k-mer weighting and repeat separation. *Genome Res.* 27, 722–736.
- Krediet, C. J., Ritchie, K. B., Paul, V. J., and Teplitski, M. (2013). Coral-associated micro-organisms and their roles in promoting coral health and thwarting diseases. *Proc. R. Soc. B Biol. Sci.* 280, 1–9.
- Kumar, S., Stecher, G., and Tamura, K. (2016). MEGA7: Molecular evolutionary genetics analysis version 7.0 for bigger datasets. *Mol. Biol. Evol.* 33, 1870–1874.
- Labbate, M., Queck, S. Y., Koh, K. S., Rice, S. A., Givskov, M., and Kjelleberg, S. (2004). Quorum sensing-controlled biofilm development in *Serratia liquefaciens* MG1. *J. Bacteriol.* 186, 692–698.
- Lamb, J., Willis, B., Fiorenza, E., Couch, C., Howard, R., Rader, D., et al., (2018). Plastic waste associated with disease on coral reefs. *Science* 359, 460–462.
- Lan, S. F., Huang, C. H., Chang, C. H., Liao, W. C., Lin, I. H., Jian, W. N., et al. (2009). Characterization of a new plasmid-like prophage in a pandemic *Vibrio parahaemolyticus* O3:K6 strain. *Appl. Environ. Microbiol.* 75, 2659–2667.
- Lane, D. J. (1991). 16S/23S rRNA sequencing. In: E. Stackebrandt and M. Goodfellow (Eds.), *Nucleic acid techniques in bacterial systematics*, JohnWiley and Sons, pp. 115–175.
- Langille, S. E., and Weiner, R. M. (1998). Spatial and temporal deposition of *Hyphomonas* strain VP-6 capsules involved in biofilm formation. *Appl. Environ. Microbiol.* 64, 2906–2913.
- Langmead, B., and Salzberg, S. L. (2012) Fast gapped-read alignment with Bowtie 2. *Nat. Methods.* 9, 357–359.
- Lau, S. C. K., Tsoi, M. M. Y., Li, X., Plakhotnikova, I., Dobretsov, S., Lau, K. W. K., et al. (2005). *Winogradskyella poriferorum* sp. nov., a novel member of the family *Flavobacteriaceae* isolated from a sponge in the Bahamas. *Int. J. Syst. Evol. Microbiol.* 55, 1589–1592.
- Law, K. L. (2010). Plastic accumulation in the North Atlantic Subtropical Gyre. *Science* 329, 1185–1188.

- Lee, S. D. (2018). *Maribius pontilimi* sp. nov., isolated from a tidal mudflat. *Int. J. Syst. Evol. Microbiol.* 68, 353–357.
- Lee, D., Cho, S. J., Kim, S. M., and Lee, S. B. (2017). *Winogradskyella damuponensis* sp. nov., isolated from seawater. *Int. J. Syst. Evol. Microbiol.* 63, 321–326.
- Lee, J.-W., Nam, J.-H., Kim, Y.-H., Lee, K.-H., and Lee, D.-H. (2008). Bacterial communities in the initial stage of marine biofilm formation on artificial surfaces. *J. Microbiol.* 46, 174–182.
- Lee, J., Whon, T. W., Shin, N. R., Roh, S. W., Kim, J., Park, S. K., *et al.*, (2012). *Ruegeria conchae* sp. nov., isolated from the ark clam *Scapharca broughtonii*. *Int. J. Syst. Evol. Microbiol.* 62, 2851–2857.
- Li, H. (2013) Aligning sequence reads, clone sequences and assembly contigs with BWA-MEM. *arXiv*: 1303.3997.
- Li, W., and Godzik, A. (2006). Cd-hit: a fast program for clustering and comparing large sets of protein or nucleotide sequences. *Bioinformatics* 22, 1658–1659.
- Lin, B., Wang, Z., Malanoski, A. P., O’Grady, E. A., Wimpee, C. F., Vuddhakul, V., *et al.* (2010). Comparative genomic analyses identify the *Vibrio harveyi* genome sequenced strains BAA-1116 and HY01 as *Vibrio campbellii*. *Environ. Microbiol. Rep.* 2, 81–89.
- Liu, J., Fu, K., Wu, C., Qin, K., Li, F., and Zhou, L. (2018). “In-group” communication in marine *Vibrio*: a review of N-acyl homoserine lactones-driven quorum sensing. *Front. Cell. Infect. Microbiol.* 8:139.
- Liu, Y. C., Huang, R. M., Bao, J., Wu, K. Y., Wu, H. Y., Gao, X. Y., *et al.* (2018). The unexpected diversity of microbial communities associated with black corals revealed by high-throughput Illumina sequencing. *FEMS Microbiol. Lett.* 365, fny167.
- Lorenz, N., Shin, J. Y., and Jung, K. (2017). Activity, abundance, and localization of quorum sensing receptors in *Vibrio harveyi*. *Front. Microbiol.* 8, 634.
- Ludwig, W. (2010). Molecular phylogeny of microorganisms: is rRNA still a useful marker? In: Oren, A., Papke, R.T. (Eds.), *Molecular phylogeny of microorganisms*, Norfolk, UK: Caister Academic Press, pp. 65–83.
- Ludwig, W., Strunk, O., Westram, R., Richter, L., Meier, H., Yadhukumar *et al.* (2004). ARB: a software environment for sequence data. *Nucleic Acids Res* 32, 1363–1371.
- Lunau, M., Lemke, A., Walther, K., Martens-Habbena, W., and Simon, M. (2005). An improved method for counting bacteria from sediments and turbid environments by epifluorescence microscopy. *Environ. Microbiol.* 7, 961–968.
- Luo, H., and Moran, M. A. (2014). Evolutionary ecology of the marine *Roseobacter* clade. *Microbiol. Mol. Biol. Rev.* 78, 573–587.
- Lusher, A. L., McHugh, M., and Thompson, R. C. (2013). Occurrence of microplastics in the gastrointestinal tract of pelagic and demersal fish from the English Channel. *Mar. Pollut. Bull.* 67, 94–99.
- Margulies, M., Egholm, M., Altman, W. E., Attiya, S., Bader, J.S., Bemben, L., *et al.* (2005) Genome sequencing in microfabricated high-density picolitre reactors. *Nature* 437, 376–380.
- Martens, T., Heidorn, T., Pukall, R., Simon, M., Tindall, B. J. and Brinkhoff, T. Reclassification of *Roseobacter gallaeciensis* Ruiz-Ponte *et al.* 1998 as *Phaeobacter gallaeciensis* gen. nov., comb. nov., description of *Phaeobacter inhibens* sp. nov., reclassification of *Ruegeria algicola* (Lafay *et al.* 1995) Uchino *et al.* 1999 as *Marinovum algicola* gen. nov., comb. nov., and emended descriptions of the genera *Roseobacter*, *Ruegeria* and *Leisingera*. *Int. J. Syst. Evol. Microbiol.* 56, 1293–1304.
- Martínez-Checa, F., Quesada, E., Martínez-Cánovas, J., Llamas, I., and Béjar, V. (2005). *Palleronia marisminoris* gen. nov., sp. nov., a moderately halophilic, exopolysaccharide-producing

- bacterium belonging to the “*Alphaproteobacteria*”, isolated from a saline soil. *Int. J. Syst. Evol. Microbiol.* 55, 2525–2530.
- Mato, Y., Isobe, T., Takada, H., Kanehiro, H., Ohtake, C., and Kaminuma, T. (2001). Plastic resin pellets as a transport medium for toxic chemicals in the marine environment. *Environ. Sci. Technol.* 35, 318–324.
- McCormick, A., Hoellein, T. J., Mason, S. A., Schluep, J., and Kelly, J. J. (2014). Microplastic is an abundant and distinct microbial habitat in an urban river. *Environ. Sci. Technol.* 48, 11863–11871.
- McDaniel, C., Su, S., Panmanee, W., Lau, G. W., Browne, T., Cox, K., et al. (2016). A putative ABC transporter permease is necessary for resistance to acidified nitrite and EDTA in *Pseudomonas aeruginosa* under aerobic and anaerobic planktonic and biofilm conditions. *Front. Microbiol.* 7, 291.
- McDevitt-Irwin, J. M., Baum, J. K., Garren, M., and Vega Thurber, R. L. (2017). Responses of coral-associated bacterial communities to local and global stressors. *Front. Mar. Sci.* 4, 1–16.
- McDougald, D., Lin, W. H., Rice, S. A., Kjelleberg, S. (2006). The role of quorum sensing and the effect of environmental conditions on biofilm formation by strains of *Vibrio vulnificus*. *Biofouling* 22, 161–172.
- McDougald, D., Rice, S. A., Barraud, N., Steinberg, P. D., and Kjelleberg, S. (2012). Should we stay or should we go: mechanisms and ecological consequences for biofilm dispersal. *Nat. Rev. Microbiol.* 10, 39–50.
- Mewborn, L., Benitez, J. A., and Silva, A. J. (2017). Flagellar motility, extracellular proteases and *Vibrio cholerae* detachment from abiotic and biotic surfaces. *Microb. Pathog.* 113, 17–24.
- Meyer, J. L., Gunasekera, S. P., Scott, R. M., Paul, V. J., and Teplitski, M. (2016). Microbiome shifts and the inhibition of quorum sensing by black band disease cyanobacteria. *ISME J.* 10, 1204–1216.
- Miller, A. W., Blackwelder, P., Al-Sayegh, H., and Richardson, L. L. (2011). Fine-structural analysis of black band disease-infected coral reveals boring cyanobacteria and novel bacteria. *Dis. Aquat. Organ.* 93, 179–190.
- Morohoshi, T., Ogata, K., Okura, T., and Sato, S. (2018). Molecular characterization of the bacterial community in biofilms for degradation of poly(3-hydroxybutyrate-co-3-hydroxyhexanoate) films in seawater. *Microbes Environ.* 33, 19–25.
- Mulhall, M. (2009). Saving the rainforests of the sea: an analysis of international efforts to conserve coral reefs. *Duke environmental law & policy forum* 19, 321–352.
- Muscantine, L., R. McCloskey, L., and E. Marian, R. (1981). Estimating the daily contribution of carbon from zooxanthellae to coral animal respiration. *Limnol. Oceanogr.* 26, 601–611.
- Muyzer, G., Waal, E. C. De, and Uitierlinden, A. G. (1993). Profiling of complex microbial populations by denaturing gradient gel electrophoresis analysis of polymerase chain reaction-amplified genes coding for 16S rRNA. *Appl. Environ. Microbiol.* 59, 695–700.
- Nanda, A. M., Thormann, K., and Frunzke, J. (2015). Impact of spontaneous prophage induction on the fitness of bacterial populations and host-microbe interactions. *J. Bacteriol.* 197, 410–419.
- Neave, M. J., Michell, C. T., Apprill, A., and Voolstra, C. R. (2017). *Endozoicomonas* genomes reveal functional adaptation and plasticity in bacterial strains symbiotically associated with diverse marine hosts. *Sci. Rep.* 7:40579.
- Nedashkovskaya, O. I., Kim, S. B., Han, S. K., Snauwaert, C., Vancanneyt, M., Swings, J., Kim, K.-O., et al., (2005). *Winogradskyella thalassocola* gen. nov., sp. nov., *Winogradskyella epiphytica* sp. nov. and *Winogradskyella eximia* sp. nov., marine bacteria of the family *Flavobacteriaceae*. *Int. J. Syst. Evol. Microbiol.* 55, 49–55.

- Nedashkovskaya, O. I., Vancanneyt, M., Kim, S. B., and Zhukova, N. V. (2009). *Winogradskyella echinorum* sp. nov., a marine bacterium of the family *Flavobacteriaceae* isolated from the sea urchin *Strongylocentrotus intermedius*. *Int. J. Syst. Evol. Microbiol.* 59, 1465–1468.
- Nedashkovskaya, O. I., Kukhlevskiy, A. D., Zhukova, N. V. (2012). *Winogradskyella ulvae* sp. nov., an epiphyte of a Pacific seaweed, and emended descriptions of the genus *Winogradskyella* and *Winogradskyella thalassocola*, *Winogradskyella echinorum*, *Winogradskyella exilis* and *Winogradskyella eximia*. *Int. J. Syst. Evol. Microbiol.* 62, 1450–1456.
- Nedashkovskaya, O. I., Kukhlevskiy, A. D., Zhukova, N. V., Kim, S., Rhee, S., and Mikhailov, V. V. (2015). *Winogradskyella litoriviva* sp. nov., isolated from coastal seawater. *Int. J. Syst. Evol. Microbiol.* 65, 3652–3657.
- Nelms, S. E., Galloway, T. S., Godley, B. J., Jarvis, D. S., and Lindeque, P. K. (2018). Investigating microplastic trophic transfer in marine top predators. *Environ. Pollut.* 238, 999–1007.
- Nelson, C. E., Goldberg, S. J., Wegley Kelly, L., Haas, A. F., Smith, J. E., Rohwer, F., et al., (2013). Coral and macroalgal exudates vary in neutral sugar composition and differentially enrich reef bacterioplankton lineages. *ISME J.* 7, 962–979.
- Ng, W.-L., and Bassler, B. L. (2009). Bacterial quorum-sensing network architectures. *Annu. Rev. Genet.* 43, 197–222.
- Nørstebø, S. F., Paulshus, E., Bjelland, A. M., and Sørum, H. (2017). A unique role of flagellar function in *Aliivibrio salmonicida* pathogenicity not related to bacterial motility in aquatic environments. *Microb. Pathog.* 109, 263–273.
- Oberbeckmann, S., Loeder, M. G. J., Gerdt, G., and Osborn, A. M. (2014). Spatial and seasonal variation in diversity and structure of microbial biofilms on marine plastics in Northern European waters. *FEMS Microbiol. Ecol.* 90, 478–492.
- Oberbeckmann, S., Osborn, A. M., and Duhaime, M. B. (2016). Microbes on a bottle: substrate, season and geography influence community composition of microbes colonizing marine plastic debris. *PLoS One* 11, e0159289.
- Oberbeckmann, S., Kreikemeyer, B., and Labrenz, M. (2018). Environmental factors support the formation of specific bacterial assemblages on microplastics. *Front. Microbiol.* 8, 2709.
- Ogonowski, M., Motiei, A., Ininbergs, K., Hell, E., Gerdes, Z., Udekwu, K. I., et al. (2018). Evidence for selective bacterial community structuring on microplastics. *Environ. Microbiol.* 20, 2796–2808.
- Oh, K. H., Jung, Y. T., Oh, T. K., and Yoon, J. H. (2011). *Ruegeria faecimaris* sp. nov., isolated from a tidal flat sediment. *Int. J. Syst. Evol. Microbiol.* 61, 1182–1188.
- Okada, K., Iida, T., Kita-Tsukamoto, K., and Honda, T. (2005). *Vibrios* commonly possess two chromosomes. *J. Bacteriol.* 187, 752–757.
- Ondov, B. D., Bergman, N. H., and Phillippy, A. M. (2011). Interactive metagenomics visualization in a Web browser. *BMC Bioinformatics* 12, 385.
- O'Toole, G., Kaplan, H. B., and Kolter, R. (2000). Biofilm formation as microbial development. *Annu. Rev. Microbiol.* 54, 49–79.
- Palmer, J., Flint, S., and Brooks, J. (2007). Bacterial cell attachment, the beginning of a biofilm. *J. Ind. Microbiol. Biotechnol.* 34, 577–588.
- Pandolfi, J. M., Connolly, S. R., Marshall, D. J., and Cohen, A. L. (2011). Projecting coral reef futures under global warming and ocean acidification. *Science* 333, 418–422.
- Pantos, O., Bongaerts, P., Dennis, P. G., Tyson, G. W., and Hoegh-Guldberg, O. (2015). Habitat-specific environmental conditions primarily control the microbiomes of the coral *Seriatopora hystrix*. *ISME J.* 9, 1916–1927.

- Pantos, O., Cooney, R. P., Le Tissier, M. D. a, Barer, M. R., O'Donnell, A. G., and Bythell, J. C. (2003). The bacterial ecology of a plague-like disease affecting the Caribbean coral *Montastrea annularis*. *Environ. Microbiol.* 5, 370–382.
- Papazisi, L., Gorton, T. S., Kutish, G., Markham, P. F., Browning, G. F., Nguyen, D. K., et al., (2003). The complete genome sequence of the avian pathogen *Mycoplasma gallisepticum* strain R_{low}. *Microbiology* 149, 2307–2316.
- Park, S., Lee, J. S., Lee, K. C., and Yoon, J. H. (2013). *Jejudonia soesokkakensis* gen. nov., sp. nov., a member of the family *Flavobacteriaceae* isolated from the junction between the ocean and a freshwater spring, and emended description of the genus *Aureitalea* Park et al., 2012. *Antonie Van Leeuwenhoek* 104, 139–147.
- Park, S., Park, J.-M., Choi, S. J., Choi, J., and Yoon, J.-H. (2018). *Pseudomaribius aestuariivivens* gen. nov., sp. nov., isolated from a tidal flat sediment. *Int. J. Syst. Evol. Microbiol.* 64, 2618–2624.
- Park, S., Park, J.-M., Won, S., Bae, K. S., and Yoon, J.-H. (2017). *Winogradskyella wandonensis* sp. nov., isolated from a tidal flat. *Int. J. Syst. Evol. Microbiol.* 64, 1520–1525.
- Park, S., Park, J.-M., Won, S. M., and Yoon, J. H. (2015). *Winogradskyella crassostreae* sp. nov., isolated from an oyster (*Crassostrea gigas*). *Int. J. Syst. Evol. Microbiol.* 65, 2890–2895.
- Park, E.-J., Yi, J., Kim, Y., Choi, K., and Park, K. (2010). Silver nanoparticles induce cytotoxicity by a Trojan-horse type mechanism. *Toxicol. In Vitro* 24, 872–878.
- Park, S., Yoon, J.-H. (2012). *Ruegeria arenilitoris* sp. nov., isolated from the seashore sand around a seaweed farm. *Antonie van Leeuwenhoek* 102, 581–589.
- Pascual, J., Macian, M. C., Arahal, D. R., Garay, E., and Pujalte, M. J. (2010). Multilocus sequence analysis of the central clade of the genus *Vibrio* by using the 16S rRNA, *recA*, *pyrH*, *rpoD*, *gyrB*, *rctB* and *toxR* genes. *Int. J. Syst. Evol. Microbiol.* 60, 154–165.
- Pathak, V. M., and Navneet (2017). Review on the current status of polymer degradation: a microbial approach. *Bioresour. Bioprocess.* 4, 1–31.
- Payne, S.M., Mey, A.R., Wyckoff, E.E. (2016). *Vibrio* iron transport: evolutionary adaptation to life in multiple environments. *Microbiol. Mol. Biol. Rev.* 80, 69–90.
- Peixoto, R., Rosado, P., and Leite, D. (2017). Beneficial microorganisms for corals (BMC): proposed mechanisms for coral health and resilience. *Front. Microbiol.* 8:341.
- Pinto, M., Langer, T. M., Hüffer, T., Hofmann, T., and Herndl, G. J. (2019). The composition of bacterial communities associated with plastic biofilms differs between different polymers and stages of biofilm succession. *PLoS One* 14, e0217165.
- Pitcher, D. G., Saunders, N. A., and Owen, R. J. (1989). Rapid extraction of bacterial genomic DNA with guanidium thiocyanate. *Lett. Appl. Microbiol.* 8, 151–156.
- Pollock, F. J., McMinds, R., Smith, S., Bourne, D. G., Willis, B. L., Medina, M., et al., (2018). Coral-associated bacteria demonstrate phyllosymbiosis and cophylogeny. *Nat. Commun.* 9, 4921.
- Pomeroy, L. R. (1974). The ocean's food web, a changing paradigm. *BioSci* 24: 499-504.
- Pruesse, E., Peplies, J., Glöckner, F. O. (2012). SINA: accurate high-throughput multiple sequence alignment of ribosomal RNA genes. *Bioinformatics* 28, 1823–1829.
- Pujalte, M. J., Lucena, T., Ruvira, M. A., Arahal, D. R., and Macian, M. C. (2013). The family *Rhodobacteraceae*. In: Rosenberg, E., DeLong, E. F., Lory, S., Stackebrandt, E., Thompson, F. L. (Eds.), *The prokaryotes: Alphaproteobacteria and betaproteobacteria*, Springer, pp. 439-512.
- Quast, C., Pruesse, E., Yilmaz, P., Gerken, J., Schweer, T., Yarza, P., et al., (2013). The SILVA ribosomal RNA gene database project: improved data processing and web-based tools. *Nucleic Acids Res.* 41, D590–D596.
- Quilliam, R. S., Jamieson, J., and Oliver, D. M. (2014). Seaweeds and plastic debris can influence the survival of faecal indicator organisms in beach environments. *Mar. Pollut. Bull.* 84, 201–207.

- Quintanilla, E., Ramírez-Portilla, C., Adu-Oppong, B., Walljasper, G., Glaeser, S. P., Wilke, T., et al., (2018). Local confinement of disease-related microbiome facilitates recovery of gorgonian sea fans from necrotic-patch disease. *Sci. Rep.* 8, 14636.
- Raina, J. B., Tapiolas, D., Motti, C., Foret, S., Seemann, T., Tebben, J., et al., (2016). Isolation of an antimicrobial compound produced by bacteria associated with reef-building corals. *PeerJ. Prepr.* 4, e2275.
- Raina, J. B., Tapiolas, D., Willis, B. L., and Bourne, D. G. (2009). Coral-associated bacteria and their role in the biogeochemical cycling of sulfur. *Appl. Environ. Microbiol.* 75:3492–3501.
- Ransome, E., Munn, C. B., Halliday, N., Cámara, M., and Tait, K. (2014). Diverse profiles of *N*-acyl-homoserine lactone molecules found in cnidarians. *FEMS Microbiol. Ecol.* 87, 315–329.
- Reichenbach, H (1992). *Flavobacteriaceae* fam. nov. In validation of the publication of new names and new combinations previously effectively published outside the IJSB, List No. 41. *Int. J. Syst. Bacteriol.* 42, 327–329.
- Reichert, J., Schellenberg, J., Schubert, P., and Wilke, T. (2018). Responses of reef building corals to microplastic exposure. *Environ. Pollut.* 237, 955–960.
- Reisser, J., Shaw, J., Hallegraeff, G., Proietti, M., Barnes, D. K. A., Thums, M., et al. (2014). Millimeter-sized marine plastics: A new pelagic habitat for microorganisms and invertebrates. *PLoS One* 9, e100289.
- Reshef, L., Koren, O., Loya, Y., Zilber-Rosenberg, I., and Rosenberg, E. (2006). The coral probiotic hypothesis. *Environ. Microbiol.* 8, 2068–2073.
- Richardson, L. L., and Aronson, R. B. (2002). Infectious diseases of reef corals. *Proc. 9th Intl. Coral Reef Symp.*, Indonesia.
- Richter, M., and Rosselló-Móra, R. (2009), Shifting the genomic gold standard for the prokaryotic species definition. *Proc. Natl. Acad. Sci.* 106, 19126–19131.
- Riedel, T., Held, B., Nolan, M., Lucas, S., Lapidus, A., Tice, H., et al., (2012). Genome sequence of the orange-pigmented seawater bacterium *Owenweeksia hongkongensis* type strain (UST20020801T). *Stand. Genomic Sci.* 7, 120–130.
- Ritchie, K. B. (2006). Regulation of microbial populations by coral surface mucus and mucus-associated bacteria. *Mar. Ecol. Prog. Ser.* 322, 1–14.
- Rochman, C. (2015). “The complex mixture, fate and toxicity of chemicals associated with plastic debris in the marine environment,” in *Marine Anthropogenic Litter*, ed. M. Bergmann, L. Gutow, and M. Klages (Springer), 117-140.
- Rodrigues, S., Paillard, C., Van Dillen, S., Tahrioui, A., Berjeaud, J.-M., Dufour, A., et al. (2018). Relation between biofilm and virulence in *Vibrio tapetis*: A transcriptomic study. *Pathogens* 7, 92.
- Rohwer, F., Breitbart, M., Jara, J., Azam, F., and Knowlton, N. (2001). Diversity of bacteria associated with the Caribbean coral *Montastraea franksi*. *Coral Reefs* 20, 85–91.
- Römling, U., Galperin, M. Y., and Gomelsky, M. (2013). Cyclic di-GMP: the first 25 years of a universal bacterial second messenger. *Microbiol. Mol. Biol. Rev.* 77, 1–52.
- Rosenberg, E., Koren, O., Reshef, L., Efrony, R., and Zilber-Rosenberg, I. (2007). The role of microorganisms in coral health, disease and evolution. *Nat. Rev. Microbiol.* 5, 355–362.
- Rosenberg, E., Kushmaro, A., Kramarsky-Winter, E., Banin, E., and Yossi, L. (2009). The role of microorganisms in coral bleaching. *ISME J.* 3, 139–146.
- Roth, O., Keller, I., Landis, S. H., Salzburger, W., and Reusch, T. B. H. (2012). Hosts are ahead in a marine host-parasite coevolutionary arms race: Innate immune system adaptation in pipefish *Syngnathus typhle* against *Vibrio* phylotypes. *Evolution.* 66, 2528–2539.

- Rubio-Portillo, E., Gago, J. F., Martínez-García, M., Vezzulli, L., Rosselló-Móra, R., Antón, J., et al., (2018). *Vibrio* communities in scleractinian corals differ according to health status and geographic location in the Mediterranean Sea. *Syst. Appl. Microbiol.* 41, 131–138.
- Rubio-Portillo, E., Santos, F., Martínez-García, M., de los Ríos, A., Ascaso, C., Souza-Egipsy, V., et al. (2016). Structure and temporal dynamics of the bacterial communities associated to microhabitats of the coral *Oculina patagonica*. *Environ. Microbiol.* 18, 4564–4578.
- Rüger, H. J., Höfle, M. G. (1992). Marine star-shaped-aggregate-forming bacteria: *Agrobacterium atlanticum* sp. nov.; *Agrobacterium meteori* sp. nov.; *Agrobacterium ferrugineum* sp. nov., nom. rev.; *Agrobacterium gelatinovorum* sp. nov., nom. rev.; and *Agrobacterium stellulatum* sp. nov., nom. rev. *Int. J. Syst. Bacteriol.* 42, 133–143.
- Ruby, E. G., Urbanowski, M., Campbell, J., Dunn, A., Faini, M., Gunsalus, R., et al. (2005). Complete genome sequence of *Vibrio fischeri*: a symbiotic bacterium with pathogenic congeners. *Proc. Natl. Acad. Sci. U. S. A.* 102, 3004–3009.
- Rypien, K. L., Ward, J. R., and Azam, F. (2010). Antagonistic interactions among coral-associated bacteria. *Environ. Microbiol.* 12, 28–39.
- Saitou, N., Nei, M. (1987). The neighbor-joining method: a new method for reconstructing phylogenetic trees. *Mol. Biol. Evol.* 4, 406–425.
- Salta, M., Wharton, J. A., Blache, Y., Stokes, K. R., and Briand, J. F. (2013). Marine biofilms on artificial surfaces: structure and dynamics. *Environ. Microbiol.* 15, 2879–2893.
- Sato, Y., Civiello, M., Bell, S. C., Willis, B. L., and Bourne, D. G. (2016). Integrated approach to understanding the onset and pathogenesis of black band disease in corals. *Environ. Microbiol.* 18, 752–765.
- Sawabe, T., Ogura, Y., Matsumura, Y., Feng, G., Rohul Amin, A. K. M., Mino, S., et al., (2013). Updating the *Vibrio* clades defined by multilocus sequence phylogeny: Proposal of eight new clades, and the description of *Vibrio tritonius* sp. nov. *Front. Microbiol.* 4, 414.
- Schellenberg, J., Busse, H., Hardt, M., Schubert, P., Wilke, T., Peter, K., et al. (2017). *Winogradskyella haliclona* sp. nov., isolated from a marine sponge of the genus *Haliclona*. *Int. J. Syst. Evol. Microbiol.* 67, 4902–4910.
- Schmidt, V. T., Reveillaud, J., Zettler, E., Mincer, T. J., Murphy, L., and Amaral-Zettler, L. A. (2014). Oligotyping reveals community level habitat selection within the genus *Vibrio*. *Front. Microbiol.* 5, 563.
- Sekar, R., Kaczmarek, L., and Richardson, L. (2008). Microbial community composition of black band disease on the coral host *Siderastrea siderea* from three regions of the wider Caribbean. *Mar. Ecol. Prog. Ser.* 362, 85–98.
- Sellstedt, A., and Richau, K. H. (2013). Aspects of nitrogen-fixing *Actinobacteria*, in particular free-living and symbiotic *Frankia*. *FEMS Microbiol. Lett.* 342, 179–186.
- Seemann, T. (2014). Prokka: rapid prokaryotic genome annotation. *Bioinformatics* 30, 2068–2069.
- Séré, M. G., Tortosa, P., Chabanet, P., Quod, J.-P., Sweet, M. J., and Schleyer, M. H. (2015). Identification of a bacterial pathogen associated with *Porites* white patch syndrome in the Western Indian Ocean. *Mol Ecol* 24, 4570–4581.
- Setälä, O., Fleming-Lehtinen, V., and Lehtiniemi, M. (2014). Ingestion and transfer of microplastics in the planktonic food web. *Environ. Pollut.* 185, 77–83.
- Setiyono, E., Heriyanto, Pringgenies, D., Shioi, Y., Kanesaki, Y., Awai, K., et al. (2019). Sulfur-containing carotenoids from a marine coral symbiont *Erythrobacter flavus* strain KJ5. *Mar. Drugs* 17, 1–15.
- Sharon, C., and Sharon, M. (2012). Studies on biodegradation of polyethylene terephthalate: A synthetic polymer. *J. Microbiol. Biotech. Res* 2, 248–257.

- Sharp, K. H., Sneed, J. M., Ritchie, K. B., McDaniel, L., and Paul, V. J. (2015). Induction of larval settlement in the reef coral *Porites astreoides* by a cultivated marine *Roseobacter* strain. *Biol. Bull.* 228, 98–107.
- Smith, J. E., Shaw, M., Edwards, R. A., Obura, D., Pantos, O., Sala, E., et al., (2006). Indirect effects of algae on coral: algae-mediated, microbe-induced coral mortality. *Ecol. Lett.* 9, 835–845.
- Stamatakis, A. (2006). RAxML-VI-HPC: Maximum likelihood-based phylogenetic analyses with thousands of taxa and mixed models. *Bioinformatics* 22, 2688–2690.
- Stolz, A., Busse, H. J., and Kämpfer, P. (2007). *Pseudomonas knackmussii* sp. nov. *Int. J. Syst. Evol. Microbiol.* 57, 572–576.
- Sunagawa, S., DeSantis, T. Z., Piceno, Y. M., Brodie, E. L., DeSalvo, M. K., Voolstra, C. R., et al., (2009). Bacterial diversity and white plague disease-associated community changes in the Caribbean coral *Montastraea faveolata*. *ISME J.* 3, 512–521.
- Sunagawa, S., Woodley, C. M., and Medina, M. (2010). Threatened corals provide underexplored microbial habitats. *PLoS One* 5, 1–7.
- Sweet, M., and Bythell, J. (2012). Ciliate and bacterial communities associated with White Syndrome and Brown Band Disease in reef-building corals. *Environ. Microbiol.* 14, 2184–2199.
- Szmant, A. M., and Gassman, N. J. (1990). The effects of prolonged “bleaching” in the tissue biomass characteristics and reproduction of the reef coral *Montastraea annularis*. *Coral Reefs* 8, 217–224.
- Szurmant, H. and Ordal, G. W. (2004). Diversity in chemotaxis mechanisms among the bacteria and archaea. *Microbiol. Mol. Biol. Rev.* 68, 301–319.
- Tang, K. W. and Grossart, H. P. (2007). Iron effects on colonisation behavior, motility, and enzymatic activity of marine bacteria. *Can. J. Microbiol.* 53, 968–974.
- Tarazona, E., Lucena, T., Arahall, D. R., Macián, M. C., Ruvira, M. A., Pujalte, M.J. (2014) Multilocus sequence analysis of putative *Vibrio mediterranei* strains and description of *Vibrio thalassae* sp. nov. *Syst. Appl. Microbiol.* 37, 320–328.
- Tebben, J., Tapiolas, D. M., Motti, C. A., Abrego, D., Negri, A. P., Blackall, L. L., et al., (2011). Induction of larval metamorphosis of the coral *Acropora millepora* by tetrabromopyrrole isolated from a *Pseudoalteromonas bacterium*. *PLoS One* 6, e19082.
- Tercero-Albuero, J. J., González-Márquez, H., Bonilla-González, E., Quiñones-Ramírez, E. I., and Vázquez-Salinas, C. (2014). Identification of capsule, biofilm, lateral flagellum, and type IV pili in *Vibrio mimicus* strains. *Microb. Pathog.* 76, 77–83.
- Thompson, C. C., Vicente, A. C. P., Souza, R. C., Vasconcelos, A. T. R., Vesth, T., Alves, N., et al. (2009). Genomic taxonomy of vibrios. *BMC Evol. Biol.* 9, 258.
- Thompson, F. L., Gomez-Gil, B., Ribeiro Vasconcelos, A. T., and Sawabe, T. (2007). Multilocus sequence analysis reveals that *Vibrio harveyi* and *V. campbellii* are distinct species. *Appl. Environ. Microbiol.* 73, 4279–4285.
- Thompson, F. L., Gevers, D., Thompson, C. C., Dawyndt, P., Hoste, B., Munn, C. B., et al. (2005a). Phylogeny and molecular identification of Vibrios on the basis of Multilocus Sequence Analysis. *Appl. Environ. Microbiol.* 71, 5107–5115.
- Thompson, F.L., Iida, T., Swings, J. (2004a). Biodiversity of Vibrios. *Microbiol. Mol. Biol. Rev.* 68, 403–431.
- Thompson, J.R., Pacocha, S., Pharino, C., Klepac-Ceraj, V., Hunt, D.E., Benoit, J., et al., (2005b). Genotypic diversity within a natural coastal bacterioplankton population. *Science* 307, 1311–1313.
- Thompson, J. R., Randa, M. A., Marcelino, L. A., Tomita-Mitchell, A., Lim, E., and Polz, M. F. (2004b). Diversity and dynamics of a North Atlantic coastal *Vibrio* community. *Appl. Environ. Microbiol.* 70, 4103–4110.

- Tindall, B. J. (1990a). A comparative study of the lipid composition of *Halobacterium saccharovorum* from various sources. *Syst. Appl. Microbiol.* 13, 128–130. doi: 10.1016/S0723-2020(11)80158-X
- Tindall, B. J. (1990b). Lipid composition of *Halobacterium lacusprofundi*. *FEMS Microbiol. Lett.* 66, 199–202.
- Tokiwa, Y., Calabia, B. P., Ugwu, C. U., and Aiba, S. (2009). Biodegradability of plastics. *Int. J. Mol. Sci.* 10, 3722–3742.
- Tout, J., Jeffries, T. C., Petrou, K., Tyson, G. W., Webster, N. S., Garren, M., et al., (2015a). Chemotaxis by natural populations of coral reef bacteria. *ISME J* 9, 1764–77.
- Tout, J., Siboni, N., Messer, L. F., Garren, M., Stocker, R., Webster, N. S., et al., (2015b). Increased seawater temperature increases the abundance and alters the structure of natural *Vibrio* populations associated with the coral *Pocillopora damicornis*. *Front. Microbiol.* 6:432.
- Uchino, Y., Hirata, A., Yokota, A., and Sugiyama, J. (1998). Reclassification of marine *Agrobacterium* species: Proposals of *Stappia stellulata* gen. nov., comb. nov., *Stappia aggregata* sp. nov., nom. rev., *Ruegeria atlantica* gen. nov., comb. nov., *Ruegeria gelatinovora* comb. nov., *Ruegeria algicola* comb. nov., and *Ahrensia kielense* gen. nov., sp. nov., nom. rev. *J. Gen. Appl. Microbiol.* 44, 201–210.
- Urbanczyk, H., Ast, J. C., Higgins, M. J., Carson, J., and Dunlap, P. V. (2007). Reclassification of *Vibrio fischeri*, *Vibrio logei*, *Vibrio salmonicida* and *Vibrio wodanis* as *Aliivibrio fischeri* gen. nov., comb. nov., *Aliivibrio logei* comb. nov., *Aliivibrio salmonicida* comb. nov. and *Aliivibrio wodanis* comb. nov. *Int. J. Syst. Evol. Microbiol.* 57, 2823–2829.
- Urbanczyk, H., Ogura, Y., and Hayashi, T. (2013). Taxonomic revision of Harveyi clade bacteria (family *Vibrionaceae*) based on analysis of whole genome sequences. *Int. J. Syst. Evol. Microbiol.* 63, 2742–2751.
- Urbanek, A. K., Rymowicz, W., and Mironczuk, A. M. (2018). Degradation of plastics and plastic-degrading bacteria in cold marine habitats. *Appl. Microbiol. Biotechnol.* 102, 7669–7678.
- Ushijima, B., and Häse, C. C. (2018). Influence of chemotaxis and swimming patterns on the virulence of the coral pathogen *Vibrio coralliilyticus*. *J. Bacteriol.* 200. e00791-17.
- Ushijima, B., Richards, G. P., Watson, M. A., Schubiger, C. B., and Häse, C. C. (2018). Factors affecting infection of corals and larval oysters by *Vibrio coralliilyticus*. *PLoS One* 13. e0199475.
- Ushijima, B., Smith, A., Aeby, G. S., and Callahan, S. M. (2012). *Vibrio owensii* induces the tissue loss disease *Montipora* White Syndrome in the Hawaiian Reef coral *Montipora capitata*. *PLoS One* 7, e46717.
- Ushijima, B., Videau, P., Burger, A. H., Shore-Maggio, A., Runyon, C. M., Sudek, M., et al., (2014). *Vibrio coralliilyticus* strain OCN008 is an etiological agent of acute *Montipora* white syndrome. *Appl. Environ. Microbiol.* 80:2102–2109.
- Ushijima, B., Videau, P., Poscablo, D., Stengel, J. W., Beurmann, S., Burger, A. H., et al., (2016). Mutation of the *toxR* or *mshA* genes from *Vibrio coralliilyticus* strain OCN014 reduces infection of the coral *Acropora cytherea*. *Environ Microbiol* 18, 4055–4067.
- Van Cauwenberghe, L., Devriese, L., Galgani, F., Robbens, J., and Janssen, C. R. (2015). Microplastics in sediments: A review of techniques, occurrence and effects. *Mar. Environ. Res.* 111, 5–17.
- Vandenberghe, J., Thompson, F. L., Gomez-Gil, B., Swings, J. (2003). Phenotypic diversity amongst *Vibrio* isolates from marine aquaculture systems. *Aquaculture* 219, 9–20.
- Vaysse, P. J., Prat, L., Mangenot, S., Cruveiller, S., Goulas, P., and Grimaud, R. (2009). Proteomic analysis of *Marinobacter hydrocarbonoclasticus* SP17 biofilm formation at the alkane-water interface reveals novel proteins and cellular processes involved in hexadecane assimilation. *Res. Microbiol.* 160, 829–837.

- Vega-Thurber, R., Willner-Hall, D., Rodriguez-Mueller, B., Desnues, C., Edwards, R. A., Angly, F., et al., (2009). Metagenomic analysis of stressed coral holobionts. *Environ. Microbiol.* 11, 2148–2163.
- Vezzulli, L., Colwell, R.R., Pruzzo, C. (2013) Ocean warming and spread of pathogenic vibrios in the aquatic environment. *Microbial. Ecol.* 65, 817–825.
- Vezzulli, L., Pezzati, E., Brettar, I., Höfle, M., and Pruzzo, C. (2015). Effects of global warming on *Vibrio* ecology. *Microbiol. Spectr.* 3, 1-9.
- Vezzulli, L., Previati, M., Pruzzo, C., Marchese, A., Bourne, D. G., and Cerrano, C. (2010). *Vibrio* infections triggering mass mortality events in a warming Mediterranean Sea. *Environ Microbiol* 12, 2007–2019.
- Viršek, M. K., Lovšin, M. N., Koren, Š., Kržan, A., and Peterlin, M. (2017). Microplastics as a vector for the transport of the bacterial fish pathogen species *Aeromonas salmonicida*. *Mar. Pollut. Bull.* 125, 301–309.
- Wagner-Döbler, I. and B. H. (2006). Environmental biology of the marine *Roseobacter* lineage. *Annu. Rev. Microbiol.* 60, 255–280.
- Wagner, M., Scherer, C., Alvarez-Muñoz, D., Brennholt, N., Bourrain, X., Buchinger, S., et al., (2014). Microplastics in freshwater ecosystems: what we know and what we need to know. *Environ. Sci. Eur.* 26, 1–9.
- Walker, B. J., Abeel, T., Shea, T., Priest, M., Abouelliel, A., Sakthikumar, S., et al. (2014) Pilon: an integrated tool for comprehensive microbial variant detection and genome assembly improvement. *PLoS One.* 9, e112963.
- Wang, X., Zhang, Y., Qin, G., Luo, W., and Lin, Q. (2016). A novel pathogenic bacteria (*Vibrio fortis*) causing enteritis in cultured seahorses, *Hippocampus erectus* Perry, 1810. *J. Fish Dis.* 39, 765–769.
- Wen, Y., Behiels, E., Felix, J., Elegheert, J., Vergauwen, B., Devreese, B., et al. (2014). The bacterial antitoxin HipB establishes a ternary complex with operator DNA and phosphorylated toxin HipA to regulate bacterial persistence. *Nucleic Acids Res.* 42, 10134–10147.
- Whitman, W. B., Coleman, D. C., and Wiebe, W. J. (1998). Prokaryotes: the unseen majority. *Proc. Natl. Acad. Sci. U. S. A.* 95, 6578–6583.
- Wick, R. R., Judd, L. M., Holt, K. E. (2019). Performance of neural network basecalling tools for Oxford Nanopore sequencing. *Genome Biol.* 20, 129.
- Wright, S. L., Thompson, R. C., and Galloway, T. S. (2013). The physical impacts of microplastics on marine organisms: A review. *Environ. Pollut.* 178, 483–492.
- Yang, J., Yang, Y., Wu, W. M., Zhao, J., and Jiang, L. (2014). Evidence of polyethylene biodegradation by bacterial strains from the guts of plastic-eating waxworms. *Environ. Sci. Technol.* 48, 13776–13784.
- Yarza, P., Richter, M., Peplies, J., Euzéby, J., Amann, R., Schleifer, K.H. et al., (2008). The all-species living tree project: A 16S rRNA-based phylogenetic tree of all sequenced type strains. *Syst Appl Microbiol* 31, 241-250.
- Yi, H., Lim, Y. W., and Chun, J. (2007). Taxonomic evaluation of the genera *Ruegeria* and *Silicibacter*: A proposal to transfer the genus *Silicibacter* Petursdottir and Kristjansson 1999 to the genus *Ruegeria* Uchino et al. 1999. *Int. J. Syst. Evol. Microbiol.* 57, 815–819.
- Yoon, S. H., Ha, S. M., Kwon, S., Lim, J., Kim, Y., Seo, H., et al., (2017). Introducing EzBioCloud: A taxonomically united database of 16S rRNA gene sequences and whole- genome assemblies. *Int J. Syst. Evol. Microbiol.* 67, 1613–1617.
- Yoshida, S., Hiraga, K., Takehana, T., Taniguchi, I., Yamaji, H., Maeda, Y., et al., (2016). A bacterium that degrades and assimilates poly(ethylene terephthalate). *Science* 351, 1196–1199.

- Zettler, E.R., Mincer, T.J., Amaral-Zettler, L. A. (2013). Life in the "plastisphere": microbial communities on plastic marine debris. *Environ. Sci. Technol.* 47, 7137–7146
- Zhang, D., Liu, Y., Huang, H., Weber, K., and Margesin, R. (2016). *Winogradskyella sediminis* sp. nov., isolated from marine sediment. *Int. J. Syst. Evol. Microbiol.* 66, 3157–3163.
- Zhang, G., Haroon, M. F., Zhang, R., Dong, X., Wang, D., Liu, Y., *et al.*, (2017). *Ruegeria profundis* sp. nov. and *Ruegeria marisrubri* sp. nov., isolated from the brine-seawater interface at Erba Deep in the Red Sea. *Int. J. Syst. Evol. Microbiol.* 67, 4624–4631.
- Zhang, L., Wang, K.-L., Yin, Q., Liang, J.-Y., and Xu, Y. (2018). *Ruegeria kandeliae* sp. nov., isolated from the rhizosphere soil of a mangrove plant *Kandelia candel.* *Int. J. Syst. Evol. Microbiol.* 68, 2653–2658.
- Zhang, Y. Y., Ling, J., Yang, Q. S., Wang, Y. S., Sun, C. C., Sun, H. Y., *et al.*, (2015a). The diversity of coral associated bacteria and the environmental factors affect their community variation. *Ecotoxicology* 24, 1467–1477.
- Zhang, Y. Y., Ling, J., Yang, Q. S., Wen, C., Yan, Q., Sun, H. Y., *et al.*, (2015b). The functional gene composition and metabolic potential of coral-associated microbial communities. *Sci. Rep.* 5:16191.
- Zhuang, L., Liu, Y., Wang, L., Wang, W., and Shao, Z. (2015). *Erythrobacter atlanticus* sp. nov., a bacterium from ocean sediment able to degrade polycyclic aromatic hydrocarbons. *Int. J. Syst. Evol. Microbiol.* 65, 3714–3719.

Appendix

Partial 16S rRNA gene sequences obtained during the clone screening and library construction of clones by using the *Vibrio*-specific primers 567F/680R and Vibrio-744F/Vibrio-849R. Due to their short length these sequences could not be deposited in the GenBank.

Sequences obtained with the primer system Vibrio-744F/Vibrio-849R:

>Seq1 C2_744F

TAGATACTGACACTCAGATGCGAAAGCGTGGGGAGCAAACGGGATTAGATACCCCGGTA
GTCCACGCCCGTAAACGATGTCTACTTGGAGGTTGTGGCCTTGAGCCA

>Seq2 C3_744F

TAGATACTGACACTCAGATGCGAAAGCGTGGGGAGCAAACAGGATTAGATACCCTGGTA
GTCCACGCAGTAAACGATGTCTACTTGGAGGTTGTGGCCTTGAGCCA

>Seq3 C4_744F

TAGATACTGACACTCAGATGCGAAAGCGTGGGGAGCAAACGGGATTAGATAACCCCGGTA
GTCCACGCCCGTAAACGATGTCTACTTGGAGGTTGTGGCCTTGAGCCA

>Seq4 C5_744F

TAGATACTGACACTCAGATGCGAAAGCGTGGGGAGCAAACGGGATTAGATAACCCCGGTA
GTCCACGCCCGTAAACGATGTCTACTTGGAGGTTGTGGCCTTGAGCCA

>Seq5 C7_744F

TAGATACTGACACTCAGATGCGAAAGCGTGAGGAGCAAACGGGATTAGATACCCTGGTA
GTCCACGCCCGTAAACGATGTCTACTTGGAGGTTGTGGCCTTGAGCCA

>Seq6 C8_744F

TAGATACTGACACTCAGATGCGAAAGCGTGGGGAGCAAACAGGATTAGATACCCTGGTA
GTCCACGCCCGTAAACGATGTCTACTTGGAGGTTGTGGCCTTGAGCCA

>Seq7 C12_744F

TAGATACTGACACTCAGATGCGAAAGCGTGGGGAGCAAACAGGATTAGATACCCTGGTA
GTCCACGCCCGTAAACGATGTCTACTTGGAGGTTGTGGCCTTGAGCCA

>Seq8 C15_744F

TAGATACTGACACTCAGATGCGAAAGCGTGGGGAGCAAACGGGATTAGATACCCCGGTA
GTCCACGCCCGTAAACGATGTCTACTTGGAGGTTGTGGCCTTGAGCCA

>Seq9 C18_744F

TAGATACTGACACTCAGATGCGAAAGCGTGGGGAGCAAACAGGATTAGATACCCTGGTA
GTCCACGCCCGTAAACGATGTCTACTTGGAGGTTGTGGCCTTGAGCCA

>Seq10 C22_744F

TAGATACTGACACTCAGATGCGAAAGCGTGGGGAGCAAACAGGATTAGATACCCTGGTA
GTCCACGCCCGTAAACGATGTCTACTTGGAGGTTGTGGCCTTGAGCCA

>Seq11 C25_744F

TAGATACTGACACTCAGATGCGAAAGCGTGGGGAGCAAACGGGATTAGATACCCCGGTA
GTCCACGCCCGTAAACGATGTCTACTTGGAGGTTGTGGCCTTGAGCCA

>Seq12 C28_744F

TAGATACTGACACTCAGATGCGAAAGCGTGGGGAGCAAACGGGATTAGATACCCCGGTA
GTCCACGCCTTAAACGATGTCTACTTGGAGGTTGTGGCCTTGAGCCA

>Seq13 C29_744F

TAGATACTGACACTCAGATGCGAAAGCGTGGGGAGCAAACGGGATTAGATACCCCGATA
GTCCACGCCGTAAACGATGTCTACTTGGAGGTTGTGGCCTTGAGCCA

>Seq14 C32_744F

TAGATACTGACACTCAGATGCGAAAGCGTGGGGAGCAAACGGGATTAGATACCCTGGTA
GTCCACGCCGTAAACGATGTCTACTTGGAGGTTGTGGCCTTGAGCCA

>Seq15 C34_744F

TAGATACTGACACTCAGATGCGAAAGCGTGGGGAGCAAACAGGATTAGATACCCTGGTA
GTCCACGCCGTAAACGATGTCTACTTGGAGGTTGTGGCCTTGAGCCA

>Seq16 C41_744F

TAGATACTGACACTCAGATGCGAAAGCGTGGGGAGCAAACAGGATTAGATACCCTGGTA
GTCCACGCCGTAAACGATGTCTACTTGAAGGTTGTGGCCTTGAGCCA

>Seq17 C2_744F

TAGATACTGACACTCAGATGCGAAAGCGTGGGGAGCAAACAGGATTAGATACCCTGGTA
GTCCACGCCGTAAACGATGTCTACTTGGAGGTTGTGGCCTTGAGCCA

Sequences obtained with the primer system 567F/680R

>Seq18 C1_567F

GGCGTAAAGCGCATGCAGGTGGTTTGTTAAGTCAGATGTGAAAGCCCCGGGGCTCAACCT
CGGAATTGCATTTGAGACTGGCAGACTAGAGTACTGTAGAGGGGGGTAGAATTTC

>Seq19 C2_567F

GGCGTAAAGCGCATGCAGGTGGTTTGTTAAGTCAGATGTGAAAGCCCCGGGGCTCGACCT
CGGAATTGCATTTGAAACTGGCAGACTAGAGTACTGTAGAGGGGGGTAGAATTTC

>Seq20 C3_567F

GGCGTAAAGCGCATGCAGGTGGTCTGTCAAGTCGGATGTGAAATCCCCGGGGCTCAACCT
GGGAACTGCATTTCGAAACTGGCAGGCTAGAGTCCTGTAGAGGGGGGTAGAATTTC

>Seq21 C4_567F

GGCGTAAAGCGCATGCAGGTGGTCTGTTAAGCAAGATGTGAAAGCCCCGGGGCTTAACCT
GGGAACCGTATTTTGAAGTGGCAGGCTAGAGTCCTGTAGAGGGGGGTAGAATTTC

>Seq22 C6_567F

GGCGTAAAGCGCATGCAGGTGGTCTGTTAAGCAAGATGTGAAAGCCCCGGGGCTTAACCT
GGGAACCGCATTTTGAAGTGGCAGGCTAGAGTCCTGTAGAGGGGGGTAGAATTTC

>Seq23 C8_567F

GGCGTAAAGCGCATGCAGGTGGATGATTAAGTCAGATGTGAAAGCCCCGGGGCTCAACCT
CGGAATTGCATTTGAAACTGGCAGACTAGAGTACTGTAGAGGGGGGTAGAATTTC

>Seq24 C10_567F

GGCGTAAAGCGCATGCAGGTGGATGATTAAGTCAGATGTGAAAGCCCCGGGGCTCAACCT
CGGAATTGCATTTGAAACTGGCAGACTAGAGTACTGTAGAGGGGGGTAGAATTTC

>Seq25 C17_567F

GGCGTAAAGCGCATGCAGGTGGATGATTAAGTCAGATGTGAAAGCCCCGGGGCTCAACCT
CGGAATTGCATTTGAAACTGGCAGACTAGAGTACTGTAGAGGGGGGTAGAATTTC

>Seq26 C21_567F

GGCGTAAAGCGCATGCAGGTGGTTTGTTAAGTCAGATGTGAAAGCCCCGGGGCTCAACCT
CGGAACTGCATTTGAAACTGGCAAAGTACTGTAGAGGGGGGTAGAATTTC

>Seq27 C22_567F

GGCGTAAAGCGCATGCAGGTGGTCTGTTAAGCAAGATGTGAAAGCCCCGGGCTTAACCT
TGGAACCGCATTTTGAAGTGGTAGACTAGAGTACTGTAGAGGGGGGTAGAATTTC

>Seq28 C28_567F

GGCGTAAAGCGCATGCAGGTGGTTTGTTAAGTCAGATGTGAAAGCACGGGGCTCAACCT
CGGAATAGCATTTGTAAATGGCAGACTAGAGTACTGTAGAGGGGGGTAGAATTTC

>Seq29 C29_567F

GGCGTAAAGCGCATGCAGGTGGTTTGTTAAGTCAGATGTGAAAGCACGGGGCTCAACCT
CGGAATAGCATTTGTAAATGGCAGACTAGAGTACTGTAGAGGGGGGTAGAATTTC

>Seq30 C35_567F

GGCGTAAAGCGCATGCAGGTGGTTTGTTAAGTCAGATGTGAAAGCCCCGGGCTCAACCT
CGGAATAGCATTTGAAACTGGCAGACTGGAGTACTGTAGAGGGGGGTAGAATTTC

>Seq31 C36_567F

GGCGTAAAGCGCATGCAGGTGGTTTGTTAAGTCAGATGTGAAAGCCCCGGGCTCAACCT
CGGAATTGCATTTGAAACTGGCAGACTAGAGTACTGTAGAGGGGGGTAGAATTTC

>Seq32 C39_567F

GGCGTAAAGCGCATGCAGGTGGTCTGTTAAGCAAGATGTGAAAGCCCCGGGCTTAACCT
GGGAACCGCATTTTGAAGTGGCAGGCTAGAGTCCTGTAGAGGGGGGTAGAATTTC

>Seq33 C40_567F

GGCGTAAAGCGCATGCAGGTGGTCTGTTAAGCAAGATGTGAAAGCCCCGGGCTTAACCT
GGGAACCGCATTTTGAAGTGGCAGGCTAGAGTCCTGTAGAGGGGGGTAGAATTTC

>Seq34 C50_567F

GGCGTAAAGCGCATGCAGGTGGTCTGTTAAGCAAGATGTGAAAGCCCCGGGCTTAACCT
GGGAACCGCATTTTGAAGTGGCAGGCTAGAGTCCTGTAGAGGGGGGTAGAATTTC

Acknowledgements

First, I want to thank my supervisors for the guidance, helpful comments and suggestions during all the stages of the Ph.D., writing abstracts, listening to oral presentations, manuscript preparations, and this thesis. I am very thankful to Prof. Dr. Peter Kämpfer for the great opportunity of being part of his working group and develop the project, as well as for all his support during these years. Likewise, I want to thank Prof. Dr. Thomas Wilke for letting me participate on this interesting project, using the animal facility of his working group to perform the experiments. I always found excellent scientific and personal support and his research expertise and dedication to science are a great role model to take into account for my future professional life. I also have to thank Prof. Dr. Catalina Arévalo-Ferro since she encouraged me to do the Ph.D. in Germany, for which I am very grateful, as well as for her support during these years. I want to thank Dr. Stefanie Glaeser for her thorough guidance and follow-up of my daily work and for all the knowledge transfer and discussions, which are reflected in this work.

I want to express my gratitude to the DAAD Center of Excellence in Marine Sciences (CEMarin) and all its funding partners for the opportunity I got to perform my Ph.D. at JLU, through the scholarship and the grant I received to conduct the project as part of the Global Change simulation project 'Ocean 2100'. For me it is very important to thank all the scientists that contributed notably and in diverse ways to the results presented in this thesis, who are also co-authors of the papers resulting from this project: Prof. Dr. Hans-Jürgen Busse, Prof. Dr. Jörn Kalinowski, Prof. Dr. Alexander Goesmann, Dr. Martin Hardt, Dr. Patrick Schubert, Dr. Jessica Reichert, Dr. Jochen Blom, Dr. Christian Rückert, and Dr. Tobias Busche. Likewise, I want to thank Katja Grebing, Maria Sowinsky, Gundi Will, and Jan Rodrigues for their excellent laboratory assistance.

I am extremely grateful to my family, my mother Cecilia and my brother Felipe, because even from far distances, they always supported and encouraged me to continue with this personal project until the end, as examples of strength, perseverance, and dedication. Likewise, I am very thankful to Steffi for her understanding, since she had to deal and share day by day the happiest and toughest periods of this process, but who always highlighted the bright sides of this effort and gave many reasons for me to stay positive for the future. Special thanks to all the friends, colleagues, and staff of the Institute of Applied Microbiology especially to Yina, Christian, Ebru, Ole, Johannes, Olga, Dipen, Julian, David, Rita, Bellinda, Renate, Corina, Martina, Monika, and other several bachelor and master students. All of them contributed in different ways to the completion of this thesis, but I also thank them for their support in laboratory activities and fruitful discussions that improved the results presented in this thesis, as well as unforgettable moments that made the everyday life easier.

All the people mentioned here were decisive to achieve this goal and I will always be grateful for their help.

**Der Lebenslauf wurde aus der elektronischen Fassung der
Dissertation entfernt**

**The curriculum vitae was removed from the electronical version of
the thesis**

Publications

- Franco, A., Cadavid, L. F., and Arévalo-Ferro, C. (2019). Biofilms and extracts from bacteria producing “*quorum sensing*” signalling molecules promote chemotaxis and settlement behaviors in *Hydractinia symbiolongicarpus* (Cnidaria: Hydrozoa) larvae. *Acta Biológica Colomb.* 24, 150–162. doi:10.15446/abc.v24n1.73642
- Franco, A., Busse, H.-J., Schubert, P., Wilke, T., Kämpfer, P., and Glaeser, S. P. (2018). *Winogradskyella pocilloporae* sp. nov. isolated from healthy tissue of the coral *Pocillopora damicornis*. *Int. J. Syst. Evol. Microbiol.* 68, 1689-1696. doi:10.1099/ijsem.0.002731
- Franco, A., Jaeger, A., Rückert, C., Blom, J., Hardt, M., Cifuentes, Y., Reichert, J., Schubert, P., Busche, T., Kalinowsky, J., Goesmann, A., Kämpfer, P., Wilke, T., and Glaeser, S. P. (in preparation). Insights into genetic features of abundant bacteria colonizing sterile polyethylene microplastic particles incubated in a marine aquaria system.
- Franco, A., Rückert, C., Blom, J., Reichert, J., Schubert, P., Wilke, T., Goesmann, A., Busche, T., Kalinowsky, J., Kämpfer, P., Glaeser, S. P. (in preparation). High diversity of *Vibrio* spp. associated with different ecological niches in a marine aquaria system and description of *Vibrio aquimaris* sp. nov.
- Franco, A., Busse, H.-J., Schubert, P., Wilke, T., Kämpfer, P., and Glaeser, S. P. (in preparation). *Pseudomaribius plastisphaeri* sp. nov., a new moderately halophilic species isolated from the surface of a polyethylene microplastic particle after incubation in a marine aquaria system
- Franco, A., Busse, H.-J., Schubert, P., Wilke, T., Kämpfer, P., and Glaeser, S. P. (in preparation). *Ruegeria sedimentorum* sp. nov., a moderately halophilic bacterium isolated from the surface of a sediment particle present in a marine aquaria system.

Conference contributions

- Franco, A., Reichert, J., Hardt, M., Schubert, P., Kämpfer, P., Wilke, T., and Glaeser, S. P. (2018). Microplastic: the Trojan horse of the ocean that might affect coral health. International Conference on Marine Science. Medellín, Colombia. (Oral presentation).
- Franco, A., Reichert, J., Hardt, M., Schubert, P., Kämpfer, P., Wilke, T., and Glaeser, S. P. (2018). Microplastics harbor non-native bacterial communities, which could develop into different genotypes of bacteria potentially harmful for corals. Vereinigung für Allgemeine und Angewandte Mikrobiologie (VAAM) Meeting. Wolfsburg, Germany. (Poster).
- Franco, A., Reichert, J., Hardt, M., Arnold, A., Schubert, P., Kämpfer, P., Wilke, T., and Glaeser, S. P. (2017). Microplastics act as new surfaces for the development of non-native

- bacterial communities in marine systems. 15th Symposium on Aquatic Microbial Ecology (SAME 15). Zagreb, Croatia. (Oral presentation).
- Franco, A., Reichert, J., Hardt, M., Arnold, A., Schubert, P., Kämpfer, P., Wilke, T., and Glaeser, S. P. (2017). Marine bacterial communities colonizing microplastic surfaces differ from those colonizing natural particles. Vereinigung für Allgemeine und Angewandte Mikrobiologie (VAAM) Meeting. Würzburg, Germany. (Poster).
- Franco, A., Cadavid, L. F., and Arévalo-Ferro, C. (2016). Quorum sensing signalling molecules produced by bacteria modulate behaviours of marine eukaryotic organisms. Vereinigung für Allgemeine und Angewandte Mikrobiologie (VAAM) Meeting. Jena, Germany. (Poster).
- Franco, A., Cadavid, L. F., and Arévalo-Ferro, C. (2015). *Hydractinia symbiolongicarpus* larvae use bacterial quorum sensing molecules to modulate their migration and metamorphosis on shells of a hermit crab. Bogota Microbial Meeting (BOMM). Bogotá, Colombia. (Oral presentation).
- Franco, A., Cadavid, L. F., and Arévalo-Ferro, C. (2014). Influence of quorum sensing molecules produced by symbiotic bacteria of shells of *Pagurus longicarpus* crab on *Hydractinia symbiolongicarpus* larvae. 114th American Society for Microbiology (ASM) General Meeting. Boston, USA. (Poster).
- Franco, A., Cadavid, L. F., and Arévalo-Ferro, C. (2012). Differential settlement of *Hydractinia symbiolongicarpus* larvae on bacterial biofilms. XXI Latin American Microbiology Congress. Santos, Brazil. (Poster).

Declaration

Ich erkläre: Ich habe die vorgelegte Dissertation selbständig und ohne unerlaubte fremde Hilfe und nur mit den Hilfen angefertigt, die ich in der Dissertation angegeben habe. Alle Textstellen, die wörtlich oder sinngemäß aus veröffentlichten Schriften entnommen sind, und alle Angaben, die auf mündlichen Auskünften beruhen, sind als solche kenntlich gemacht. Ich stimme einer evtl. Überprüfung meiner Dissertation durch eine Antiplagiat-Software zu. Bei den von mir durchgeführten und in der Dissertation erwähnten Untersuchungen habe ich die Grundsätze guter wissenschaftlicher Praxis, wie sie in der „Satzung der Justus-LiebigUniversität Gießen zur Sicherung guter wissenschaftlicher Praxis“ niedergelegt sind, eingehalten.

Gießen, April 2020

Ángel Germán Franco Franco